



SAFETY ANALYSIS REPORT

(CHAPTERS 1-7)



University of Massachusetts Lowell

Research Reactor (UMLRR)

License R-125

Docket 50-223

(2015 REV. 0)

TABLE OF CONTENTS

CHAPTERS

- 1. THE FACILITY**
- 2. SITE CHARACTERISTICS**
- 3. DESIGN OF STRUCTURES, SYSTEMS, AND COMPONENTS**
- 4. REACTOR DESCRIPTION**
- 5. REACTOR COOLANT SYSTEMS**
- 6. ENGINEERED SAFETY FEATURES**
- 7. INSTRUMENTATION AND CONTROL SYSTEMS**

Table of Contents

1 The Facility..... 1-2

1.1 Introduction..... 1-2

1.2 Summary and Conclusions on Principal Safety Considerations 1-2

1.3 General Description..... 1-4

1.3.1 Reactor Pool and Structure 1-4

1.3.2 Containment Building..... 1-6

1.3.3 Reactor Core 1-8

1.4 Shared Facilities and Equipment..... 1-10

1.5 Comparison with Similar Facilities..... 1-13

1.6 Summary of Operations 1-14

1.6.1 History..... 1-14

1.6.2 Summary..... 1-14

1.7 Compliance with the Nuclear Waste Policy Act of 1982..... 1-15

1.8 Facility Modifications and History 1-15

Tables of Figures

Figure 1-1:University of Massachusetts Lowell Reactor..... 1-5

Figure 1-2: Shared Electric Power Feed..... 1-12

Table of Tables

Table 1-1: Physical data for the UMLRR and WPI standard fuel elements..... 1-9

Table 1-2: Reactor Design Characteristics 1-10

Table 1-3: Comparison Similar Facilities..... 1-13

Table 1-4: License Amendments 1-15

Table 1-5: Changes Requiring 10CFR50.59 Review 1-16

1 The Facility

1.1 Introduction

The University of Massachusetts Lowell Research Reactor (UMLRR) open pool reactor is owned and operated by the University of Massachusetts Lowell. The UMLRR is located in Lowell MA, (Figure 1) on the North Campus of University of Massachusetts Lowell. The site is located at [N42°39'18", W71°19'30"] as determined by the U.S Geological Survey topographical maps.

As originally installed, the reactor and support systems built by General Electric Company are adequate for operation at two(2) MW thermal(t), however the facility is only licensed for operation at one(1) MW thermal(t). Reactor License R-125 was issued by the United States Atomic Energy Commission (USAEC) on December 24, 1974 and initial criticality was achieved in January 1975.

This SAR is submitted pursuant to 10 CFR 50.64 by the University of Massachusetts Lowell to apply for a twenty-year license renewal. The University of Massachusetts Lowell is responsible for the contents of this report.

1.2 Summary and Conclusions on Principal Safety Considerations

The analyses presented in this report demonstrate that the UMLRR has been designed and constructed and can be operated, as described herein, without undue risk to the health and safety of personnel in the facility and the general public. This document only addresses the safety issues associated with the operation of the MURR reflecting the as-built condition of the reactor facility, and includes the experience observed in the operation and performance of the reactor systems.

The UMLRR fuel, instrumentation, and control systems are based on past operating systems with the same or similar design, which have been approved for operation by U.S. Government agencies;

- The operating and accident conditions of the UMLRR are no greater than those of other similar reactors using the same fuel systems, and therefore present no undue risk to the health and safety of the public;
- The UMLRR has been maintained and its components and systems have been updated and/or replaced as needed;

The UMLRR has safely operated for more than 40 years. The UMLRR fuel, control-rod drives, control rods, and experimental systems are similar to many other systems used throughout the United States. These items have well-established operating experience. Conversion of the UMLRR to LEU fuel was accomplished in 1997. The reactor operates at a nominal steady-state power of one(1) MW(t). Abnormal conditions or postulated accidents discussed in this report (See Chapter 13) include:

- Maximum Hypothetical Accident (MHA);
- Reactivity insertion;
- Loss of coolant;
- Loss of heat-removal system, and;
- Fuel cladding failure

The limiting fault condition (i.e., the Maximum Hypothetical Accident) assumes complete failure of fuel cladding and an air release of all the fission products from a single fuel plate. This will result in acceptable thyroid and whole body radiation doses to both UMLRR personnel and the general public. Chapter 13 contains a detailed discussion of this accident scenario.

Radiation exposures to personnel working in the UMLRR from both direct and airborne radiation during normal operation have been analyzed and actual radiation levels have been measured. These analyses and measurements show that the highest exposures occur when personnel are working on the beam floor when the reactor is operating. Under these conditions, personnel will be subjected to a maximum radiation field of 0.5 mrem/hr. Chapter 11 contains the personnel exposure analysis. All personnel entering radiation areas will be closely monitored, their exposures will be kept as low as possible, and in no case will they be allowed to exceed the 10 CFR Part 20 guidelines.

The effects of Ar-41 and N-16 concentrations during normal operation of the reactor have also been evaluated for both UMLRR personnel and the general public. These isotopes result in exposures of only a few mrem/yr to UMLRR personnel. Their release to the atmosphere, via the exhaust stack, results in a maximum downwind concentration below the 10 CFR Part 20 guidelines for unrestricted areas; see Chapter 9 and Chapter 11 for this analysis. Radiation monitoring equipment has been installed at key locations throughout the facility to monitor radiation levels and to sound alarms and/or activate the containment isolation system if preset values are exceeded.

1.3 General Description

The reactor is licensed to operate at one (█) MW(t). The original design of the reactor permits later conversion to two (█) MW(t) operation after specific NRC review and approval. It operates with forced-convection cooling at power levels up to one (█) MW(t), or natural convection cooling at power levels below (█) MW(t). It is presently licensed to operate at one (█) MW(t).

In general, the facility provides a fast neutron irradiation facility adjacent to the reactor, three beam tubes for neutron experiments, a thermal column for thermal neutron use, gamma ray experiment facilities, a hot cell and one pneumatic tube system for activation analysis. Laboratory support services are also made available for researchers.

The reactor facility is composed of five basic systems: (1) the pool and biological shielding; (2) the reactor core, core suspension, drives, and drive shafts; (3) the controls and instrumentation systems; (4) the experiment facilities; and (5) the process and cooling systems.

1.3.1 Reactor Pool and Structure

The open pool reactor is a light water moderated and cooled, graphite and water reflected, heterogeneous reactor (Figure 1-1). The fuel is uranium enriched to 19.75% U-235. Many major experimental facilities converge toward the core and allow for simultaneous performance of a number of different experiments.

The core consists of fuel elements surrounded by reflector elements. Four safety control blades and a servo-actuated regulating blade are utilized to control reactivity in the reactor core. The control blades move vertically within a pair of shrouds that extend the length of the core. Core elements are contained in a grid box that is enclosed on four sides to confine the flow of cooling water between elements. A suspension frame supports the grid box, core, and the drive mechanisms. It should be noted that the beam tubes illustrated in Figure 1-1 have been removed to make way for the Fast Neutron Irradiation (FNI) facility. The three beam ports located on the opposite side of the core remain in service.

Direct visual and mechanical access to the core and mechanical components is available from the top of the pool for inspection, maintenance, and fuel handling. The pool water provides adequate shielding of personnel standing over the pool. The mechanical components of the bridge and frame are designed to permit the structure to be mechanically moved along a rail

system mounted on the top of the pool walls. The mechanical components are described in greater detail in Chapter 4, Reactor Description.

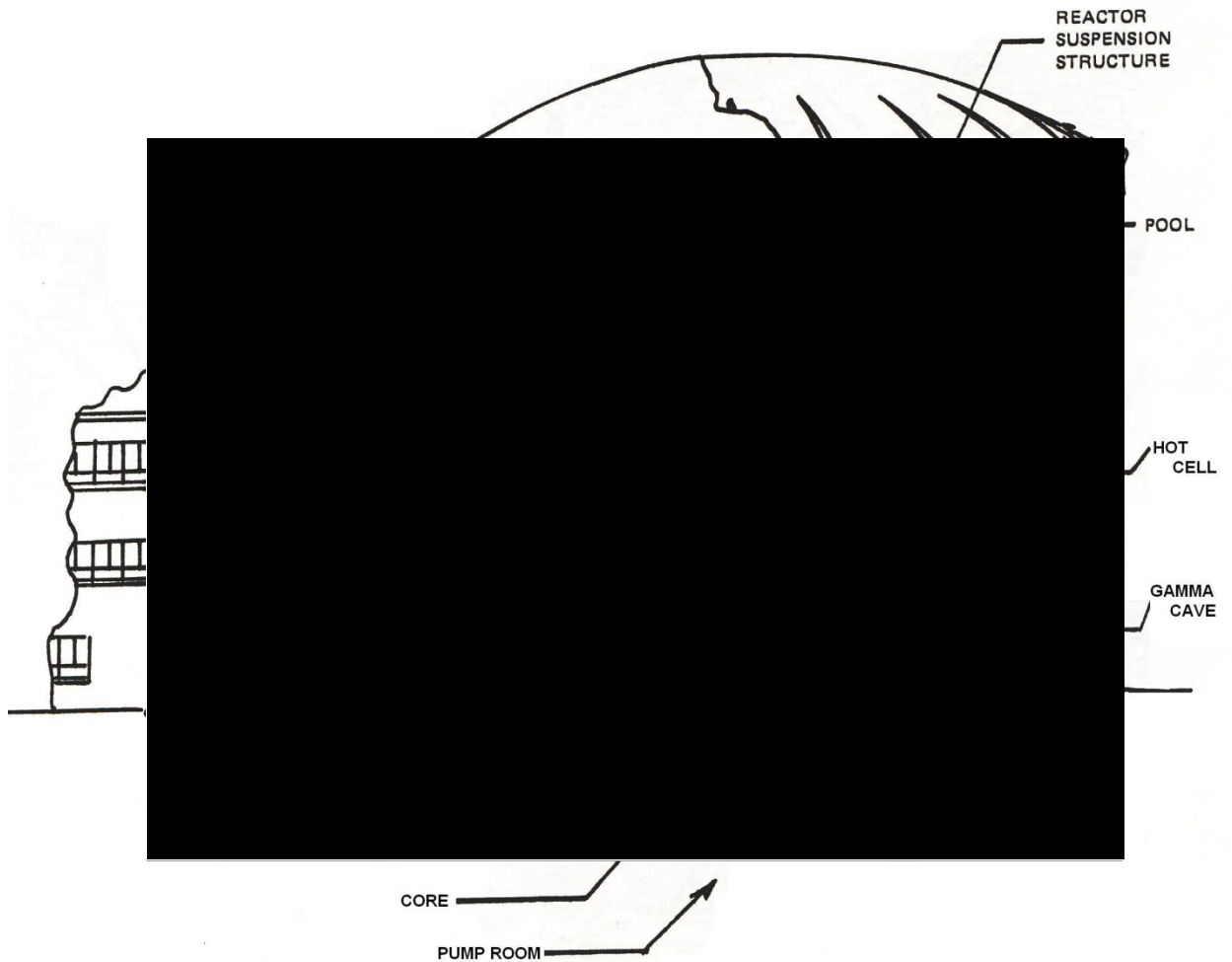


Figure 1-1: University of Massachusetts Lowell Reactor

The pool area is lined with aluminum which aids in maintaining water purity and minimizes water leakage into the concrete. Coolant piping protrudes through the concrete shield structure to allow connections to the core. Major experimental facilities converge towards the core and afford ample opportunity for the simultaneous performance of a number of different experiments.

The heart of the reactor consists of a core supported by a suspension frame in an open pool of water. The frame is bolted to a bridge, which is movable from one end of the pool to the other by means of a hand crank that, when turned, moves the wheel-mounted bridge along rails mounted at the top of the concrete structure. The reactor core sits on a [REDACTED] grid plate with

the four corner grid positions occupied by the suspension frame support posts. These support posts connect the grid plate box to the reactor bridge that spans the open pool. The support posts are water-filled, providing a convenient neutron detector location. The grid plate box is suspended about [REDACTED] meters ([REDACTED] feet) below the pool water surface.

This grid plate is installed at the bottom of a grid box whose four-sides are enclosed. The top of the grid box is open to the pool and the bottom connects to an enclosed plenum for coolant flow. The grid box also contains two permanently installed shrouds in which four BORTEC Metal Matrix Composite (MMC) control blades move. The Boral™ regulating blade is located in the reflector region adjacent to the LEU core.

During operation, each grid position must contain a fuel element, a reflector, or an irradiation basket; otherwise, the coolant flow would by-pass the active core through the vacant grid position. At the time of the HEU-LEU conversion four radiation baskets were permanently capped to further restrict by-pass coolant flow and increase the flow to fueled elements. A three-inch lead thermal shield is positioned in the pool between the grid box and the thermal column.

Surrounding the reactor, at the main floor level, is approximately [REDACTED] of reinforced high density concrete. The basic purpose of the massive concrete structure is to provide biological shielding for personnel working in the reactor building. The reactor control room [REDACTED] [REDACTED] allow operators access to the reactor.

The reactor control console is located in the control room and manages all control blade movements and contains devices that provide interlocks, scrams, and systems indication. It processes and displays information on control blade positions, power levels, and coolant system parameters. The reactor instrumentation includes chart recorders to display information graphically and the data can also be saved for future reference. A complete description of the reactor instrumentation and the data acquisition systems can be viewed in Chapter 7.

1.3.2 Containment Building

The UMLRR is housed in a containment building specifically designed for reactor operation. It includes the many systems needed to support this type of operation. The UMLRR facility consists of one building which houses the reactor and support areas. The containment building is a steel-reinforced concrete building normally maintained under a negative pressure.

Normal operation results from containment exhaust air being removed by the main exhaust blower. Air passes through a valve located within the containment wall penetration followed by a second valve approximately [REDACTED] feet downstream from the first valve, then onto the reactor exhaust stack. Air intake comes through a butterfly valve that leads to a second valve at the building wall penetration into the building heated air duct. The butterfly valve closes air tight on activation of the emergency exhaust system; when in the closed position, it provides dilution air to the emergency exhaust system. Additionally, off gas is removed from experimental facilities by blowers and filter systems. The blowers remove gases from the thermal column, beam port drain and vents, etc. and discharges into a dedicated exhaust line that includes a containment isolation valve. A pneumatic system blower discharges its gas removal into the dedicated “facilities” discharge line. The ventilation and pneumatic systems operation are fully described in Chapters 9 and 10.

The pool is divided into two interconnected sections: (1) the high-power section (Stall Pool) and (2) the low-power section (Bulk Pool). A movable gate can be used to separate the Stall and Bulk pool and allows for individual draining of the two different sections. The reactor core is moved to the high-power section and coupled to the coolant lines for operation in power ranges above [REDACTED] MW(t) using [REDACTED]. For operation in power ranges of [REDACTED] MW(t) and below, the reactor may be operated in any of the sections using [REDACTED].

As spent fuel elements are generated, they are placed in the [REDACTED]. [REDACTED]. The spent elements may be used as a [REDACTED]. [REDACTED] Co-60 sources are also utilized to perform gamma irradiation, with a licensed limit of [REDACTED]. The UMLRR gamma irradiation facility is capable of irradiating sample at dose rates in excess of [REDACTED]/hr.

The facility has a radiation monitoring system consisting of area monitors with audible/visible warnings to prevent personnel from inadvertent exposure to high radiation levels. Beam port position indications are [REDACTED]. The pneumatic system sample stations have lead receiving boxes and radiation monitors for personnel protection. Manual reactor scram buttons are located in the [REDACTED] [REDACTED] the facility.

The facility contains proven and reliable electrical, water, makeup water and waste water systems. In addition, the facility has fire detection and suppression capabilities, intercom system,

radiation monitoring systems, [REDACTED] [REDACTED] and [REDACTED] [REDACTED] system. Primary and secondary cooling systems and a primary water cleanup system are used for heat removal and pool water purification.

1.3.3 Reactor Core

The UMLRR is a water moderated and cooled open pool-type reactor that has a [REDACTED]-[REDACTED] fuel element design. The fueled core region is reflected primarily by a combination of water basket and graphite reflector elements. The standard UMLRR [REDACTED] uranium (LEU) fuel design uses uranium-silicide (U_3Si_2-Al) fuel, with [REDACTED] of U-235 per element. The UMLRR also currently has a possession-only license for [REDACTED] slightly used uranium-aluminide (UAl_x-Al) LEU fuel elements that were obtained from the Worcester Polytechnic Institute (WPI) when their research reactor was shut down.² The UMLRR U_3Si_2-Al and WPI UAl_x-Al fuel elements are similar in overall size and shape, so both elements fit interchangeably within the UMLRR grid support structure. However, the material composition of the fuel meat is different (aluminide vs. silicide fuel), the U-235 loading is quite different ([REDACTED] for the WPI element vs. [REDACTED] for the UMLRR assembly), the number of fuel plates per element differs ([REDACTED] vs. [REDACTED] for the WPI and UMLRR fuel, respectively), and there are also some small differences in meat thickness, plate thickness, water gap thickness, etc., so formal analyses that include both types of fuel design are required.

The core grid plate, consisting of a [REDACTED] by [REDACTED] rectangular array of spaces in an egg-crate shaped bottom aluminum plate, is capable of being loaded with fuel elements, reflector elements (graphite or water), experimental radiation baskets, and lead-void boxes. The availability of both water and graphite reflector elements gives flexibility in adjusting the core excess reactivity by simply interchanging some of the water vs. graphite elements closest to the fuel. The Pb-void elements were installed within the UMLRR in 2002 as part of a new core arrangement (the M-2-5 core) that included a new experimental facility, referred to as the fast neutron irradiator (FNI), on one side of the core.

Excess reactivity is limited to 4.7% $\Delta k/k$ (Facility Technical Specifications). Four safety blades and one servo-actuated regulating blade control core reactivity. The blades move vertically within a pair of shrouds extending the length of the core. Core elements are contained in a grid box, enclosed on four sides to confine the flow of cooling water between elements. The

grid box and contents, as well as the drive mechanisms, are supported by a suspension frame from the reactor bridge.

Heat Produced in the reactor is removed by natural convection at power levels below [REDACTED] kW, and by forced convection above [REDACTED] kW. A double loop coolant system transfers heat from the reactor to atmosphere via the primary coolant system, heat exchanger, a secondary coolant system, and a cooling tower. Pool water make-up and clean-up systems maintain water purity at prescribed values.

The principal reactor fuel characteristics are tabulated below.

Table 1-1: Physical data for the UMLRR and WPI standard fuel elements.

| Parameter | UMLRR Full Fuel Element | WPI Fuel Element |
|-------------------------------|------------------------------------|-------------------------|
| Plate Data: | | |
| fuel type | U ₃ Si ₂ -Al | UAl _x -Al |
| enrichment (w/o) | [REDACTED] | [REDACTED] |
| U235 loading (g/plate) | [REDACTED] | [REDACTED] |
| [REDACTED] | [REDACTED] | [REDACTED] |
| meat width (cm) | 6.085 | 6.085 |
| plate thickness (cm) | 0.1270 | 0.1524 |
| meat thickness (cm) | 0.0510 | 0.0762 |
| clad thickness (cm) | 0.0380 | 0.0381 |
| plate height (cm) | 63.50 | 62.55 |
| meat height (cm) | 59.69 | 59.69 |
| Assembly Data: | | |
| fuel plates/element | [REDACTED] | [REDACTED] |
| aluminum plates/element | 2 | 0 |
| U235 loading (g/element) | [REDACTED] | [REDACTED] |
| side plate thickness (cm) | 0.5080 | 0.4572 |
| channel thickness (cm) | 0.2963 | 0.2709 |
| assembly dimension (cm × cm) | 7.620 × 7.620 | 7.620 × 7.620 |
| assy. dim. with gap (cm × cm) | 7.7724 × 7.7724 | 7.7724 × 7.7724 |

The principal reactor design characteristics are tabulated below in Table 1-2.

Table 1-2: Reactor Design Characteristics

| <u>Reactor Characteristics</u> | |
|---|------------------------------------|
| Clean, cold core loading (█ elements █ partials)) | █ U-235 |
| Operating excess reactivity | 3.5% Δk/k |
| Reactivity in safety blades (shutdown) | 2.7% Δk/k |
| Temperature (Cool + Fuel) coefficient | -1.43x10 ⁻⁴ Δk/k/°C |
| Void coefficient (core average) | -2.59x10 ⁻³ Δk/k/% void |
| Prompt neutron lifetime | 6.45x10 ⁻⁵ sec |

| <u>Thermal Characteristics (Based on 21 Installed Elements)</u> | |
|---|-------------------------|
| Heat output | █ W(th) |
| Hot Channel Factor | █ |
| Maximum heat flux | █ BTU/h-ft ² |
| Specific power (clean, cold) | █ Watts/gm U-235 |
| Maximum gamma heat in core | █ Watts/cc |
| Coolant flow | █ gpm |
| Maximum water temperature (hot channel) | █ °F |
| Maximum fuel surface temperature (rated power) | █ °F |
| Pool water temperature (pool) | █ °F |
| Outlet water temperature (average bulk) | █ °F |
| Primary water pressure at heat exchanger | ~ █ psig |
| Secondary water pressure at heat exchanger | ~ █ psig |
| Pressure drop through core | █ psi |

| <u>Control</u> | |
|-----------------------------------|-------------------------------------|
| Safety elements | Four 10.6 inch wide vertical blades |
| Regulation element | One 2 ½ inch square vertical rod |
| Composition | BORTEC MMC (24% w/o B4C) |
| Withdrawal rate of safety blades | 3 ½ inches/minute |
| Withdrawal rate of regulating rod | 55 inches/minute |

1.4 Shared Facilities and Equipment

The UMLRR facility has a shared heating system with the adjacent █ building. This building supplies heat and cooling (circulated water) directly into the existing reactor building ventilation system. The hot water heating supply is generated by the central gas-fired boiler system for the North Campus of University of Massachusetts.

Electricity is supplied at 13,800 V from a pole on Riverside Street, down to underground conduits leading to switch and metering gear near the Power Plant (Figure 1-1), from which

point it is distributed to the area buildings. The [REDACTED] Building is fed by a 4160 V line, which runs in underground conduit from the Power Plant.

The incoming 4160 V supply is fed through two transformers in the [REDACTED] Building to two main distribution switchboards. The first transformer is rated at 750 kVA and supplies 277/408 V, three phase output to the first distribution switchboard; the second transformer is rated at 300 kVA and supplies 120/208 V, three phase output to the second distribution switchboard.

The [REDACTED] Building is also served by a [REDACTED] natural-gas fired three-phase generator. This available load is split between the reactor, accelerator, and emergency lighting within the greater [REDACTED] Building. This generator can support all operations necessary to shut down and secure the UMLRR during any power events which may occur.

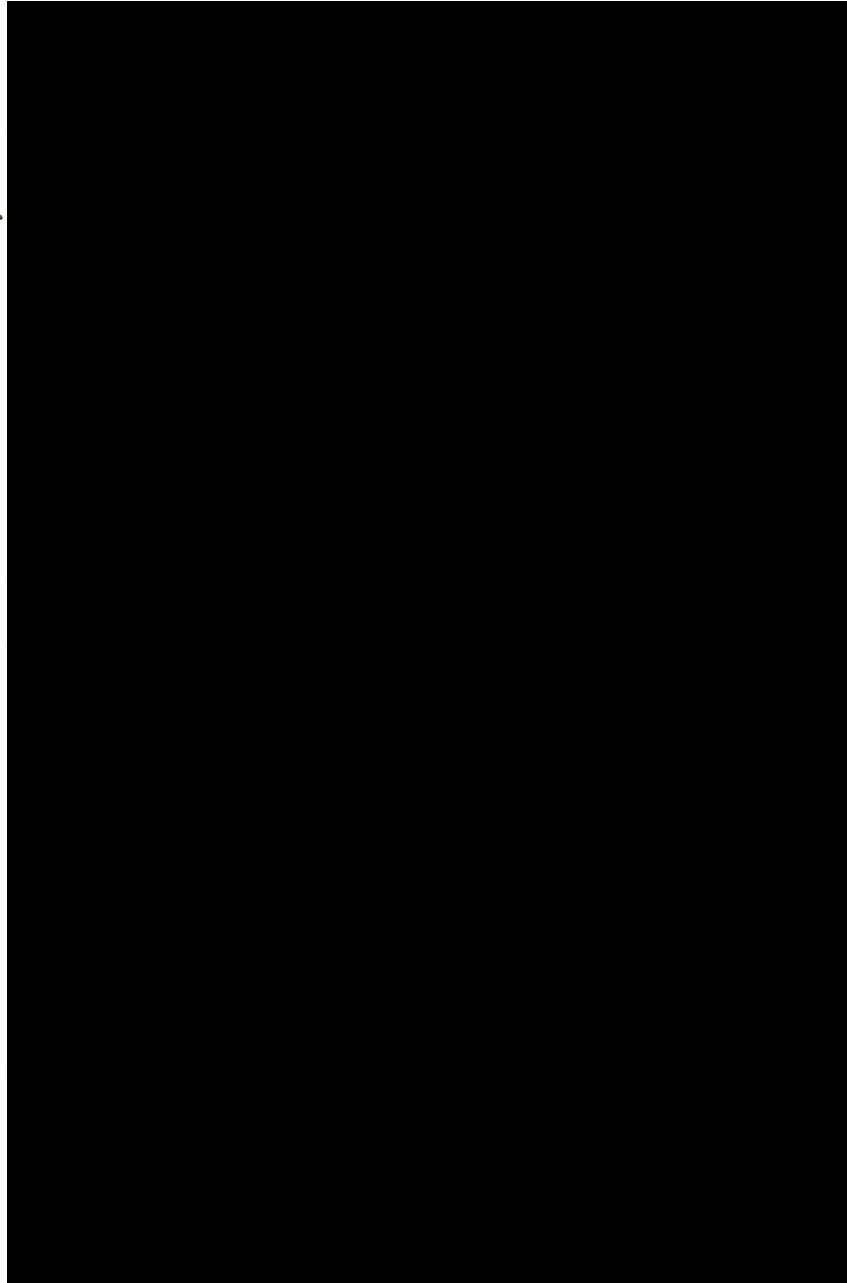


Figure 1-2: Shared Electric Power Feed

1.5 Comparison with Similar Facilities

Table 1-3: Comparison Similar Facilities

| Facility | Power Rating Max. Thermal Flux | Plate Fuel Type | Reflector | Control | Coolant | Containment/ Confinement | Initial Critical Year | Dimensions |
|--|--------------------------------------|-----------------|--|---|--|-----------------------------|-----------------------------|--|
| University of Massachusetts Lowell Research Reactor | | | Graphite H ₂ O | Four 10.65x0.38 in. wide safeties One 2.13 in. square Reg Rod. Boral | H ₂ O Forced (1600 gpm) and Natural Convection | Containment | 1975 | Pool type Stall Pool: [REDACTED] ft. Bulk Pool: [REDACTED] ft. |
| Massachusetts Institute of Technology Reactor-II | | | D ₂ O H ₂ O Graphite | Six 7.0x0.3 in. wide safeties (Boron) One 0.88x18 in. cylindrical Reg Rod (Cadmium) | H ₂ O Forced Convection 2000 gpm | Containment | 1958 | Tank type [REDACTED] ft. inner diameter at core [REDACTED] inner diameter above core [REDACTED] high |
| The Ohio State University Research Reactor | | | Graphite H ₂ O | Three 2.25x0.88 in. wide safeties (Boron) One 0.88x27 in. oval Reg Rod Stainless Steel (Water filled) | H ₂ O Natural Convection | Confinement | 1961 | Pool type [REDACTED] ft. |

1.6 Summary of Operations

1.6.1 History

The Lowell Technological Institute merged with Lowell State College to form the University of Lowell during 1975. As a result, the reactor facility became the University of Lowell Reactor (ULR). In the early 1980's, the name of the Nuclear Center was officially changed to the "██████ Building." The purpose was to reflect the change in emphasis of work at the center from strictly nuclear studies. At that time, the ULR became part of a newly established Radiation Laboratory. In 1992, the University formally became the University of Massachusetts Lowell (UML).

The Radiation Laboratory is a major research focal point of the University. Much research is correlated with safety and efficiency in the nuclear and radiation industries, including public utilities, pharmaceuticals, medical applications, health effects, etc; however, much research is also done by workers in other fields who use the unique facilities as analytical tools.

The Laboratory's facilities are used in the course work of various departments of the University. It provides these services to other Universities in the New England area, government agencies and, to a limited extent, industrial organizations in Massachusetts and the New England area.

1.6.2 Summary

The University of Massachusetts Lowell (UML) has been operating the research reactor for more than 40 years. As one of the higher flux reactors (when compared with other University Research Reactors [URR]), the UMLRR has significant potential to carry out a wide range of research and educational programs. As a public institution, the UMLRR is responsible for providing tours, briefings and training to high school students, college classes and the general public from a large geographical area. Reactor utilization by outside users is fostered and encouraged. The UMLRR actively supports the local research and industrial community in the area of nuclear science and technology.

The operating schedule makes the reactor available for full power operation during most of the year on a daily (one shift) basis.

1.7 Compliance with the Nuclear Waste Policy Act of 1982

The UMLRR has an agreement with Battelle Energy Alliance (BEA), LLC. under subcontract No. C87-101424-001 for reactor fuel assistance under Prime Contract No. DE-AC07-05ID14517 between BEA and the United States Department of Energy (DOE). The contract includes the disposal of spent fuel. A copy of the contract is enclosed herein and satisfies the requirements of the Nuclear Waste Policy Act of 1982.

1.8 Facility Modifications and History

The UMLRR has had six (6) license amendments since the 1985 License renewal. In addition, seventeen facility changes that required a 10CFR50.59 review were made. All changes are listed below in Table 1-4 & Table 1-5. These changes have been reviewed and approved by both the UMLRR Safety Sub-Committee and USNRC Reviewers, either at the time of the Amendment or during USNRC Site Inspections.

Table 1-4: License Amendments

| License Amendment # | Date | Description |
|---------------------|---------|---|
| 14 | 06/2010 | SNM & Byproduct Materials Possession Limit WPI Fuel |
| 13 | 06/2010 | SNM Possession Limit Increase for WPI Fuel |
| 12 | 07/1997 | HEU - LEU Conversion |
| 11 | 02/1992 | Changes name to University of Massachusetts. Changes minimum personnel for reactor operation. |
| 10 | 01/1992 | Changes 15 second period inhibit to control blade from regulating Blade. Changes pool water channel from protective to measuring. |
| 9 | 11/1985 | 1985 License Renewal Incorporates Amendments 1 through 8 |

Table 1-5: Changes Requiring 10CFR50.59 Review

| YEAR | TITLE | REVIEWED |
|------|---|------------|
| 2015 | Control Blade Replacement | 03/18/2015 |
| 2014 | Linear Channel Replacement | 12/17/2014 |
| 2014 | Addition of Panel Indicators | 10/7/2014 |
| 2013 | Log-N Channel Replacement | 12/18/2013 |
| 2013 | Beam Port Irradiation Facility | 06/25/2013 |
| 2012 | Stack Monitor Replacement | 12/21/2012 |
| 2012 | Cooling Tower Replacement | 03/29/2012 |
| 2012 | Chart Recorder Replacement | 01/12/2012 |
| 2011 | Pneumatic Tube Control System Upgrade | 09/29/2011 |
| 2010 | Reactor Test Using Down-comer Flow Mode | 02/25/2010 |
| 2008 | Secondary Cooling System Remote Control | 03/14/2008 |
| 2003 | Drives Control System | 02/20/2003 |
| 2002 | Clean-up and Make-up System Upgrade | 04/11/2002 |
| 2001 | Upgrade of UMLRR Process Control Cabinet | 10/25/2001 |
| 2001 | Installation of Ex-Core Fast Neutron Irradiation Facility | 01/17/2001 |
| 1998 | Power Detector Mechanical Height Adjusters | 12/17/1998 |
| 1997 | Instrumentation Upgrade | 09/11/1997 |

Table of Contents

2.0 Site Characteristics..... 2-4

2.1 Geography and Demography 2-4

2.1.1 Site Location and Description..... 2-4

2.1.2 Population Distribution..... 2-8

2.2 Nearby Industrial, Transportation, and Military Facilities..... 2-11

2.2.1 Location and Routes 2-11

2.2.2 Air Traffic 2-14

2.2.3 Analysis of Potential Accidents at Facilities 2-14

2.3 Meteorology 2-15

2.3.1 General and Local Climate 2-15

2.3.2 Meteorology..... 2-22

2.4 Hydrology..... 2-25

2.4.1 UMLRR Impact on Groundwater 2-27

2.5 Geology, Seismology, and Geotechnical Engineering..... 2-28

2.5.1 Regional Geology 2-28

2.5.2 Site Geology..... 2-30

2.5.3 Seismicity..... 2-31

2.5.4 Maximum Earthquake Potential 2-33

2.5.5 Vibratory Ground Motion 2-34

2.5.6 Surface Faulting..... 2-35

2.5.7 Liquefaction Potential..... 2-35

2.6 Bibliography (Geology Section) 2-35

Table of Figures

Figure 2-1: US Geological Topographical Map of Lowell Quadrangle. 2-5

Figure 2-2: US Geological Topographical Map. 2-6

Figure 2-3: UMLRR Location Relative to Local Streets. 2-6

Figure 2-4: Reactor Site Location (Google Earth Pro). 2-7

Figure 2-5: Reactor Containment Building on North Campus. 2-8

Figure 2-6: 2010 Census Tracts for Lowell, Mass. 2-9

Figure 2-7: 1, 2, 3, 4, 5, 8 & 10 km Radius From UMLRR Site (Google Earth Pro) ... 2-10

Figure 2-8: UMLRR in Relation to the Route 3 and 495 2-11

Figure 2-9: UMLRR in Relation to Active Railways 2-12

Figure 2-10: Hanscom Air Force Base 2-13

Figure 2-11: Lawrence Municipal Airport..... 2-14

Figure 2-12: Middlesex County Tornado 1955-2011 2-18

Figure 2-13: Tornado Days Per Year in the US (NOAA NSSL)..... 2-19

Figure 2-14: Wind Speed/Direction for Hanscom AFB (1/1/2013-12/31/2013)..... 2-22

Figure 2-15: Wind Rose for Hanscom Air Force Base (1/1/2013-12/31/2013) 2-24

Figure 2-16: Flood Vulnerability Assessment – ██████ Campus (Mitigation Plan) 2-27

Figure 2-17: Tectonic terranes, lithologic units, and fault zones of eastern Massachusetts.
From Skehan (2001). 2-29

Figure 2-18: Rose diagram showing the orientation of mafic dikes in the Candia and
Pawtuckaway quadrangles, New Hampshire (Kerwin, 2007). 2-30

Figure 2-19: Historical and recent earthquakes in eastern North America. Maps are from
the Weston Observatory web site. 2-32

Figure 2-20: All historical and measure earthquakes with $M > 5.0$. From Ebel (2013). 2-32

Figure 2-21: Modified Mercalli intensity map for the 1727 Newbury, MA, earthquake. Modified from Ebel (2000). 2-34

Table of Tables

Table 2-1: 2010 Census Tract and Recorded Population..... 2-9

Table 2-2: Monthly Climate Data for Lowell 1981-2010..... 2-15

Table 2-3: Summary of Lowell Weather Conditions..... 2-15

Table 2-4: Massachusetts Hurricane Major Disaster Declarations (1954 – Present) 2-17

Table 2-5: Lightning Event Data for City of Lowell (Jan. 1, 2000 – Feb. 28, 2013) ... 2-19

Table 2-6: Winter Storm/Blizzard Data Middlesex County (Jan. 1, 2000 – Feb. 28, 2013)
..... 2-20

Table 2-7: Wind Speed Frequency (Knots) 2-23

Table 2-8: US Army Engineering Corp. Historic Flood Levels 2-25

Table 2-9: Massachusetts Flooding Major Disaster Declarations (1954 – Present)..... 2-26

Table 2-10: Recurrence Intervals for New England Earthquakes* 2-33

Table 2-11: New England Seismic Hazard* 2-33

2.0 Site Characteristics

This chapter discusses and describes the geographical, geological, seismological, hydrological, and meteorological characteristics of the reactor facility site and vicinity in conjunction with present and projected population distributions, industrial facilities, land use, site activities and controls.

The conclusion reached in this chapter and throughout the SAR is that the site is well suited for the location of the facility when considering the relatively benign operating characteristics of the reactor including the Maximum Hypothetical Accident (MHA).

2.1 Geography and Demography

The geography and demographics of the location selected for the UMLRR site are described here.

2.1.1 Site Location and Description

2.1.1.1 Specification and Location

The University of Massachusetts Lowell Research Reactor (UMLRR) is located at [REDACTED] as determined by the U.S Geological Survey topographical maps. The research reactor is attached to the [REDACTED] g on the [REDACTED] Campus of the University of Massachusetts Lowell. The physical address of the [REDACTED] building is [REDACTED] [REDACTED] [REDACTED] Lowell Massachusetts, [REDACTED] which is within [REDACTED] County. The North Campus is located in an area just north of the Middlesex River known as Pawtuckeville, and features a majority of classrooms, offices and laboratories. The US Geological Survey topographical map of the Lowell Quadrangle can be found in Figure 2-1. This map provides details of the surrounding area.

Figure 2-2 provides more topographical and geological details of the physical area occupied by the University of Massachusetts Lowell (UML). This magnified selection provides an illustration of the local geological features that surround the UMLRR site on UML's [REDACTED] Campus. . The UMLRR is essentially located at the center of UML's [REDACTED] Campus and is approximately bounded by [REDACTED] Street to the South, [REDACTED] Street to the [REDACTED], [REDACTED]'s Street to the [REDACTED]h and [REDACTED] to the [REDACTED]. The map from Figure 2-3 illustrates the location of the [REDACTED] Energy Center and UMLRR relative to the local streets. The UML [REDACTED] [REDACTED] Campus locations encompass the highlighted regions on the map.

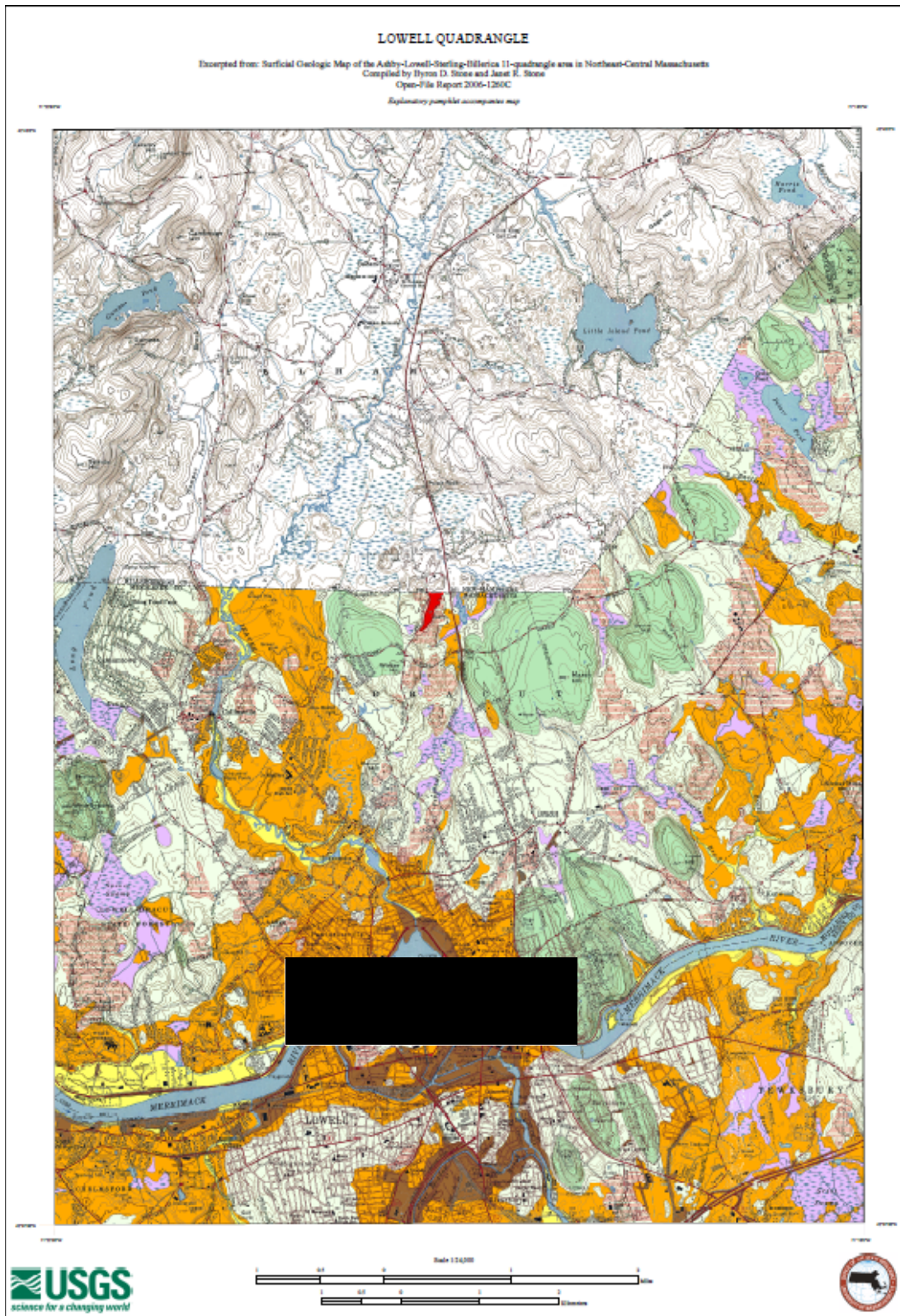


Figure 2-1: US Geological Topographical Map of Lowell Quadrangle.



Figure 2-2: US Geological Topographical Map.

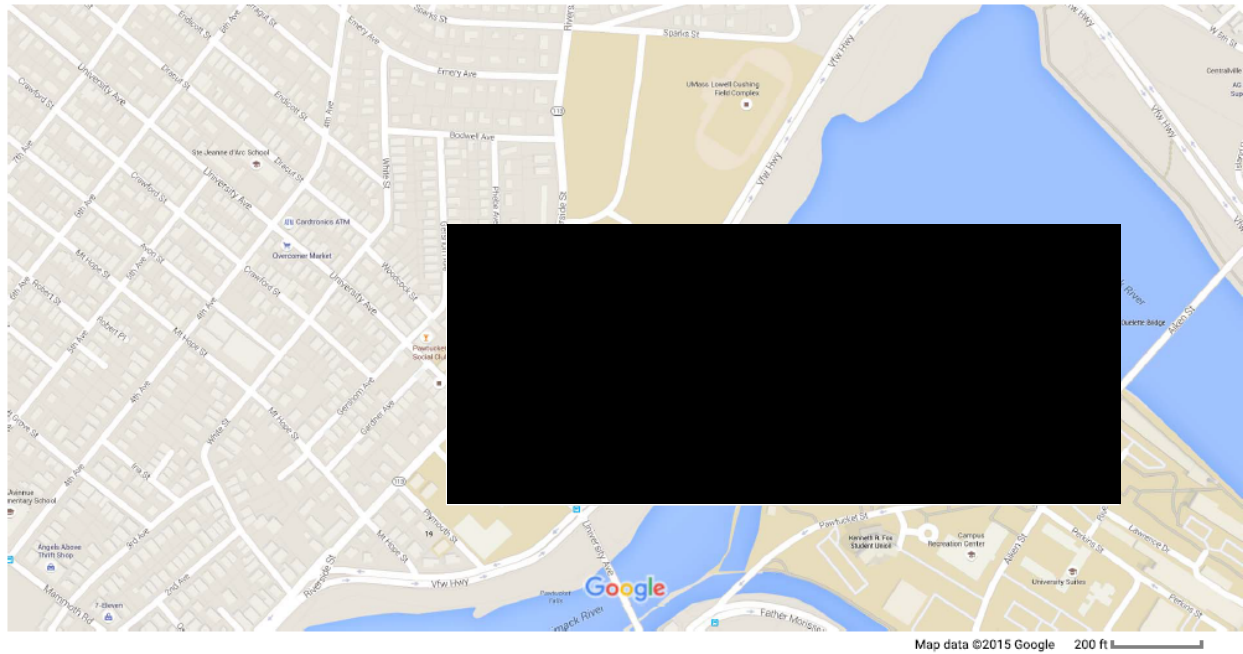


Figure 2-3: UMLRR Location Relative to Local Streets.

The reactor site is situated [REDACTED] highway and [REDACTED] Merrimack River. The Merrimack River is 117 miles (188km) long and originates in Franklin, New Hampshire at the meeting of the Pemigewasset River and Winnepesaukee River and

empties into the Atlantic Ocean at Newburyport, Massachusetts. The reactor containment dome is shown in relation to the [REDACTED] Energy Center Building in Figure 4

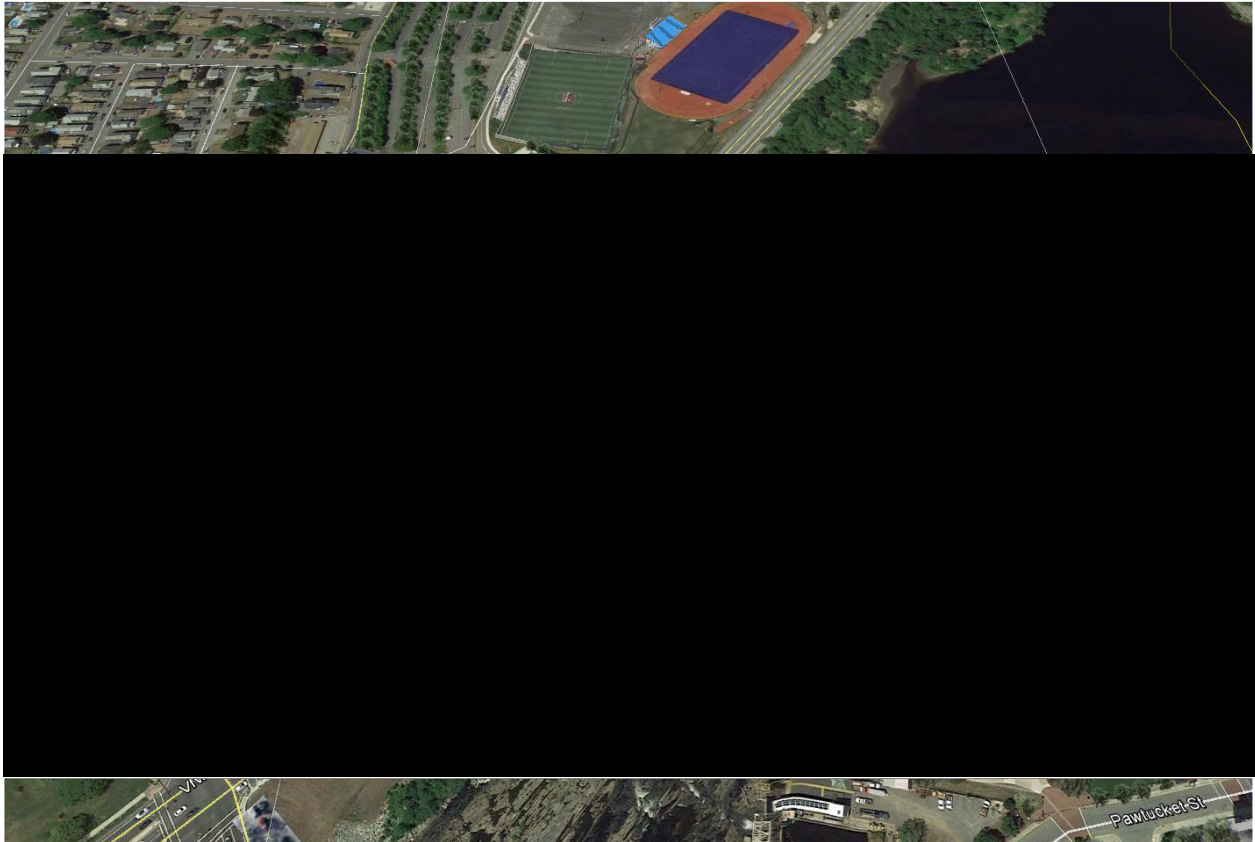


Figure 2-4: Reactor Site Location (Google Earth Pro).

2.1.1.2 Boundary and Zone Area Map

The reactor facility is associated with three main boundaries. [REDACTED]

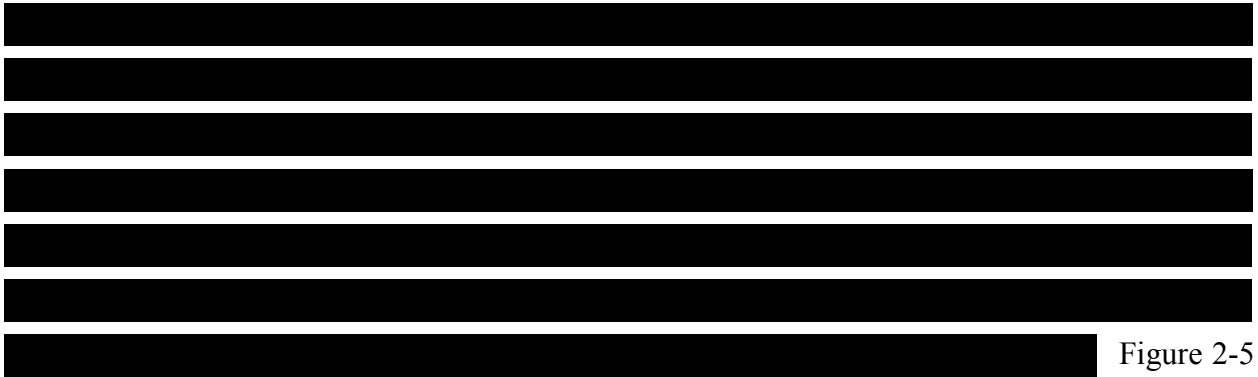


Figure 2-5

below shows the Reactor Containment Building in relation to the adjoining Pawtucket Building, as well as the UMass Lowell Campus.

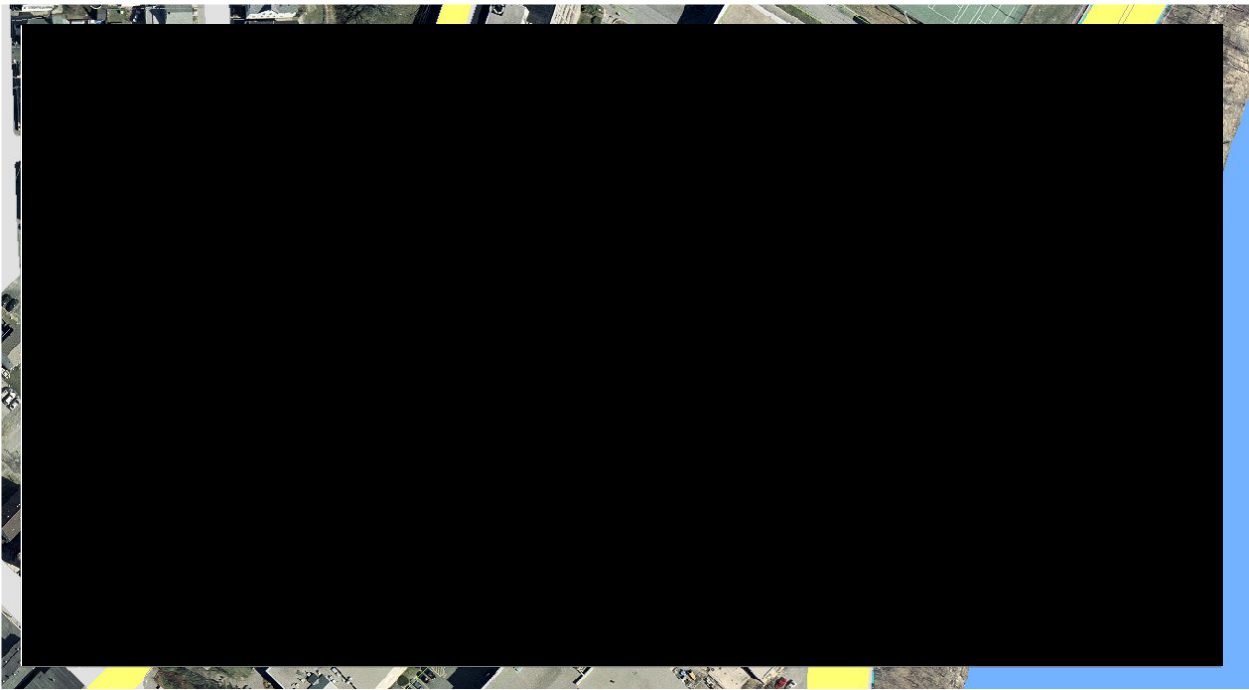


Figure 2-5: Reactor Containment Building on North Campus.

2.1.2 Population Distribution

The 2010 census lists Lowell having a population of 106,519 people, a 1.3% increase on the 2000 census. The population density is listed as 7,842.1 persons per square mile with a total of 41,431 housing units, making Lowell the fourth largest city in Massachusetts. Based on the 1.3% growth seen between the 2000 and 2010 census, an estimate of the population of Lowell for 2020 and 2035 will be 107,211 and 110,016 people respectively. Figure 2-6 below shows the 2010 Census Tract for Lowell, Massachusetts. The facility falls within census tract number 310500, which corresponds to 3,449 people and can be found in Table 2-1: 2010 Census Tract and Recorded Population.

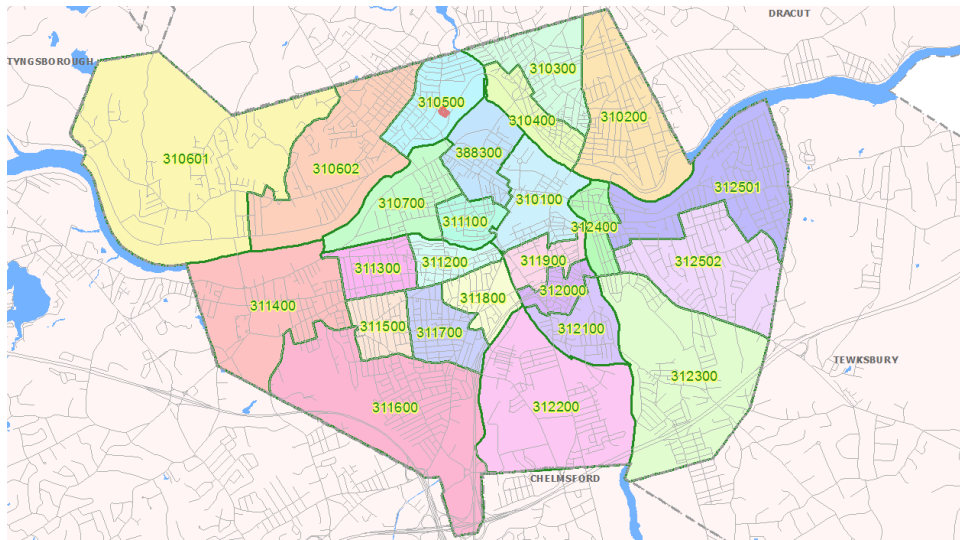


Figure 2-6: 2010 Census Tracts for Lowell, Mass.

Table 2-1: 2010 Census Tract and Recorded Population

| Community Lowell | Tract | Tract Population | Tract | Tract Population |
|---------------------|--------|------------------|------------------------------|------------------|
| | | | continued from adjacent list | |
| | 310100 | 5,267 | 311600 | 5,295 |
| | 310200 | 5,976 | 311700 | 5,098 |
| | 310300 | 6,016 | 311800 | 3,513 |
| | 310400 | 3,245 | 311900 | 2,429 |
| | 310500 | 3,449 | 312000 | 2,938 |
| | 310601 | 5,746 | 312100 | 3,149 |
| | 310602 | 5,825 | 312200 | 4,309 |
| | 310700 | 4,441 | 312300 | 4,931 |
| | 311100 | 2,410 | 312400 | 2,354 |
| | 311200 | 3,267 | 312501 | 4,464 |
| | 311300 | 4,057 | 312502 | 3,960 |
| | 311400 | 5,986 | 388300 | 5,420 |
| | 311500 | 2,974 | | |
| Total Population | | | | 106,519 |

There are seasonal fluctuations in population closest to the reactor when students leave for semester breaks. During the winter and summer semester breaks, the students return home and do not reside on the UML campuses. The winter break extends from mid-December to mid-January and the summer break extends from the first week of May to the last week of August. As of 2013 there are 9,832 undergraduate students and 4,117 graduate students attending the UML’s north, south and east campuses. It is estimated nearly half of the student population lives on campus, roughly 6,974 students.

Figure 2-7 provides a map with illustrations of the distance in kilometers (1,2,3,4,5,8 &10) from the UMLRR site. In addition to the city of Lowell, the other major population center within the 8 kilometer distance around the site is the city of Dracut, MA. Located north of the site, Dracut has a 2010 population of 29,422 people. Based on a 3.1% growth seen between the 2000 and 2010 census an estimate of the population in Dracut for 2020 and 2030 will be 29,863 and 31744 people, respectively. Portions of the following cities and towns are also located within the 8 kilometer zone, with minimal population relative to that of Lowell and Dracut: Tyngsboro, Chelmsford, Billerica, Tewksbury, Andover, Methuen, Pelham NH and Hudson NH.

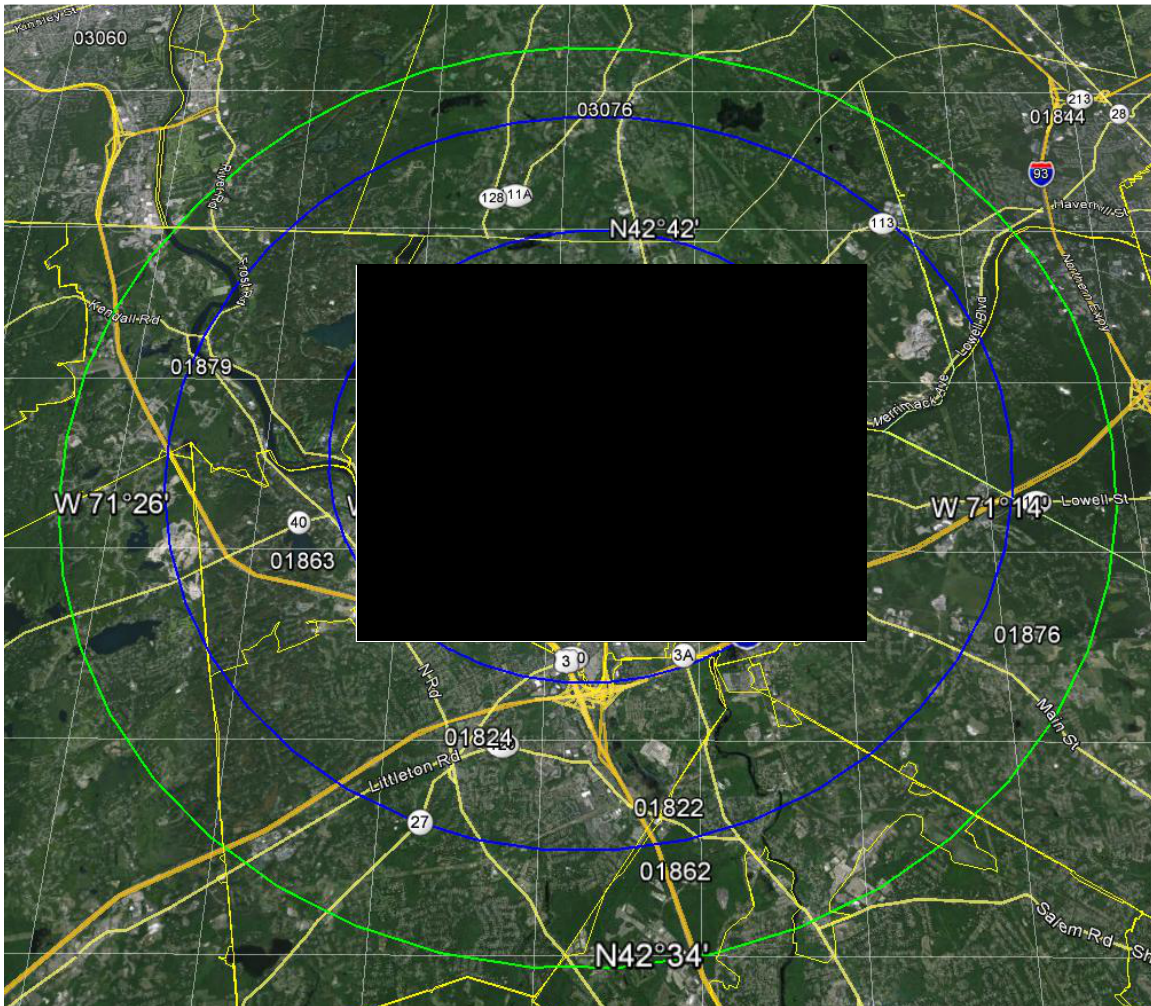


Figure 2-7: 1, 2, 3, 4, 5, 8 & 10 km Radius From UMLRR Site (Google Earth Pro)

2.2 Nearby Industrial, Transportation, and Military Facilities

2.2.1 Location and Routes

There are no industrial, transportation, or Military Facilities in the vicinity that poses a significant threat to the operations at the UMLRR. The UMLRR is located [REDACTED] from the Lowell Connector which connects Route [REDACTED] as seen in Figure 2-8. Lowell has a Massachusetts Commuter Rail Station as well as an active freight line used by Guilford railways. The UMLRR is located [REDACTED] miles north of the Lowell Line Commuter Rail Station and [REDACTED] from the closest freight line as seen in Figure 2-9.

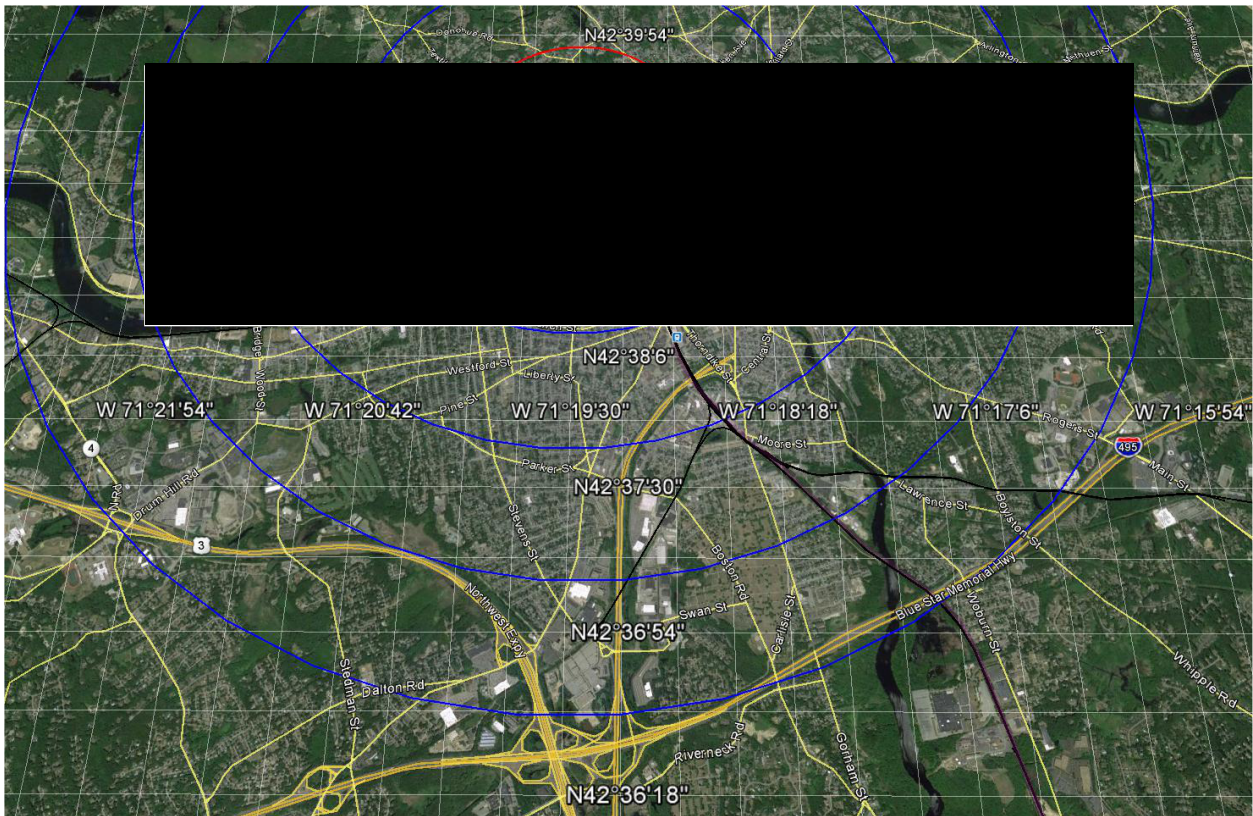


Figure 2-8: UMLRR in Relation to the Route 3 and 495

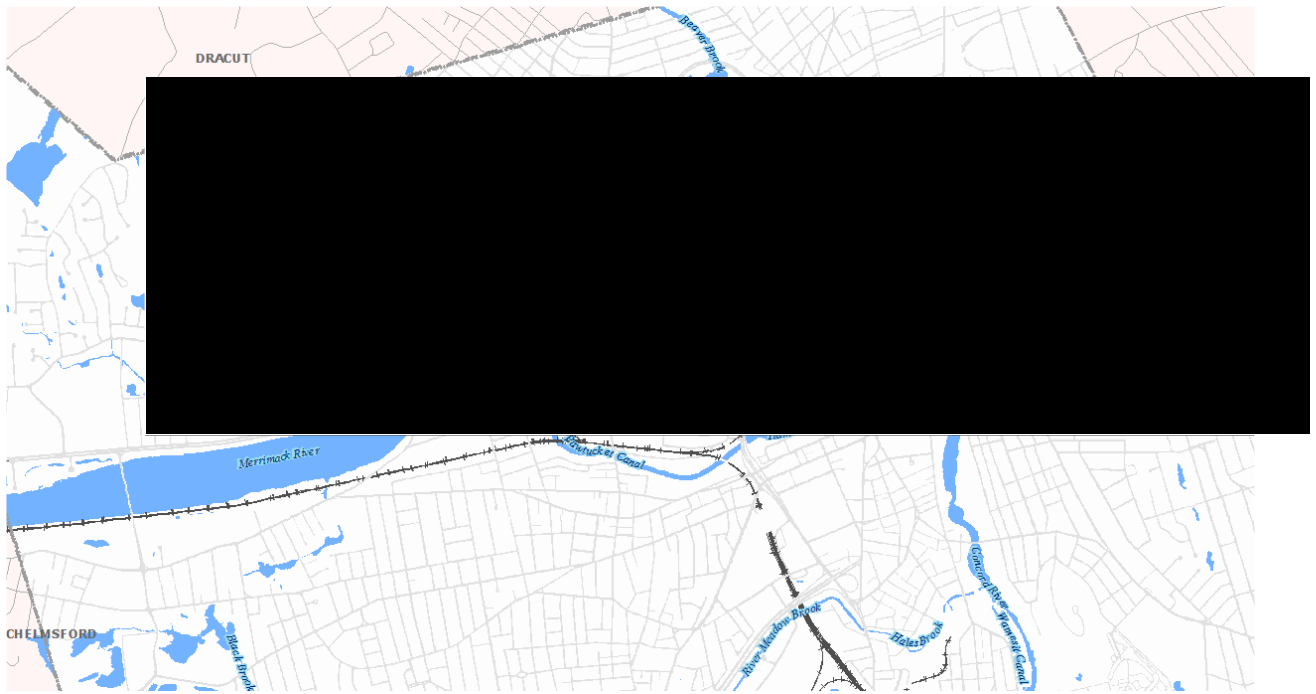


Figure 2-9: UMLRR in Relation to Active Railways

The closest military base is Hanscom Air Force Base in Bedford, Mass which is [REDACTED] miles from the UMLRR, well outside the 8 kilometer zone. Figure 2-10 shows the relative location of the Hanscom Air Force Base.

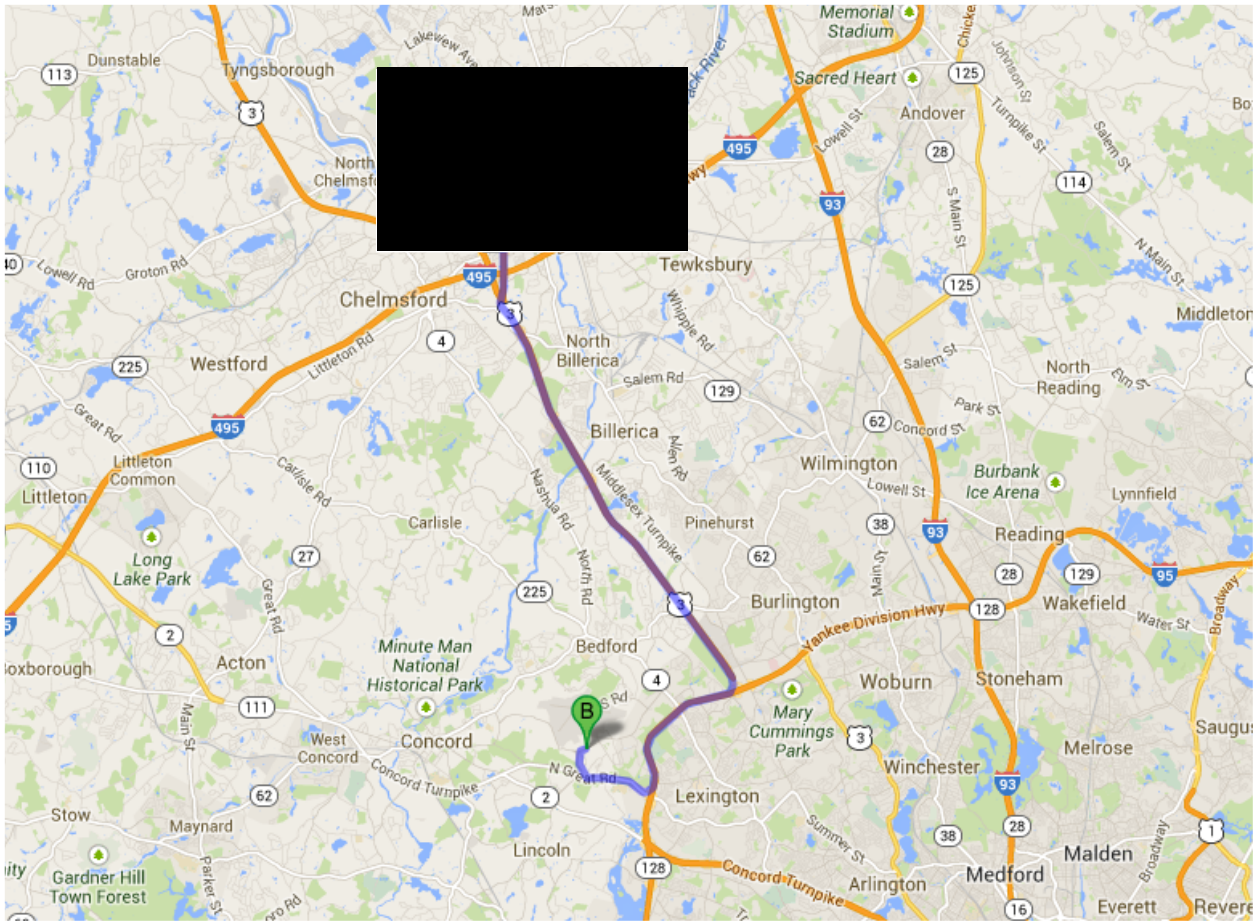


Figure 2-10: Hanscom Air Force Base

Lawrence Municipal Airport (LMA) located in North Andover Massachusetts is [REDACTED] miles east of the UMLRR as seen in Figure 2-11. LMA is home to an average of 200 aircrafts and caters to smaller jets. The airport consists of only 2 runways. The main runway is 5000 ft and the second runway 3900 ft.

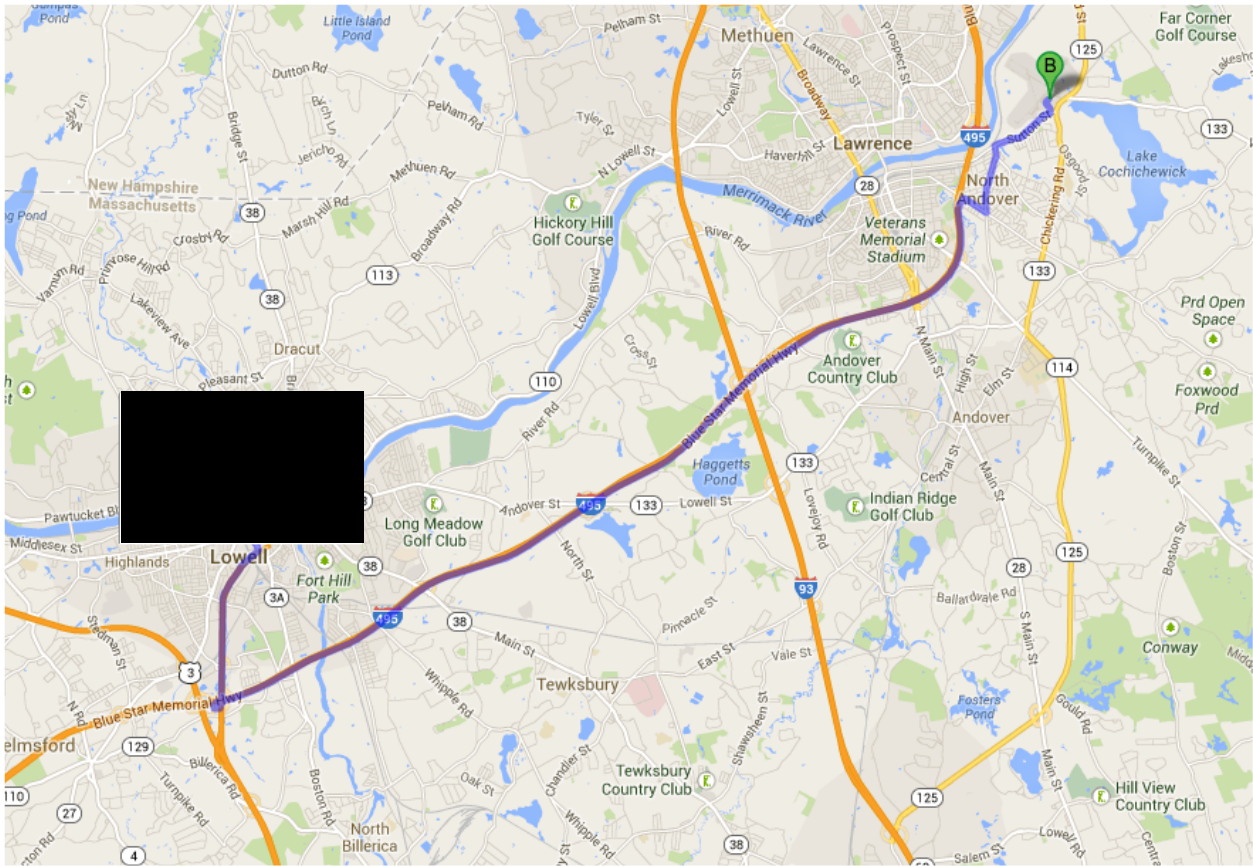


Figure 2-11: Lawrence Municipal Airport

2.2.2 Air Traffic

As mentioned previously, the closest commercial airports to the UMLRR is Lawrence Airport, located in North Andover MA at [REDACTED] miles east of the site and Boire Field Airport, located in Nashua NH, [REDACTED] miles north of the site. Neither of these airfields have any impact on the safety or integrity of the UMLRR.

2.2.3 Analysis of Potential Accidents at Facilities

No potential accident, at current and planned offsite facilities, has the capability to produce an effect which would impact the safe operation of the UMLRR.

2.3 Meteorology

2.3.1 General and Local Climate

Lowell Massachusetts, located in New England, northwest of Boston, is affected by two different air masses. Maritime tropical and continental polar are the two air masses causing four seasons. Each season is roughly three months in length.

The climate in Lowell is typically cold and snowy in the winter and warm in the summer with moderate amounts of rainfall. The monthly temperature and precipitation data for Lowell are listed in Table 2-2 . The summary of annual conditions can be found in Table 2-3.

The average annual temperature of Lowell is 49.1 °F based on data collected since 1893. A ten year average has shown a decrease in the average temperature by a half of a degree, to 48.6 °F. Average annual precipitation has been increasing. The overall average of annual precipitation (1893-2012) is 43.03 inches. Over the past 20 years (1992-2012), precipitation has increased to 46.92 inches per year. The ten year average of precipitation (2002-2012) has increased also to 51.11 inches per year.

Table 2-2: Monthly Climate Data for Lowell 1981-2010

| | JAN | FEB | MAR | APR | MAY | JUN | JUL | AUG | SEP | OCT | NO V | DEC |
|--|------|------|------|------|------|------|------|------|------|------|---------|------|
| Average High | 33 | 37 | 46 | 58 | 70 | 79 | 85 | 82 | 74 | 62 | 49 | 38 |
| Average Low | 14 | 18 | 25 | 35 | 45 | 54 | 60 | 59 | 50 | 38 | 31 | 21 |
| Average Rainfall | 3.78 | 2.91 | 3.5 | 3.86 | 3.39 | 3.66 | 3.23 | 3.27 | 3.62 | 3.94 | 4.33 | 3.62 |
| Average Snowfall | 15.7 | 11.7 | 10.1 | 2.4 | 0 | 0 | 0 | 0 | 0 | 0 | 3.0 | 10.7 |
| <i>Source: NOAA Climate Data for Lowell (1981 – 2010) & UMass Lowell MET Lab</i> | | | | | | | | | | | | |

Extremes in Lowell include a high temperature of 103 °F and a low temperature of -29 °F. Both extremes have occurred before 1960. In the past 50 years, the extremes have been less severe. A summary of Min/Max/Average temperature and precipitation data is listed in Table 2-3.

Table 2-3: Summary of Lowell Weather Conditions

| Condition | Survey Time Span | | | |
|---------------------------------|------------------|-----------|-----------|-----------|
| | 1992-2012 | 2002-2012 | 1893-2012 | 1962-2012 |
| Maximum Temperature | 102 °F | 102 °F | 103°F | 102°F |
| Minimum Temperature | -17 °F | -11 °F | -29°F | -17 °F |
| Maximum Rainfall in 24 h period | 5.48 in. | 3.39 in. | 6.64 in. | 5.48 in. |
| Average Annual Temperature | 48.6 °F | 48.6°F | 49.1°F | 48.8°F |
| Average Annual Precipitation | 46.92 in. | 51.11 in. | 43.03 in. | 42.96 in. |

Source: National Climatic Data Center, National Oceanic and Atmospheric Administration

The sea level pressure for Lowell has varied from a low value of 978 mb to a maximum of 1041 mb. The average mean sea level pressure since 1980 is 1016 mb. The average dew point during this same time frame is 46 degrees Fahrenheit, with a minimum of -11 and maximum of 76 degrees Fahrenheit.

2.3.1.1 Historical Site Weather Phenomena

In 2012, the University of Massachusetts Lowell, in conjunction with the Massachusetts Emergency Management Agency (MEMA) began an effort to develop a Hazard Mitigation Plan that would fulfill federal, state and local hazard mitigation planning requirements. The elements of this plan provide the frequency and durations of historical weather related hazards for the UMLRR site.

2.3.1.2 Hurricane & Occurrences of the Hazard

According to the State of Massachusetts Hazard Mitigation Plan, Massachusetts is susceptible to hurricanes and tropical storms. Since 1954, there have been six Major Disaster Declarations in the State of Massachusetts due to a hurricane or tropical storm, four of which have resulted in Middlesex County receiving a designated area status from MEMA.

A tropical storm is classified as having winds between 39 mph and 73 mph. Of the six storms, the most severe was Tropical Storm Irene in 2008. Irene's center passed through New York and Vermont and produced gales of 57 mph. The most severe hurricane to affect Massachusetts occurred in 1938 when a category 3 hurricane moved through with sustained winds greater than 100 mph. Gusts in some locations exceeded 150 mph.

Table 2-4: Massachusetts Hurricane Major Disaster Declarations (1954 – Present)

| | Disaster No. | Incident Period | Date Disaster Declared | Middlesex Co? | Notes |
|--|--------------|-------------------------|------------------------|---------------|---|
| Hurricane Sandy | 4097 | 10/27/2012 – 11/08/2012 | 12/19/2012 | No | Second costliest hurricane in U.S. history. Impacted 24 states with severe damage in New York and New Jersey. |
| Tropical Storm Irene | 4028 | 8/27/2011 – 8/29/2011 | 9/23/2011 | No | Impacted most of east coast and is ranked as 6th costliest hurricane in United States history. |
| Hurricane Bob | 914 | 8/19/1991 | 8/26/1991 | Yes | 60% southern MA and RI residents lost power and the storm surge in Buzzards Bay was 10-15 feet. |
| Hurricane Gloria | 751 | 9/27/1985 | 10/28/1985 | Yes | Dramatic coastal impact including beach erosion and many flooding issues caused over 2 million without power. |
| Hurricane Diane | 43 | 8/20/1955 | 8/20/1955 | Unknown | Was a Tropical Storm when it reached New England, had heavy rain of 10” – 20”, setting flood records for the time. |
| Hurricane | 22 | 9/2/1954 | 9/2/1954 | Unknown | There was heavy storm surge to Narragansett Bay and New Bedford Harbor, water up to 12 feet in downtown Providence, and massive power loss. |
| Source: FEMA Major Disaster Declarations 1954 – Present, State of Massachusetts Hazard Mitigation Plan | | | | | |

Impacts to the Commonwealth, in addition to a direct hit, include effects from tropical storm remnants such as heavy rain, localized flooding and storm surge. In Middlesex County, where the UMLRR is situated, heavy rains associated with hurricanes [and flooding events that occur as a result] present the greatest risk to the area.

Based on NOAA’s Adapting to Climate Change Guideⁱ, the power, frequency, and intensity of Atlantic Ocean hurricanes has increased in recent decades and is likely to increase over the extended long term. Within the short term, NOAA makes yearly predictions at the start of hurricane season to forecast the number of Atlantic Ocean based hurricanes. For 2013, NOAA is forecasting an active or extremely active season with a 70 percent likelihood of 13 to 20 named storms, of which 7 to 11 could become hurricanes. These ranges are above the seasonal average of 12 named storms, 6 hurricanes, and 3 major hurricanes. According to the State Hazard Mitigation Plan, based on past hurricane landfalls and the frequency of tropical systems, the

likelihood of a hurricane or tropical storm to hit Massachusetts is once out of every six years on average.

2.3.1.3 Tornadoes & Occurrences of the Hazard

Since 1955, approximately 17 tornadoes have touched down in Middlesex County, several of which have impacted the City of Lowell directly as shown in Figure 2-12.

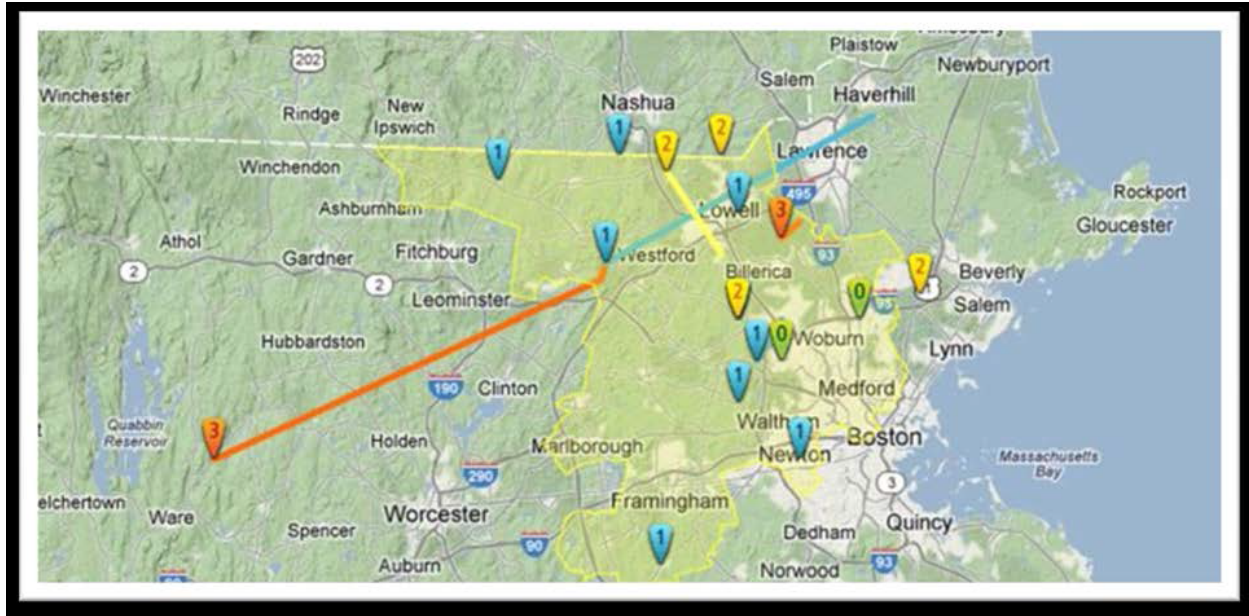


Figure 2-12: Middlesex County Tornado 1955-2011

NOAA's National Severe Storm Laboratory (NSSL) has estimated the likelihood for a tornado on a given day in the United States. Figure 2-13 shows that the probability for a tornado in Massachusetts is 0.2 to 0.4 days per year based on tornado data collected from 1995 to 1999.

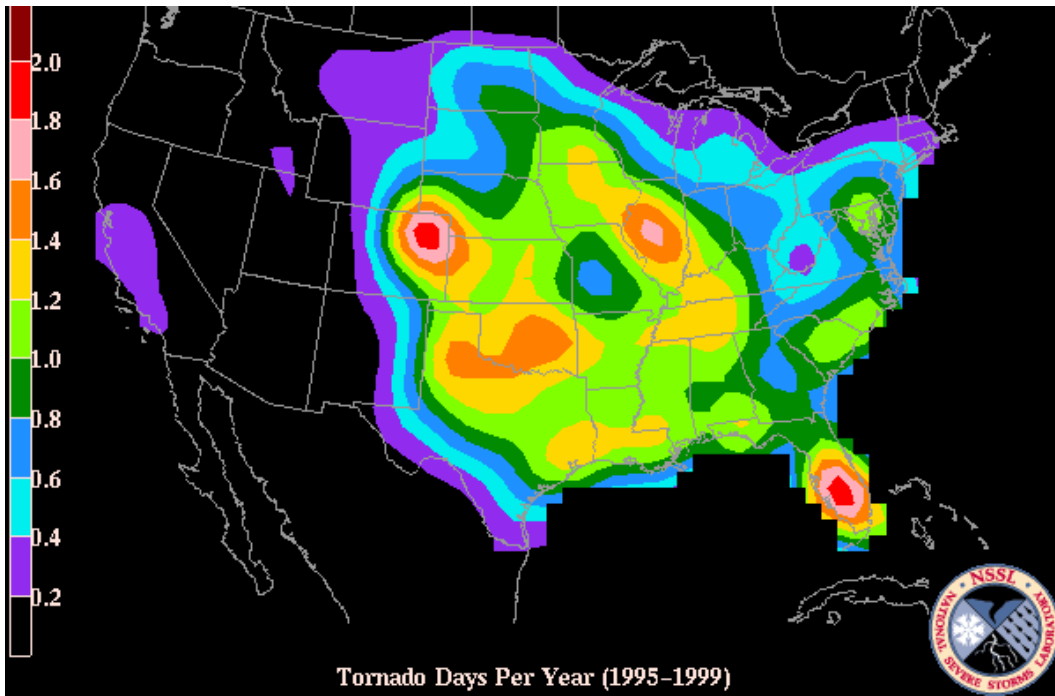


Figure 2-13: Tornado Days Per Year in the US (NOAA NSSL)

2.3.1.4 Thunderstorm/Lightning & Occurrences of the Hazard

Since 1995 there has been an average of 70 lightning strikes per year, 1.5 tornadoes, 41.5 incidents of hail, and 84 cases of extreme wind reported (>50 knots or 57 mph). The greatest number of each occurred in 2005, 1997, 2008, and 2008 respectively. The reports of this data are for the entire state of Massachusetts. Lowell will see severe storms which sometimes include hail, and frequent lightning. Winds are most consistent with thunderstorms in Massachusetts, and are usually sustained around 40 to 60 mph with higher gusts.

The National Climatic Data Center (NCDC) tracks storm events Table 2-5 provides information for the City of Lowell regarding lightning occurrences.

Table 2-5: Lightning Event Data for City of Lowell (Jan. 1, 2000 – Feb. 28, 2013)

| Location | Date | Death | Injury | Property Damage |
|----------|-----------|-------|--------|-----------------|
| Lowell | 6/29/2008 | 0 | 0 | 0.50K |
| Lowell | 5/24/2004 | 0 | 0 | 15.00K |
| Lowell | 6/27/2002 | 0 | 0 | 25.00K |
| Totals: | | | | 40.50K |

Specific details from the more significant lightning events noted in Table 5 that have occurred in the City of Lowell and other areas of Middlesex County include:

- **June 29, 2008** – Lightning struck a home on Marlborough Street in Lowell, resulting in a power surge that blew out several light switches.
- **May 24, 2004** – Severe thunderstorms formed in southeast Massachusetts, causing minor damage to homes in Lowell.
- **June 27, 2002** – Severe thunderstorms moved through parts of central and northeast Massachusetts. Several lightning strikes were reported from Lowell to Billerica, causing scattered power outages.

The probability of a future lightning and thunderstorm occurrence in Massachusetts and the City of Lowell is highly likely. Future lightning events will continue, but do not produce any abnormal events or require a response at UMLRR.

2.3.1.5 Severe Winter Weather & Occurrences of the Hazard

Between 1986 and 2012 the average snowfall was about 50 inches. The maximum seasonal snowfall occurred in 2005 when 102 inches of snow fell. In 2012 there was only a total of 11.4 inches of snow. During this same time frame, average snowfall was 16.2 inches. The maximum snow accumulation was 31 inches and occurred in 2000 and 2014. Table 2-6 lists winter storms for Middlesex County where the UMLRR is located.

Table 2-6: Winter Storm/Blizzard Data Middlesex County (Jan. 1, 2000 – Feb. 28, 2013)

| Location (County Zone) | Date | Type` | Death | Injury | Property Damage |
|----------------------------|------------|--------------|-------|--------|-----------------|
| Southeast Middlesex | 2/8/2013 | Blizzard | 0 | 0 | 0.00K |
| Western Middlesex | 2/8/2013 | Blizzard | 0 | 0 | 0.00K |
| Southeast Middlesex | 3/1/2012 | Winter Storm | 0 | 0 | 0.00K |
| Southeast Middlesex | 2/29/2012 | Winter Storm | 0 | 0 | 0.00K |
| Northwest Middlesex | 2/1/2011 | Winter Storm | 0 | 0 | 0.00K |
| Southeast Middlesex | 2/1/2011 | Winter Storm | 0 | 0 | 183.50K |
| Western Middlesex | 2/1/2011 | Winter Storm | 0 | 0 | 926.00K |
| Northwest Middlesex County | 1/21/2011 | Winter Storm | 0 | 0 | 0.00K |
| Southeast Middlesex | 1/21/2011 | Winter Storm | 0 | 0 | 0.00K |
| Western Middlesex | 1/21/2011 | Winter Storm | 0 | 0 | 0.00K |
| Northwest Middlesex County | 1/18/2011 | Winter Storm | 0 | 0 | 0.00K |
| Western Middlesex | 1/18/2011 | Winter Storm | 0 | 0 | 0.00K |
| Southeast Middlesex | 1/12/2011 | Winter Storm | 0 | 0 | 50.00K |
| Northwest Middlesex County | 12/26/2010 | Winter Storm | 0 | 0 | 0.00K |
| Southeast Middlesex | 12/26/2010 | Winter Storm | 0 | 0 | 0.00K |
| Western Middlesex | 12/26/2010 | Winter Storm | 0 | 0 | 0.00K |
| Western Middlesex | 1/28/2009 | Winter Storm | 0 | 0 | 0.00K |
| Southeast Middlesex | 3/16/2007 | Winter Storm | 0 | 0 | 0.00K |
| Western Middlesex | 3/16/2007 | Winter Storm | 0 | 0 | 0.00K |
| Northwest Middlesex County | 2/14/2007 | Winter Storm | 0 | 0 | 0.00K |
| Southeast Middlesex | 2/14/2007 | Winter Storm | 0 | 0 | 0.00K |
| Western Middlesex | 2/14/2007 | Winter Storm | 0 | 0 | 0.00K |
| Southeast Middlesex | 2/12/2006 | Winter Storm | 0 | 0 | 10.00K |
| Western Middlesex | 2/12/2006 | Winter Storm | 0 | 0 | 10.00K |
| Western Middlesex | 3/12/2005 | Winter Storm | 0 | 0 | 0.00K |
| Western Middlesex | 3/8/2005 | Winter Storm | 0 | 0 | 0.00K |
| Southeast Middlesex | 3/1/2005 | Winter Storm | 0 | 0 | 0.00K |
| Western Middlesex | 3/1/2005 | Winter Storm | 0 | 0 | 0.00K |
| Southeast Middlesex | 1/22/2005 | Winter Storm | 0 | 0 | 0.00K |
| Western Middlesex | 1/22/2005 | Winter Storm | 0 | 0 | 0.00K |
| Western Middlesex | 1/8/2005 | Winter Storm | 0 | 0 | 50.00K |
| Southeast Middlesex | 1/5/2005 | Winter Storm | 0 | 0 | 0.00K |
| Western Middlesex | 1/5/2005 | Winter Storm | 0 | 0 | 0.00K |
| Southeast Middlesex | 12/26/2004 | Winter Storm | 0 | 0 | 0.00K |

| | | | | | |
|---------------------|------------|--------------|---|---|---------|
| Western Middlesex | 12/26/2004 | Winter Storm | 0 | 0 | 0.00K |
| Western Middlesex | 12/14/2003 | Winter Storm | 0 | 0 | 0.00K |
| Southeast Middlesex | 12/5/2003 | Winter Storm | 0 | 0 | 0.00K |
| Western Middlesex | 12/5/2003 | Winter Storm | 0 | 0 | 0.00K |
| Southeast Middlesex | 2/17/2003 | Winter Storm | 0 | 0 | 0.00K |
| Western Middlesex | 2/17/2003 | Winter Storm | 0 | 0 | 0.00K |
| Southeast Middlesex | 2/7/2003 | Winter Storm | 0 | 0 | 0.00K |
| Western Middlesex | 2/7/2003 | Winter Storm | 0 | 0 | 0.00K |
| Southeast Middlesex | 1/3/2003 | Winter Storm | 0 | 0 | 0.00K |
| Western Middlesex | 1/3/2003 | Winter Storm | 0 | 0 | 0.00K |
| Southeast Middlesex | 12/25/2002 | Winter Storm | 0 | 0 | 15.00K |
| Western Middlesex | 12/25/2002 | Winter Storm | 0 | 0 | 15.00K |
| Totals: | | | | | 1.2595M |

Specific details from the more significant events for Middlesex County noted in **Table 3-32** include:

- **February 8, 2013** – A historic winter storm deposited large amounts of snow all over southern New England during February 8-9, 2013. Most locations received 2 to 2.5 feet of snow. The blizzard produced a prolonged period of strong winds.
- **February 1, 2011** – A total of 9 to 14 inches of snow fell across sections of Middlesex County on February 1 and 2. Damage included 34 roof collapses due to 81 inches of snow accumulation between December 26, 2010 and February 2, 2011.
- **January 12, 2011** – 12 to 24 inches of snow fell across southeast Middlesex County. Strong winds resulted in numerous downed trees and wires.
- **January 8, 2005** – A mix of snow, sleet, and freezing rain occurred in southern New England. The Merrimack Valley, inclusive of Lowell, was especially hit hard where a combination of 4 to 7 inches of snow and one quarter inch of icing brought down trees and power lines with scattered power outages.

At the UMLRR there have been several winter storm impacts related to the campus. In 2012, a winter storm cut out power to the campus for two days. There are some general concerns regarding navigating around campus during the winter, which include high snow banks at intersections and increased weight of snow on roofs, among others.

2.3.2 Meteorology

The prevailing wind for the area is westerly, with northeast winds being noticeable. The wind speed and direction was taken at Hanscom Air Force Base in Bedford, MA and the data is shown in Figure 9 for the year 2013. Calm winds occur less than 1% of the time, while wind speeds greater than 10 mph occur about 15% of the time. The most frequent wind speeds are between 5 and 10 mph and occur over 50% of the time.

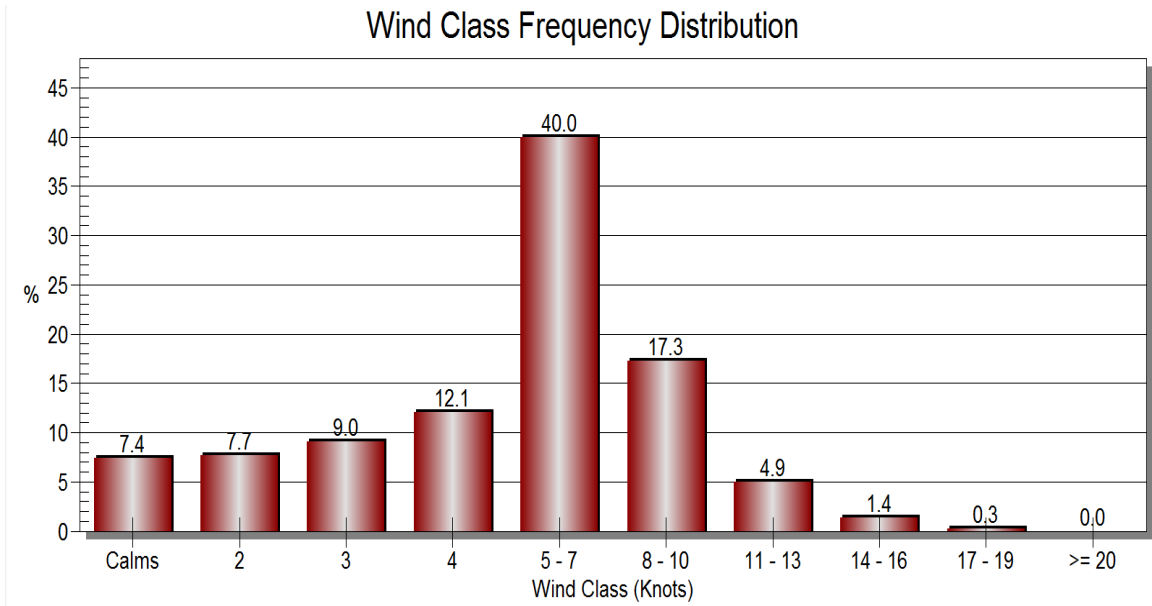
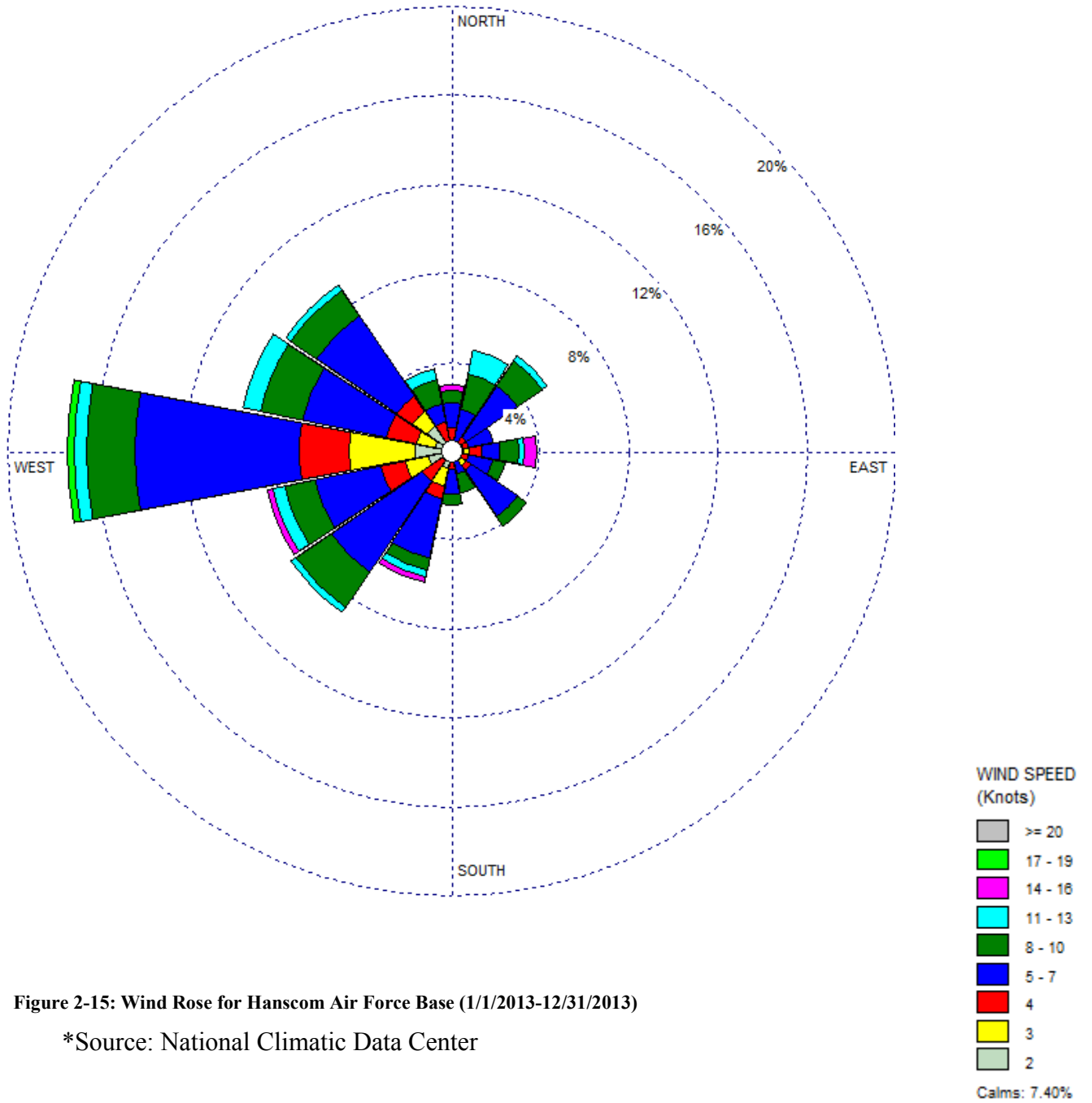


Figure 2-14: Wind Speed/Direction for Hanscom AFB (1/1/2013-12/31/2013)

Table 2-7: Wind Speed Frequency (Knots)

| Wind Direction (knots) | 2 | 3 | 4 | 5-7 | 8-10 | 11-13 | 14-16 | 17- 19 | >20 | Total (%) |
|------------------------|---------|---------|----------|----------|----------|---------|---------|---------|---------|-----------|
| 348.75-11.25 | 0.27397 | 0.27397 | 0.54795 | 1.09589 | 0.54795 | 0.00000 | 0.27397 | 0.00000 | 0.00000 | 3.01370 |
| 11.25-33.75 | 0.00000 | 0.00000 | 0.27397 | 1.64384 | 1.64384 | 1.09589 | 0.00000 | 0.00000 | 0.00000 | 4.65753 |
| 33.75-56.25 | 0.00000 | 0.27397 | 0.54795 | 2.73973 | 1.36986 | 0.27397 | 0.00000 | 0.00000 | 0.00000 | 5.20548 |
| 56.25-78.75 | 0.00000 | 0.54795 | 0.27397 | 1.09589 | 0.00000 | 0.00000 | 0.00000 | 0.00000 | 0.00000 | 1.91781 |
| 78.75-101.25 | 0.54795 | 0.27397 | 0.54795 | 0.82192 | 0.82192 | 0.27397 | 0.54795 | 0.00000 | 0.00000 | 3.83562 |
| 101.25-123.75 | 0.27397 | 0.00000 | 0.54795 | 1.09589 | 0.54795 | 0.00000 | 0.00000 | 0.00000 | 0.00000 | 2.46575 |
| 123.75-146.25 | 0.54795 | 0.27397 | 0.27397 | 2.46575 | 0.54795 | 0.00000 | 0.00000 | 0.00000 | 0.00000 | 4.10959 |
| 146.25-168.75 | 0.00000 | 0.00000 | 0.27397 | 0.82192 | 0.82192 | 0.00000 | 0.00000 | 0.00000 | 0.00000 | 1.91781 |
| 168.75-191.25 | 0.00000 | 0.27397 | 0.54795 | 1.09589 | 0.54795 | 0.00000 | 0.00000 | 0.00000 | 0.00000 | 2.46575 |
| 191.25-213.75 | 0.82192 | 0.82192 | 0.54795 | 2.73973 | 0.54795 | 0.27397 | 0.27397 | 0.00000 | 0.00000 | 6.02740 |
| 213.75-236.25 | 0.00000 | 0.54795 | 1.09589 | 4.93151 | 1.91781 | 0.27397 | 0.00000 | 0.00000 | 0.00000 | 8.76712 |
| 236.25-258.75 | 1.09589 | 1.09589 | 1.09589 | 3.01370 | 1.36986 | 0.54795 | 0.27397 | 0.00000 | 0.00000 | 8.49315 |
| 258.75-281.25 | 1.64384 | 3.01370 | 2.19178 | 7.39726 | 2.19178 | 0.54795 | 0.00000 | 0.27397 | 0.00000 | 17.26030 |
| 281.25-303.75 | 0.82192 | 0.82192 | 1.36986 | 3.83562 | 1.91781 | 0.82192 | 0.00000 | 0.00000 | 0.00000 | 9.58904 |
| 303.75-326.25 | 1.36986 | 0.82192 | 0.82192 | 4.38356 | 1.36986 | 0.27397 | 0.00000 | 0.00000 | 0.00000 | 9.04110 |
| 326.25-348.75 | 0.27397 | 0.00000 | 1.09589 | 0.82192 | 1.09589 | 0.54795 | 0.00000 | 0.00000 | 0.00000 | 3.83562 |
| Sub-Total | 7.67123 | 9.04110 | 12.05480 | 40.00000 | 17.26030 | 4.93151 | 1.36986 | 0.27397 | 0.00000 | 92.60270 |
| Calms | | | | | | | | | | 7.39726 |
| Total | | | | | | | | | | 100.00000 |



2.4 Hydrology

Drainage in the reactor site in the Pawtucket Falls area is directly toward the Merrimack River. Average and minimum flow rates of the river measured at the Lowell Gauging Station between 1925 and 1976 were 6,540 cfs and 181 cfs, respectively. During the record flood of 1936, the flow rate was 157,430 cfs.

Flooding from rainfall or melting snow is not an issue in the reactor site area because of the drainage provided by the river and the height above the river which the facility occupies. Minor flooding of local roads that parallel the river is a chronic problem when the river is above flood stage, but this does not affect the UMLRR site. Vehicles that would respond to an emergency at the UMLRRR do not use this road.

The U.S. Army Engineer Division, New England, of the Corps of Engineersⁱⁱ has tabulated flood data for 1936 and 1938 for locations near the University. The data is reproduced below in Table 2-8 along with relevant reactor building elevations.

Table 2-8: US Army Engineering Corp. Historic Flood Levels

| Location | Elevation in feet above mean sea level | |
|--|--|--------------|
| Upstream from Moody Street Bridge | 89.6 | (1936 Flood) |
| | 84.2 | (1938 Flood) |
| Downstream from Moody Street Bridge (about 200 ft. downstream of section opposite the reactor) | 82.5 | (1936 Flood) |
| | 76.5 | (1938 Flood) |
| Reactor Building | █ | (Ground) |
| | 98 | (Basement) |

After the floods of the 1930s, the Corps of Engineers completed four flood control reservoirs in New Hampshire to reduce the flood potential of the Merrimack River. The effect of the controls is estimated to be equivalent to a reduction of the 1936 flood level by 6.5 feet and the 1938 level by █ feet in the reactor site region.

The corps developed a Standard Project Flood which is a synthetic flood reflecting the storm and runoff potential of a river basin. For Lowell, this synthetic flood would cause stages about 3 feet below the 1936 flood levels. Since the █ of the █ building is some █ feet above the potential flood level, there is no flood risk involved in the site.

Since 1954 there have been 14 Presidential Disaster Declarations made for the State of Massachusetts, eight of which directly impacted the Middlesex County. The tabulated data taken from the Multi-Campus Hazard Mitigation Plan created in 2013 can be seen in Table 2-9.

Table 2-9: Massachusetts Flooding Major Disaster Declarations (1954 – Present)

| | Disaster No. | Incident Period | Date Disaster Declared | Middlesex County a Designated Area? |
|--|---------------------|-------------------------|-------------------------------|--|
| Severe Winter Storm, Snowstorm, Flooding | DR-4110 | 2/8/2013 – 2/9/2013 | 4/19/2013 | Yes |
| Severe Storm and Flooding | DR-1895 | 3/12/2010 – 4/26/2010 | 3/29/2010 | Yes |
| Severe Winter Storm and Flooding | DR-1813 | 12/11/2008 – 12/18/2008 | 1/5/2009 | Yes |
| Severe Storms, Inland and Coastal Flooding | DR-1701 | 4/15/2007 – 4/25/2007 | 5/16/2007 | No |
| Severe Storms and Flooding | DR-1642 | 5/12/2006 – 5/23/2006 | 5/25/2006 | Yes |
| Severe Storms and Flooding | DR-1614 | 10/7/2005 – 10/16/2005 | 11/10/2005 | Yes |
| Flooding | DR-1512 | 4/1/2004 – 4/30/2004 | 4/24/2004 | Yes |
| Severe Storms and Flooding | DR-1364 | 3/5/2001 – 4/16/2001 | 4/10/2001 | Yes |
| Heavy Rain and Flooding | DR-1224 | 6/13/1998-7/6/1998 | 6/23/1998 | Yes |
| Severe Storms and Flooding | DR-1142 | 10/20/1996-10/25/1996 | 10/25/1996 | Yes |
| Severe Storms and Flooding | DR-790 | 3/30/1987-4/13/1987 | 4/18/1987 | Yes |
| Coastal Storms, Flood, | DR-546 | 2/6/1978-2/8/1978 | 2/10/1978 | No |
| Severe Storms, Flooding | DR-325 | 3/6/1972 | 3/6/1972 | No |
| Hurricane, Floods | DR-43 | 8/20/1955 | 8/20/1955 | Unknown |

The State of Massachusetts Hazard Mitigation plan notes that flooding is the most common hazard to affect New England. It is certain that flood events will continue to impact the City of Lowell and the UMass Lowell campus. Figure 2-16 below shows the risk potential on UMass Lowell’s North Campus, denoting the [REDACTED] Building is well outside the flood area.



Figure 2-16: Flood Vulnerability Assessment – North Campus (Mitigation Plan)

2.4.1 UMLRR Impact on Groundwater

UMLRR operations, normal or abnormal, do not possess any significant potential impact on groundwater. This fact arises from the documented history of the relatively small amount of tritium production in the reactor pool water. If the reactor pool were to have a significant leak, it would be confined to the Reactor Containment. Should the water be released to the ground or sewer system in an uncontrolled manner, the concentrations are not of radiological concern. The

tritium concentration in the pool has been measured to be [REDACTED] [REDACTED] [REDACTED]. 10 CFR 20 Appendix B Table 3 indicates that the concentration limit for the release of tritium to the sewer system is 1×10^{-2} pCi /ml. Consequently, the concentration in the reactor pool is one order of magnitude less than the release limit. This indicates that there is no significant potential facility impact on the groundwater.

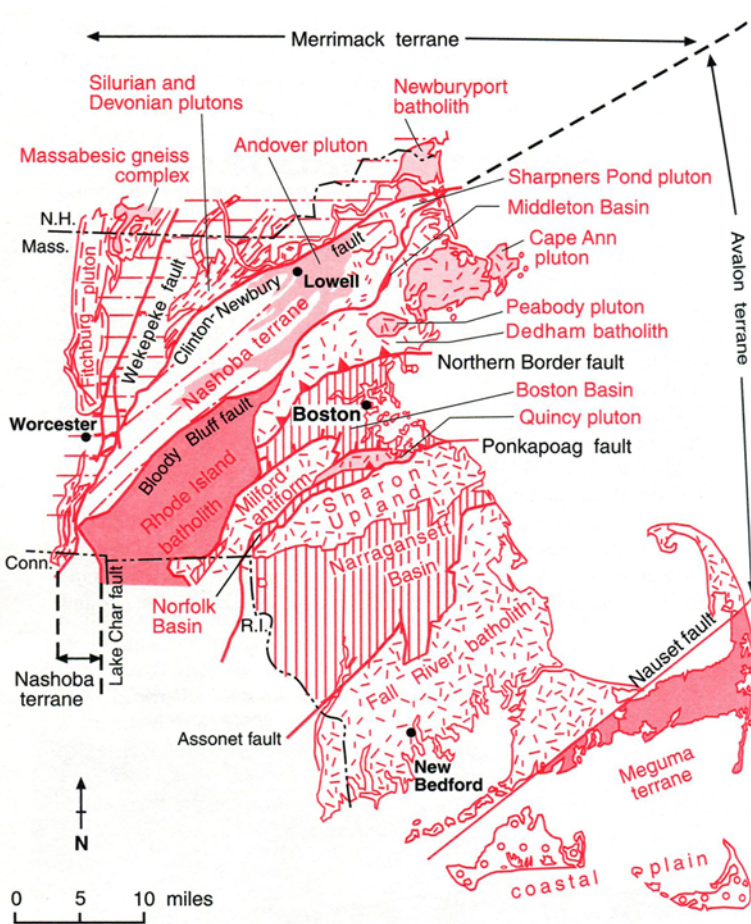
2.5 Geology, Seismology, and Geotechnical Engineering

2.5.1 Regional Geology

Geologically Massachusetts and adjoining states consist of accreted terranes that were added during the construction of Pangea (in the Paleozoic) to the cratonic core (of Precambrian age) of North America. Central and Eastern Massachusetts consists of four accreted terranes, Merrimack, Nashoba, Avalon, and Meguma, which are separated from each other by SW-NE trending faults. These terranes extend into New Hampshire and eastern Connecticut and form the geologic framework for eastern New England. The western part of Massachusetts and neighboring states encompass the geologically older (Precambrian to early Paleozoic) Laurentian terranes.

The various terranes that comprise eastern Massachusetts (Figure 2-17) were formed at different times in response to plate tectonic processes. Avalon is the oldest terrane and radiometric ages vary from 610 Ma to 595 Ma. The other three terranes are younger with radiometric ages between 500 Ma and 400 Ma. These four terranes were welded to Laurentia during the Acadian mountain building event (~370 Ma). The terranes are largely composed of granitic and gabbroic intrusions and metamorphosed sediments and metamorphosed volcanics ranging in metamorphic grade from phyllite to gneiss.

The UMLRR lies in the Merrimack terrane just to the northwest of the Clinton-Newbury fault which separates the Nashoba terrane from the Merrimack terrane. The fault is interpreted as marking a subduction zone (Skehan, 2001). The fault zone is west-dipping and characterized by abundant mylonite and ductile faults. The fault zone had an extended history from 450 Ma to 370 Ma, but is no longer active.



Geology of eastern Massachusetts. —Modified from Zen and others, 1983

Figure 2-17: Tectonic terranes, lithologic units, and fault zones of eastern Massachusetts. From Skehan (2001).

The Merrimack quartzite, which underlies the UMLRR reactor, is part of the Berwick formation of the Merrimack terrane. The Berwick formation is of Silurian age (443.8 Ma – 419.2 Ma) and consists of thin- to-thick bedded calcareous phyllites and schists. Structural studies of the Berwick formation in southern New Hampshire, based on the occurrence of basaltic dikes, outline a SW-NE trending fracture zone (Figure 2-18). The dikes were emplaced at ~120 Ma in response to the initial rifting of Gondwana which led to the formation of the Atlantic Ocean. These dikes represent the most recent occurrence of active faulting at the surface of New England.

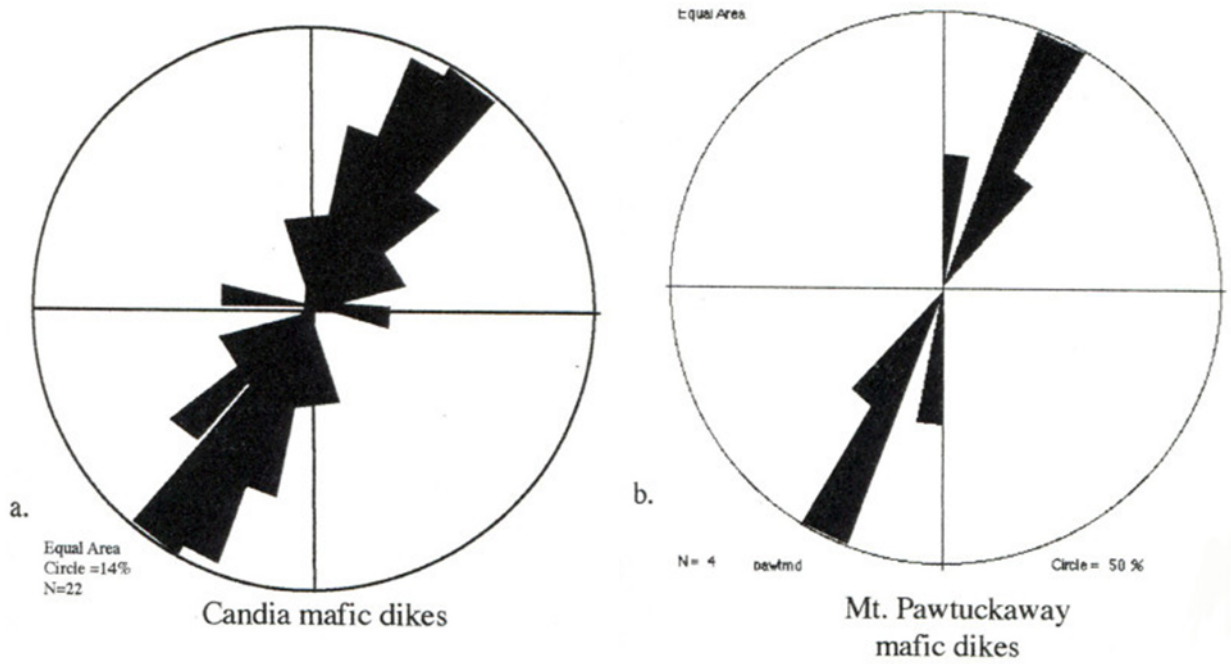


Figure 2-18: Rose diagram showing the orientation of mafic dikes in the Candia and Pawtuckaway quadrangles, New Hampshire (Kerwin, 2007).

2.5.2 Site Geology

The North Campus of the University of Massachusetts Lowell and surrounding area is underlain by the Merrimack quartzite, a unit within the Berwick formation. The quartzite is exposed in the Pawtucket Falls section of the Merrimack River next to the site. The consultant [Haley & Aldrich] described the rock as thinly bedded quartzite ranging in color from gray through greenish gray to brown. The brown color was due to the occurrence of minute particles of red biotite. Thin layers of slaty quartzite and quartz schist were also observed in the unit. At this location the quartzite strikes NE-SW and dips 30° to 50° to the NW. Quartzite with similar strike and dip was observed behind the UML library and in the foundation excavation for Costello gym. Jointing, with a NW-SE strike and near vertical dip, was also noted in these outcrops.

Haley & Aldrich made five borings at the reactor site. Each [REDACTED] [REDACTED] for [REDACTED] feet into bedrock. The material recovered from the cores was the same as that seen in outcrop. With the exception of one core, jointing was absent and there was no observable weathering. Haley & Aldrich concluded that the quartzite was essentially sound, free from weathering, and had only

minor jointing. In their opinion the bedrock had an allowable bearing pressure in excess of 20 tons per square foot, which is about four or five times the maximum bearing pressure beneath the foundation mat for the reactor containment building. Differential settlement of the structure under these conditions will be insignificant. The rock is hard, chemically stable, and insoluble.

2.5.3 Seismicity

New England is located in the interior of a tectonic plate (the North American plate) whose eastern boundary is the Mid-Atlantic Ridge and western boundary is the San Andreas fault system of California. Earthquakes in New England are believed to be due to far field stresses originating from the Mid-Atlantic Ridge spreading center. Earthquake focal mechanisms and borehole stress direction measurements indicate that these far field stresses lead to maximum stress directions in northeastern North America that are primarily NE-SW to E-W (Ebel and Bouck, 1988; Ebel, 2013). The focal mechanisms for the earthquakes due to this stress field indicate that the faults are generally thrust to oblique slip with a strong thrust component. The faults are apparently cross faults that are not associated with the predominately NE-SW fault systems seen at the surface. It is believed that the minor fault directions are preferred because of the orientation of the current plate tectonics stress field (Ebel, 2013). Focal mechanisms for earthquakes also reveal that earthquakes that occur in the accreted terranes of New England have shallow focal depths, frequently less than 4 km. Deeper focus earthquakes (>10 km) are extremely rare. To the west, in the stable craton, focal depths can reach 30 km (Ebel, 2013).

The epicenters for historical and recent earthquakes are shown on Figure 2-19. Both present day seismicity (1735 – 2014) and historical seismicity (1638 – 1974) show similar distributions of earthquakes. Earthquake clusters are found in the St. Lawrence lowlands, in southwestern Quebec and Ontario, and through central New Hampshire in the Ossipees. In the first two instances the earthquake activity is associated with ancient rift systems. All known earthquakes (historical and measured) with $M > 5.0$ are shown on Figure 2-20.

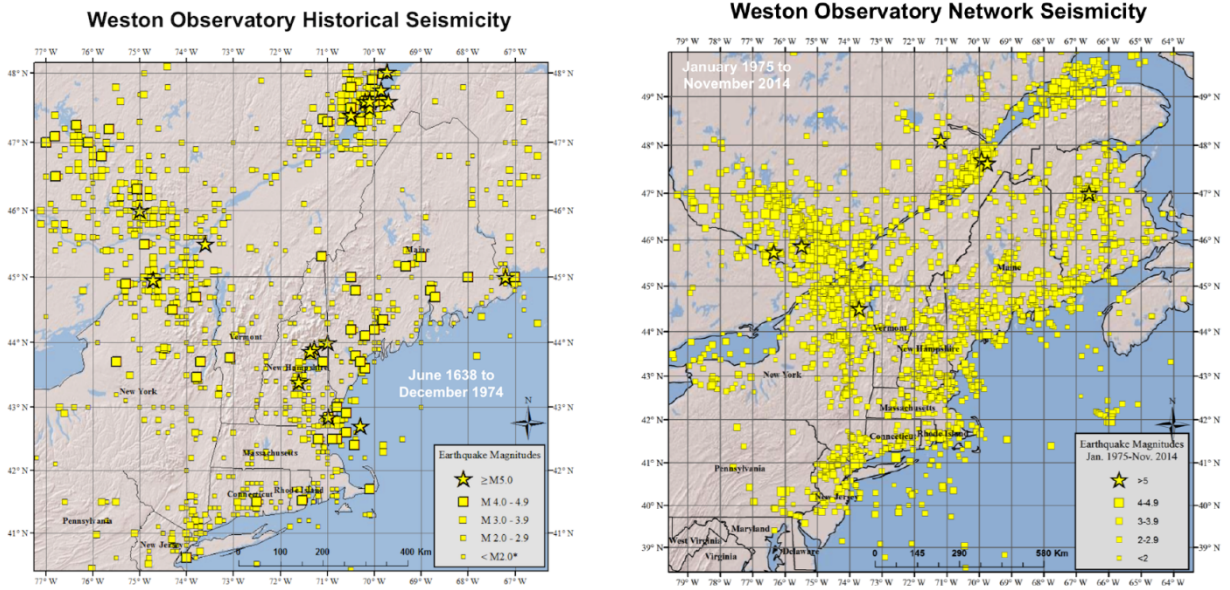


Figure 2-19: Historical and recent earthquakes in eastern North America. Maps are from the Weston Observatory web site.

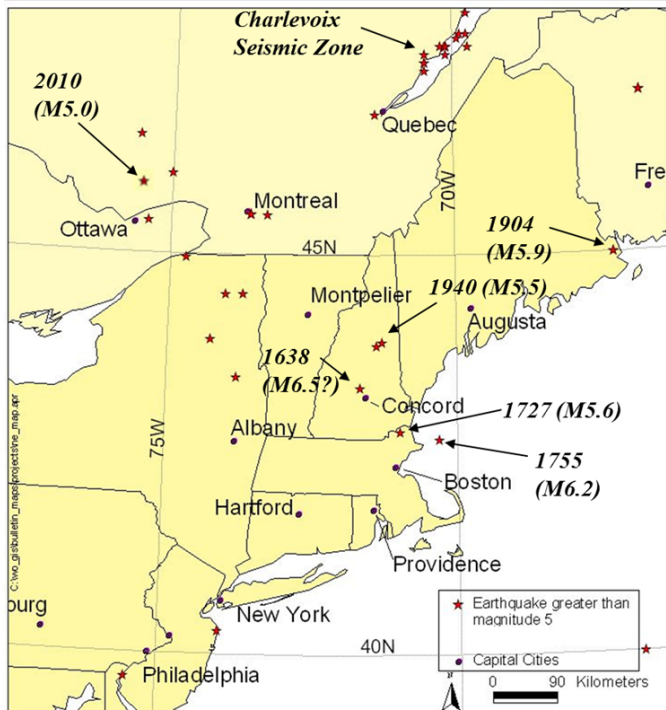


Figure 2-20: All historical and measure earthquakes with M > 5.0. From Ebel (2013).

The recurrence interval (Table 2-10) and seismic hazard (Table 2-11) for New England earthquakes has been estimated using the recent instrumental record (Ebel, 1984). These estimates are for the entire New England region. Earthquake distribution across the region is not uniform. Currently the most seismically active area in New England is near Concord, NH (Ebel, 2013).

Table 2-10: Recurrence Intervals for New England Earthquakes*

| | | | | | | | | | |
|-----|---|---|---|---|---|---|---|---|---|
| MMI | ■ | | ■ | | ■ | | ■ | | ■ |
| | ■ | ■ | ■ | ■ | ■ | ■ | ■ | ■ | ■ |
| | ■ | ■ | ■ | ■ | ■ | ■ | ■ | ■ | ■ |

*From Ebel (1984). MMI – Modified Mercalli Intensity. Mc – coda magnitude.

Table 2-11: New England Seismic Hazard*

| Mc | Time (yrs) | | | | | | | |
|-----|------------|------|------|------|------|------|------|------|
| | 1 | 7 | 10 | 50 | 100 | 200 | 500 | 1000 |
| 4.6 | 0.10 | 0.51 | 0.64 | 0.99 | 1.00 | 1.00 | 1.00 | 1.00 |
| 5.0 | 0.05 | 0.28 | 0.38 | 0.91 | 0.99 | 1.00 | 1.00 | 1.00 |
| 5.2 | 0.03 | .020 | 0.28 | 0.80 | 0.96 | 1.00 | 1.00 | 1.00 |
| 5.5 | 0.01 | 0.12 | 0.17 | 0.60 | 0.84 | 0.97 | 1.00 | 1.00 |
| 5.8 | 0.01 | 0.07 | 0.10 | 0.40 | 0.64 | 0.87 | 0.99 | 1.00 |
| 6.0 | 0.01 | 0.05 | 0.07 | 0.29 | 0.50 | 0.75 | 0.97 | 1.00 |
| 6.4 | 0.003 | 0.02 | 0.03 | 0.15 | 0.27 | 0.47 | 0.80 | 0.96 |
| 6.5 | 0.003 | 0.02 | 0.03 | 0.12 | 0.23 | 0.41 | 0.73 | 0.93 |
| 7.0 | 0.001 | 0.01 | 0.01 | 0.05 | 0.10 | 0.18 | 0.40 | 0.63 |

*Values represent probability of an earthquake of a particular magnitude in the specified time interval. From Ebel (1984).

2.5.4 Maximum Earthquake Potential

The areas closest to Lowell that currently show persistent earthquake activity are the Amesbury, MA, area northeast of Lowell and the Littleton, MA, area southwest of Lowell. The Amesbury, MA area has averaged a felt earthquake every 3.6 years. The Littleton, MA area has averaged a felt earthquake every 2.2 years. As of spring 2013 the last detected earthquake in the Amesbury areas was a M 0.9 event SE of Amesbury on 2/21/2013 and for the Littleton area the last earthquake was M 2.5 on 10/19/2007 (Ebel, 2013). No significant felt earthquakes have occurred in the Lowell area since the start of instrumental records.

With reference to the historical record of seismicity, the largest relevant event was the Newbury earthquake of 1727. This earthquake was felt as far as Philadelphia and Casco Bay, ME. The estimated magnitude for the earthquake is 5.6 (Ebel, 2000). The estimated MMI for the Lowell area was V (Figure 2-21). Other large earthquakes in the historical record (Figure 2-20) are the Cape Ann M 6.2 event of 1755 and the 1638 event NW of Concord, NH, with estimated M 6.5 (but note that there is a large degree of uncertainty in the estimate). The Concord area, as noted above, continues to have a relatively high frequency of seismic activity to the present day.

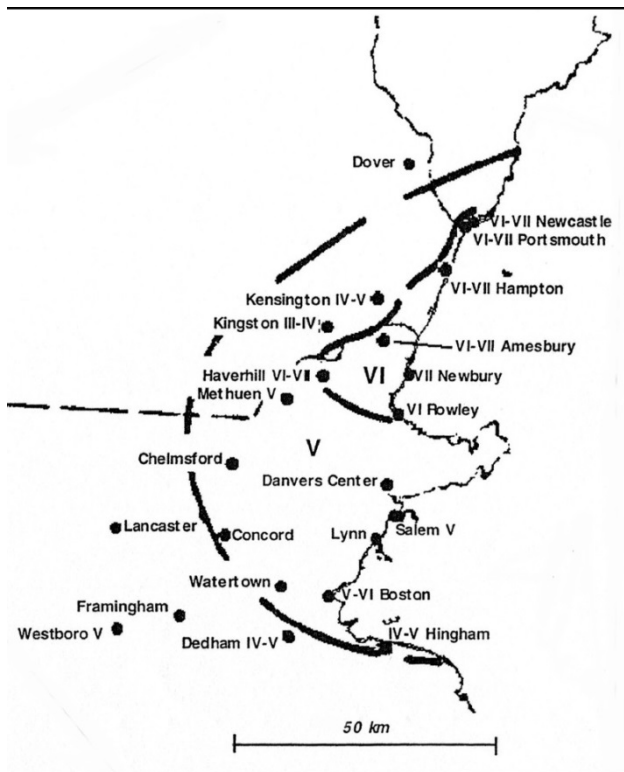


Figure 2-21: Modified Mercalli intensity map for the 1727 Newbury, MA, earthquake. Modified from Ebel (2000).

2.5.5 Vibratory Ground Motion

The Area Zoning Map of the Uniform Building Code³ shows the Lowell area included in Seismic Probability Zone 2, in which the Code recommends designing to withstand shocks equivalent to intensity ■■■ on the Modified Mercalli Scale. The center of intensity ■■■ corresponds to an acceleration of ■■■ g⁴, and the reactor building foundation, the pool, the reinforced concrete parts of the reactor building, and the steel containment have been designed to

withstand ■ g acceleration. From the discussion in ■ Maximum Earthquake Potential, this design criteria exceeds the expected felt intensity of earthquakes in the Lowell area.

2.5.6 Surface Faulting

There are no active faults at the surface as previously discussed.

2.5.7 Liquefaction Potential

Previous to human disturbance the site was covered with stratified glacial deposits. These are described on the surficial geologic map that encompasses Lowell as Gravel deposits composed mainly of gravel sized clasts; cobbles and boulders predominate; minor amounts of sand within gravel beds, and sand comprises few separate layers. Gravel layers generally are poorly sorted and bedding commonly is distorted and faulted due to post-depositional collapse related to melting of ice. Sand and gravel deposits are composed of mixtures of gravel and sand within individual layers and as alternating layers. Sand and gravel layers generally range from 25 to 50 percent gravel particles and from 50 to 75 percent sand particles. Layers are well to poorly sorted; bedding may be distorted and faulted due to post-depositional collapse. Sand deposits composed mainly of very coarse to fine sand, commonly in well-sorted layers. Coarser layers may contain up to 25 percent gravel particles, generally granules and pebbles; finer layers may contain some very fine sand, silt, and clay.” Observations made during an in progress excavation for a new building on the UMass Lowell North Campus indicate that the surficial deposits consist of approximately 40% boulders in mostly sand-sized material. This type of material is moderately resistant to liquefaction (Geotechnical Engineering Bureau, 2007). Therefore the material surrounding the UML reactor should not pose a significant liquefaction risk.

With respect to the UML reactor structure, all the overburden was removed during construction of the facility. The reactor is built on bedrock and thus there is no liquefaction potential directly related to the structure.

2.6 Bibliography (Geology Section)

Ebel, J., 1984. Statistical aspects of New England seismicity from 1975 to 1982 and implications for past and future earthquake activity. *Bulleting of the Seismological Society of America* 74, 1311-1329.

Ebel, J., 2000. A reanalysis of the 1727 earthquake at Newbury, Massachusetts. *Seismological Research Letters* 71, 364-374.

Ebel, J., 2013. Neotectonics and the accreted terranes of New England. *Geological Society of America Abstracts with Programs* 45, 1, p. 45.

Ebel, J. E., Bouck, B. R., 1988. New focal mechanisms for the New England region: constraints on the regional stress regime. *Seismological Research Letters* 59, 183-187.

Geotechnical Engineering Bureau, 2007. Geotechnical design procedure: liquefaction potential of cohesionless soils. GDP-9, State of New York Department of Transportation, 80p.

Kerwin, Charles M., 2007. Mapping, Petrological and Geochemical Explorations of the Massabesic Gneiss Complex in New Hampshire. Ph.D. Thesis, University of New Hampshire, Durham, NH, 151p.

Skehan, James W., 2001. *Roadside Geology of Massachusetts*. Mountain Press Publishing Company, Missoula, MT, 378p.

Stone, B.D., Stone, J.R., compilers, 2007. Surficial Geologic Map of the Ashby-Lowell-Sterling-Billerica 11-Quadrangle Area in Northeast-Central Massachusetts: U.S. Geological Survey Open-File Report 2006-1260-C.

ⁱ Adapting to Climate Change: A Planning Guide for State Coastal Managers. NOAA Office of Ocean and Coastal Resource Management. <http://coastalmanagement.noaa.gov/climate/adaptation.html>

ⁱⁱ University of Massachusetts | 225646.00 October 2013 DRAFT UMass Lowell Campus Annex Plan

Table of Contents

3.0 Design of Structures, Systems and Components 3-3

3.1 Design Criteria 3-3

3.1.1 Environmental and Dynamic Effects Design Bases..... 3-3

3.1.2 Prevention of Release of Radioactive Material..... 3-4

3.1.3 Provisions to Avoid or Mitigate Consequences of Fire or Explosion..... 3-5

3.1.4 Inspection, Testing and Maintenance..... 3-6

3.1.5 Quality Standards and Records 3-6

3.2 Meteorological Damage 3-6

3.2.1 Wind Loading..... 3-7

3.2.2 Snow and Ice Loads 3-8

3.3 Water Damage..... 3-8

3.4 Seismic Damage..... 3-8

3.5 Systems and Components 3-9

3.5.1 Containment System 3-9

3.5.2 Instrumentation and Control..... 3-15

3.5.3 Reactor Protection System (RPS) Function 3-16

3.5.4 Reactor Design 3-17

3.5.5 Fuel System..... 3-17

3.5.6 Electric Power Systems..... 3-18

3.5.7 Fluid Systems 3-18

3.5.8 Anti-Siphon System 3-19

3.5.9 Fuel Storage and Radioactivity Control 3-20

Table of Figures

Figure 3-1: Plan View of [REDACTED] Building..... 3-12

Figure 3-2: Elevation View of the UML Research Reactor and [REDACTED] Building..... 3-13

Figure 3-3: Longitudinal Section through Building to River..... 3-14

3.0 Design of Structures, Systems and Components

This chapter identifies and describes the principal architectural and engineering design

[REDACTED]

[REDACTED] The material presented emphasizes the safety and protective functions and related design features that help provide defense-in-depth against the uncontrolled release of radioactive material to the environment. The bases for the design criteria for some of the systems discussed in this chapter are developed in other chapters and are appropriately cross-referenced, where required.

3.1 Design Criteria

Design criteria for various components and systems of the UMLRR are summarized here. Complete descriptions of these components and systems are deferred to the cognizant chapter of this report. The UMLRR is designed and licensed for operation at a maximum steady-state power level of 1 MW. The fission-product inventory produced is substantially less than that of conventional nuclear power plants. In addition, a conservative upper limit of the energy released for an entire year of operation would be about [REDACTED] MW-Days. This comparison illustrates why the UMLRR should be placed in a much lower risk category than conventional nuclear power plants.

The UMLRR does not have [REDACTED] that are important to safety in the same context as nuclear power plants. For the UMLRR, a loss of coolant event, failure of the Reactor Protection System (RPS), or any other credible accident does not have the potential for causing off-site exposure comparable to those listed in the guideline for accident exposures of ANSI 15.7.

The UMLRR does not have [REDACTED] requiring a Category 1 classification. However, certain [REDACTED] have been designed to withstand potential site-specific natural phenomena. These design considerations are discussed in the following subsections.

3.1.1 Environmental and Dynamic Effects Design Bases

The design of the UMLRR accommodates the effects of, and is compatible with, the environmental conditions associated with normal operation, maintenance, testing, and postulated

accidents. The design and construction of the facility preclude the [REDACTED] of the [REDACTED]. There is no postulated accident which could occur in the reactor containment building which would generate a positive pressure differential sufficient enough to compromise [REDACTED]

Operating procedures control the use and exclusion of [REDACTED] materials in any [REDACTED] facility or in the reactor containment building. The amount of [REDACTED] materials irradiated or allowed in any experiment are limited to reduce the likelihood of damage to the reactor or pool should they [REDACTED]. The reactor core is protected from [REDACTED] by being located within the reactor containment which is surrounded by and anchored to a reinforced concrete biological shield. [REDACTED] effects of conditions such as whipping pipes, are not a concern because there are no [REDACTED] within the facility. The primary and pool coolant systems operate at atmospheric pressures with all piping and components suitably supported and anchored. The primary coolant does not [REDACTED]. The supply and return lines for the secondary coolant systems [REDACTED]

[REDACTED]. The probability of an event or condition resulting from the [REDACTED], is, therefore, very small.

3.1.2 Prevention of Release of Radioactive Material

Operation of the UMLRR results in the production of fission products in the fuel itself and activation of both core components and irradiated samples. There are multiple barriers to the release of these radioactive materials. They include the following:

- a. Fission Products from the Core: The fuel matrix and the fuel cladding.
- b. Activation Byproducts: The confines of the location where it is produced (e.g., the core tank, the sample irradiation facility or the hot cell chemistry area) and the containment building.

3.1.2.1 Fuel and Cladding

Specifications for the UMLRR fuel were developed and are maintained by the Idaho National Engineering and Environmental Laboratory (INEEL) for the U.S. Department of Energy. This specification in turn incorporates the applicable portions of relevant ASTM

International (Technical Society Standards), ANSI (American National Standards Institute), ISO (International Standards Organization), MIL-STD (Military Standards), and AWS (American Welding Society) standards as well as drawings prepared by INEEL for the manufacture of individual plates. The specifications include the plate loading, void volume, fuel homogeneity, fuel particle location relative to the core of the plate, radiography procedures, cladding and fuel core thickness, evaluation methods, surface finish, dimensions, and surface alpha contamination. The specifications also cover materials of construction, element assembly from the individual plates, test and inspection requirements, packaging and shipping processes, and acceptance inspections.

3.1.2.2 Primary Coolant System and Reactor Pool

The UMLRR reactor is located in an open pool containing approximately [REDACTED] gallons of high purity water, with a maximum depth of [REDACTED] feet. The design pressures and ratings for the components that comprise the primary coolant system and core tank are adequate for all foreseen operations at the licensed 1 MW power level. The primary coolant does not leave the containment structure under normal operating conditions.

3.1.3 Provisions to Avoid or Mitigate Consequences of Fire or Explosion

The UMLRR containment building and most of the structures therein are built of steel and concrete and/or aluminum and are highly fire resistant. In addition, the following features reduce both the likelihood and consequences of a fire:

- a. The reactor is fail-safe and would shut down if fire should damage the reactor protection system.
- b. Appropriate fire extinguishers are strategically located throughout the facility.
- c. [REDACTED]
- d. The large volume of water in the core tank would protect the core from a fire.
- e. Closed-circuit television can be used to survey the experimental areas from the control room. Also, the control room itself can be monitored by [REDACTED]
[REDACTED].

The UMLRR fire protection program has passive, active, and preventive elements with the objective of ensuring that safety-related systems can perform their required functions. The program conforms to the intent of ANSI/ANS-15.17-1987.

3.1.4 Inspection, Testing and Maintenance

UMLRR structures, systems, and components whose integrity is important to the prevention of radioactive material release, the prevention of core damage and to reactivity control are designed to facilitate inspections, testing, and maintenance. Some examples include:

- a. Acceptance inspections of fuel elements.
- b. Visual inspections of all in-core components for material condition.
- c. Tests of all interlocks associated with the discharge of radioactive effluent.
- d. Verification of safety control blade drop times.
- e. Channel checks and calibrations of the nuclear and process safety systems.

Written procedures have been prepared and reviewed for the conduct of all system inspections and tests. Approved written procedures are also implemented following the maintenance of major equipment such as control devices.

3.1.5 Quality Standards and Records

Structures, systems, and components important to safety were designed, fabricated, constructed, and tested to the original design specifications and associated codes and standards. All design and construction work was monitored by the contractors to assure that the specifications incorporated appropriate standards and that the design and construction was in accordance with these specifications. Modifications to the facility have been made in accordance with existing standards and requirements.

3.2 Meteorological Damage

Tornadoes are relatively rare in Massachusetts. Based on the small probability of occurrence, postulated low intensity, the intermittent type of reactor operation and low fission-product inventory, no criteria for tornadoes have been established for the UMLRR containment. The UMLRR reactor core is protected from damage by high winds or tornadoes by its containment dome, and the location in the thick reinforced concrete structure surrounding the reactor tank. The containment structure of the UMLRR was designed for area wind loads

including those associated with the infrequent hurricanes reaching into Middlesex County, MA. Facility design also accounts for snowstorms and severe cold weather, which has not presented significant problems in the past.

3.2.1 Wind Loading

The greatest one-minute sustained wind speed ever recorded in the Boston area was 86 km per hour (54 miles per hour) and the greatest gust was 130 km per hour (81 miles per hour). If the axial profiles associated with these winds are assumed to be constant from the ground to an elevation of [REDACTED] ([REDACTED]) and if a flat surface is also assumed, then the associated dynamic pressures are [REDACTED] pounds per square foot and [REDACTED] pounds per square foot, respectively. These values are in line with the UMLRR wind load design of [REDACTED] per square foot. These values are computed using the ASCE/SEI 7-12 design code:

$$P = [REDACTED] K_z K_{zt} K_d V^2 I \text{ (lb/ft}^2\text{)}$$

Where K_z is the velocity pressure exposure factor, K_{zt} is the topographic factor, K_d is the wind directionality factor, V is the basic wind speed/velocity, and I is the importance factor.

With: $K_z = 0.93$ (most critical)

$$K_{zt} = (1 + 0.43 * 0.50 * 0.5)^2 = 1.226 \text{ (--> This part is about the topographic effect accounting for the location of the structure w.r.t. on a hill.)}$$

$$K_d = [REDACTED] \text{ for round structures}$$

$$I = [REDACTED]$$

$$\text{Load Correction factor } [REDACTED]$$

$$V = [REDACTED]$$

$$\text{--> } P = [REDACTED] \text{ lb/ft}^2$$

If use gust speed,

$$\text{--> } P = [REDACTED] \text{ lb/ft}^2$$

These numbers are calculated based on ASCE Minimum Design loads for Buildings and Other Structures (ASCE/SEI 7-12).

3.2.2 Snow and Ice Loads

The loading of the 100-year return snowpack is approximately [REDACTED] [REDACTED] pounds per square foot - contrasted to a UMLRR live load design of [REDACTED] pounds per square foot). This is equivalent to [REDACTED] cm ([REDACTED] inches) of liquid water. The depth of this moisture in solid form would depend on the density of the snow. However, it would be in the range of [REDACTED] feet of snow. This amount of moisture, whether in liquid or solid form, presents a danger to structures only if it is allowed to accumulate as could occur, for example, on a flat roof. The torospherical shape of the reactor containment building causes rain to be shed at once and snow to slide off as soon as a small amount accumulates. The presence of any wind or solar heating accelerates the snow removal process.

3.3 Water Damage

As was discussed on Section 2 of this report, the UMLRR site is not subject to flooding. Moreover, even if water were to accumulate around the containment building exterior, it would not impact reactor safety because the building itself (including the foundation) is water tight. In the event of a severe storm or flood, the reactor will be shut down, secured and locked if there appears to be even a remote chance of danger in operating the reactor at the time.

3.4 Seismic Damage

The seismic characteristics of the UMLRR site are summarized in Section 2.5 of this report. The major conclusions are as follows:

- a. The earthquake for the Lowell area has an associated acceleration of [REDACTED]
- b. The maximum earthquake potential is a repeat of the Cape Ann earthquake that occurred in [REDACTED]. It had an epicentral intensity of [REDACTED] on the MMI scale.
- c. The soil at the UMLRR site is not prone to liquefaction.

The Massachusetts area is classified as being in Seismic Zone [REDACTED] as defined in the Uniform Building Code. The UMLRR containment, shielding structure, reactor tank, and core support structure have been [REDACTED] in [REDACTED]. Seismic activity in the region has registered as high as Richter [REDACTED] in historical time, which indicates an upper limit on the most likely seismic event. Due to design, there is ample conservatism in the design for the maximum expected event and it is most likely that the reactor can be returned to

operation without structural repairs following an earthquake likely to occur during the facilities lifetime. The UMLRR structures may suffer some damage from a seismic event of the highest possible yield, but as previously noted, even in the event of the incredible seismic scenario, the resultant radiological doses would be within the ranges evaluated in Chapter 13 and the consequences found acceptable from the standpoint of public safety. In the event of a beyond design basis earthquake, the frequency of vibration of the pool unit may well be different from that of the building, causing dislocations between the reactor and immediate surroundings. Any resultant break in the primary coolant pipes would allow the pool to drain no lower than [REDACTED] feet above the core, due to the pipe location in the pool concrete and anti-siphon provision.

The facility has a seismic detector (switch) mounted on the biological shield which, when tripped, initiates an automatic reactor scram. Maintenance and testing of the detector is performed in accordance with the UMLRR Operating Procedures and Technical Specifications (see Chapter 14). The switch is set to scram at a Modified Mercalli Scale IV. ANSI/ANS-15.7.1 (rev. 1977) section 3.2 (2) requires a reactor scram for intensities [REDACTED] or greater. The reactor would not be started up again until an examination of the structure could be made to insure that no damage had occurred to the reactor.

3.5 Systems and Components

3.5.1 Containment System

The containment building is a welded steel shell with a flat bottom, cylindrical sides, and a domed top. The structural specifications meet the design criteria listed below.

- a. Design pressure: Internal, [REDACTED] lb in.⁻²; External, [REDACTED] lb in.
- b. Design internal volume: ([REDACTED] x 10³ ft³)
- c. Design internal temperature: [REDACTED] ± 3°F
- d. Leak rate: No more than 1 [REDACTED]
- e. Roof live load: [REDACTED]/ft²
- f. Wind load: [REDACTED]/ft²
- g. Dead load: [REDACTED]b/ft²
- h. Earthquake load: Intensity [REDACTED] on the Modified Mercalli scale.

- i. Design stresses: In accordance with the ASME Boiler and Pressure Vessel Code, Section 8, "Rules for Construction of Unfired Pressure Vessels."
- j. Design analysis: Based on elastic analysis.

The flat bottom of the shell is lined with [REDACTED] and [REDACTED] [REDACTED] feet of poured concrete. The cylindrical walls are lined with [REDACTED] feet of poured concrete to serve as a [REDACTED] [REDACTED] and to support a fifteen ton polar crane. The inside clear diameter is nominally [REDACTED] feet. From the flat steel bottom to the highest point of the domed top the distance is about [REDACTED] feet, of which the lower [REDACTED] feet are below grade. The domed or ceiling portion is insulated with two inches of fiberglass held in place by stud welded pins and speed washers and sealed on the underside with a finish coat of white lagging adhesive to provide a continuous vapor and dust barrier. The outside of the shell is painted with a red lead undercoat and a weather resistant finish coat. A beam level plan view and an elevation view are shown in Figures 3-1 & 3-2.

Beneath the flat steel bottom, a concrete pad rests on the underlying light gray quartzite rock . Core borings were taken [REDACTED] feet into the rock by the Atlantic Test Boring Company and analyzed by soil engineers*. The tests indicated some jointing, but excellent bearing capacity was concluded by the engineers. The rock slopes generally downward (Figure 3) to the Merrimack River bed with an average slope of 0.086. The containment building foundation is firmly keyed to the bedrock.

The prime contractor for the reactor building, including excavation and foundation work, was the Wexler Construction Company, Inc. The welded steel containment shell was furnished and erected by the Chicago Bridge & Iron Company.

3.5.1.1 Containment Building Ventilation Isolation

The criteria for containment building ventilation isolation are that the ventilation valves close upon detection of abnormal effluent activity and that the closure time is such that the activity is not released. The containment building ventilation system is automatically sealed upon

* Haley and Aldrich, Inc., Cambridge, Mass. 02142. See also Chapter 2.

detection of abnormal airborne effluent radiation levels. Both the intake and the exhaust ducts are equipped with redundant sets of pneumatic valves that allow for the rapid release of pressure from the isolation valves. Exhaust air is monitored for radioactivity at the entrance to a holdup plenum. The main and secondary exhaust valves are located at the exit of this plenum. The transit delay time in the plenum is such that the main exhaust valves will close in response to a signal from the monitor before the exhaust air that contains the abnormal radioactivity has been discharged. The secondary valve also automatically closes, providing redundancy should the main one fails to do so. The main and auxiliary intake valves respond to the monitor's signal in similar fashion. Intake dampers are interlocked to close so that effluent cannot exit via the intake duct when building ventilation is off.



Figure 3-1: Plan View of [REDACTED] Building

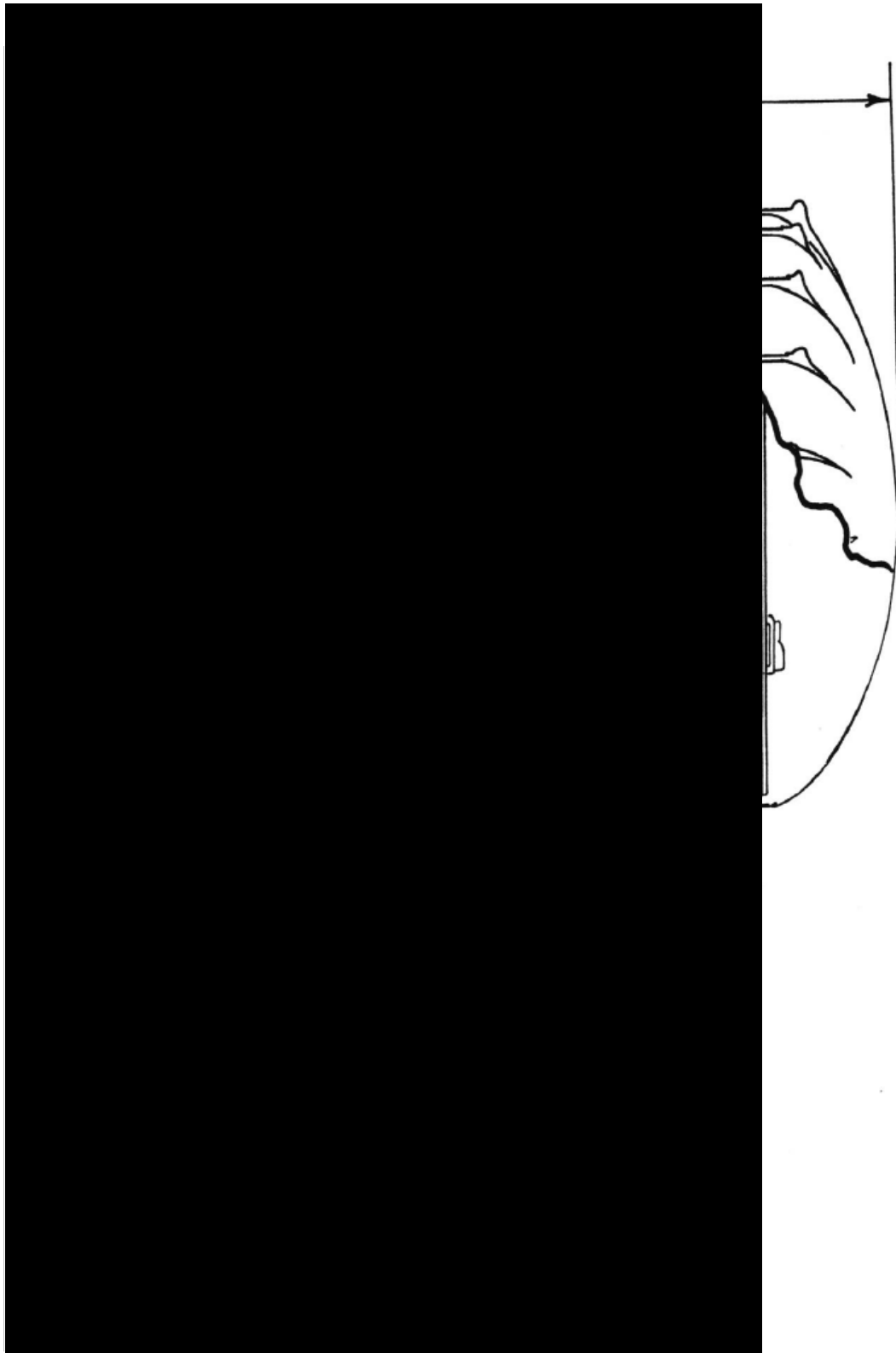


Figure 3-2: Elevation View of the UML Research Reactor and [REDACTED] Building

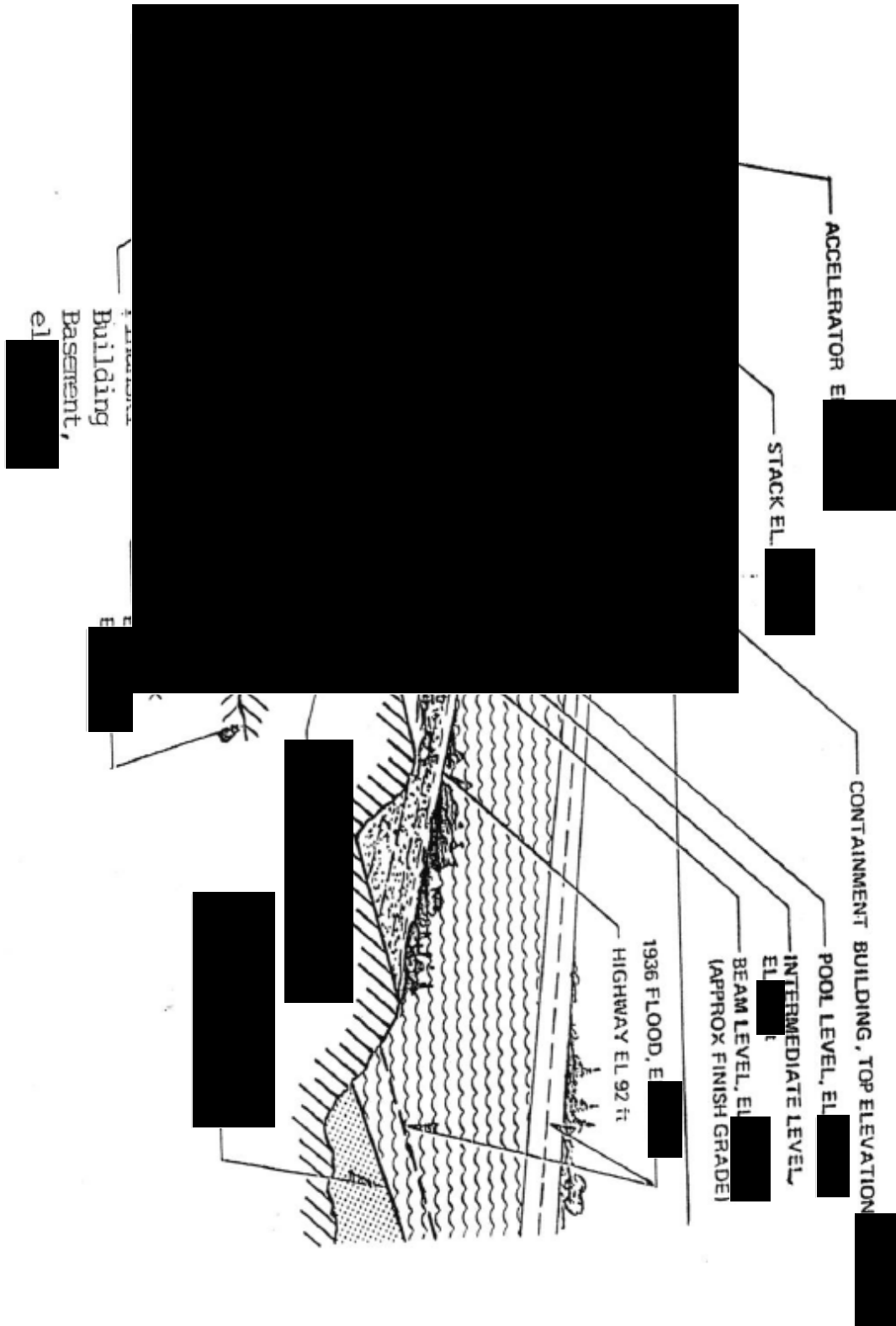


Figure 3-3: Longitudinal Section through Building to River

3.5.2 Instrumentation and Control

The UMLRR uses a hybrid analog system for instrumentation and control. The Drive Control System (DCS) is an essential element whose sole function is to safely operate the reactor drive system components. The UMLRR reactor can be operated in two control modes: manual and automatic. Operations are controlled from the reactor console and blade control panels. The manual and automatic control modes are used for reactor operation from source level to 100% power. The manual mode is used for reactor startup, while either manual or automatic control can be used to change power level or maintain steady-state operation.

The UMLRR has five independent reactivity control blades: four safety control blades and one regulating blade. Each of the blades has its own drive mechanism and control circuit and are operated individually. The control and regulating blades and drives are similar. The regulating blade is used to control reactor power either manually or by automatic control as described in Chapter 7.

The control blade drive assemblies are mounted on the reactor bridge structure. The drives are commercial dc motors, equipped with rotary encoders to determine position. The drive assembly mechanism consists of the DC motor and reduction gear, a rack and pinion, an electromagnet and armature, a dashpot assembly, and a control-blade extension shaft. Blade drive position data is obtained from the rotary encoder. Limit switches are provided to indicate the positions limits of the blades, either full in or full out (0.00” and approximately 25” respectively). The nominal drive speed for the control blade is approximately 3.5 inches per minute or less. The nominal drive speed for the regulating blade is 78 inches per minute.

During a scram, the control blade, blade extension, and magnet armature are detached from the electromagnet and drop by gravity. The dashpot assembly slows the rate of insertion near the bottom of the stroke to limit deceleration forces. Upon receipt of a scram signal, all the control blades are released from their drives and dropped into the core. Insertion of at least three of the control blades ensures reactor shutdown. The total worth of the blades is more than adequate to maintain the core at a sub-critical level with the most reactive blade stuck out of the core.

The time from initiation of a scram signal for a control blade to go from its full-out position to its 80% inserted position shall be less than 1.0 second. The term "initiation of a scram signal" refers to the time at which the true value of the parameter in question attains its scram setting.

No conceivable malfunction of the reactivity control systems could result in a reactivity accident worse than the conditions encountered during the startup accident. As shown in Chapter 13, neither continuous blade withdrawal nor loss of coolant will cause undue heating of the fuel. Identified accidents will not result in significant movement of adjacent fuel elements or otherwise disturb the core so as to add reactivity to the system. Since the primary coolant system operates at atmospheric pressure, control blade ejection is not a credible event. The control blades and the regulating blade cannot drop out of the core because the blades in the full down position are approximately one inch above the safety plate located near the bottom of the tank. Travel out of the core in the downward position is therefore eliminated.

The RPS and DCS satisfy all existing design standards. Periodic checks (i.e., startup, shutdown, and maintenance procedures) of all reactor protective system channels and drive control systems demonstrate that they perform their intended function.

3.5.3 Reactor Protection System (RPS) Function

The UMLRR Reactor Protection System (RPS) was designed to initiate automatic actions to assure that fuel design limits are not exceeded by anticipated operational occurrences or accident conditions. The RPS initiates a drop of the control blades when trip settings are exceeded (see Chapter 7). There are no other automatic actions required by the RPS to keep fuel temperature limits from being exceeded. The RPS is designed with the intent of having redundancy, diversity, power loss fail safe protection and isolation. The reactor protection system conforms to the intent of the former IEEE-323-1974.

The UMLRR Reactor Protection System (RPS) is designed to be fail-safe. Any sub-channel loss that causes the channel to lose its ability to perform its intended function results in initiation of shutdown action. Protective action is manifested through several independent scram inputs arranged in series such that action by any one interrupts current to the scram magnets resulting in shutdown of the reactor. Redundancy of channels is provided and in addition, a loss

of any channel due to open circuit or loss of power will result in a scram. Scram action is, therefore, on a one-out-of-one basis. All instrumentation and channels are provided with testing capability.

The reactor protective system complies with the single failure criterion of IEEE-279. A malfunction in one of the reactor safety system trip actuator amplifiers (TAAs) could result in, at most, the failure to interrupt the current to two control blade electromagnets, in which case the other two control blades would drop and successfully shut down the reactor. The reactor safety system channels are designed with 1/N logic: any one of N signal inputs to either logic unit will cause the TAAs to trip and initiate a reactor scram. Manual initiation of a scram by switch opens an input to each channel as well as interrupting power to the TAAs. While there is only one short reactor period scram channel; the high power level scram channels are redundant, with separate detectors and electronic chassis. This arrangement satisfies the single failure criterion, although the relative physical location of the signal cables and electronics leaves them [REDACTED] to an [REDACTED]. However, resulting damage would cause a reactor scram. Furthermore, an operator is always stationed in the control room during normal operation of the reactor and, therefore, is in the immediate vicinity of the cables and electronics.

3.5.4 Reactor Design

Safety limits for the reactor for period, excess reactivity, and fuel surface temperature are established in Chapter 14 “Technical Specifications”. Accident analyses presented in Chapter 13 show that under credible accident conditions, the safety limits will not be exceeded. Consequently, there would be no fission product release that would exceed allowable radiation levels.

There is a significant prompt negative temperature reactivity coefficient because of fuel material and core design. Routine steady-state power operation is performed with the control and regulating blades partially withdrawn. As shown in Chapters 4 and 13, the most rapid possible reactivity insertion rates are adequately compensated for by period alarm and trip provisions.

3.5.5 Fuel System

The specification for the fuel and cladding is described in Section 4 of this report. It addresses all aspects of the fuel's manufacture and characteristics. UMLRR is fueled primarily

by U_3Si_2 type fuel and may also be fueled using a UAl alloy fuel. Parameters enumerated in the fuel specifications (UAl alloy or U_3Si_2) include:

- a. Form: UAl alloy or U_3Si_2 with a maximum of 20 w/o uranium in the fuel matrix.
- b. Cladding: Aluminum with a nominal clad thickness of 0.038 inches, but not less than [REDACTED] inches. U_3Si_2
- c. U_3Si_2 Nominal Fuel Loading: [REDACTED] gr/U-235 per plate; [REDACTED] gr/U-235 per element.
- d. UAl Nominal Fuel Loading: [REDACTED] gr/U-235 per plate; [REDACTED] gr/U-235 per element.

3.5.6 Electric Power Systems

The primary power distribution system that supplies commercial electric power to the UMLRR is maintained by electrical utility maintenance crews. In case of a power failure, the UMLRR is provided with a [REDACTED] emergency natural gas-fired backup generator (see Chapter 8). All RPS channels are also independently powered on a 3KVA un-interruptible battery backup power supply that ensures continuous operation through any power transient that may occur during generator start lag times.

Routine surveillance and inspection of the electric power system is performed on a monthly basis to ensure the proper operation and function of the emergency backup power system.

3.5.7 Fluid Systems

A secondary coolant system is utilized to cool reactor pool water during normal operation of the reactor. The UMLRR requires no auxiliary cooling system for cooling of reactor pool water upon shutdown. Natural convection cooling is adequate to dissipate core afterheat.

The reactor pool and cooling systems operate at low pressure and temperature. The pool is [REDACTED] and no means for pressurizing the system exist. The reactor pool is constructed of [REDACTED], while the primary coolant system components are aluminum or stainless steel. The system components outside the reactor pool have a low probability of serious leakage or of gross failure. Further, the design of the system is such that even if a line or component ruptures, only a small amount of water would be removed from the tank. Rupture of the tank is virtually impossible, since it is supported on the bottom and sides by reinforced concrete. All components containing primary coolant (i.e. reactor pool, primary

coolant system, and the purification system) are constructed of aluminum and stainless steel, using standard codes for quality control. There is no requirement for leak detection in the primary coolant or purification loop since no conceivable leak condition can result in the pool water level to lower more than [REDACTED] below the suspension frame base plate elevation without a scram. There is also a requirement to test the secondary water for sSodium-24 which would indicate a leak from the primary water into the secondary water.

The reactor pool is [REDACTED] the maximum pressure in the primary system is that due to the static head. The primary, secondary, and purification systems are pressurized by their circulating pumps. Piping and valves in the primary and purification systems are stainless steel or aluminum and of such size to provide adequate operating margins. The secondary system components are manufactured from either PVC or carbon steel. The cooling system is described in detail in Chapter 5. The UMLRR water purification system design also includes a “Make Up Water Source” for replacing of primary coolant water lost through experimentation and evaporation.

Cooling equipment used in normal operation of the reactor is located either in the reactor room, equipment room, or outside the building with adequate space provided to permit inspection and testing of all components. Operation of the bulk coolant and cooling tower system is checked on a daily basis prior to reactor operation. During this checkout, the performance of each system is monitored with emphasis on pump outlet pressures, pressure differentials, temperatures and system flow rates.

3.5.8 Anti-Siphon System

The anti-siphon system functions as a backup system to the various safety instrumentation and equipment (e. g., pressure sensors, pump and valve interlocks, etc.) ensuring that the reactor core does not become uncovered during a LOCA. A rupture of the primary coolant system followed by a decrease in pool water height causes the anti-siphon system to admit a fixed volume of air to the high point of the reactor outlet piping, thus breaking any potential siphon which may have been created by the pipe rupture. Redundancy is incorporated into the system to ensure no single component or circuit failure will render any portion of the anti-siphon system inoperative. This system does not rely on electrical circuitry, as the

activation of the system is initiated by a drop in pool level to below the height of the primary piping penetrations.

3.5.9 Fuel Storage and Radioactivity Control

There is no readily available path for radioactive liquid waste to be discharged directly to the environment. Liquids in the reactor containment that could subsequently be released into the environment may result from regeneration of the demineralizer, spills, wash down of the floor, etc. These liquids are collected in storage tanks outside of UMLRR, analyzed for radioactivity and disposed of accordingly according to procedures and relevant environmental regulations regarding discharges.

The major concerns relative to storage, handling, and control of radioactivity of irradiated fuel are shielding and criticality. All irradiated fuel elements are stored in [REDACTED]. When fuel is stored in the [REDACTED], the water provides a minimum shield thickness of at least [REDACTED] feet. This amount of water also provides scavenging of any fission products should any escape from the fuel elements. Irradiated fuel elements are handled either under [REDACTED] in the fuel element. The elements are transferred [REDACTED], so they are in a [REDACTED]-safe configuration. For some experiments, special core loadings may be required. Fuel elements removed from the core can be placed in a [REDACTED]. As described in more detail, in Chapter 11 “Radiation Protection and Waste Management”, samples of both primary and secondary water are monitored for the presence of unexpected isotopes. Primary water samples are analyzed for the presence of fission products, while secondary water is analyzed for the presence of induced radioactive elements. Over the 40 year operating history of UMLRR, no fission products or induced radioactivity have been detected in either primary or secondary coolants.

Table of Contents

4 Reactor Description 4-4

 4.1 Summary Description 4-4

 4.2 Reactor Core 4-6

 4.2.1 Reactor Fuel 4-7

 4.2.2 Control Blades 4-11

 4.2.3 Neutron Moderator and Reflector 4-17

 4.2.4 Neutron Startup Source 4-19

 4.2.5 Core Support Structure 4-19

 4.3 Reactor Pool 4-21

 4.3.1 Retention Tank 4-23

 4.4 Biological Shield 4-24

 4.5 Nuclear Design 4-24

 4.5.1 Normal Operating Conditions (Reference Core) 4-26

 4.5.2 Reference Parameters for the Safety Analyses 4-29

 4.5.3 Peaking Factors and Axial Power Profile: 4-30

 4.5.4 Basic Kinetics Data and Reactivity Coefficients 4-32

 4.5.5 Blade Worth Distribution and Drop Times 4-34

 4.5.6 Pump-On and Pump Coast-Down Characteristics 4-36

 4.5.7 Flow Distribution and Assembly Flow Rates 4-37

 4.6 Thermal Hydraulics Design 4-43

 4.6.1 Steady State Operating Limits 4-46

Table of Figures

Figure 4-1: Core Box 4-6

Figure 4-2: Reactor Reference Core Layout..... 4-7

Figure 4-3: Fuel Element and End Box Detail..... 4-9

Figure 4-4: UMLRR LEU 16/18 Fuel Element with Dimensions..... 4-10

Figure 4-5: Control Blade (front)..... 4-12

Figure 4-6: Control Blade (ortho/side) 4-12

Figure 4-7: Control Blade Drive Mechanism Illustration..... 4-14

Figure 4-8: Regulating Rod Cross Sectional View..... 4-16

Figure 4-9: Graphite Reflector Element 4-18

Figure 4-10: Lead Void Element 4-18

Figure 4-11: Reactor Core Suspension Structure..... 4-21

Figure 4-12: Reactor Pool Layout..... 4-22

Figure 4-13: Summary PARET results for feedback-free reference test (see Ref.). 4-29

Figure 4-14: Summary results for a natural convection test case (see for details). 4-29

Figure 4-15: Normalized axial power profile in thermal analysis calculations. 4-32

Figure 4-16: Pump coast-down curve for the UMLRR primary pump 4-37

Figure 4-17: ONB power to flow map for steady state operation in the UMLRR 4-47

Table of Tables

Table 4-1: Physical data for the UMLRR and WPI standard fuel elements..... 4-10

Table 4-2: Reactor Pool Penetrations 4-23

Table 4-3: Measured blade worths ($\% \Delta k/k$) 4-26

Table 4-4: Point kinetics data used in the UMLRR PARET models..... 4-33

Table 4-5: Reactivity coefficient evaluation for BOL reference core ($\beta_{eff} = 0.0078$).. 4-34

Table 4-6: Blade worth vs. insertion distance for PARET input file..... 4-36

Table 4-7: Flow Fraction Versus Time 4-37

Table 4-8: (a) Normalized flow areas by element type with UMLRR fuel..... 4-39

Table 4-9: Fraction of flow in the fuel channels with and without friction losses. 4-40

Table 4-10: Coolant flow rate information for a ■-element core..... 4-42

Table 4-11: Hot channel factor data used in NATCON and PLTEMP computations... 4-45

Table 4-12: ONB flow rate data for $P = \blacksquare$ MW for both UMLRR and WPI fuel..... 4-48

Table 4-13: ONB power levels for free flow for both UMLRR and WPI fuel..... 4-48

4 Reactor Description

This chapter discusses and describes the principal features, operating characteristics, and parameters of the reactor. The analysis in this chapter supports the conclusion that the reactor is conservatively designed for safe operation and shutdown under all credible operating conditions. The information in this chapter provides the design bases for many systems, subsystems, and functions discussed elsewhere in the SAR and for many of the Technical Specifications.

4.1 Summary Description

The UMass-Lowell Research Reactor (UMLRR) is a water-moderated and cooled, graphite reflected, open pool-type reactor that has a flat-plate fuel element design. The fueled core region is reflected primarily by a combination of water basket and graphite reflector elements. The standard UMLRR low enriched uranium (LEU) fuel design uses uranium-silicide U_3Si_2 -Al fuel, with 200 g of U-235 per element. The UMLRR also currently has a possession-only license for [REDACTED] slightly used uranium-aluminide UAl_x -Al LEU fuel elements that were obtained from the Worcester Polytechnic Institute (WPI) when their research reactor was shut downⁱ. The UMLRR U_3Si_2 -Al and WPI UAl_x -Al fuel elements are similar in overall size and shape, so both [REDACTED] [REDACTED] [REDACTED] the UMLRR [REDACTED] re. However, the material composition of the fuel meat is different (aluminide vs. silicide fuel), the U-235 loading is quite different ([REDACTED] g for the WPI element vs. [REDACTED] g for the UMLRR assembly), the number of fuel plates per element differs ([REDACTED] vs. [REDACTED] for the WPI and UMLRR fuel, respectively), and there are also some small differences in meat thickness, plate thickness, water gap thickness, etc., so formal analyses that include both types of fuel design were performed for this Safety Analysis Report. Detailed results of the formal analyses can be found in Chapter 13.

The reactor core assembly is located near the bottom of a [REDACTED]-foot deep, aluminum-lined pool. It can be moved into any of two sections by means of a mechanical rail system located on top of the pool wall. The two sections are the high power (Stall) section (for operation at power levels above [REDACTED] MW(t) with forced circulation) and the low power (Bulk Pool) section. At power levels below [REDACTED] MW(t), the reactor may be operated, with core cooling by natural convection, in any of the sections. As spent fuel elements are generated, they are placed in the fuel storage racks located in the low-power section. The spent elements may be used as a source of gamma

radiation; however, the [REDACTED] kCurie Cobalt-60 source is available as an alternative gamma source. A description of the Cobalt-60 sources can be found in Chapter 10.

The reactor accommodates an experiments position (flux trap at peak flux location) at the center of the core within an aluminum reflector element. This flux trap has a diameter of [REDACTED] inches and was manufactured from a standard water filled radiation basket. In-core devices can be placed in irradiation baskets along the edge of the core. These devices are designed for large capacity of samples and long duration irradiations. The reactor also provides irradiation for experiments by utilizing a pneumatic tube for small targets; horizontal beam ports for long-term irradiations and neutron beam extraction experiments such as medical irradiations and neutron spectroscopy; a thermal column containing graphite for neutron radiography, etc.; and a dry irradiation room located adjacent to the low power section of the pool for gamma irradiations.

The reactor core is based on fuel elements in a [REDACTED] array, surrounded on four sides by reflector elements. Four safety control blades and a servo actuated regulating rod control the reactivity. The control blades move vertically within a pair of shrouds extending the length of the core. Core elements are contained in a grid box that is enclosed on four sides to confine the flow of cooling water between elements. The grid box assembly, including the drive mechanisms, is supported by the suspension frame. The elements that make up the core sit on a [REDACTED] grid plate with the four corner positions occupied by the suspension frame corner posts. These corner posts connect the grid plate to the reactor bridge that spans the open pool. The neutron detectors are suspended within the water filled corner posts. The grid plate is suspended about [REDACTED] meters ([REDACTED] feet) below the pool water surface. The core suspension system includes the reactor bridge, the suspension frame, the locating plate, and the blade drive mechanisms.

The core assembly is cooled by water under either natural or forced convection mode. A single primary pump operation circulates approximately [REDACTED] gpm of coolant through the grid box assembly. The heat from the pool and primary coolant systems is transferred to the secondary coolant system by means of heat exchangers. The heat is then dissipated to the atmosphere through cooling towers located adjacent to the reactor containment.

4.2 Reactor Core

The core consists of a [REDACTED] array of [REDACTED]-inch square modules with the four corners occupied by posts as illustrated in Figure 4-1. Four safety blades subdivide the fuel element array into [REDACTED] sections. The modules surrounding the fuel array may be utilized for graphite reflectors or radiation baskets and are filled with one or the other to ensure proper flow distribution with forced circulation.

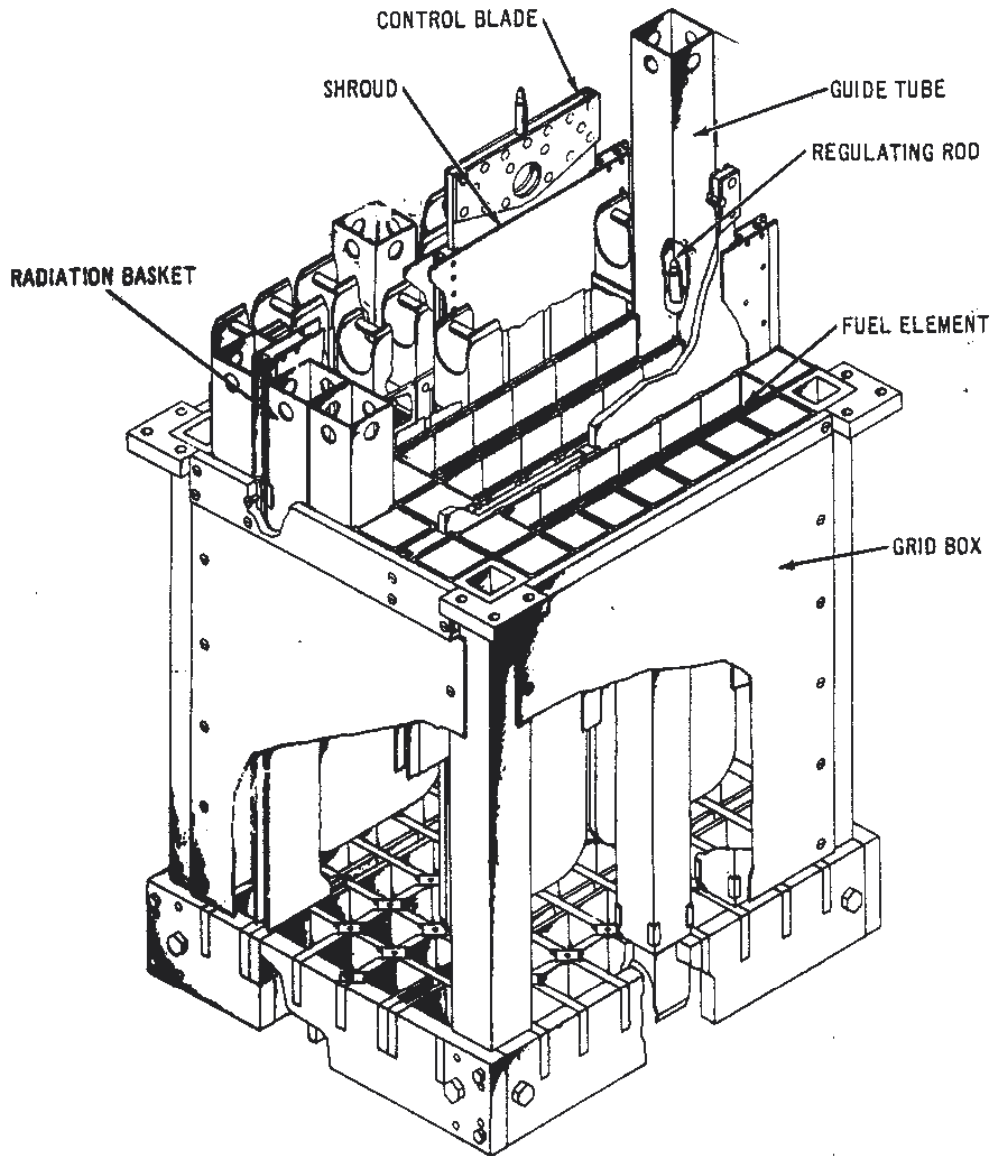


Figure 4-1: Core Box

A sketch of the reference core material configuration is shown in Figure 4-2. This figure identifies the row and column grid notation; for example, the D5 location refers to row D and

column 5 in the core grid, which is directly in the center of the core. This position is commonly referred to as the flux trap location. Additional features such as, the regulating rod located in position D9, a partial fuel element in C3 (which contains [REDACTED] the uranium loading of a full UMLRR fuel assembly), five Pb-void elements in row A, are also shown in Figure 4-1. The four control blades are numbered 1 to 4 in the clockwise direction starting in the lower left quadrant in Figure 4-1. This sketch also clearly identifies the location of the beam tubes, the FNI, and the large graphite thermal column relative to the core layout.

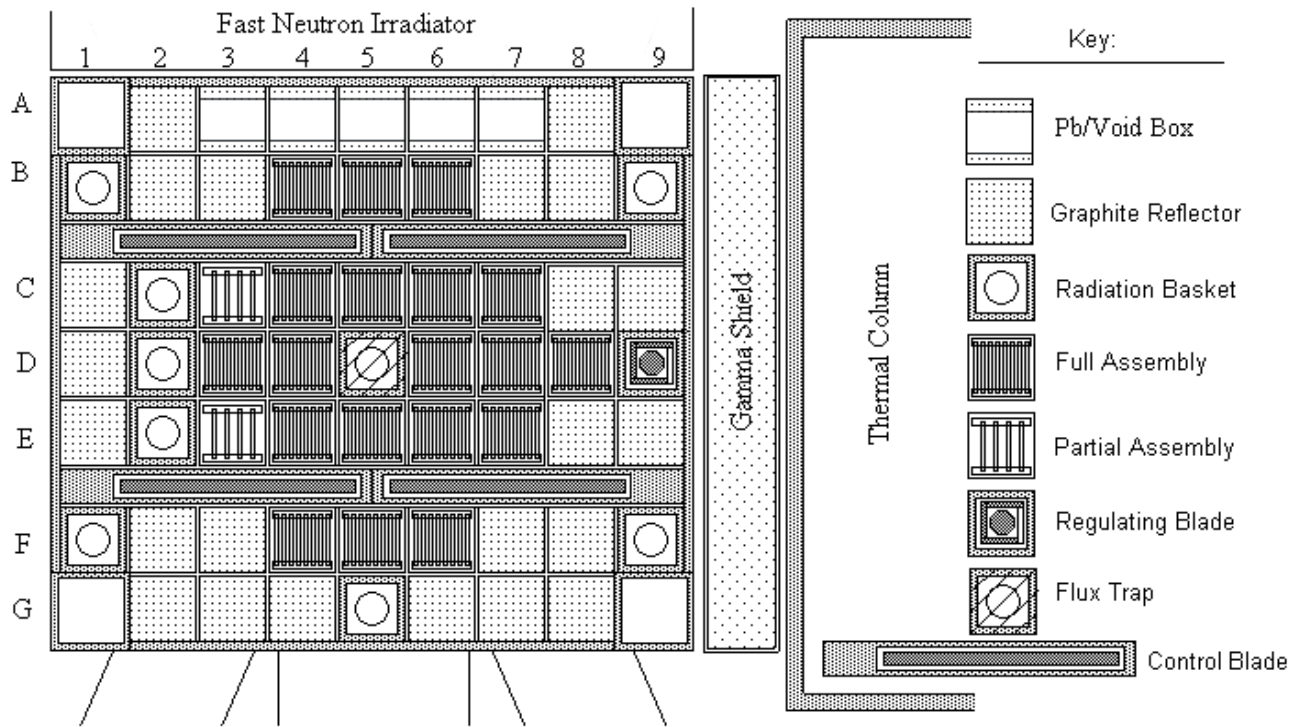


Figure 4-2: Reactor Reference Core Layout

4.2.1 Reactor Fuel

The fuel is of the flat plate Material Testing Reactor (MTR) type. The meat of the Standard Fuel plate is a uranium-silicon intermetallic compound, U_3Si_2 , enriched to [REDACTED]% U-235, and clad with 0 [REDACTED] inches of aluminum. Fabrication of the fuel begins by blending metallic Uranium and Silicon in a zirconia crucible superheated to [REDACTED]. The uranium-silicide ingot is then ground and powdered to an even consistency in an Argon filled environment due to its pyrophoric characteristics. After this, the powder is cold pressed to form a briquette. Aluminum powder is added to the briquette to achieve the necessary density. After repressing,

the U_3Si_2 -Al briquette is vacuum degassed at [REDACTED] $^{\circ}C$. The U_3Si_2 -Al briquette is set in an aluminum frame and placed between two aluminum plates, which are then welded and rolled to the desired specifications. The finished plates are radiographed to ensure proper fuel meat alignment within the plate and for proper uranium distribution. The plates are then assembled into fuel elements.

Fuel element integrity is assured during the manufacturing process. Swelling is reduced by preventing the formation of impurities such as U, USi and U_3Si in the ingot during blending. Hot spots are avoided by ensuring proper Uranium homogeneity during blending, aluminum addition and rolling. Cladding integrity is maintained by heating and degassing prior to rolling. Radiographic analysis of the fuel plates allows for the identification and subsequent removal of stray particles within the edges of the plate. Plates with stray particles are rejected and sent back for Uranium reclamation. Physical tolerances, including the water channel width between plates within the elements are quality controlled during manufacturing.

Two identical end boxes position the fuel element in the grid and provide handles for refueling (Figure 4-3). Including end boxes, the elements are nearly [REDACTED] inches wide and [REDACTED]. Each UMLRR element has [REDACTED] equally spaced plates with [REDACTED] containing fuel and two outside plates of aluminum. Each plate is [REDACTED] inches long, [REDACTED] inches wide and [REDACTED] in thick. When assembled in the fuel element, plates are separated by a [REDACTED] inch gap for water passage. This results in a fuel loading of approximately [REDACTED] grams of U-235 per plate and [REDACTED] \pm [REDACTED] grams of U-235 per element. The partial fuel element is identical to the standard type but with [REDACTED] the uranium loading. The elements may be inverted and rotated to achieve more efficient utilization of fuel.

Additional fuel elements made from a Uranium-Aluminum alloy are also available for use. Physically they are identical to the Standard Fuel Element with [REDACTED] U-235 enrichment, except they have U-235 loading of [REDACTED] grams per plate and [REDACTED] grams per element. A Uranium-Aluminum variable load element, with removable plates is also available for use. The physical data is summarized below in Table 4-1, it contains the data for both UMLRR and WPI standard fuel elements.

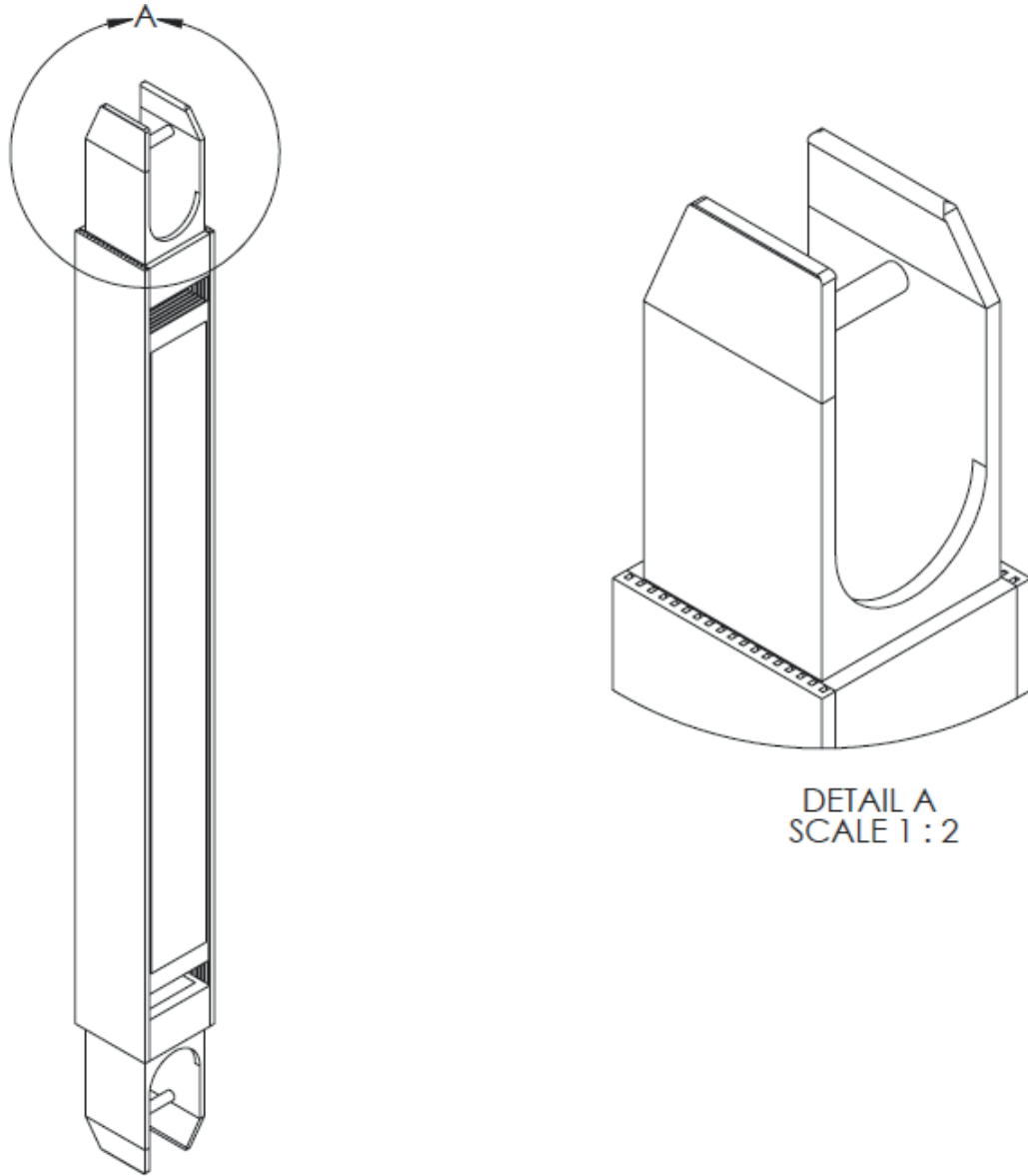


Figure 4-3: Fuel Element and End Box Detail

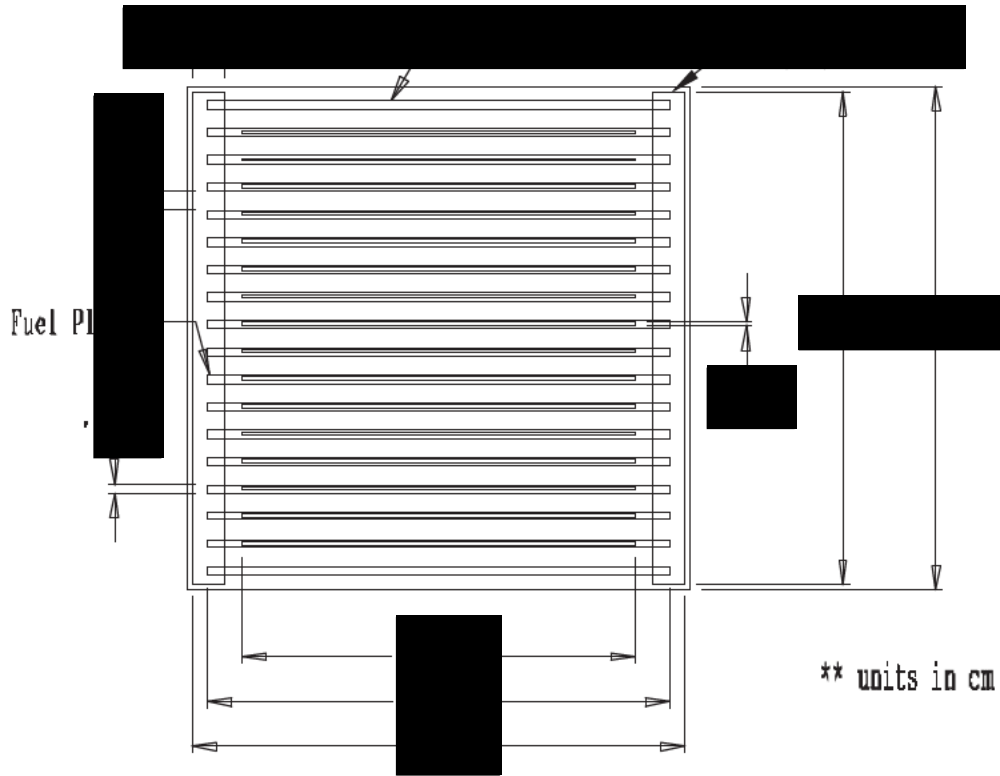


Figure 4-4: UMLRR LEU 16/18 Fuel Element with Dimensions

Table 4-1: Physical data for the UMLRR and WPI standard fuel elements.

| Parameter | UMLRR Full Fuel Element | WPI Fuel Element |
|-------------------------------|------------------------------------|----------------------|
| <u>Plate Data:</u> | | |
| fuel type | U ₃ Si ₂ -Al | UAl _x -Al |
| enrichment (w/o) | 19.75 | 19.75 |
| U-235 loading (g/plate) | 12.5 | 9.28 |
| plate width (cm) | 7.140 | 7.049 |
| meat width (cm) | 6.085 | 6.085 |
| plate thickness (cm) | 0.1270 | 0.1524 |
| meat thickness (cm) | 0.0510 | 0.0762 |
| clad thickness (cm) | 0.0380 | 0.0381 |
| plate height (cm) | 63.50 | 62.55 |
| meat height (cm) | 59.69 | 59.69 |
| <u>Assembly Data:</u> | | |
| fuel plates/element | 16 | 18 |
| aluminum plates/element | 2 | 0 |
| U-235 loading (g/element) | 200.0 | 167.0 |
| side plate thickness (cm) | 0.5080 | 0.4572 |
| channel thickness (cm) | 0.2963 | 0.2709 |
| assembly dimension (cm × cm) | 7.620 × 7.620 | 7.620 × 7.620 |
| assy. dim. with gap (cm × cm) | 7.7724 × 7.7724 | 7.7724 × 7.7724 |

There are nine storage racks with spaces that house nine elements of unused fuel. The racks are located around the inside perimeter of the pool at various depths, the highest of which is located [REDACTED] feet from the top of the pool surface.

4.2.1.1 Evaluation of the Fuel

The Onset of Nucleate Boiling (ONB) was used to determine operational limits of the fuel. ONB is typically reached at a plate temperature of [REDACTED] to [REDACTED] depending heat flux and flow conditions. If the maximum plate temperature under any potential abnormal condition does not exceed [REDACTED] there is no possibility of fuel damage, since the melting point of aluminum is [REDACTED]. Thermal analysis results using hot spot channel factors show, at a nominal flow rate of [REDACTED] gpm and operation at [REDACTED] the margin to ONB is over [REDACTED]. Natural convection testing indicates that ONB occurs at a power of [REDACTED] MW using conservative hot spot channel factors. The thermal analysis later in this chapter provides the detailed results of the thermal performance of the reactor fuel and core configurations.

4.2.2 Control Blades

Reactor control for startup and shutdown is accomplished by four blade-type control blades working vertically within a pair of shrouds located parallel to the major axis of the core. Blades and shrouds are depicted in Figure 4-1 by the two vertical sections that effectively divide the core into three regions. The control blade active region consists of a single homogeneous metal matrix composite (MMC) material with no explicit clad. The material (trade name BORTECⁱⁱ) is a homogeneous MMC mix of B₄C and Al.

Ceradyne manufactures BORTEC MMC in the Canadian ISO and NQA-1 facility. The MMC is extruded and rolled into shapes with B₄C contents up to [REDACTED] by volume using various aluminum alloys. The resulting composites have outstanding properties for structural or non-structural design applications, and are lightweight and adaptable for neutron capture in both wet and dry environments. For the UMLRR control blades, a [REDACTED] w/o B₄C composition is used with a total thickness of [REDACTED] inches.ⁱⁱⁱ This composition, in conjunction with the additional volume occupied by the absorber material, provides an areal boron density of [REDACTED] g B₁₀/cm².

The entire blade is a poison, it is 52 inches in vertical length by 10.65 inches in width and 0.375 in thickness, the lower 26 inches of length which provide active control of the core. The

remaining materials connect the blade to the drive tube. The control blades are illustrated below in Figure 4-5 & Figure 4-6.

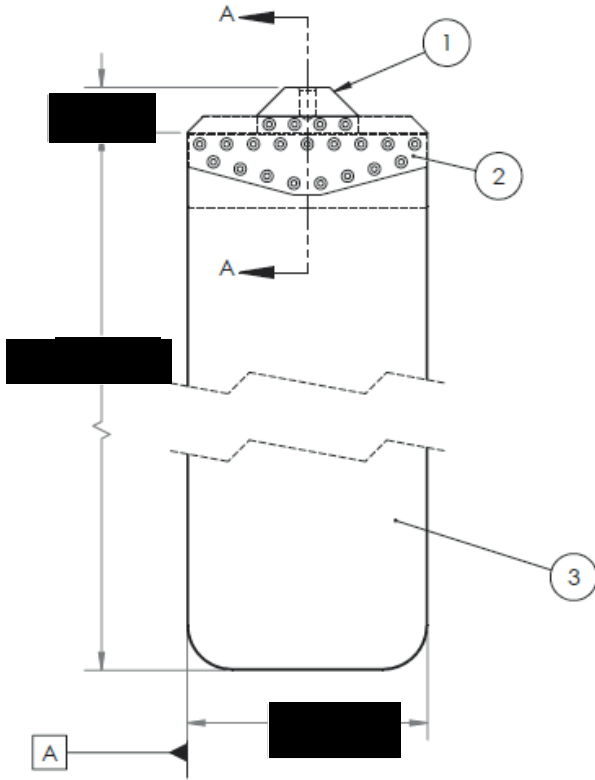


Figure 4-5: Control Blade (front)

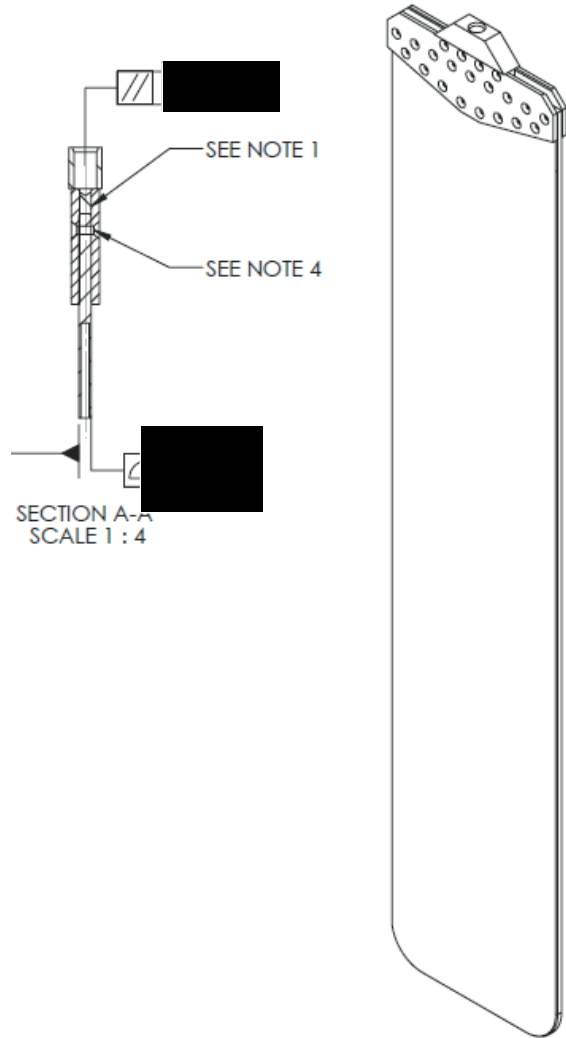


Figure 4-6: Control Blade (ortho/side)

The shrouds act as guides for the control blades throughout its travel. When a control blade is fully withdrawn from the core, at least 3 inches of the control blade remain engaged in the shroud. The shroud consists of two thin aluminum plates 38 inches high, separated by aluminum spacers to provide an eighth-inch water annulus around the blade. The shroud is fastened to the sides of the grid box by screws. Small flow holes at the bottom of the shroud minimize the effect of viscous damping on the blade drop time.

4.2.2.1 Control Blade Drive Systems

These four control blades are actuated by electromechanical drives that position, hold, and scram each control blade. The drives, mounted on the locating plate above the core, are coupled to the control blades through electromagnets that provide gravity scram when de-energized. The control blade drive mechanisms includes a brushless DC motor, helical coupler, torque limiting clutch, ball bearing screw assembly, limit switches, scram magnet assembly, housing, and related mounting and connecting hardware. An optical encoder is provides a continuous position indication within \pm [REDACTED] inches. The drives are housed in aluminum enclosures to minimize any stray electromagnetic interference (EMI) that may be present in and around the reactor bridge.

The drive motor is a reversible electric motor with an integral reducing-gear assembly to reduce speed and an integral brake assembly to prevent drift of the control blade. A mechanical slip clutch on the output shaft limits the force on the control blade to approximately [REDACTED] foot-pounds. The ball-bearing screw and nut are utilized to raise and lower the-control blade. The lead screw assembly converts the rotation of the drive motor to the linear motion of the control blades. The motion is transmitted through ball bearings, which limits wear on the rotating member and produces a uniform rotation. The ball nut is coupled directly to the drive tube and is driven inward or outward by the lead screw. In order to minimize friction and possible binding, large clearances are provided in guide bearings of the control shafts. All lubricants are sealed to prevent leakage into the reactor pool. The working parts of the drive are enclosed in the drive tube, which is sealed off at the lower end by attachment to the scram magnet assembly, or to the solid coupling in the case of the regulating rod. At a point above the reactor pool water level, the electromagnet, engages a cadmium-plated carbon steel anvil that is attached to the end of the lift-rod assembly. The lift-rod assembly connects to the control blade through a support and guiding (offset) mechanism mounted on a bracket attached to the core structure.

The control drive mechanism can operate through a stroke of [REDACTED] inches at a maximum speed of [REDACTED] inches per minute in either direction. Coasting of the mechanism is limited to less than [REDACTED] of an inch of blade travel. Limit switches at the ends of the stroke de-energize the drive motor and are used to provide indications in the control room. In addition, a limit switch within the scram magnet gives indication in the control room when the magnet engages the control

blade anvil. The control blade can be withdrawn when the electromagnet is engaged with the anvil and is energized. When the reactor is scrammed, the electromagnet is de-energized, releasing the anvil, and allowing the control blade and lift-rod assembly to drop into the core under the force of gravity. A dash pot assembly cushions the fall of the shim blade during the final 20% of travel. To recover the control blade after a scram, the drive mechanism is run down and the magnet attaches to the top of the control blade shaft. Figure 4-7 below illustrated the general geometry of the control blade drives, as well as the regulating rod and start-up counter drive systems.

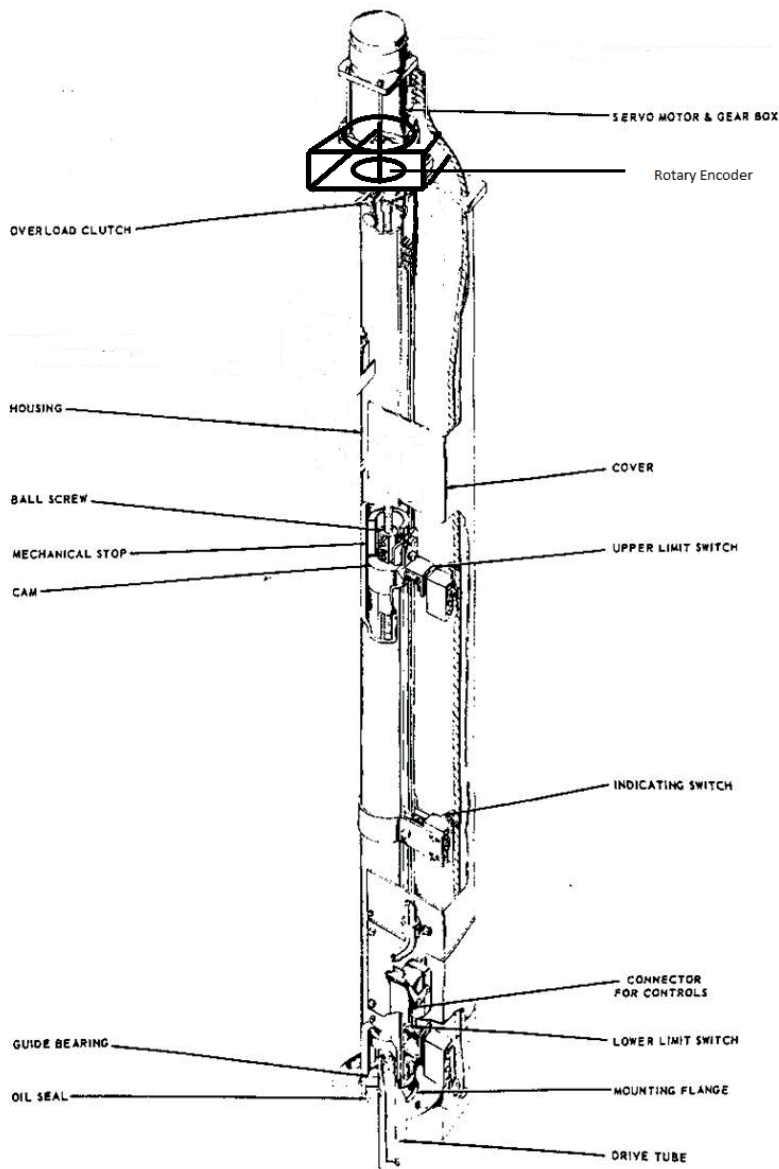


Figure 4-7: Control Blade Drive Mechanism Illustration

4.2.2.2 Evaluation of the Control Blades

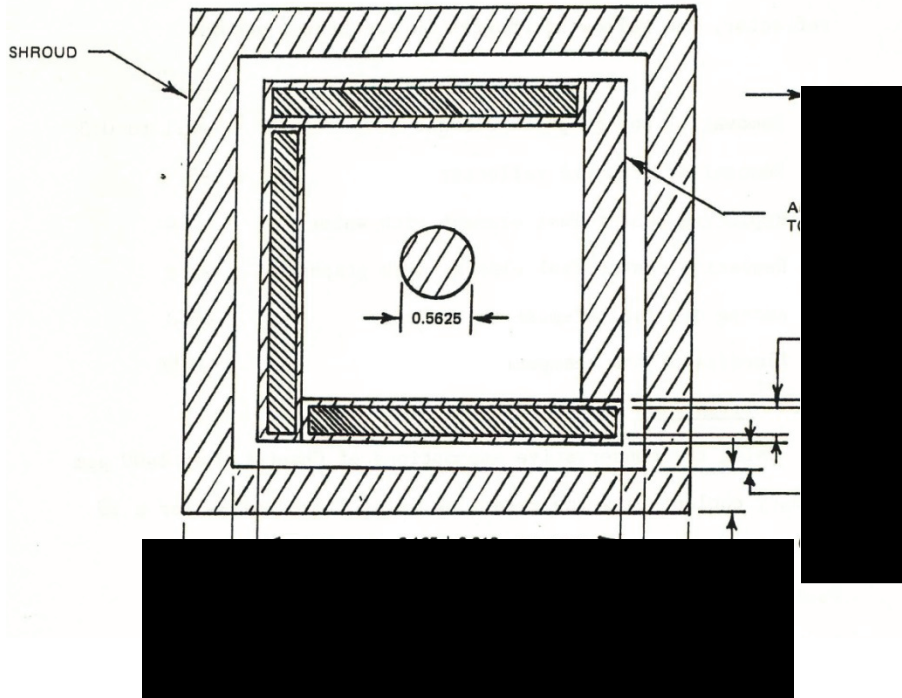
The reactivity worth and speed of travel for the control blades are sufficient to allow complete control of the reactor system from a shutdown condition to full power operation. The insertion rate for the control blades is adequate to ensure prompt shutdown of the reactor in the event a scram signal is received. The control blades have been configured to control the excess reactivity needed for 1-MW continuous operation (including xenon override) and will provide a minimum shutdown margin of 2.7 % $\Delta k/k$ (Chapter 14, TS 3.1.1). This shutdown margin ensures that the reactor can be shut down from any operating condition even if the most reactive control blade and the regulating rod should remain in the fully withdrawn position.

The drop times of each of the four control blades are measured at intervals as stated in the Technical Specifications (Chapter 14, TS 4.2.1). Insertion of the control blades to the 20% withdrawn position from the fully withdrawn position in less than 1 second ensures that the reactor will be promptly shut down when required. This test provides a means for detecting degradation of the control blades which could affect their mechanical operability. In more than forty years of conducting this surveillance, the control blades have never failed to meet this specification.

The control blades are inspected at intervals as stated in the Technical Specifications. Periodic inspection of the control blades provides detection of singular blade abnormalities and any potential generic blade deficiencies.

4.2.2.3 Regulating Rod and Drive

The servo-regulating rod provides continuous control of the reactor by actuation of an automatic servo control system to compensate for small changes in reactivity. The regulating rod is fabricated of a [REDACTED] inch long, [REDACTED] inch square BORAL tube of [REDACTED] inch wall thickness which is lock screwed to the servo regulating rod drive shaft. A [REDACTED] h square aluminum shell guide tube is seated in the reflector region of the grid to ensure proper rod travel. The regulating rod has a reactivity worth less than 0.5% $\Delta k/k$.



The servo-controlled regulating element drive actuates the servo element allowing regulations of reactor power within closer limits than those attainable with use of the control blades alone. The servo drive mechanism is similar to the control blade mechanism in that the two units have an identical slip clutch, ball bearing screw assembly, limit switches, housing, and position indicator. However, a solid coupling replaces the scram magnet assembly, negating the scram provision. The servo control drive is operated by a servo motor and reducing gear train through a total stroke of 26 inches at a maximum travel speed of 78 in./min, which corresponds to a maximum reactivity addition rate of 0.054% $\Delta k/k/\text{sec}$ based on a rod worth of 0.5% $\Delta k/k$, an effective length of 24 inches, and the assumption that the maximum rod worth is twice the average. The element guide tube is a 3-inch square aluminum shell seated in the reflector region of the grid.

The servo-controlled drive automatically regulates reactor power within closer limits than those attainable by using the control blades. The regulating rod is driven by a stepper motor-controlled mechanism. The drive positions are derived from rotary encoders that are mechanically attached to each drive train. The rotary encoders provide blade position indication to the control console. A solid coupling replaces the holding magnet; therefore the regulating

rod does not scram. The maximum speed of travel of the regulating rod is 78 inches per minute, with a total stroke of 26 inches.

4.2.3 Neutron Moderator and Reflector

In addition to removing the heat generated from the fission process, coolant from the primary pool also serve as the neutron moderator. Water filled radiation baskets are used to reflect the core in conjunction with graphite reflector elements.

The graphite reflector element is a reactor grade graphite block contained in a 3-inch square aluminum can. By reducing neutron flux leakage from the active core, the reflector elements increase the neutron flux at the core perimeter and improve utilization of the fuel. The graphite log in the reflector element extends about 3 inches above and below the active 24-inch length of the adjacent fuel elements. The thin-walled aluminum can is evacuated to collapse the walls onto the graphite and thus provide good heat transfer to the pool water. Figure 4-8 provides an illustration of a Graphite Reflector Element.

The design of the reflector element allows for thermal expansion, and for an increase in graphite dimensions of 1.1% due to irradiation growth and gas evolution from an integrated flux of 2 ■■■ ■■ vt. Irradiation tests in the Hanford reactor and at the MTR, in environmental conditions at least equivalent to those at this reactor, have revealed no other significant changes in the graphite properties. The reactor is designed to allow the removal and/or replacement of any neutron reflectors. Graphite or water elements can be replaced on an individual basis or if a breach of the aluminum cladding is suspected (in the case of graphite).

4.2.3.1 Lead Void Elements

In order to help facilitate the neutronic decoupling of the reactor from the Fast Neutron Irradiator; Lead/Void elements were developed. The illustration in Figure 4-10 depicts the lead void element. These elements provide a 1.5 inch void sandwiched between two, 0.5 inch thick lead layers housed in an aluminum assembly. The elements are built on the standard 3" pitch used for all in-core positions. Their use is restricted to the 5 core positions adjacent to the FNI. The large potential reactivity due to the displacement of the volume of FNI container is offset by through the use of these elements. These elements limit neutron feedback to the core.

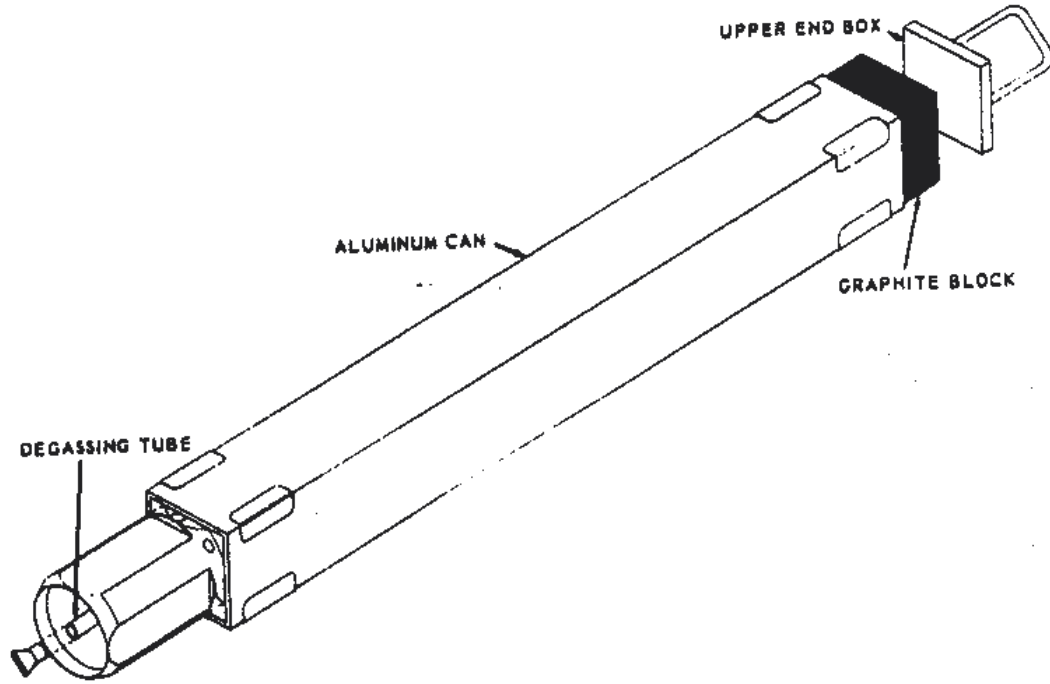


Figure 4-9: Graphite Reflector Element

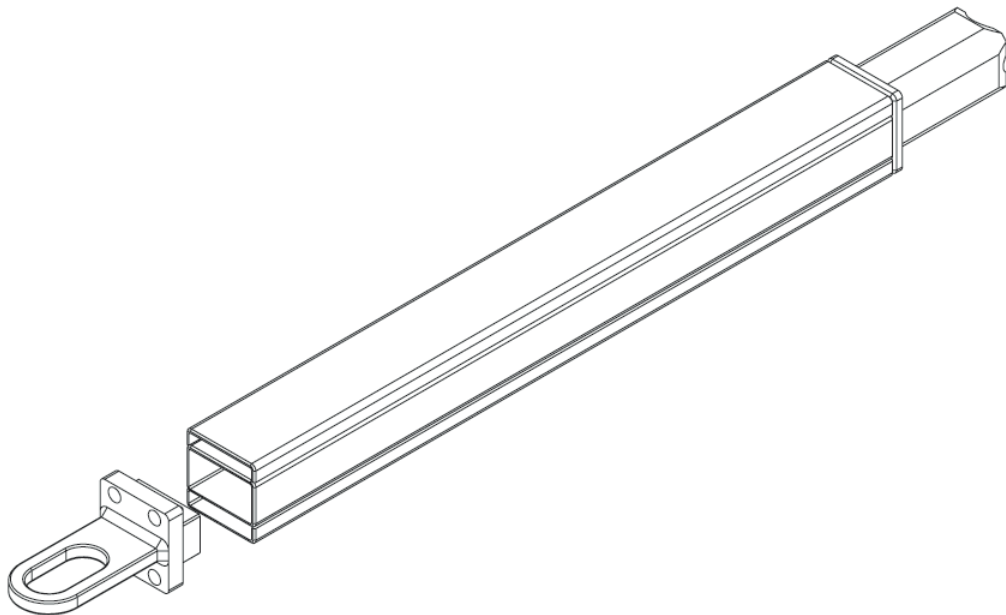


Figure 4-10: Lead Void Element

4.2.4 Neutron Startup Source

A [REDACTED] curie americium-beryllium neutron source is provided for routine startup of the reactor. This source is located inside a water-filled radiation basket, which in turn is seated in the reflector region of the core grid. This ensures that the source is in the active region of the core. The source holder is an aluminum shell, 3 inches square and 42 inches long, normally water filled. This source is normally removed for operation of the core above 10 kW to ensure that excess fission product production does not occur within the source. A handling line allows the neutron source to be lowered into an irradiation position located in the graphite reflector region. Insertion and removal of the startup source is controlled via procedural mechanisms to ensure that it is removed from the core and re-inserted after the reactor is shutdown. The source is currently positioned in core position G-5, in a standard radiation basket.

4.2.5 Core Support Structure

The reactor bridge is provided as a means of supporting the reactor core and core suspension frame, as well as serving [REDACTED]. The reactor bridge spans the entire width of the reactor pool. The bridge consists of two separate sections of structural frame-work set horizontally one above the other and supported on each side of the pool by a two-wheel, rail-mounted truck assembly. The truck assembly allows the reactor bridge to be positioned at the desired location within the reactor pool. The upper section, or upper bridge, is supported independently over the [REDACTED]. The lower section, or lower bridge, supports the weight of the suspension frame and core.

A [REDACTED] crank and gear drive are provided for [REDACTED] the bridge on the pool rails at a rate of approximately [REDACTED] inches per full turn. The bridge is equipped with a brake assembly to allow securing the bridge in the desired operating or inspection position. The bridge is interlocked to prevent any movement while the reactor control blades are withdrawn. Limit switches are provided to ensure that power operation above [REDACTED] kW is limited to the high-power operating positions at each end of the reactor pool.

4.2.5.1 Core Suspension and Support

The core suspension frame is suspended from the lower reactor bridge as seen in Figure 4-8. The suspension frame is an aluminum rectangular column built of four square corner posts

forming a rigid structure. The core box is attached to the lower end of the suspension frame. Cross braces and stiffeners are utilized to provide structural rigidity and alignment in the upper half of the suspension frame. Coolant flow channels are used to provide this function in the lower half of the suspension frame. Stiffeners are provided on three sides of the frame while the [REDACTED]. The [REDACTED]. [REDACTED].

The manipulation is performed using a manual grapple thus enabling the operator to position an element in any one of the spaces in the grid box. Neutron detectors for monitoring power and period are located in each of three corner posts of the suspension frame. The startup counter is located in the fourth corner post of the frame. The ion chambers and fission chambers are electrically insulated from the suspension frame to eliminate possible ground current effects. The three neutron detectors are suspended from the corner posts by cables and held in place by cable clamps at the bridge level. Positioning of the detectors is as needed and verified prior to each reactor run. Height for each detector can be adjusted and locked into place, using the screw adjusted linear positioner on each chamber. A locating plate which spans the upper end of the suspension frame serves as a mounting for the startup drive, the servo regulating rod drive, and the control blade drives. The control blade guide tubes are flanged to the bottom of the locating plate.

The core [REDACTED] is designed primarily to support the reactor core, to provide means for moving it along the major axis of the pool, and to secure the core in any desired operating or service positions, including one readily reproducible position with respect to the coolant header and experimental facilities. The core suspension is also arranged to ensure positive alignment of the shafts between the control and servo drive mechanisms and the respective driven elements as well as [REDACTED] and experiments. To ensure that the reactor bridge is in the proper position to allow for high-power operations, a mechanical latch yoke is connected between the biological shield and the reactor. This yoke is illustrated in Figure 4-11.

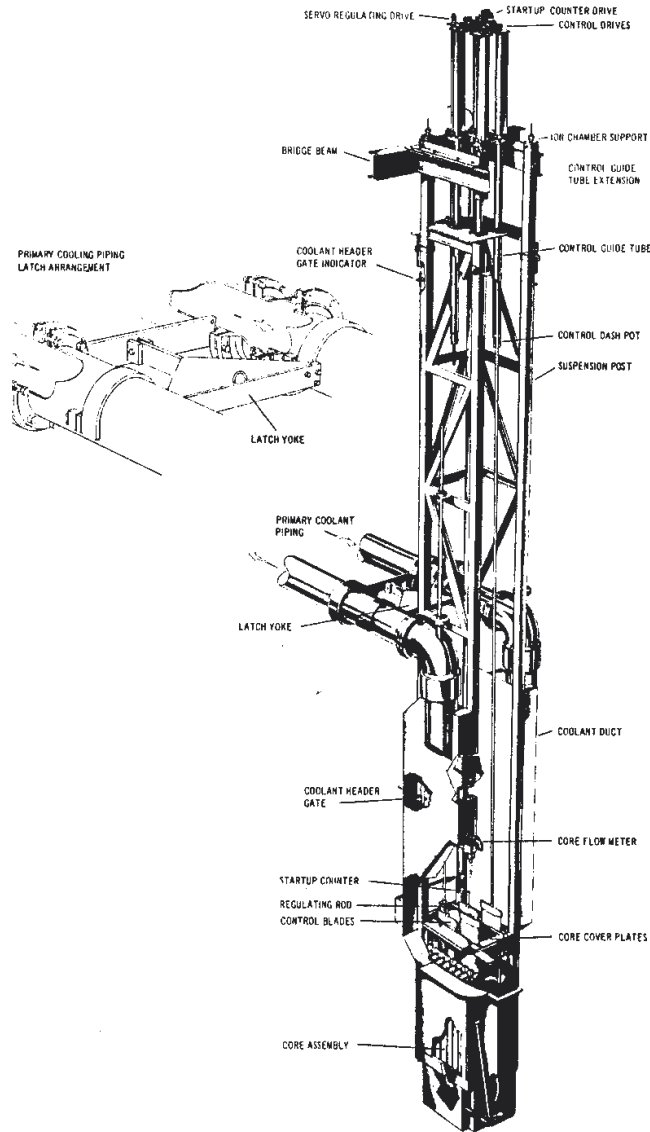


Figure 4-11: Reactor Core Suspension Structure

4.3 Reactor Pool

The reactor pool is comprised of two principal sections, a stall pool and a bulk irradiation pool. The overall dimensions of the reactor pool are approximately [REDACTED] feet deep by [REDACTED] feet long and together hold a combined [REDACTED] gallons of high purity deionized water. The clean water minimizes corrosion and prevents the activation of impurities. See Chapter 14, "Technical Specifications" for more information relating to the pool water quality. Normally, the reactor core centerline sits beneath approximately [REDACTED] feet of water. Each pool is equipped with primary cooling connections necessary for operation at powers over [REDACTED] kW. The North (Bulk Pool) connections are not in service due to modifications for handling Co-60 [REDACTED] and due to the

cross-stall flow path used for the primary coolant system. The pool walls are constructed of heavy aggregate concrete and ordinary concrete as required to provide adequate biological shielding.

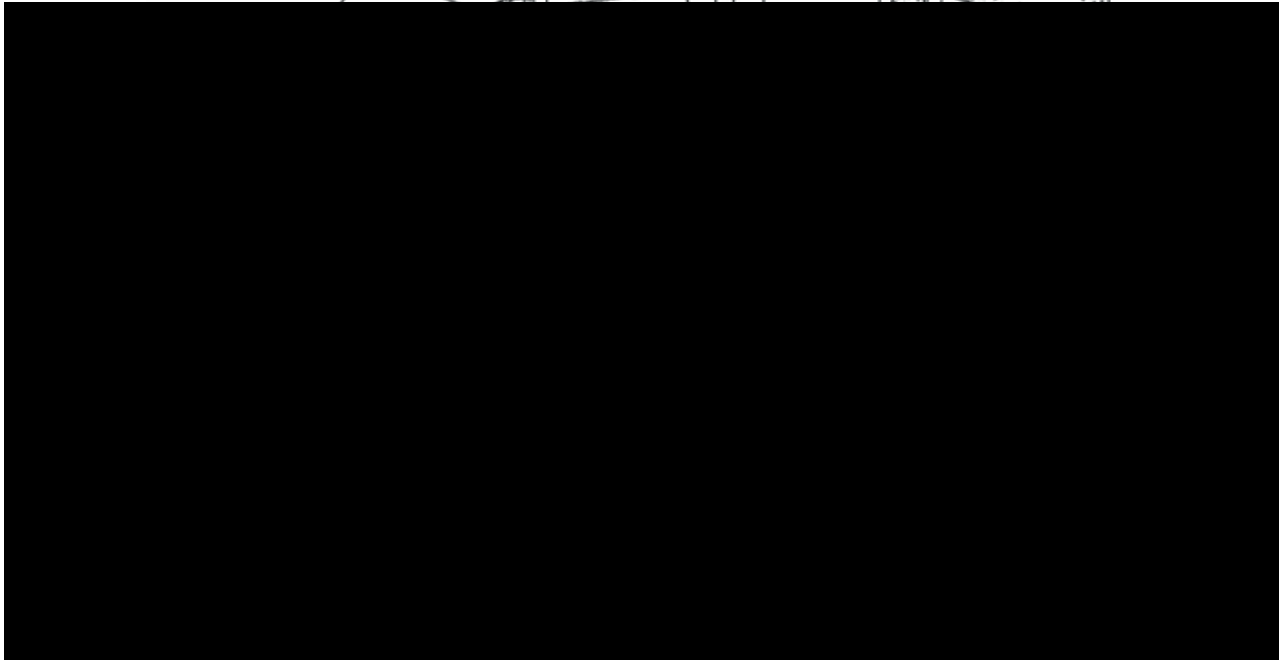
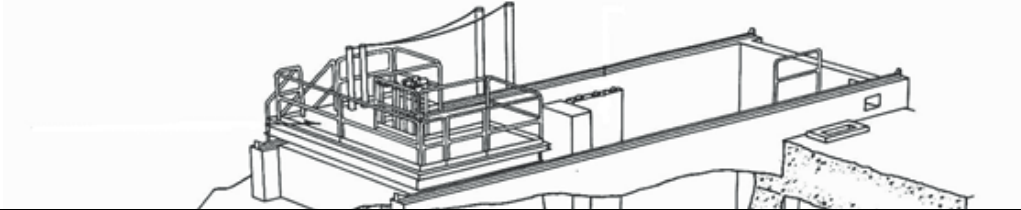


Figure 4-12: Reactor Pool Layout

In Figure 4-11, three beamports are visible, these beamports were removed to install the Fast Neutron Irradiator (FNI) Facility. They remain in this drawing for illustrative purposes to depict the symmetrically located remaining three beamports on the opposite side of the reactor core.

Penetrations to the pool are seal-welded to a [REDACTED] inch thick aluminum liner. Penetrations in the pool wall are summarized in Table 4-2 and discussed further in Chapter 5, “Reactor Coolant Systems”. There are no penetrations made in the pool floor. Fuel storage racks are provided along the walls of the pool.

High power operation is conducted in a section of the stall pool approximately [REDACTED] feet in diameter and [REDACTED] feet deep. The stall pool is separated from the bulk irradiation pool by a [REDACTED] feet

wide, [REDACTED] feet deep pool divider. An approximately [REDACTED] feet wide by [REDACTED] feet high aluminum pool divider gate is available to isolate a given section of the pool. A rubber gasket located about the edges of the gate provides a watertight seal. The gate permits independent drainage of either pool section. When in position the gate rests on six equally spaced aluminum supports. The supports have a J-type bend to prevent shifting or falling of the pool divider gate. The gate is moved into position using the overhead crane and two personnel.

Table 4-2: Reactor Pool Penetrations

| Reactor Pool Penetrations Heights | | | | | |
|-----------------------------------|------------|-----------------------|--------------|-------------------------------|---|
| Penetration | Location | Amount | Depth (feet) | Dimensions | Method of Isolation |
| Primary piping | [REDACTED] | [REDACTED] | [REDACTED] | [REDACTED] in diameter | Anti-Siphon Valves (see Chapter 5) |
| 8" Beam Port | [REDACTED] | [REDACTED] (1 in use) | C.C.C. | [REDACTED] in diameter. | (1)Welded End Cap. (1)Bolted Closed |
| 6" Beam Port | [REDACTED] | [REDACTED] (2 in use) | C.C.C. | [REDACTED] in diameter | (2)Welded End Cap. (2) Bolted Closed |
| Pneumatic Transfer Tubes | [REDACTED] | [REDACTED] (1 in use) | [REDACTED] | [REDACTED] inches in diameter | Sealed End Cap |
| Pneumatic Transfer Tubes (Unused) | [REDACTED] | [REDACTED] | [REDACTED] | [REDACTED] in diameter | Bolted Closed |
| Pool Skimmer (Inlet) | [REDACTED] | [REDACTED] | [REDACTED] | [REDACTED] inches in diameter | Turn line valves to closed positions |
| Pool Skimmer (Outlet) | [REDACTED] | [REDACTED] | [REDACTED] | [REDACTED] inches in diameter | Turn line valves to closed positions |
| Medical Embedment | [REDACTED] | [REDACTED] | C.C.C. | [REDACTED] | Bolted Closed |
| Hot Cell Transfer Port | [REDACTED] | [REDACTED] | [REDACTED] | [REDACTED] | Water Tight Gates |

4.3.1 Retention Tank

A [REDACTED] gallon retention tank located underground adjacent the containment building, is available for partial drainage of the reactor pool. The tank, approximately [REDACTED] feet and [REDACTED] feet high with a [REDACTED] feet hatchway area, is constructed of reinforced concrete and lined with ironite. The interior of the tank is coated and lined with polyvinylchloride sheets [REDACTED] inch thick. When the pool is drained, flow passes through a 10-inch aluminum discharge line located between the holdup tank and primary pump. This discharge line has two valves to isolate the retention tank. The first provides a scram signal when opened and the second is normally chain locked shut. The pool may also be drained to the retention tank via a 4-inch aluminum line from the cleanup system. This line also has two valves providing isolation of the tank. The first valve provides a scram signal when opened and the second valve is normally chain locked shut.

4.4 Biological Shield

The biological shields for the reactor are the pool water and the reinforced concrete walls of the pool structure. The entire facility was designed for operations at █ MW. Additionally, the facility and the pool wall structure were also designed to withstand an earthquake of intensity █ under the Modified Mercalli Scale. Concrete thicknesses and pool water heights were based of these conditions. The reactor core sits underneath approximately █ feet of water. The wall structure is composed of high density and regular concrete, were appropriate. At the thinnest point, the reactor wall is █ feet thick. The concrete and water combination ensures that no radiation fields exist around the periphery of the pool wall structure, aside from experimental facilities, like the Beam Port and Thermal Column where such fields are expected and utilized. For a complete list of all the experimental facilities, and their respective radiation hazards, see Chapter 10, “Experimental Facilities.” The activation and irradiation of ground water or soil surrounding the facility is beyond the realm of credibility.

4.5 Nuclear Design

The UMLRR is a water moderated and cooled open pool-type reactor using MTR-type fuel as described in Section 4.2.1. The fueled core region is reflected primarily by a combination of graphite reflector elements (Section 4.2.3) and water baskets. Water baskets are radiation baskets (Section 10.2.8) with the central aluminum tube blocked to increase coolant flow to the fuel elements.

The standard UMLRR low enriched uranium (LEU) fuel design uses uranium-silicide U_3Si_2 -Al fuel, with 200 g of U-235 per element. The UMLRR also possesses 27 slightly used uranium-aluminide UAl_x -Al LEU fuel elements obtained from the decommissioned Worcester Polytechnic Institute (WPI) teaching reactor^{iv}. The UMLRR U_3Si_2 -Al and WPI UAl_x -Al fuel elements are similar in overall size and shape. Both elements fit interchangeably within the UMLRR grid support structure. However, the material composition of the fuel meat is different (aluminide vs. silicide fuel), the U-235 loading is different (█ g for the WPI element vs. █ g for the UMLRR assembly), the number of fuel plates per element differs (18 vs. 16 for the WPI and UMLRR fuel, respectively), and there are also some small differences in meat thickness, plate thickness, and water gap thickness. A detailed comparison of the two fuel types is given in Table 4-1. Reference 3^v provides a more detailed comparison of the two fuel element types and

Reference 4^{vi} provides an analysis of the behavior and performance of the WPI elements within the WPI reactor.

The data in Table 4-1 were used in all the physics and thermal hydraulics models developed for the current UMLRR analyses. As detailed later in this chapter, the UMLRR physics and safety analysis studies were performed for a variety of core arrangements containing only UMLRR fuel, only WPI fuel, and for a variety of mixed core configurations. In all cases, the original [REDACTED], primarily because it is more [REDACTED] U-235 [REDACTED] and it has a higher average plate power due the smaller [REDACTED] per [REDACTED]. By analyzing both fuel types in a variety of configurations, any reasonable homogeneous or mixed core configuration meeting the UMLRR Technical Specifications criteria for excess reactivity and shutdown margin (Chapter 14, TS 4.1) will be acceptable for use within the UMLRR.

The core grid plate (Figure 4-1) consists of a [REDACTED] array of spaces in an egg-crate shaped bottom aluminum plate. The grid plate is capable of being loaded with fuel elements, reflector elements (graphite or water), experimental radiation baskets, and lead-void boxes. The availability of both water and graphite reflector elements gives flexibility in adjusting the core excess reactivity by simply interchanging some of the water vs. graphite elements closest to the fuel. The Pb-void elements were installed within the UMLRR in 2002 as part of a new core arrangement that included a new experimental facility, referred to as the fast neutron irradiator (FNI), on one side of the core (Section 10.2.2). In addition to the FNI, the UMLRR also has a number of additional experimental facilities, including three beam tubes, a graphite thermal column, a pneumatic tube assembly, and several in-core radiation basket elements.

Reactivity control in the UMLRR is accomplished with four large safety blades and one low-worth regulating rod (Section 4.2.2). The neutron poison material in all the control elements is B₄C in various geometries and loadings. The control blades consist of a single homogeneous metal matrix composite (MMC) material. The material is a homogeneous MMC mix of B₄C and Al having a 23 w/o B₄C composition and a total thickness of 0.375 inches and a B-10 areal density of 0.0815g B-10/cm². The regulating rod is a hollow square, with three sides of the square geometry made from BORAL plates containing a 35 w/o B₄C composition, with the last

side consisting of an aluminum plate of the same thickness as the BORAL plates^{vii}. This arrangement allows some flexibility in establishing the regulating rod worth. The rod can be rotated to have the poison material facing towards or away from the fuel region thereby allowing either a “high worth” or “low worth” arrangement, respectively. The “high worth” configuration has been in use since the HEU to LEU fuel conversion took place back in Aug. 2000^{viii,ix}. Table 4-3 provides the total blade worths for the reference core measured during annual surveillance activities in January 2015.

Table 4-3: Measured blade worths (%Δk/k)

| Blade # | Reference Core |
|--------------------|-----------------------|
| 1 | 2.56 |
| 2 | 2.16 |
| 3 | 3.29 |
| 4 | 3.54 |
| total worth | 11.55 |

4.5.1 Normal Operating Conditions (Reference Core)

The core design depicted in Figure 4-2 was utilized to derive many of the parameters used in the subsequent safety analyses calculations. The diagram clearly identifies the row and column grid notation. For example, the D5 location refers to row D and column 5 in the core grid, which is directly in the center of the core. Additionally, one can identify various core elements and components such as the regulating rod in position D9, a partial fuel element in C3 (which contains half the uranium loading of a full UMLRR fuel assembly), and the five Pb-void elements in row A. The diagram also clearly identifies the location of the beam tubes, the FNI, and the large graphite thermal column relative to the core layout.

4.5.1.1 Computer Codes and Model Validation

The physics calculations performed for reference core include 3-D UMLRR models in both the VENTURE diffusion theory code^x and MCNP Monte Carlo code.^{xi} The two-group cross sections for VENTURE are generated using a variety of modules from the SCALE

package.^{xii} In general, VENTURE is used to obtain the power and few-group flux distributions within the UMLRR and for most routine reactivity evaluations including blade worth distributions and excess reactivity evaluations. In addition, VENTURE is used for most of the depletion analyses performed to date. Note, however, that burnup effects within the UMLRR are relatively minor since the accumulated burnup is so low. There has been approximately 70 MWD in the first 13 years of operation of the LEU core. Thus, for most applications, a beginning of life (BOL) model with fresh fuel compositions is used with the blade positions adjusted to account for the current critical height. The critical height for all four control blades in the BOL reference core was about 14.9 inches withdrawn. After about [REDACTED] MWD, it was about [REDACTED] inches.

In contrast, the MCNP code is used for general validation purposes, for the evaluation of specific detailed experiments, and for certain studies where the VENTURE model has known deficiencies. For example, the VENTURE model predicts a small negative worth associated with a dry experimental bayonet inserted into the D5 flux trap position, whereas the MCNP model predicts a positive worth that is reasonably consistent with measure data. Thus, the MCNP model is generally better suited for a comparative analysis of certain core component changes. The combined use of both the VENTURE and MCNP models provide a good representation of the physics behavior of the UMLRR. References 17-19 provide detail concerning both the 3-D VENTURE and MCNP models, along with several inter-comparisons and evaluations relative to actual measured data for the UMLRR. The studies support the use of these computational models as part of the current safety analyses.

For the safety analysis, the majority of the thermal calculations were completed using three computer codes - NATCON, PLTEMP, and PARET-ANL. All three codes are suitable for the analysis of plate-type fuel operated in a low-pressure environment. This set of codes^{xiii} was originally obtained for use in the UMLRR HEU to LEU conversion project from the RERTR group at Argonne National Laboratory (ANL) in 1988. A newer version was obtained in late 1999 to support a preliminary study that looked at the possibility of upgrading the UMLRR to the 2 MW level.^{xiv} More recently, however, a 2001 version of PARET-ANL was obtained from the Radiation Safety Information Computational Center.^{xv} The 1999 versions of NATCON and PLTEMP were used to do the steady-state studies, and the 2001 version of PARET was used to do all the transient analyses for this SAR.

The NATCON code is a relatively simple natural convection steady state analysis tool used to simulate the conditions of natural convection flow in a thin rectangular fuel channel. For a given power level, it balances buoyancy and friction forces to determine the steady state flow rate in the channel for the given heat source. For this SAR, it was used to find the power level at which the onset of nucleate boiling (ONB) occurs under steady state natural convection conditions. Similarly, PLTEMP also models a steady state system, but it assumes forced convection flow instead of natural convection. The PLTEMP code was used to simulate pump flow through the entire reactor core to determine the amount of flow in the fuel vs. the bypass channels (control regions, experimental basket elements, etc.). In addition, it was also used to do a hot channel analysis at steady state forced flow conditions to determine the thermal characteristics of the fuel, clad, and coolant as a function of power level and flow rate. The hot channel analysis in PLTEMP was used to determine a power-to-flow map to identify, at a given power level, what flow rate would lead to ONB conditions.

PARET-ANL (PARET) is a transient analysis code that simulates the behavior associated with both reactivity and flow-induced transients within the system. For the UMLRR analysis, PARET was used to evaluate the consequence of both rapid and ramped reactivity changes in the reactor core, and to determine how a loss of flow scenario affects reactor performance and safety. The PARET results for the UMLRR show that ONB conditions would not be reached under a series of limiting credible reactor transients.

Unfortunately, the UMLRR does not have any devices that give a direct measurement of the temperatures that develop within a fuel channel. As a result, direct validation of the results from NATCON and PLTEMP is not possible. However, during transient operation, the power level, $P(t)$, is recorded and, by using a recently developed inverse kinetics technique,^{xvi} the total core reactivity, $\rho(t)$, can also be measured. Thus, with this information, some formal testing of the PARET model can indeed be performed. In particular, a recent set of PARET benchmark tests were performed with the goal of validating the base PARET model and a set of reactivity coefficients to be used within subsequent PARET safety analyses.^{xvii} The reactor conditions and both the simulated and measured results are discussed in detail in Ref. ^{xviii}. In general, the UMLRR PARET simulations for the series of reactivity and flow transients show very good overall performance. As an illustration, Figure 4-12 and Figure 4-13 show two particular test

cases. Figure 4-12 shows a low-power (feedback-free) reactivity transient that tests the base PARET model and basic kinetics parameters used within PARET’s point kinetics model. Figure 4-13 shows a natural convection test with the temperature feedbacks. These results show the PARET model for the UMLRR can simulate actual reactor behavior with reasonable accuracy. In both cases, the $P(t)$ and $\rho(t)$ behavior are reasonably represented with the PARET simulations.

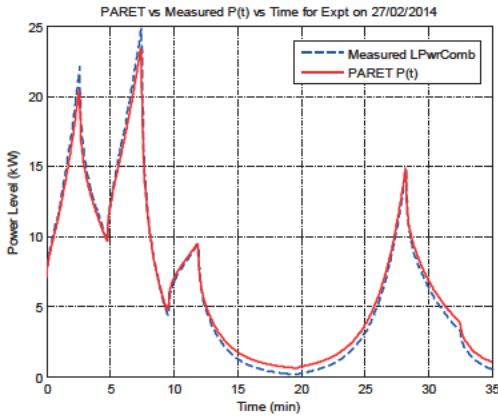


Figure 4-13: Summary PARET results for feedback-free reference test (see Ref. ³³).

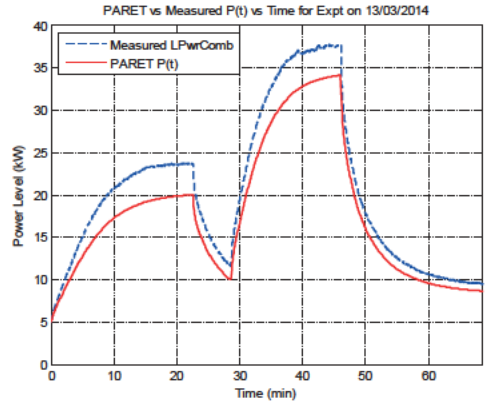
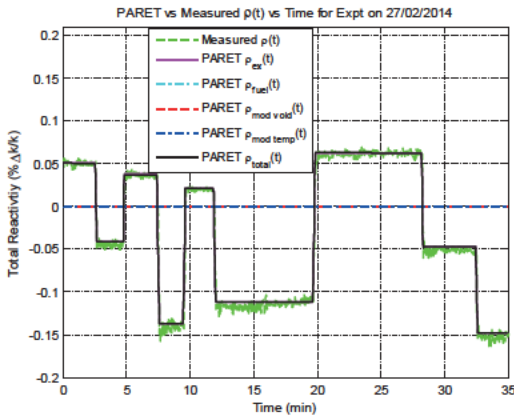
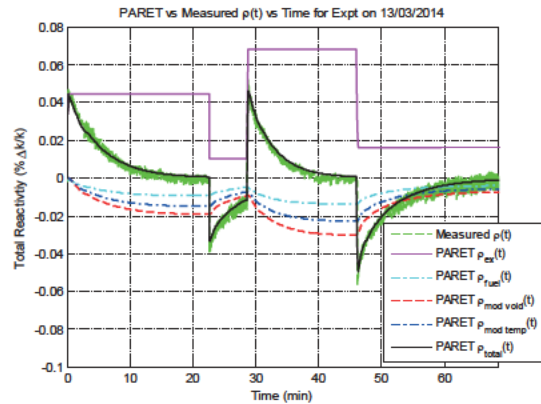


Figure 4-14: Summary results for a natural convection test case (see ³³ for details).



4.5.2 Reference Parameters for the Safety Analyses

The safety analyses for a particular reactor design typically involve a series of calculations that model the behavior of the system under a series of off-normal conditions to

show that fuel integrity will not be compromised under any credible scenario. These computer analyses require extensive modeling data such as the worst-case power peaking factors and axial power distribution, appropriate basic kinetics data and reactivity feedback coefficients, blade worth distributions and drop times (including instrument delay times), typical fluid flow rates and pump-on and pump coast-down characteristics, as well as standard operational conditions at the beginning of a particular transient scenario including: power level, inlet temperature and pressure, and prior operating conditions for decay heat considerations. This section will briefly discuss and tabulate many of the needed parameters for the subsequent analyses. Additional detail may be found in the references.

4.5.3 Peaking Factors and Axial Power Profile:

From previous physics studies of the UMLRR, it was determined that the more severe power peaking condition is associated with the blades inserted substantially into the core. Thus, an core arrangement with a high excess reactivity which is made nearly critical via blade insertion often gives the desired limiting peaking factors. In particular, the excess reactivity in the BOL reference core was about 3.5 % $\Delta k/k$. Though less than the maximum excess of 4.7 % $\Delta k/k$ allowable under the Technical Specifications (Chapter 14, TS 3.1.1), this is sufficiently large enough for extended operation of the UMLRR. Thus, the BOL reference core model with the blades at their critical height of about 14.9" withdrawn was selected as a good candidate configuration for determining the maximum peaking factors.

A practical lower limit on excess reactivity is somewhere in the range of 1.5-2.0 % $\Delta k/k$, since sufficient excess reactivity is needed to override temperature and xenon feedbacks, to allow for additional fuel burnup, and to the counter negative reactivity effects of experiments. In addition, a Technical Specification minimum shutdown margin of 2.7 % $\Delta k/k$ also limits the asymmetry that can be allowed in the blade worths, since the shutdown margin is computed with the most reactive blade in its least reactive position (i.e., withdrawn). All these conditions tend to constrain the allowable configurations that can be realized in practice.

The maximum peaking factors are strongly affected also by the design of the experimental element that is placed in the central D5 flux trap location. The use of a water radiation basket (WRB) in D5 produces the largest thermal fluxes and flux gradients, leading to

the highest peaking factors in the nearby fuel elements. Though not typically used in core position D5, the WRB design was selected for determining the worst case situation.

Within these considerations, the 3-D VENTURE model was used to evaluate a variety of core configurations containing all UMLRR fuel, all WPI fuel, and a mix of both fuel types. In addition, fresh cores and cores with some accumulated burnup were also addressed, again with the goal of addressing as wide a range as possible of practical configurations in order to find a reasonable upper limit for both the radial and axial peaking factors.

Of the many feasible configurations investigated^{xxi}, the worst case core layout identified was a BOL 21-element core with the following conditions: blades at 14.9" out, a WRB in D5, eight (8) fresh UMLRR uranium silicide elements immediately surrounding the D5 position (i.e. the inner ring of fuel) and, to emphasize the power peaking in the inner ring, the remaining thirteen (13) elements in the outer ring contained the less reactive WPI uranium aluminide fuels assemblies. Although rather contrived, this is a feasible configuration and it had the largest computed peak power density, with a radial peaking factor of $f_{xy} = 1.993$ and an axial peaking factor of $f_z = 1.383$. With these values as a base, it was recommended that these peaking factors both be increased by 5% and rounded up to obtain two significant figures for the quoted values of f_{xy} and f_z . This approach adds some conservatism and gives recommended worst-case peaking factors of about $f_{xy} = 2.1$ and $f_z = 1.5$. These values, which combined leads to a total peaking factor of over 3.1, are the peaking factors used in the subsequent NATCON, PLTEMP, and PARET safety analysis calculations.

Related to the axial power profile, the fuel element in location B5 of the reference core has an axial peaking factor of approximately 1.50. The axial power distribution in this location was selected for use in the thermal analysis codes. In the code models, 20 discrete axial intervals are used (21 points). The VENTURE calculated profile was normalized and then interpolated to the 21 points used within the thermal codes, as shown in Figure 4-14. This axial profile was used for all the subsequent thermal calculations. For an average channel, the values shown in Figure 4-14 were used as displayed. However, for a hot channel analysis, the values shown were multiplied by the radial peaking factor, $f_{xy} = 2.1$, to represent the axial profile in the hottest channel in the core.

4.5.4 Basic Kinetics Data and Reactivity Coefficients

The PARET code uses the point kinetics approximation, along with a set of reactivity coefficients to treat the inherent temperature feedback effects, to model the transient power and reactivity behavior during the off-normal transient scenario being simulated. One common form of the point kinetics equations can be written as:

$$\frac{dT}{dt} = \frac{(\rho - \beta)}{\Lambda} T + \sum_i \lambda_i c_i + q \tag{1}$$

$$\frac{dc_i}{dt} = \frac{\beta_i}{\Lambda} T - \lambda_i c_i \quad \text{for } i = 1, 2, \dots, 6 \tag{2}$$

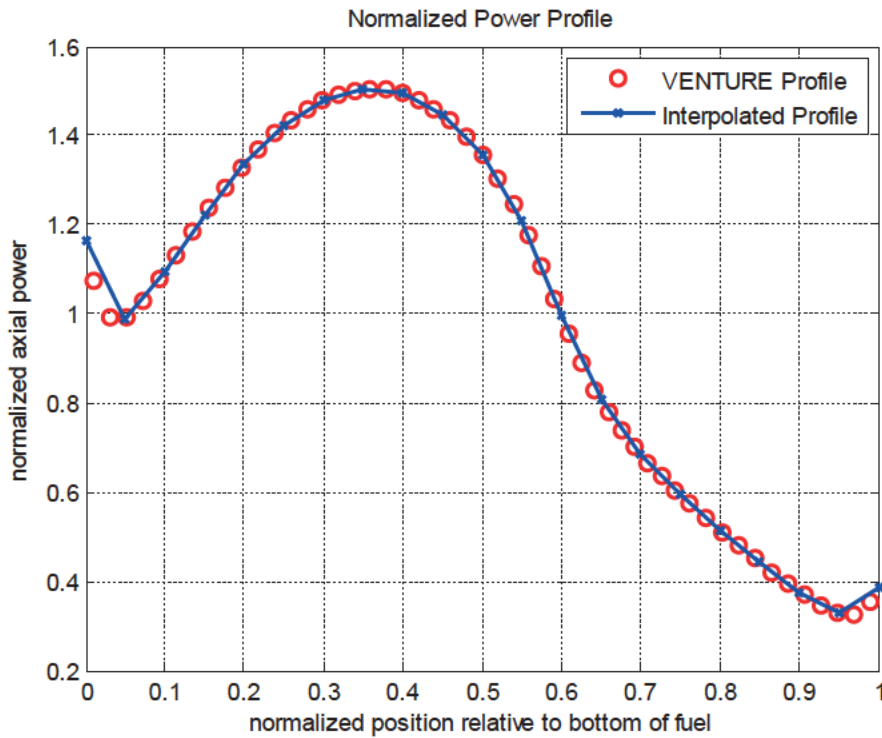


Figure 4-15: Normalized axial power profile in thermal analysis calculations.

where $T(t)$ and $c_i(t)$ are, respectively, the normalized neutron amplitude and normalized precursor levels, and the quantities, β_i , λ_i , Λ , and $\beta = \sum \beta_i$, are referred to as the kinetics parameters (where β refers to the effective delayed neutron fraction, β_{eff}). For application to the analyses in this SAR, the source term, q , is set to zero, the neutron amplitude is replaced by the

reactor power, $P(t)$, since the two quantities are proportional, and the kinetics parameters are treated as constants for a particular reactor design. The total reactivity, $\rho(t)$, includes both the external reactivity, $\rho_{ex}(t)$, that is under operator control via control blade movement, and the compensated or feedback reactivity, $\rho_c(t) = \rho_f(t)$, that is due to inherent temperature changes in the system. In PARET, the feedback reactivity components are represented in the form of reactivity coefficients multiplied by a change in the parameter of interest (fuel and moderator temperature and moderator %void). The feedback reactivity, in dollars, is given as

$$\rho_f(t) = \alpha_{Tf} \{T_f(t) - T_{f,ref}\} + \alpha_{Tm} \{T_m(t) - T_{m,ref}\} + \alpha_v \{V_m(t) - V_{m,ref}\} \quad (3)$$

where the reactivity coefficients, α_{Tf} , α_{Tm} , and α_v for the fuel temperature, moderator temperature, and moderator void, respectively, are given in either $\$/^\circ\text{C}$ or $\$/\%void$. More complicated expressions are available to account for the temperature dependence of the reactivity coefficients, but the current PARET models of the UMLRR assume that these are relatively constant, so this additional detail is not used.

The kinetics parameters used for the PARET safety studies are the same as those used for the initial HEU to LEU conversion studies^{xxii}. These parameters are summarized in Table 4-4. The RERTR program at ANL computed the generation time and β_{eff} values,^{xxiii} and the decay constants and the delayed neutron distribution among the six precursor groups were derived from ENDF/B-V data.^{xxiv} The comparisons shown in Figure 4-12 were generated within PARET using the kinetics data from Table 4-4. These data also are suitable for use with the current UMLRR PARET calculations.

Table 4-4: Point kinetics data used in the UMLRR PARET models

| | | | |
|-----------------|---|-------------------------------|---|
| β_{eff} | 0.0078 | Λ (μsec) | 65 |
| Precursor Group | Precursor Weights β_i/β_{eff} | | Decay Constants λ_i (sec^{-1}) |
| 1 | 0.038 | | 0.0127 |
| 2 | 0.213 | | 0.0317 |
| 3 | 0.188 | | 0.1160 |
| 4 | 0.407 | | 0.3111 |
| 5 | 0.128 | | 1.400 |
| 6 | 0.026 | | 3.871 |

Feedback coefficients for the UMLRR were generated as part of a graduate thesis (Pike).^{xxv} To validate the current PARET model for the UMLRR, including the reactivity coefficients, the raw data generated by Pike were re-evaluated and a new slightly modified set of coefficients were derived. The resultant coefficients developed in this re-evaluation are summarized in Table 4-5. These values were used in the full benchmark analysis.

The values in bold in Table 4-5 were those used in the PARET input file, with the unit of reactivity in dollars (\$), and these correspond to the three reactivity coefficients needed within eqn. (3). For added conservatism in the subsequent “worst-case” transient studies to establish the safety limits, the coefficients in Table 4-5 were conservatively modified by 25% to account for any uncertainties that may exist in both the models and the input reactivity coefficient information. Thus, the magnitude of the PARET input values in the safety analysis calculations are 25% lower or 25% larger, as appropriate, than those in Table 4-5.

Table 4-5: Reactivity coefficient evaluation for BOL reference core ($\beta_{eff} = 0.0078$)

| Component | Reactivity Coefficients | |
|--------------------------|--------------------------------|------------------------|
| Water Temp Only | -5.30e-5 $\Delta k/k/^\circ C$ | -6.79e-3 $\$/^\circ C$ |
| Water Density Only | -6.91e-5 $\Delta k/k/^\circ C$ | -8.86e-3 $\$/^\circ C$ |
| total $T_{coolant}$ | -1.22e-4 $\Delta k/k/^\circ C$ | -1.56e-2 $\$/^\circ C$ |
| T_{fuel} | -2.12e-5 $\Delta k/k/^\circ C$ | -2.72e-3 $\$/^\circ C$ |
| $T_{coolant} + T_{fuel}$ | -1.43e-4 $\Delta k/k/^\circ C$ | -1.83e-2 $\$/^\circ C$ |
| Coolant Void | -2.59e-3 $\Delta k/k/\%void$ | -3.32e-1 $\$/\%void$ |

4.5.5 Blade Worth Distribution and Drop Times

When performing both reactivity-induced and flow-induced transient simulations in PARET, the code provides an option to scram the reactor on either a high-power signal or a low-flow indication. This capability models the safety control blades being de-energized and dropping rapidly into the core, thereby “scramming the reactor” and causing the power level to drop rapidly. This simulation scenario in PARET assumes some delay time from when the preset scram limit is reached to when the magnets de-energize, and then the blades drop into the core using a user-specified blade speed and blade worth curve.

The UMLRR Technical Specifications (Chapter 14, TS 3.2.1) stipulate the scram time must be less than 1 second from a fully withdrawn position, which includes the instrument delay time and the physical time to drop by gravity through the approximately 25-inch length of the blade. The last approximate four inches of free-fall travel are dampened by a piston-type arrangement known as a dashpot to prevent mechanical damage to the blade. The scram time is verified annually. Using the total 1-second requirement as the actual travel time gives a minimum average blade speed of $(25 - 4) \text{ inches/sec} = 0.533 \text{ m/sec}$, and this is the value used in the PARET input for the safety calculations. This value is conservative because the usual measured total drop time includes the instrumentation delay as well as the physical travel time, and these combined times are always less than the 1-second limit.

As noted above, PARET treats the instrument delay as a separate time interval, during which no blade movement occurs. In practice, this delay time is a very important quantity in the overall simulation, since as soon as the blades start to drop, the transient power and temperatures very quickly start to fall. The measured delay time value is approximately 185 msec.^{xxvi} For added conservatism, 210 msec is used in the subsequent PARET safety computations for the instrument delay time.

For the blade worth curves that are input to PARET, the assumption is made that the reactor is critical with the blades at roughly 15 inches withdrawn. For additional conservatism, it is assumed the most reactive blades is stuck in the fully withdrawn position and does not scram. The blade worth curves associated with Table 4-3 were used to collect data at 1-inch intervals starting at 15 inches withdrawn. The inserted worths for the least reactive control blades were summed and both the position and reactivity were converted into proper units for use in PARET. The results of these manipulations are summarized in Table 4-6, with the last two columns representing data actually input to the code. The average blade speed (0.533 m/s) coupled with the worth vs. distance inserted data in Table 4-6 are converted into reactivity vs. time and used as the external reactivity component, $\rho_{\text{ex}}(t)$, for the particular transient under study.

Table 4-6: Blade worth vs. insertion distance for PARET input file.

| Inches Withdrawn | Inserted Worth (% $\Delta k/k$) | Inserted Worth (\$) | Distance Inserted (m) |
|------------------|----------------------------------|---------------------|-----------------------|
| 15 | 0.000 | 0.00 | 0.000 |
| 14 | -0.539 | -0.69 | 0.025 |
| 13 | -1.109 | -1.42 | 0.051 |
| 12 | -1.693 | -2.17 | 0.076 |
| 11 | -2.274 | -2.92 | 0.102 |
| 10 | -2.836 | -3.64 | 0.127 |
| 9 | -3.363 | -4.31 | 0.152 |
| 8 | -3.842 | -4.93 | 0.178 |
| 7 | -4.262 | -5.46 | 0.203 |
| 6 | -4.618 | -5.92 | 0.229 |
| 5 | -4.905 | -6.29 | 0.254 |
| 4 | -5.126 | -6.57 | 0.279 |
| 3 | -5.285 | -6.78 | 0.305 |
| 2 | -5.390 | -6.91 | 0.330 |
| 1 | -5.454 | -6.99 | 0.356 |
| 0 | -5.487 | -7.03 | 0.381 |

4.5.6 Pump-On and Pump Coast-Down Characteristics

Two flow transients analyzed as part of the overall safety analysis (SAR Section 13.2) include a pump-on “cold water insertion event” and a pump-off “loss-of-flow scenario.” Particular versions of both of these events were analyzed as part of the documented validation tests. These actual tests were performed under a set of rather mild and specialized operating conditions such that the reactor would not approach any of its limiting safety system settings and initiate an automatic scram. In contrast during normal forced flow operation, if the primary pump suddenly fails, the flow rate will decrease in an exponential-like fashion and a reactor trip will be triggered when the flow rate reaches the low-flow setpoint. Similarly, if the primary pump is inadvertently turned on during natural convection operation, the power increase due to the positive reactivity insertion following the rapid addition of colder water in the core will cause the reactor power to eventually reach the natural convection limiting safety system setting of 115 kW (assuming no operator intervention) and initiate a reactor scram. To formally simulate both these scenarios in PARET, the pump characteristics need to be known following both a pump-on and pump-off event.

A series of pump-off and pump-on tests were performed to generate pump flow curves for analysis. For a pump-on event, the pump approaches full flow rate capacity in approximately

2 seconds. This is modeled in PARET as a simple ramp function that goes from zero flow to full flow in 2 seconds. For the pump-off scenario, the pump coast down is more gradual, occurring over a period of about 10 seconds. The measured flow rate data and an average coast-down curve for a series of four pump-off events is shown in Figure 4-15. Numerical data from this curve was extracted at 1-second intervals to generate the flow fraction data in Table 4-1. These data were then used within PARET to represent the fraction of full flow following a pump trip, with the value set to exactly zero for $t \geq 10$ seconds.

Table 4-7: Flow Fraction Versus Time

| | | | | | | | | | | |
|---------------|-------|-------|-------|-------|-------|-------|-------|-------|-------|-------|
| Time (secs) | 0.0 | 1.0 | 2.0 | 3.0 | 4.0 | 5.0 | 5.0 | 7.0 | 8.0 | 9.0 |
| Flow Fraction | 1.000 | 0.923 | 0.551 | 0.316 | 0.194 | 0.138 | 0.107 | 0.084 | 0.057 | 0.044 |

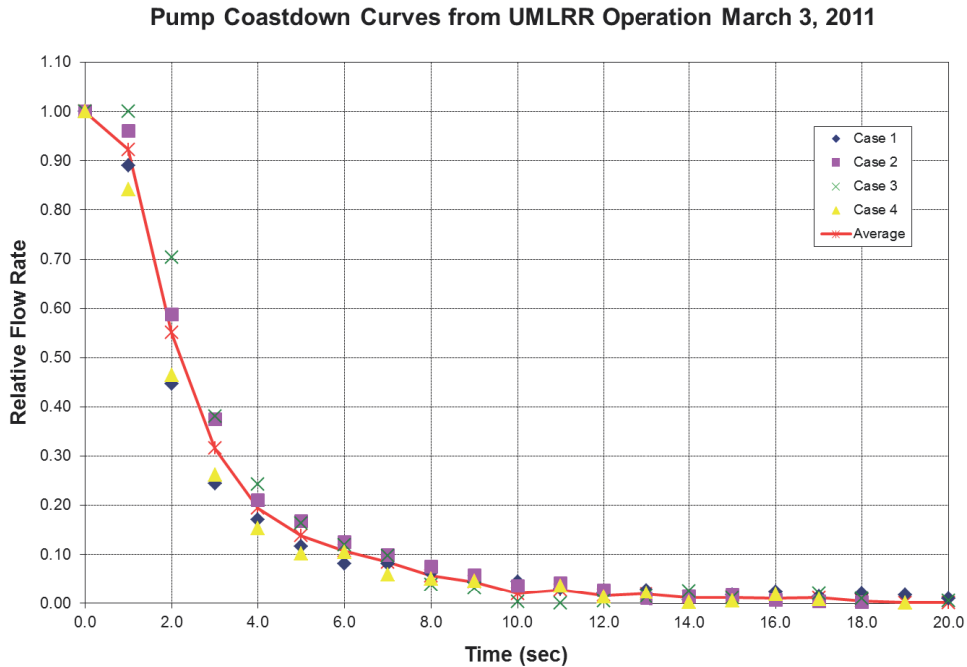


Figure 4-16: Pump coast-down curve for the UMLRR primary pump

4.5.7 Flow Distribution and Assembly Flow Rates

When operating in forced flow mode with the primary pump on, the coolant flows downward through the core with a nominal pump flow rate of approximately [REDACTED] gpm. Refer to Section [REDACTED] for a complete description of the primary coolant system. In steady state, a pressure drop (ΔP) across the core is established due to wall friction, inlet/exit effects, and elevation changes. Due to mixing in the common inlet and outlet plena, the same ΔP is imposed

across each fuel and bypass channel. For a specific ΔP across the core, the flow rate in all the individual channels (e.g., fuel, control elements, and radiation baskets) can be determined, and summed to find the relative flow distribution (i.e., fraction of total flow) in each region.

Full core models within PLTEMP for various core sizes (i.e., number of fuel assemblies) were generated to determine the fraction of pump flow that is expected per fuel element. These models were relatively detailed geometrically, with three axial regions for determining pressure drop in the fuel channels and three different bypass channels (radiation baskets, control blades, and regulating rod) to account for non-fuel flow. Due to the different fuel channel sizes, calculations were performed separately for the UMLRR U_3Si_2 -Al fuel elements and for the WPI UAl_x -Al fuel assemblies.

The information needed for these calculations includes the flow area, hydraulic diameter, region length, and entrance and exit loss coefficients for each axial region for each element type. There are four assembly types in the model: N fuel assemblies, where N varied from 20 to 26 fuel elements, and three types of bypass regions including five radiation baskets, four large control blades, and one regulating rod. A maximum of five open radiation baskets can be present in the core at one time to limit the amount of bypass flow and to assure that there is sufficient flow in the fuel channels (Chapter 14, TS 3.1.1.4). Flow on the outside of the assemblies is assumed to be negligible since the bottom grid plate has essentially zero flow area and blocks direct downward flow.

With data on the flow regions and various assumptions concerning the loss coefficients associated with the entrance and exit effects of each axial region for the fuel and bypass regions, PLTEMP is able to compute the flow distributions that can be expected in both the UMLRR and WPI-fueled cores. These calculations were performed for several power level and core ΔP specifications. The actual relative flow distributions were found to be essentially independent of both power and total flow. As an upper bound on the fuel element flow fraction, the flow distribution also was computed based solely on minimum flow area. This latter computation represents an upper estimate of the fraction of flow in the fuel region since the fuel channel generally has the largest wall friction and loss coefficient components. This results in a ΔP common to the other bypass channels only if the flow rate is lower relative to the bypasses with less friction loss.

A summary of the results from the above computations is given in Table 4-8 and Table 4-9. In particular, Table 4-8(a) and 4-8(b) show the minimum flow area distribution for both the UMLRR and WPI fuel elements respectively as a function of the number of fuel assemblies present in the core. These data show, based on only flow area, that roughly 77% – 82% of the total pump flow is expected through the fuel elements. Slightly less flow is expected in the WPI vs. UMLRR fuel due to the smaller channel dimensions in the WPI element design (see Table 4-1). However, the total flow area data ignores the friction loss differences in the different channels. The friction loss is greater in smaller fuel channels with their associated wall surface friction and larger contraction and expansion losses at the entrance and exit of each channel. The PLTEMP calculations take these friction effects into account and the summary comparisons are presented in Table 4-9. The importance of the increased friction in the fuel channels is obvious since it leads to a significant decrease in core flow (i.e., fraction of flow in the fuel channels) relative to that estimated from a simple analysis of flow areas.

Table 4-8: (a) Normalized flow areas by element type with UMLRR fuel.

| | Normalized Flow Areas for UMLRR Fuelled Core | | | | |
|-------------------|--|---------------------|------------------------|----------|-------|
| # Fuel Assemblies | Fuel Elements | 5 Radiation Baskets | 4 Large Control Blades | 1 RegRod | Total |
| █ | 0.783 | 0.093 | 0.113 | 0.011 | 1.000 |
| █ | 0.792 | 0.090 | 0.108 | 0.010 | 1.000 |
| █ | 0.799 | 0.087 | 0.104 | 0.010 | 1.000 |
| █ | 0.806 | 0.084 | 0.101 | 0.009 | 1.000 |
| █ | 0.813 | 0.081 | 0.097 | 0.009 | 1.000 |
| █ | 0.819 | 0.078 | 0.094 | 0.009 | 1.000 |
| █ | 0.825 | 0.076 | 0.091 | 0.009 | 1.000 |

Table 4-8: (b) Normalized flow areas by element type with UMLRR fuel.

| | Normalized Flow Areas for WPI Fuelled Core | | | | |
|-------------------|--|---------------------|------------------------|----------|-------|
| # Fuel Assemblies | Fuel Elements | 5 Radiation Baskets | 4 Large Control Blades | 1 RegRod | Total |
| █ | 0.771 | 0.099 | 0.119 | 0.011 | 1.000 |
| █ | 0.779 | 0.095 | 0.115 | 0.011 | 1.000 |
| █ | 0.787 | 0.092 | 0.111 | 0.010 | 1.000 |
| █ | 0.794 | 0.089 | 0.107 | 0.010 | 1.000 |
| █ | 0.801 | 0.086 | 0.103 | 0.010 | 1.000 |
| █ | 0.808 | 0.083 | 0.100 | 0.009 | 1.000 |
| █ | 0.814 | 0.080 | 0.097 | 0.009 | 1.000 |

As noted above, because of the slightly smaller channels, the WPI element design has a smaller portion of the total flow through the fuel region by roughly 1-2% relative to the original UMLRR LEU fuel element design. To be conservative, the last column of Table 9 is used to obtain the fraction of fuel flow for both the WPI and UMLRR elements. A simple linear fit through these data gives the following expression

$$f = 0.50 + 0.0088 N \tag{4}$$

where f is the fraction of total pump flow that goes through the fuel and N is the number of fuel elements in the core.

Table 4-9: Fraction of flow in the fuel channels with and without friction losses.

| # Fuel Assemblies | UMLRR Fuelled Core | | WPI Fuelled Core | |
|-------------------|--------------------------|---|--------------------------|---|
| | Based only on flow areas | PLTEMP calculation with friction losses | Based only on flow areas | PLTEMP calculation with friction losses |
| █ | █ | █ | █ | █ |
| █ | █ | █ | █ | █ |
| █ | █ | █ | █ | █ |
| █ | █ | █ | █ | █ |
| █ | █ | █ | █ | █ |
| █ | █ | █ | █ | █ |
| █ | █ | █ | █ | █ |

For the 21-element reference core, eqn. (4) indicates that approximately 68.5% of the nominal █ gpm flow rate goes through the fuel elements. Since flow in the bypass regions (radiation baskets and control elements) is not modeled explicitly in the safety calculations, eqn. (4) is used to relate the total pump flow rate, Q_{pump} , to the flow rate through the fuel elements, Q_{assy} , and individual fuel channels, Q_{chan} , or

$$Q_{assy} = \frac{\text{flow rate in all fuel}}{\text{number of assemblies}} = \frac{Q_{pump} \times f}{N} \quad \text{and} \quad Q_{chan} = \frac{Q_{assy}}{\text{█}} \tag{5}$$

where both the UMLRR and WPI elements have 18 plates and 18 “effective” coolant channels per assembly. While there are only 16 fuel plates in the UMLRR element, the additional two aluminum edge plates give 18 total plates. Also, with 18 plates, there are actually 19 channels (see Figure 4-4). However, the two edge channels only have half the width of an interior channel, resulting in 18 “effective” coolant channels.

For the input data, it is convenient to have a conversion factor that relates a single assembly or single channel mass flow rate, w , in kg/s (as used by the codes) to the measured total pump volumetric flow rate in gallons per minute (gpm). Since the water density change over the range of normal operating temperatures is small, a constant value of [REDACTED] kg/m³ is assumed in determining the desired conversion factor, as follows:

$$w_{\text{assy}} = Q_{\text{assy}}\rho = \frac{f}{N} \times Q_{\text{pump}} \left(\frac{\text{gal}}{\text{min}} \right) \times \frac{1 \text{ min}}{60 \text{ sec}} \times \frac{1 \text{ m}^3}{[\text{REDACTED}]} \times [\text{REDACTED}] \frac{\text{kg}}{\text{m}^3} = \frac{[\text{REDACTED}] f}{N} \times Q_{\text{pump}}$$

or $w_{\text{assy}} = \frac{[\text{REDACTED}] f}{N} \times Q_{\text{pump}}$

(6)

where Q_{pump} is given in gpm and the assembly mass flow rate, w_{assy} , is in kg/s. For $N = 21$, the conversion factor in eqn. (6) evaluates to 2.054e-3 kg/s per gpm of pump flow. Stated differently, Q_{pump} in gpm is 487 times the assembly mass flow rate, w_{assy} , in kg/s for a 21 element core. This latter conversion factor is used to convert the assembly flow rates obtained from the PLTEMP code to overall UMLRR primary pump flow rates in gpm.

Another related quantity of interest is the mass flux, w'' , which has units of mass flow rate per unit area, or kg/s/m². This quantity is useful since it is independent of the entity of interest. For example, the mass flux in a single channel, in the assembly, or in all N fuel elements is the same value. In particular, PARET requires the mass flux in the fuel region to compute various parameters such as the flow velocity, the Reynold's number, the pertinent flow regime (laminar or turbulent), and the heat transfer coefficient.

For convenience, a short tabulation of flow rate information is given in Table 4-10 for several pump volumetric flow rates of interest in the [REDACTED] fuel element reference core case. Note the fraction of core flow through the fuel as given by eqn. (4) is the same for both the UMLRR and WPI assemblies (as discussed above). As a result, the channel mass flow rates are the same for the two fuel types for a given number of elements; however, the mass fluxes are slightly different due to the different flow areas within the UMLRR and WPI elements. The values of Q_{pump} correspond to typical operational flow-rate conditions utilized for the UMLRR ([REDACTED] and [REDACTED] gpm), also to the anticipated trip setting flow rate ([REDACTED] gpm), and to the

transient analysis flow rate (█ gpm). PARET calculations have been performed primarily for the pump flow rates listed in Table 4-10.

Table 4-10: Coolant flow rate information for a █-element core

| Q _{pump} (gpm) | w _{chan} (kg/s) | mass flux, w'' (kg/s/m ²) | |
|-------------------------|--------------------------|---------------------------------------|----------|
| | | UMLRR fuel | WPI fuel |
| █ | █ | █+02 | █+03 |
| █ | █ | █+02 | █+03 |
| █ | █ | █+02 | █+03 |
| █ | █ | █+02 | █+02 |
| █ | █ | █+02 | █+02 |

The power-to-flow ratio vs. number of fuel assemblies is also considered. For a given power level, as the number of elements increases, the power per element or power per fuel plate decreases. Within the same context, the flow rate per element also decreases as the number of elements increases. Of particular interest is the determination of how the power-to-flow ratio (i.e. kW/gpm) varies with the number of fuel elements in the core. This can be expressed in mathematical form as:

$$\left. \frac{\text{power}}{\text{flow}} \right|_{\text{ave}} = \frac{\text{ave power per assy}}{\text{flow rate per assy}} = \frac{P_{\text{tot}} / N}{(Q_{\text{pump}} \times f) / N} = \frac{P_{\text{tot}}}{Q_{\text{pump}} f} = \frac{P_{\text{tot}} / Q_{\text{pump}}}{\text{█} \text{█}} \quad (7)$$

where the fraction of flow through the fuel, f, as given by eqn. (4), is included directly in the last version of this expression.

This relationship shows that, for a given power level and pump flow rate, the power-to-flow ratio decreases with increasing N. The decrease is slow, only changing from 0.█ kW/gpm to █ kW/gpm over the range from N = █ to N = █ for the case of P_{tot} = █ kW and Q_{pump} = █ gpm. Nevertheless, this suggests that smaller cores are more limiting since the power-to-flow ratio is larger for small N. This assumes that the peaking factors do not increase significantly with increasing N, which is not expected and has not been observed in the physics calculations performed to date. The focus for these analyses has been on a reference core with N = █. This represents a reasonable lower limit for most practical core configurations for the UMLRR and also represents a near-limiting arrangement for the safety analyses.

A core configuration with 20 fresh fuel elements, including a graphite radiation basket in D5 and three water baskets in C2, D2, and E2 for in-core irradiation applications, is the practical minimum number of elements needed for routine reactor operations. This takes into account having sufficient excess reactivity to overcome temperature effects, xenon reactivity, and to allow for limited burnup. However, to achieve sufficient regulating rod reactivity worth, a fuel element must be in the D8 position. In addition, symmetry considerations and the desire to have high fluxes for experiments placed in the beam tubes as well as in the fast neutron irradiator (FNI), requires another fuel element (N=21) to balance the number of fuel elements outside of the control blade regions (i.e., Rows B and F as seen in Figure 4-2). From an education and training perspective, many different core configurations are possible (some with less than 21 elements), but these are mostly limited to low power criticality evaluations for demonstration, training, and/or code validation purposes, not for long-term routine operations. Thus, with all these considerations and the fact that smaller tends to be more limiting, the 21-element reference core configuration has been selected as the basis for performing the UMLRR safety analyses.

4.6 Thermal Hydraulics Design

The NATCON and PLTEMP codes were used to establish the steady state operating limits within the LEU fuelled UMLRR during the conversion from HEU to LEU fuel^{1,31-32}. The same basic procedure has been used for the current safety analysis. The major differences include a different radial peaking factor, axial power profile, and the inclusion of WPI fuel.

Using PLTEMP, a power vs. flow curve is generated that identifies the relationship of power and overall pump flow rate at which the onset of nucleate boiling (ONB) point is reached. The purpose of which is to assure that the forced convection steady-state operating point is well within the limits set by this curve. For natural convection operation, NATCON is used to establish the power level where ONB occurs, and again, the nominal operation point is set well below this limit. In establishing these ONB limits, it is important to take into account the effect of uncertainties in the data and models used in the analysis. In particular, one or more engineering hot channel factors are introduced that account for fuel and assembly design tolerances and for uncertainties in various calculated and measured parameters. In NATCON and PLTEMP, these hot channel factors are applied as three separate components,

1. F_q -- accounts for heat flux uncertainties
2. F_b -- treats uncertainties in bulk flow or enthalpy change in a channel
3. F_h -- quantifies the uncertainty in the heat transfer process

These factors (which are greater than or equal to unity) are used to either increase or decrease (as appropriate) the nominal estimate of the heat flux, channel flow rate (which affects the coolant ΔT directly), and calculated heat transfer coefficient. Specifically, each time these quantities are used in the codes, they are modified by the hot channel factors as follows:

$$\text{heat flux:} \quad q'' = q''_{\text{nom}} \times F_q$$

$$\text{mass flow rate:} \quad w = w_{\text{nom}} / F_b$$

$$\text{heat transfer:} \quad h = h_{\text{nom}} / F_h$$

Each of these hot channel factors, in turn, is composed of a number of subfactors. The values of the subfactors are estimated (usually quite conservatively) based on specified design tolerances and experience with various measurement devices and empirical correlations. These subfactors are then combined statistically (usually assuming uncorrelated uncertainties) to give the three factors used within the codes. The only exception to this procedure was for the F_h value, which included the heat transfer coefficient uncertainty as a multiplicative safety factor (see Note 3 in Table 4-11 below).

The individual values of the subfactors for the UMLRR LEU fuel used previously as part of the safety analyses for the UMLRR HEU to LEU conversion effort^{xxvii,xxviii} have been reviewed and compared to the values used in the WPI safety analyses⁴ performed by the RERTR Program at ANL. In most cases the individual factors were very similar and the resultant values of F_q and F_b were nearly identical as shown in Table 4-11. As apparent in this comparison, the largest difference in the estimated subfactors was the channel thickness contribution to F_h , where [REDACTED] was used for the UMLRR fuel and [REDACTED] was used for the WPI fuel. This difference resulted in F_h values of 1.35 and 1.41, respectively, for the UMLRR and WPI fuel. Since the underlying assumptions associated with the individual subfactors for the WPI fuel are not available, the values taken directly from the original references are used without modification. The F_q , F_b , and F_h factors used for the UMLRR fuel are [REDACTED], [REDACTED], and [REDACTED] respectively.^{xxix} The same

quantities for the WPI fuel are [REDACTED] [REDACTED] and [REDACTED] respectively.^{xxx} These are the values used in the NATCON and PLTEMP calculations reported below in the section “Steady State Operating Limits”.

It should be noted that data and modeling uncertainties are treated differently in the transient calculations, since the PARET code does not include explicit usage of the hot channel factors noted above. Instead, for the transient calculations, very conservative assumptions and initial operating points are used to account for the inherent modeling uncertainties that exist in any simulation of a real system. For example, the heat flux hot channel factor, F_q , accounts for a number of physical and measurement uncertainties that affect the heat flux seen in the real system. In PLTEMP, a nominal power level is input to the code, but then internally the code multiplies the calculated heat flux (which is directly proportional to the power) by F_q to account for the uncertainties associated with this quantity. In PARET, the user simply inputs a larger value of initial power to account for the inherent uncertainties. For example, nominal full power for the UMLRR in forced flow mode is 1 MW, but the worst-case reactivity-induced transient analyzed has the input power at the LSSS value of [REDACTED] MW \times [REDACTED] = [REDACTED] MW. Similarly, the nominal pump flow rate is [REDACTED] gpm, but the transient calculations are run at the LSSS flow rate value of [REDACTED] gpm / [REDACTED] = [REDACTED] gpm. These conservative initial conditions plus a high inlet temperature, large peaking factors, conservative reactivity coefficients, blade worths, instrument delay times, etc., all coupled with ONB as the safety limit, will add a significant real safety margin to more than cover any uncertainties that exist in the system.

Table 4-11: Hot channel factor data used in NATCON and PLTEMP computations

| Subfactors | UMLRR Fuel (from Ref. 26) | | | WPI Fuel (from Ref. 4) | | |
|------------------|---------------------------|------------|------------|------------------------|------------|------------|
| | F_a | F_b | F_h | F_a | F_b | F_h |
| F_u [REDACTED] | [REDACTED] | [REDACTED] | | [REDACTED] | [REDACTED] | |
| [REDACTED] | [REDACTED] | [REDACTED] | [REDACTED] | [REDACTED] | [REDACTED] | [REDACTED] |
| [REDACTED] | [REDACTED] | [REDACTED] | [REDACTED] | [REDACTED] | [REDACTED] | [REDACTED] |
| [REDACTED] | [REDACTED] | [REDACTED] | [REDACTED] | [REDACTED] | [REDACTED] | [REDACTED] |
| [REDACTED] | [REDACTED] | [REDACTED] | [REDACTED] | [REDACTED] | [REDACTED] | [REDACTED] |
| [REDACTED] | [REDACTED] | [REDACTED] | [REDACTED] | [REDACTED] | [REDACTED] | [REDACTED] |
| [REDACTED] | [REDACTED] | [REDACTED] | [REDACTED] | [REDACTED] | [REDACTED] | [REDACTED] |
| [REDACTED] | [REDACTED] | [REDACTED] | [REDACTED] | [REDACTED] | [REDACTED] | [REDACTED] |

SEE NOTES BELOW FOR ADDITIONAL DETAILS:

1. F_q corresponds to radial uncertainty, F_b relates to axial uncertainty.
2. A 10% uncertainty in channel thickness was assumed for the UMLRR fuel. The values given for the UMLRR fuel correspond to the worst-case observed uncertainty in ΔT_{water} and ΔT_{clad} , respectively.
3. In general, the total hot channel factor is computed assuming uncorrelated uncertainties. For F_h , the channel thickness and flow rate factors are combined statistically and the heat transfer component is treated as a multiplicative (safety) factor.

4.6.1 Steady State Operating Limits

For safety-related studies, some limiting criteria needs to be established that will guarantee safe operation of the reactor at all times. As stated previously, for the UMLRR, the limiting criteria for both steady state operation and for credible off-normal protected transients is the onset of nucleate boiling (ONB) point. Since the coolant saturation temperature for roughly ■ ft of water above the core (i.e. for $P = \blacksquare$ psia or ■ MPa) is about ■ °C, the ONB point is typically reached at a plate surface temperature of ■ – ■ °C depending on the heat flux and flow conditions. Thus, if the maximum clad temperature never exceeds ■ °C, there is no possibility of clad or fuel damage in the system. Fuel damage occurs with blister formation, and the blister threshold temperature for both uranium silicide and uranium aluminide fuel is above ■ C,^{xxxi} so a maximum clad temperature of ■ C guarantees that fuel damage will not occur.

For forced flow steady state operation, a relationship between the reactor power and the pump flow rate at which the onset of nucleate boiling (ONB) point is reached needs to be established. Similarly, for steady state natural convection operation, the power level where ONB occurs also needs to be determined. The goal purpose in both cases is to assure that the UMLRR nominal operating point is well within the ONB limits for both forced and free convection operation.

As discussed previously, the NATCON and PLTEMP codes were used to obtain the steady state ONB conditions for the UMLRR. The models are relatively simple, requiring such factors as a description of the fuel and channel geometry, the reference pressure and temperature, the radial peaking factor and relative axial power profile, and a set of appropriate hot channel factors. All the calculations used the geometry parameters given in Table 4-1, a radial peaking

factor of 2.1, the axial power profile shown in Figure 4-14, and an inlet temperature of [REDACTED]⁰F ([REDACTED]⁰C). A full series of cases was run for a [REDACTED]-element core with UMLRR fuel with and without the hot channel factors shown in Table 4-11. Several cases were also completed for the WPI fuel but, in all cases, these were not limiting because of the greater number of fuel plates per assembly ([REDACTED] for the WPI fuel vs. [REDACTED] for the UMLRR fuel). Subsequently, there was no need to generate a full data set.

Summary results from the PLTEMP forced flow calculations are shown in Figure 4-16, along with an indication of the margin associated with normal operation at [REDACTED] MW with a pump flow rate of [REDACTED] gpm. This figure contains curves for both best-estimate “nominal” analysis and with the hot channel factors included to account for uncertainties in the system. The lower curve with the system uncertainties included is considered the upper limit for steady state operation below the ONB point. As shown, for a nominal flow rate of [REDACTED] gpm, operation at [REDACTED] MW gives a margin to ONB of over [REDACTED]

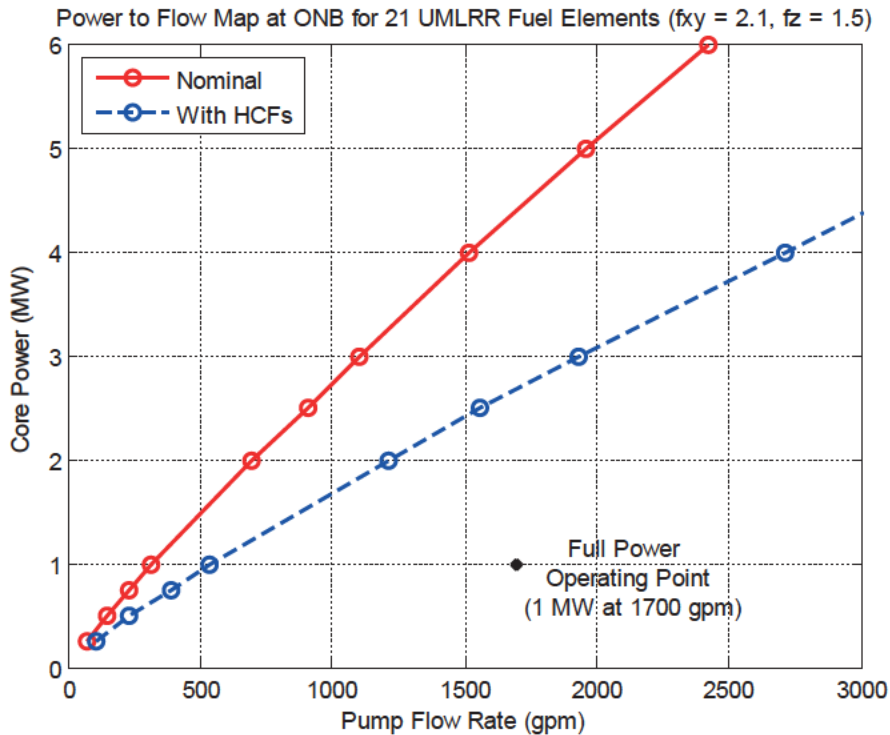


Figure 4-17: ONB power to flow map for steady state operation in the UMLRR

It was noted previously that the UMLRR fuel was more limiting than the WPI fuel due to the smaller number of fuel plates per assembly. Table 4-12 demonstrates this behavior

quantitatively for a single power level. In particular, it shows the ONB flow rate for a power of [REDACTED] MW for both the UMLRR and WPI fuel element designs. As seen here, for the case with the engineering hot channels factors HCFs listed in Table 4-11, the WPI fuel requires a pump flow rate of at least 1312 gpm to stay below the ONB point, whereas the UMLRR element requires about 1561 gpm of flow to prevent localized boiling from occurring. This behavior whereby the UMLRR fuel requires a higher flow rate to stay below ONB is similar for all cases (with and without HCFs). Thus, the UMLRR fuel clearly presents a more limiting scenario. As a result, the limiting steady-state ONB power to flow curve shown in Figure 4-16 only includes data from the UMLRR fuel cases.

Table 4-12: ONB flow rate data for P = 2.5 MW for both UMLRR and WPI fuel.

| Case Description | UMLRR Fuel | WPI Fuel |
|--|----------------|----------------|
| nominal best-estimate calculation | [REDACTED] gpm | [REDACTED] gpm |
| with hot channel factors from Table 11 | [REDACTED] gpm | [REDACTED] gpm |

Concerning steady-state free convection operation, Table 4-9 summarizes the results from the NATCON ONB runs for the 21-element core models. Here again the UMLRR fuel is more limiting than the WPI design and the cases with the hot channel factors (HCFs) are clearly more restrictive. These data suggest that the UMLRR could operate in natural convection mode below the ONB point with a power level as high as [REDACTED] kW. This power level is much larger than the nominal [REDACTED] kW operating limit which has been chosen to reduce the production and subsequent escape of nitrogen-16 from the pool surface. The free flow operating limit of [REDACTED] kW gives a margin to ONB of about 2.5.

Table 4-13: ONB power levels for free flow for both UMLRR and WPI fuel

| Case Description | UMLRR Fuel | WPI Fuel |
|--|---------------|---------------|
| nominal best-estimate calculation | [REDACTED] kW | [REDACTED] kW |
| with hot channel factors from Table 11 | [REDACTED] kW | [REDACTED] kW |

Operating Limits for Various Transient Scenarios

It should be emphasized that Figure 4-16 is only of limited use, since it only sets constraints for operation at steady state. It does not address the consequences of a transient off-normal condition that is initiated from critical steady state operation. As noted previously, there

are a series of credible accident scenarios that must be analyzed and, in practice, it is the behavior of these accident sequences that set the real operating limits on the reactor. In most cases, the various initiating events can be classified into either a reactivity-induced or a flow-induced transient. The PARET code is utilized to model and evaluate these situations. In particular, since the limiting criteria for both steady state operation and for credible off-normal protected transients within the UMLRR is the onset of nucleate boiling (ONB) point, the outcome is to establish a range of operation such that ONB does not occur during a worst-case reactivity or flow transient. Since a variety of transients can occur, including both rapid and ramp reactivity additions and pump-off and pump-on events, a full range of possibilities is evaluated. The most limiting sequence is the used to place actual operating constraints on the UMLRR. Each of the four events (fast reactivity addition, ramp reactivity insertion, loss of flow scenario, and cold water insertion event) are analyzed separately in Chapter 13.

ⁱ “Amendment No. 14 to Facility Operating License No. R-125 for the University of Massachusetts Lowell Research Reactor,” NRC Docket No. 50-223 (June 2011).

ⁱⁱ <http://www.ceradyne.com/products/nuclear/bortec-mm-c.aspx>

ⁱⁱⁱ Personal communication from G. Arsenaault, Ceradyne Sales Engineer to T. M. Regan, UMass-Lowell Reactor Engineer (Aug. 2014).

^{iv} “Amendment No. 14 to Facility Operating License No. R-125 for the University of Massachusetts Lowell Research Reactor,” NRC Docket No. 50-223 (June 2011).

^v J. R. White and J. Marcyoniak, “Comparison of the WPI and UMLRR Fuel Assembly Models,” UMass-Lowell internal project documentation (July 2011).

^{vi} J. E. Matos and K. E. Freese, “Analyses for Conversion of the Worcester Polytechnic Institute Reactor from HEU to LEU Fuel,” ANL RERTR Program (August 1987).

^{vii} J. Phelps et. al., “Final Safety Analysis Report for the Lowell Technological Institute Reactor,” Lowell Technological Institute Nuclear Center (Sept. 1973).

^{viii} “Report on the HEU to LEU Conversion of the University of Massachusetts Lowell Research Reactor,” submitted to the US Nuclear Regulatory Commission in fulfillment of Amendment No. 12 to License No. R-125 (April 2001).

^{ix} J. R. White and L. Bobek, “Startup Test Results and Model Evaluation for the HEU to LEU Conversion of the UMass-Lowell Research,” 24th International Meeting on Reduced Enrichment for Research and Test Reactors (RERTR 2002), San Carlos de Bariloche, Argentina (Nov. 2002).

^x VENTURE-PC - A Reactor Analysis Code System,” distributed through the Radiation Safety Information Computational Center, CCC-654 (1997).

^{xi} “MCNP6.1: Monte Carlo N-Particle Transport Code System,” distributed through the Radiation Safety Information Computational Center, CCC-810 (Aug. 2013).

^{xii} SCALE: A Comprehensive Modeling and Simulation Suite for Nuclear Safety Analysis and Design,” ORNL/TM-2005/39 Version 6.1, distributed through the Radiation Safety Information Computational Center, CCC-785 (July 2011).

^{xiii} NATCON, PLTEMP, and PARET code distribution from the RERTR Program at Argonne National Laboratory (ANL) (1988 and 1999). Also see R. S. Smith and W. L. Woodruff, “Thermal Hydraulics Analysis and Safety Margins for Natural Convection Cooled Research Reactors,” RERTR Program, Argonne National Laboratory, (1987) and K. Mishima, K. Kanda, T. Shibata, “Thermal Hydraulic Analysis for Core Conversion to the Use of Low Enriched Uranium Fuels in the KUR,” Research Reactor Institute, Kyoto University, KURRI-TR-258 (1984).

-
- ^{xiv} A. L. Stevens, "Thermal Hydraulic Analysis of the University of Massachusetts Lowell Research Reactor," M.S. Thesis in Energy Engineering (Nuclear Option), UMass-Lowell, (Dec. 2002).
- ^{xv} W. L. Woodruff and R. S. Smith, "A Users Guide for the ANL Version of the PARET Code, PARET/ANL (2001 Rev.)," ANL/RERTR/TM-16 (March 2001). Also see C. F. Obenchain, "PARET, A Program for the Analysis of Reactor Transients," Phillips Petroleum Company, AEC Research and Development Report (Jan. 1969). This code package is distributed through the Radiation Safety Information Computational Center, PSR-516 (Feb. 2002). Note also that the pareth2o.exe code, as distributed, incorrectly refers to the D2O properties library -- so a temporary fix was made by renaming the H2O library (pareth2o.lib) to paret2o.lib.
- ^{xvi} T. P. Michaud, "Implementation of the Inverse Kinetics Method for Reactivity Calculations at the UMLRR," M.S. Thesis in Energy Engineering (Nuclear Option), UMass-Lowell, (Dec. 2011).
- ^{xvii} J. R. White, "Reactivity Coefficients for Use in UMLRR Transient Analyses: Quantitative Analysis and Partial Validation via Comparison with Actual Reactor Data," UMass-Lowell internal project documentation (August 2015).
- ^{xviii} J. R. White, "Reactivity Coefficients for Use in UMLRR Transient Analyses: Quantitative Analysis and Partial Validation via Comparison with Actual Reactor Data," UMass-Lowell internal project documentation (August 2015).
- ^{xix} J. R. White, "Reactivity Coefficients for Use in UMLRR Transient Analyses: Quantitative Analysis and Partial Validation via Comparison with Actual Reactor Data," UMass-Lowell internal project documentation (August 2015).
- ^{xx} J. R. White, "Reactivity Coefficients for Use in UMLRR Transient Analyses: Quantitative Analysis and Partial Validation via Comparison with Actual Reactor Data," UMass-Lowell internal project documentation (August 2015).
- ^{xxi} J. R. White, "Updated Peaking Factors for Use in the UMLRR Safety Analysis," UMass-Lowell internal project documentation (July 2015).
- ^{xxii} "FSAR Supplement for Conversion to Low Enrichment Uranium (LEU) Fuel," Document submitted for review by the NRC for conversion of the UMass-Lowell Research Reactor (May 1993).
- ^{xxiii} Letter from J.R. Matos, RERTR Program at ANL, to J.R. White, UMass-Lowell (Jan. 1993).
- ^{xxiv} D. Biswas, W. P. Kovacic, and J. R. White, "Evaluation of the Delayed Neutron Importance Factor with ENDF/B-V Data," Trans. Am. Nucl. Soc., 59, 318 (June 1989).
- ^{xxv} M. Pike, "Expanding Local Capabilities for the Computational Analysis of the UMass- Lowell Research Reactor," M.S. Thesis in Energy Engineering (Nuclear Option), UMass-Lowell (May 2013).
- ^{xxvi} T. M. Regan, "Control Blade Position and Timing During UMLRR SCRAM," UMass-Lowell Radiation Laboratory internal project documentation (Aug. 2015).
- ^{xxvii} "FSAR Supplement for Conversion to Low Enrichment Uranium (LEU) Fuel," Document submitted for review by the NRC for conversion of the UMass-Lowell Research Reactor (May 1993).
- ^{xxviii} J. R. White, "Steady-State Thermal Hydraulic Analyses in Support of the HEU to LEU Conversion Effort," UMass-Lowell internal project documentation (Nov. 1991).
- ^{xxix} "FSAR Supplement for Conversion to Low Enrichment Uranium (LEU) Fuel," Document submitted for review by the NRC for conversion of the UMass-Lowell Research Reactor (May 1993).
- ^{xxx} J. E. Matos and K. E. Freese, "Analyses for Conversion of the Worcester Polytechnic Institute Reactor from HEU to LEU Fuel," ANL RERTR Program (August 1987).
- ^{xxxi} "Safety Evaluation Report related to the Evaluation of Low-Enriched Uranium Silicide-Aluminum Dispersion Fuel for Use in Non-Power Reactors, NUREG-1313," U. S. Nuclear Regulatory Commission (NRC) (July 1988).

Table of Contents

5 Reactor Coolant Systems..... 5-1

5.1 Summary Description..... 5-1

5.2 Primary Coolant System..... 5-2

5.3 Secondary Coolant System..... 5-4

 5.3.1 Cooling Tower..... 5-5

5.4 Primary Coolant Cleanup System 5-6

 5.4.1 Deionizer Unit..... 5-6

5.5 Primary Coolant Makeup Water System..... 5-7

5.6 Nitrogen-16 Control System 5-8

5.7 Auxiliary Systems Using Primary Coolant 5-8

Table of Figures

Figure 5-1: Primary Piping System Schematic..... 5-9

Figure 5-2: Secondary Piping Schematic..... 5-10

Figure 5-3: Make-Up System Piping Schematic 5-11

Figure 5-4: Demineralizer Piping Schematic..... 5-12

Figure 5-5: Clean-up Piping Schematic 5-13

Table of Tables

Table 5-1: Pool Penetration List 5-4

5 Reactor Coolant Systems

5.1 Summary Description

The reactor is located in an open pool containing, approximately, [REDACTED] gallons of high purity water occupying a volume of [REDACTED] by [REDACTED] with a [REDACTED] depth. The pool water is part of the

primary coolant loop and serves as moderator, coolant, and shielding. The high purity of the primary coolant is maintained by a cleanup system, which operates continuously to remove impurities and maintain a neutral pH and conductivity. Municipal water is admitted to the cleanup system before entering the primary coolant loop in order to maintain the reactor pool water at a certain level. Heat is transferred from the primary coolant to the secondary system through a heat exchanger. Heat removal from the secondary system is accomplished with a cooling tower located near the exterior of the reactor containment building.

5.2 Primary Coolant System

The primary coolant system functions to remove heat and maintain core temperature below a predetermined level and also serves as the neutron moderator and provides shielding. The primary system comprises the reactor pool, primary coolant pump, holdup tank, heat exchanger, retention tank, and all associated piping.

The reactor is located in the reactor pool. The reactor pool is part of the primary coolant loop and is comprised of two principle sections: the stall pool and the bulk irradiation pool. Primary coolant connections are located at the end of each section and are referred to as power positions. Power position No. 1 is located in the stall pool and power position No. 2 is located in the bulk irradiation pool. The primary coolant connections allow two locations for the reactor to be operated under forced convection. When the reactor is physically coupled to the primary coolant connections, full power operations are permitted under forced convection cooling.

Two modes exist for operations with forced convection: downcomer mode and cross-stall mode. In downcomer mode, cooling water is supplied to the core by a 10” aluminum line connected to the inlet flow channel forming one side of the suspension frame. Water is fed from the flow channel into a plenum over the core. From here it is forced down through the core flow channels into a plenum below the core. From this plenum, it flows up through the outlet flow channel forming the other side of the suspension frame, which then connects to another 10” aluminum line. Finally, the primary coolant passes through the pump room systems, completing the loop. In cross-stall mode, after the primary coolant has left the pump room systems, it is not fed into the inlet flow channel on the suspension frame, but, instead, is discharged from primary coolant connection into the pool section not occupied by the reactor. The cross-stall mode is the

preferred method of forced convection cooling as it reduces vibrations to the core suspension structure.

The reactor is also capable of operation under natural convection cooling, at any location within the reactor pool. In natural convection, the flow of primary coolant is reversed. Heated coolant flows into the inlet channel. A riser gate near the top of the inlet channel opens to facilitate convection to the pool water. Heated coolant is replaced with coolant from the outlet channel. Under natural convection cooling, reactor power is limited to [REDACTED]. The large volume of water in the reactor pool provides an adequate heat sink and the level of N-16 detected at the surface of the pool is negligible for [REDACTED] natural convection operations.

Since the reactor is capable of operating in different locations within the reactor pool under different methods of cooling, a series of limit switches enforces proper alignment. If proper alignment is not achieved, the electromagnets will not engage the blades. Five limit switches are located on the reactor bridge. One switch is located near a cogwheel for bridge movement. It prevents bridge movement while the reactor is operating. Two others are located on the outer sides of the bridge across the narrow length of the reactor pool. They are associated with the reactor power positions and, therefore, prevent operations above [REDACTED] if they are not properly aligned with the primary coolant connections. The last two limit switches on the reactor bridge are located along the stainless steel shaft that extends from the top of the bridge to the top corner of the primary coolant channels and are also associated with coolant channel alignment. The pump room also contains five limit switches associated with the primary coolant system. Each of the four gate valves (P-1 through P-4) on the pool inlet and outlet lines possesses a limit switch for determining coolant modes. A switch on one of the two valves leading to the primary retention tank through the primary piping prevents syphoning of the reactor pool while the reactor is operating. A sixth limit switch exists on the cleanup piping leading to the retention tank, but its purpose is to prevent syphoning of the reactor pool and is not associated with reactor cooling modes.

A number of radiation detectors are located in close proximity to the primary coolant system, both in the pump room and on the third floor near the reactor pool. Located on the underside of the reactor bridge above the surface of the pool, an ion chamber is installed. As it is attached to the reactor bridge, the detector will always be located directly above the core. Also

above the surface of the pool, but located in the bulk irradiation pool above the primary coolant connections, is a GM detector. Not far from this detector a second GM is located in the exhaust plenum near the bulk irradiation pool end of the reactor bay. A constant air monitor (CAM) capable of reading alpha and beta radiation is stationed between the reactor pool and the control room. In the pump room, a neutron detector is position above the primary piping located between the primary coolant pump and the holdup tank. A GM detector located on the inner containment wall provides a general dose rate in the vicinity of the pump room. All of these detectors are read from the control room and are part of the ARM system. The detectors located in the basement can also be read locally from the PC located near the primary coolant cleanup system.

Numerous penetrations in the pool allow for, purposes not limited to, areas for experiments to be performed, channels for coolant to circulate, and piping for primary to be circulated. The penetrations are listed in Table 5-1.

Table 5-1: Pool Penetration List
Pool Penetration List

| Name/Description | Distance From Core* | Distance from Pool Floor** |
|------------------------------------|---------------------|----------------------------|
| Water Level/Pool Gutter | █ -0" | █ -1" |
| Centerline of Core | █ -0" | █ -1" |
| 8" Beam Port | ~█ -0" | █ -0.5625" |
| 6" Beam Port | ~█ -0" | █ -0.4375" |
| Hot Cell Transfer Port | █ -11" | █ -0" |
| Hot Cell Transfer Port - Fill Line | █ -4" | █ -5" |
| Pneumatic Transfer Tubes (In Use) | █ -0" | █ -1" |
| Pneumatic Transfer Tubes (Spare) | █ -0" | █ -1" |
| Primary Piping Connections | █ -8.75" | █ -9.75" |
| Pool Skimmer (In) | █ -11" | █ -0" |
| Pool Skimmer (Out) | █ -5" | █ -6" |
| Medical Embedment | █ -6" | █ -7" |

*Distances are based on centerline to centerline measurements

**Measurements are made from Pool Floor to centerline of "Name/Description"

5.3 Secondary Coolant System

The secondary loop functions to transfer heat from the primary coolant in the heat exchanger to the atmosphere at the cooling tower. The secondary cooling water is neither activated by direct contact with the reactor core, nor contaminated by mixture with primary coolant in the heat exchanger. This isolation allows the heat being carried by the secondary cooling water to be reasonably and safely dissipated by evaporation of a portion of the water in a conventional cooling tower. A substantial amount of makeup water is required to replenish the resulting loss to the atmosphere. Losses are made up through a valve controlled from the PCS. The secondary cooling loop includes the heat exchanger, cooling tower, secondary pump, and temperature and flow sensors.

5.3.1 Cooling Tower

The cooling tower is a Baltimore Air Coil, model PT2-1009A-2M2, counter-flow, induced-draft, axial fan system. The unit consists of two cells with each cell housing one fan rated for an air flow rate of [REDACTED] CFM. At a wet bulb temperature of [REDACTED] the cooling tower can lower water temperature from [REDACTED] at a flow rate of [REDACTED] GPM. The total cooling capacity of the unit is 537 nominal tons.

The control system for the cooling tower is located in the basement stairwell of the containment building. It provides efficient temperature control of the secondary cooling system water and is configurable for automatic or manual control of the cooling tower fans.

The temperature of the secondary water leaving the cooling tower is measured by a passive positive temperature coefficient (PTC) sensor located in the secondary piping entering the pump room. The sensor output is connected to the Electronic Temperature Control Module (C1).

Selecting AUTO on the E7 Bypass Control Panel Control Keypad places the system in an automatic mode. In auto mode, the desired secondary coolant temperature is adjusted using the set-point dial on C1. The actual secondary coolant temperature and the set-point temperature are displayed on the Display Module (C5). When the exit temperature is above the set-point temperature, the C1 module relay is energized, which in turn energizes the lead fan via the variable frequency drive (VFD) controller. The Proportional Stage Module (C2) throttles the

VFD to vary the lead fan motor speed and adjust the water cooling capacity. If the VFD reaches the maximum frequency (motor speed) and the exit temperature continues to increase, the Temperature Slave Stage Module (C3) relay is energized, which in turn energizes the lag fan via the second VFD controller. The second Proportional Stage Slave Module (C4) throttles the second VFD to vary the lag fan motor speed and adjust the water cooling capacity.

Selecting HAND on the E7 Bypass Control Panel Digital Operator places the system in a manual mode. In HAND mode...

5.4 Primary Coolant Cleanup System

The cleanup system removes impurities that enter into the reactor pool including those resulting from water reacting with its environs and those caused by mechanical wear and damage. The cleanup system includes a pump, a US Filter VP Mixed Bed Deionizer Unit, PVC and aluminum piping, manual and air-operated valves, a UV light, and a post filter. During normal operations, the cleanup pump draws primary coolant from the primary coolant piping at a point after the heat exchanger. The primary coolant is passed through the demineralizer vessel, the UV light, and the post filter before it is discharged back into the pool at the third floor. A local PC with user-interface display is available for controlling the system and for providing status and controls for the various other pump room systems. All instrumentation signals are sent to the local PC and the control room process controls.

5.4.1 Deionizer Unit

The main component of the cleanup system is a mixed bed deionizer. It consists of the deionizer vessel, PVC piping, air-operated valves, and instrumentation panel. The air-operated valves on the unit are controlled by OPTO 22 digital control hardware and software. Air is supplied by the compressor located on the second floor of the containment building. The local instrument panel for the deionizer system contains air-operated valve control, OPTO 22 hardware, and display units for the measurement of the water's conductivity, temperature, flow rate, and pH. The deionizer vessel is a PVC lined single steel pressure vessel containing both cation and anion exchange resins. Municipal/Utility water is admitted by an air-operated valve to the cleanup system through the makeup system which allows for primary makeup and for periodic regeneration of the ion exchange resin.

Regeneration of the resin is done via the introduction of acid and caustic. The valve alignments necessary to complete the regeneration are controlled by the OPTO 22 controller or may be initiated manually. Each individual step in the system regeneration process must be initiated by an operator.

The cleanup system is located in the pump room of the containment building. Access to the [REDACTED] is through a set of [REDACTED]. A [REDACTED] on the door allows only individuals with a certain level of [REDACTED]. An ion chamber that is part of the Area Radiation Monitoring (ARM) system is located near the deionizer vessel and can be read at the local PC. This radiation monitor provides general dose rates in the immediate vicinity of the deionizer vessel. The cleanup post filter is located far downstream from the deionizer vessel, behind the wall that shields the hold-up tank and the reactor pool inlet and outlet piping.

5.5 Primary Coolant Makeup Water System

The makeup system provides the water required to fill and maintain the reactor pool at the proper level. Municipal water passes through a pressure regulator and backflow preventer, and then passes through a sediment cartridge filter and a carbon filter to provide preconditioning of the water. An air-operated valve admits this preconditioned water to a water softener before flowing into the cleanup system deionizer vessel. From the deionizer vessel, the makeup water follows the same path as when primary water passes through the cleanup system, including the particulate post filter and UV filter, before entering the pool.

The makeup system is in operation when the air-operated makeup valve is open. This valve can be controlled automatically via the control room process control system (PCS), or manually. In the default Auto mode, the PCS will shut down the cleanup pump, and open the makeup valve. In manual mode, the cleanup pump must be turned off before the makeup valve is opened. The makeup system can be monitored from the control room PCS, the pump room PC, and the cleanup system's local instrument panel.

5.6 Nitrogen-16 Control System

The primary control for decay of short-lived radionuclides (N-16 and O-19) produced in the primary coolant is the holdup tank. The holdup tank is an aluminum tank with a 3,000 gallon capacity that is part of the primary system. It is located in the pump room near the end of the bulk irradiation pool, which is opposite the pump room entrance.

Significant radiation levels are seen in the vicinity of the holdup tank during forced convection operations. To minimize radiation levels throughout the rest of the pump room, a wall [REDACTED] extends from the [REDACTED] wall to a distance just past the [REDACTED] tank to within a [REDACTED] feet of the [REDACTED] wall. The result is a large reduction in dose rates to the rest of the pump room allowing personnel to perform periodic checks and tests during forced convection operations.

5.7 Auxiliary Systems Using Primary Coolant

Water in the reactor pool provides passive cooling and shielding for some facilities. Located in the pool above each of the [REDACTED] beam ports, small diameter ports [REDACTED] the [REDACTED] wall in order to remove heat from the facility. The ports are aluminum lined, welded to the [REDACTED] and extend a very short length into the pool wall. Each beam port is also fitted with its own separate valve to supply demineralized water. The water is supplied to the beam ports through a common header, which has a solenoid controlled valve interlocked to prevent opening and flooding of the beam ports during reactor operations.

The thermal column section [REDACTED] cooled by natural convection from pool water that is allowed to enter into the [REDACTED] that surrounds the [REDACTED] cavity. The lead gamma shield, located at the front end of the thermal column extension facing the nuclear core, is cooled by natural convection to the reactor pool.

Legend

Valves:
Gate Check Globe Diaphragm Needle

Instruments:
Temperature Pressure Conductivity Flow Differential Pressure Orifice Plate

Primary Piping

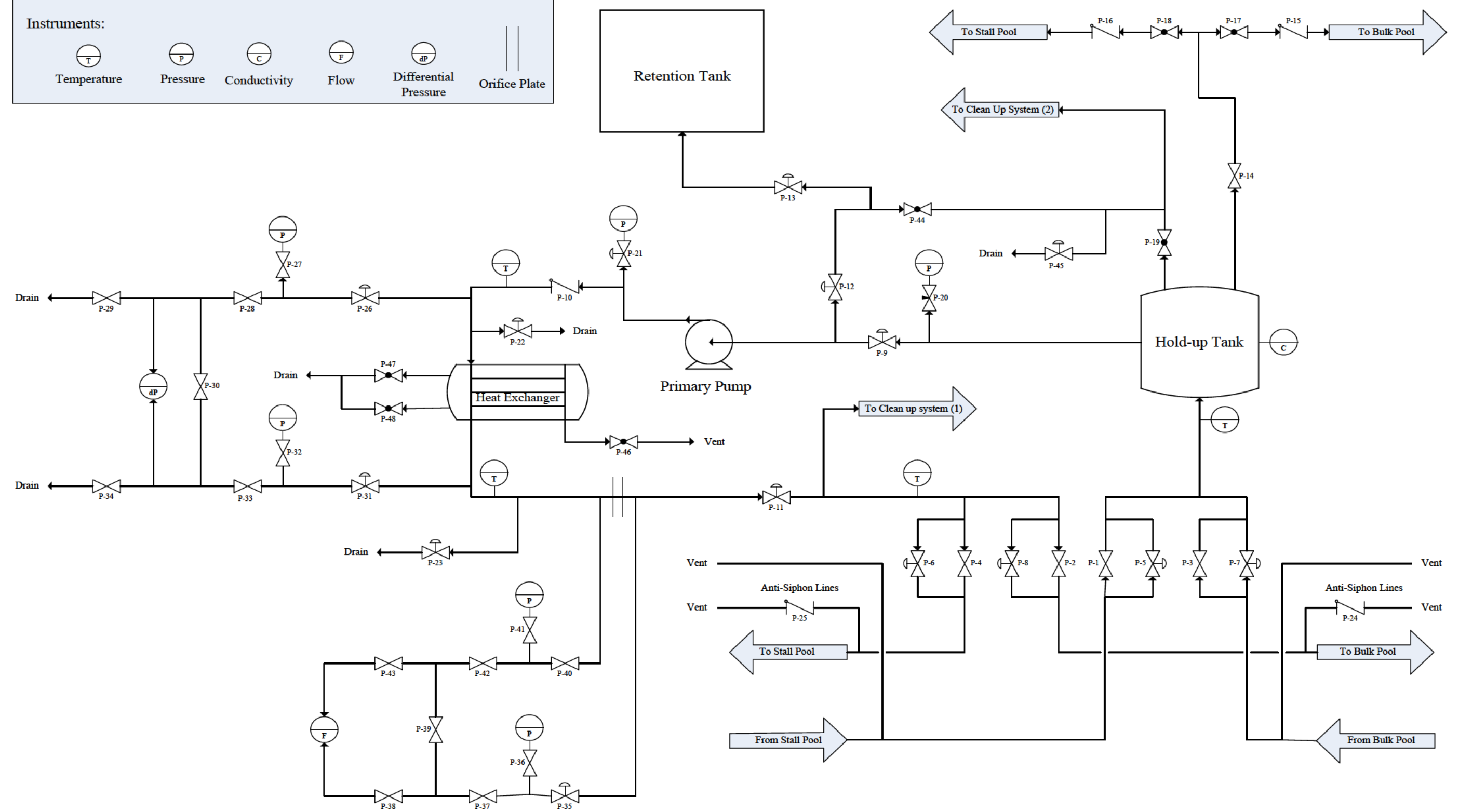


Figure 5-1: Primary Piping System Schematic

Secondary Piping

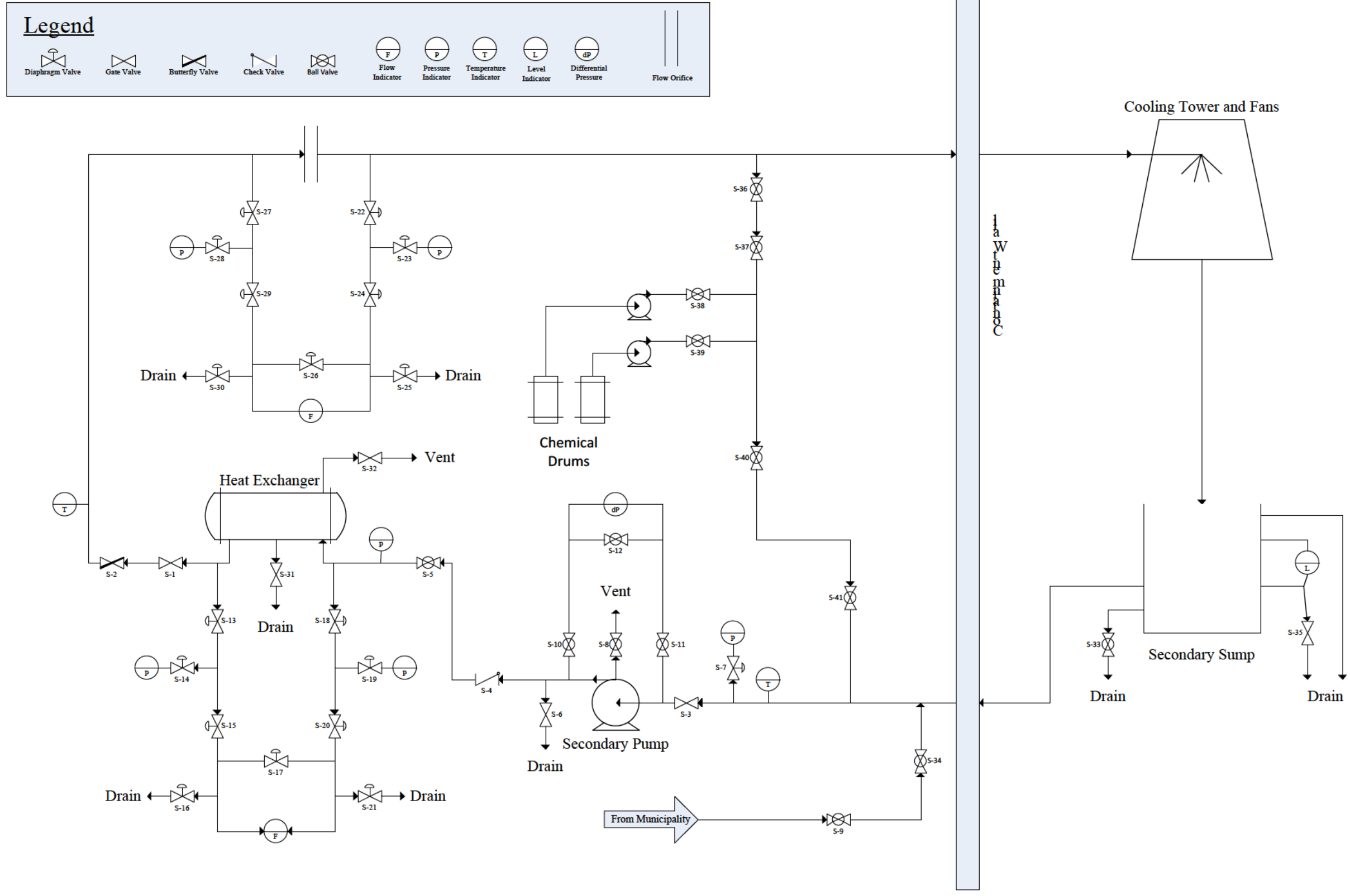


Figure 5-2: Secondary Piping Schematic

Make-Up Piping

Legend



Gate Valve



Diaphragm Valve



Check Valve



Ball Valve



Pressure

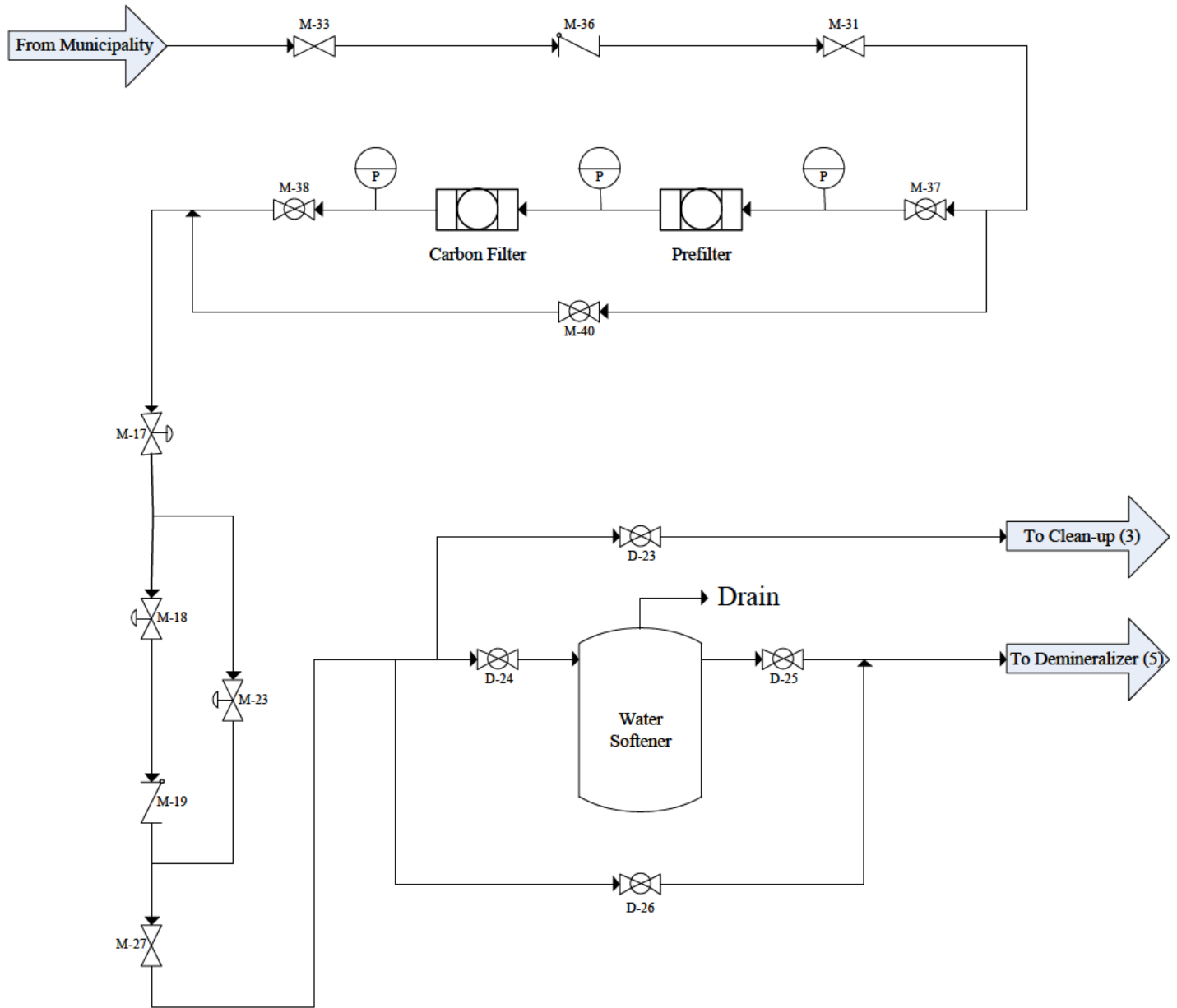


Figure 5-3: Make-Up System Piping Schematic

Demineralizer Piping

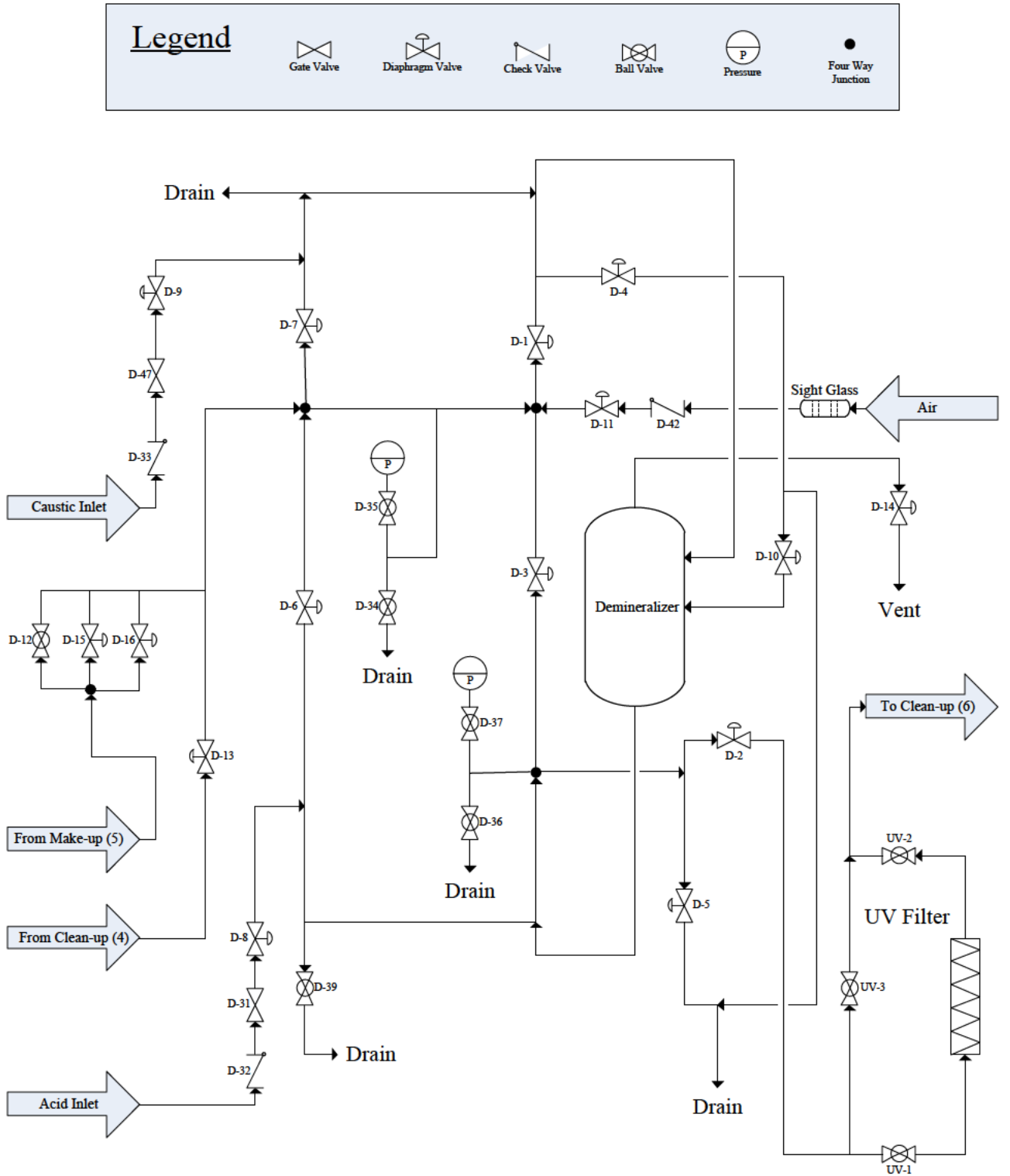


Figure 5-4: Demineralizer Piping Schematic

Clean-Up Piping

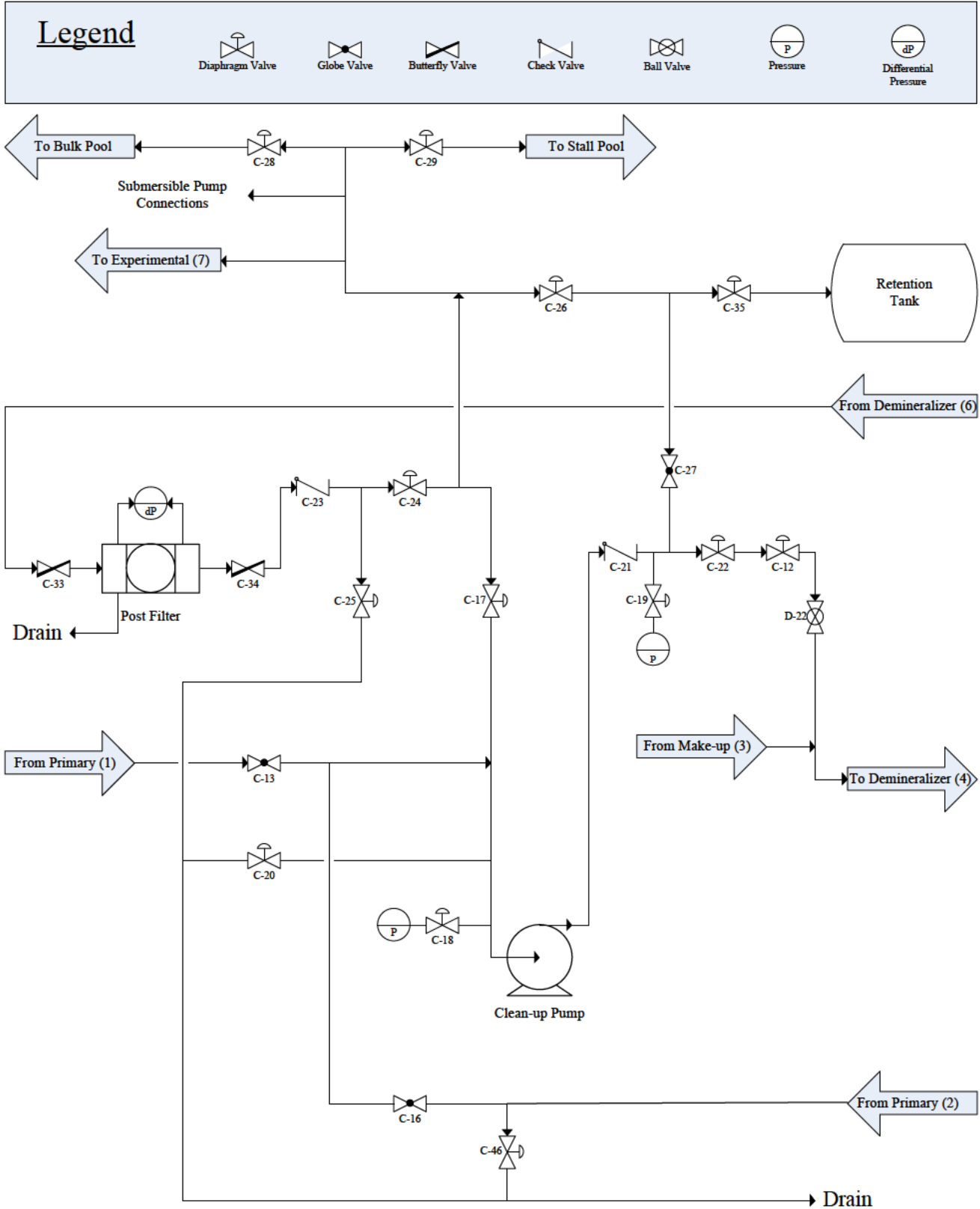


Figure 5-5: Clean-up Piping Schematic

Table of Contents

6 Engineered Safety Features..... 6-2

6.1 Summary Description..... 6-2

6.2 Containment Building Description..... 6-2

6.2.1 Penetrations..... 6-4

6.2.2 Ventilation Valves 6-7

6.2.3 System Operation..... 6-8

6.2.4 Emergency Exhaust System..... 6-10

6.2.5 Facility Filters 6-11

6.2.6 Containment Integrity with Over-pressure 6-11

6.2.7 Containment Integrity with Under-pressure 6-12

6.2.8 Acceptance Testing..... 6-13

6.3 Emergency Core Cooling System 6-15

6.4 References 6-15

Table of Figures

Figure 6-1: Reactor Containment Building Cutaway 6-3

Figure 6-2: Ventilation Schematic 6-6

Figure 6-3: 48-inch Diameter Ventilation Valve Design..... 6-7

Figure 6-4: 20-inch and 12-inch Diameter Ventilation Valve Design..... 6-8

6 Engineered Safety Features

6.1 Summary Description

Engineered Safety Features (ESFs) are designed to (1) prevent or mitigate the consequences of [REDACTED] [REDACTED] due to [REDACTED] g events, or (2) [REDACTED] [REDACTED] of any [REDACTED]. The principal engineered safety feature for the University of Massachusetts Lowell Research Reactor (UMLRR) is the reactor containment building and its associated ventilation system. A containment building functions to prevent or minimize any release of radioactive material to the environment, in addition to minimizing any dose from radiation across the containment boundary. Containment is an ESF typically associated with higher powered research reactors licensed to operate at [REDACTED] or greater. Containment is neither required nor necessary for any postulated credible reactor accident at a research reactor licensed to operate at only [REDACTED]. The results of the design bases events analyzed for the UMLRR in Chapter 13 show there are no credible reactor accidents that could lead to the release and dispersal of fission products. Nonetheless, the containment building offers unique [REDACTED] and [REDACTED] features beyond those associated with a confinement building. In [REDACTED] [REDACTED], the UMLRR containment isolation system is designed for automatic shutdown of the ventilation system and the actuation of the ventilation isolation valves. The UMLRR containment building is designed to maintain its integrity under normal and adverse conditions while providing access for electrical lines, water, conditioned air, and personnel.

6.2 Containment Building Description

The UMLRR containment building is a cylindrical welded steel shell with a flat bottom and a domed top. The flat bottom is lined with [REDACTED] inches of reinforced poured concrete and the cylindrical walls are lined [REDACTED] [REDACTED] inches of reinforced poured concrete to serve as a [REDACTED] and [REDACTED] [REDACTED] and to support a [REDACTED] polar crane. The inner clear diameter is nominally [REDACTED] ft. From the flat steel bottom to the highest point of the domed top, the distance is about [REDACTED] feet, of which the lower [REDACTED] feet are below grade as shown in Figure 6-1. The outside of the shell is painted with a red lead primer undercoat and a weather resistant finish coat. The domed or ceiling portion is insulated with [REDACTED]-inch sheets of fiberglass held in place by stud

welded pins and speed washers. The sheets are sealed on the underside with a finish coat of white lagging adhesive to provide a continuous vapor and dust barrier.

The design criteria include:

- (1) Design Pressure: Internal, [REDACTED] psi; External, [REDACTED] psi
- (2) Design Internal Volume: [REDACTED] cubic ft
- (3) Design Internal Temperature: [REDACTED] degrees Fahrenheit
- (4) Leak Rate: No more than [REDACTED] per [REDACTED] hours at [REDACTED] psig
- (5) Roof Live Load: [REDACTED] psf
- (6) Wind Load: [REDACTED] psf
- (7) Dead Load: [REDACTED] psf
- (8) Earthquake Load: Intensity [REDACTED] on the Modified Mercalli scale
- (9) Design Stresses: In accordance with the ASME Boiler and Pressure Vessel Code, Section 8, "Rules for Construction of Unfired Pressure Vessels."
- (10) Design analysis: Based on elastic analysis

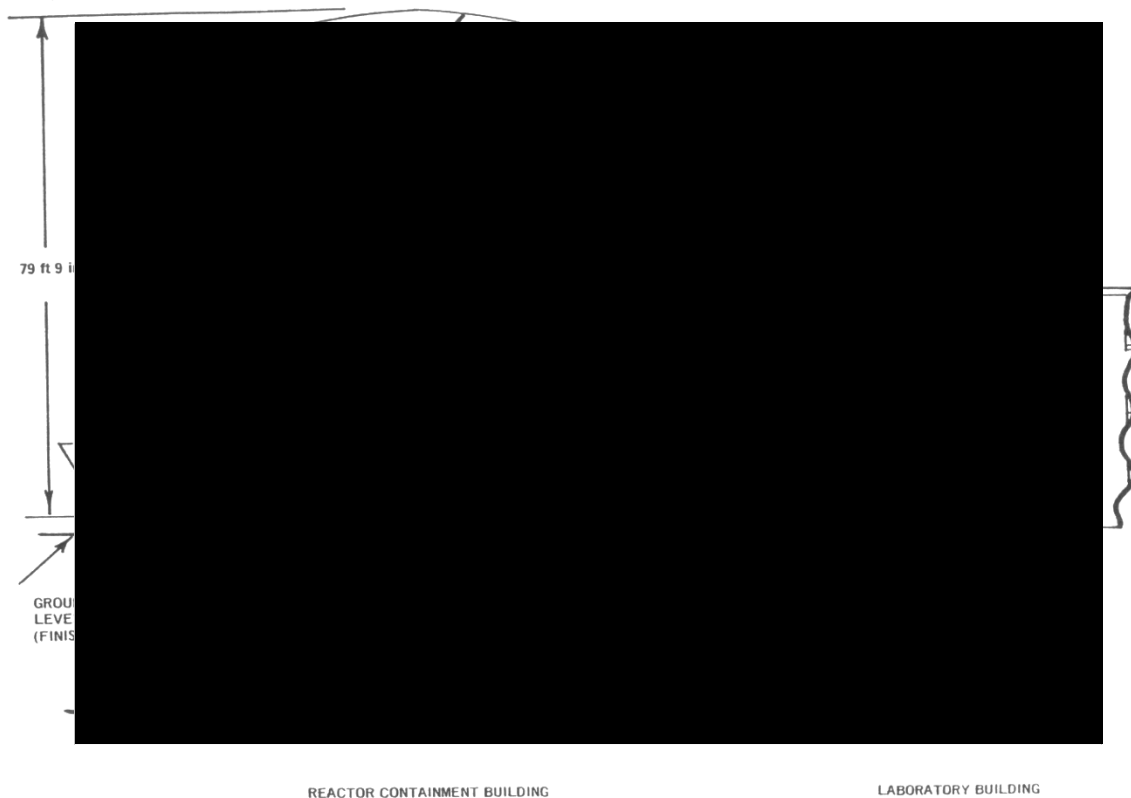


Figure 6-1: Reactor Containment Building Cutaway

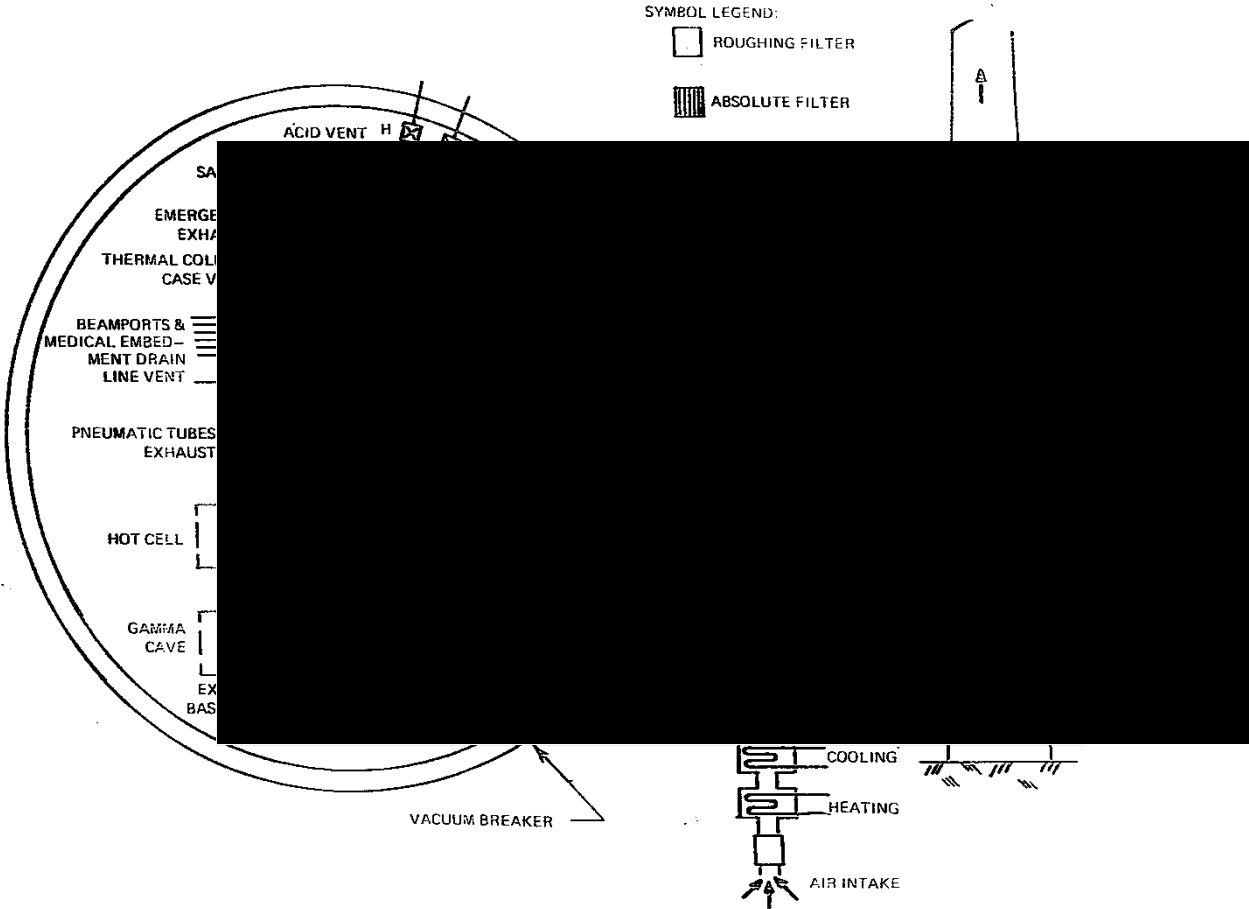


Figure 6-2: Ventilation Schematic

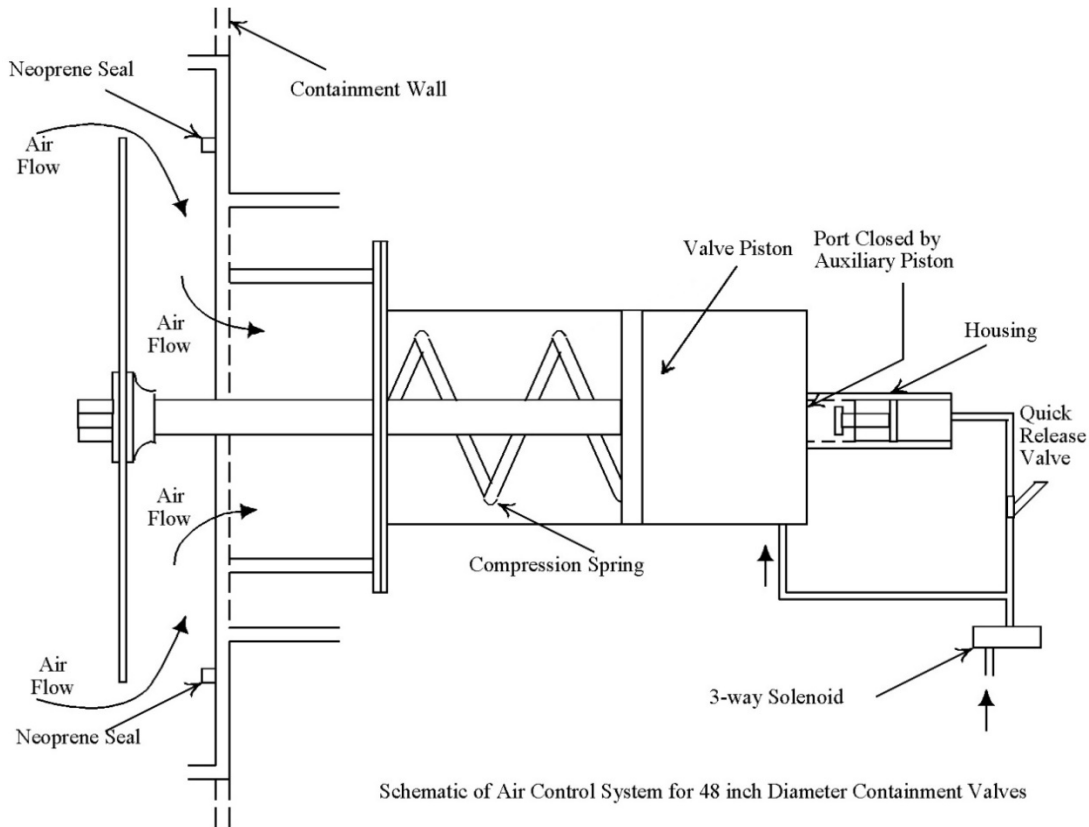
A number of penetrations exist for telephone and signal wires, and for power line conduits. One small penetration is made for comparison of containment building pressure with outside ambient pressure. Air compressors that serve pneumatically operated valves are on the same side of the shell as the valves, and the compressor that furnishes shop air and air-lock door air is inside containment, so that no high pressure air lines penetrate the containment building. Appropriate penetrations are made for the passage of secondary system water to and from the cooling tower.

All pipe and duct penetrations are welded to the steel shell or pass through special fittings designed to be airtight, which are welded to the shell. Signal wire penetrations make use of Pyle fittings, and power line conduits are sealed with Duxseal or similar material. Pipes which carry fluid are fitted with check valves, fail-safe valves which close on containment command, or deep traps, as appropriate. Some special purpose penetrations not in use during normal reactor

operation, such as the return lines to the primary pump and cleanup pump from the outside retention tank, are fitted with manual valves.

6.2.2 Ventilation Valves

The ventilation fail-safe blast valves are opened against a compression spring by compressed air, so that they close upon receipt of an appropriate signal from either the reactor operator, the radiation monitoring system, upon loss of electrical power, or upon loss of the supply air pressure. Air is supplied by a compressor located in the exterior fan room housing the main intake fan (designated AC-2 in Figure 6-2). Because the volume of air which must be exhausted to allow valve closure is larger for the large cylinders and pistons in the 48-inch diameter valves, a dual relief system is used (Figure 6-3). This allows a relatively small amount of air to be bled through a quick release valve from a secondary cylinder to relieve its piston which in turn opens a sizeable port in the main cylinder. This allows air to escape rapidly from the main piston, quickly placing the valve into the closed position. The [REDACTED] diameter and [REDACTED] diameter valves release their compressed air directly through a quick release valve (Figure 6-4).



Schematic of Air Control System for 48 inch Diameter Containment Valves

Figure 6-3: 48-inch Diameter Ventilation Valve Design

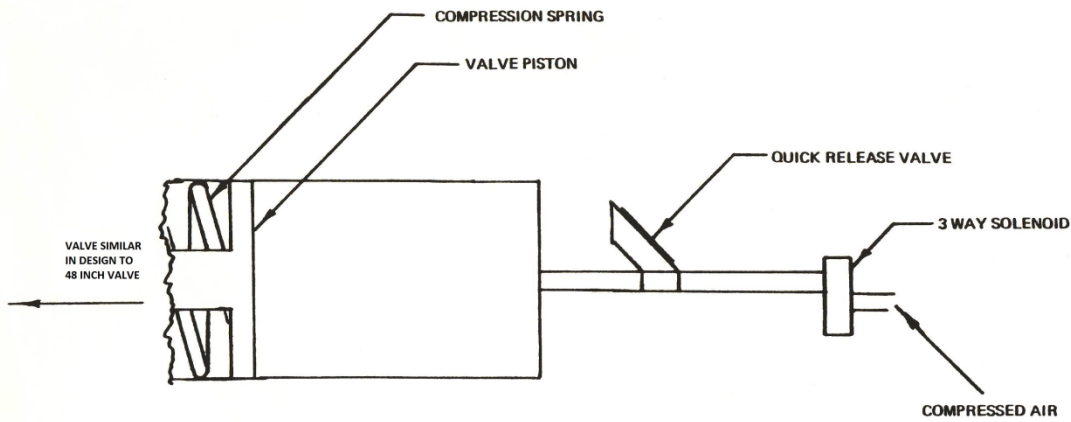


Figure 6-4: 20-inch and 12-inch Diameter Ventilation Valve Design

On all the blast valves, the valve seat is steel on neoprene and is made with a no-wipe contact to minimize wear by abrasion. Closure times are typically less than 1 second. The valves seat in a direction such that building internal overpressure assists in making the seal, as shown in Figure 6-3.

Normal operation of the ventilation system and valves is commanded from the control room process controls system (PCS). A bypass control panel for maintenance purposes is located in the AC-2 fan room for manual operation of the valves. The bypass controls have key locked switches.

6.2.3 System Operation

During normal operations, air is brought into the containment building by the intake blower through valve A at a nominal rate of [REDACTED] cubic feet per minute and exhausted out by the exhaust blower, nominally, at [REDACTED] cubic feet per minute through valves B and C to the [REDACTED] stack (Figure 6-2). The difference in flow rates maintains the negative containment building pressure (about 0.1 inch water column) relative to atmospheric pressure. The objective is to have “in” leakage rather than “out” leakage through the containment during normal operation so that all building exhaust is through the stack.

Additionally, each experimental facility is provided with its own separate exhaust capability. The experimental facility blowers include the gamma cave, hot cell, facilities, and

pneumatic tubes. While the gamma cave, hot cell, and pneumatic tubes blowers are dedicated to their own respective facility, the facilities blower services the beam ports and thermal column. The experimental facility blowers are operated at the discretion of the reactor operator. The emergency exhaust system is not operating during normal conditions, but is kept in an automatic mode capable of operating as described in the next section. The emergency exhaust system also has manual capability to allow for the performance of checks and operation at the discretion of the reactor operator.

Closure of the reactor ventilation system is initiated upon receipt of a number of signals, but it responds the same way to all signals. This response is called the General Reaction in the Ventilation System (GRVS). When the GRVS condition is activated, two major events occur (refer to Figure 6-2):

- (1) Valves A, B, C, E, G, and H close and valve F opens. These are the fail-safe positions of the valves. Valve-F is a bypass valve that allows the air flow from the main intake fan (designated AC-2 in Figure 6-2) to flow up the stack for dilution purposes. Clearance of the GRVS signal opens valves G and H, but the remaining valves operate only after the reactor operator re-starts the main exhaust fan (designated EF-12 in Figure 6-2).

- (2) The main exhaust fan and the four experimental facility blowers cease to operate. The main intake fan continues to operate, except for the case where electrical power is lost. Clearance of the GRVS signal does not reactivate the affected fans. The reactor operator must re-start the fans.

Signals which achieve a general reaction in the ventilation system (GRVS) are as follows:

- (1) Activation of a Local Radiation Emergency Alarm or General Radiation Emergency Alarm from the Area Radiation Monitoring System (see Section 7.7)
- (2) Manual control by the reactor operator
- (3) Loss of electrical power

6.2.4 Emergency Exhaust System

An emergency exhaust system draws air through charcoal filters along with absolute filters into a separate duct through a 12-inch blast valve in the containment wall. The duct connects to the main exhaust down-stream from all other valves in order to allow passage up the stack. The emergency exhaust blower (designated EF-14 in Figure 6-2) is located above the sample preparation area on the third level of the containment building and is rated at [REDACTED] cubic feet per minute. The emergency exhaust operates independently and is not affected by a GRVS signal. It responds automatically through the Process Control System by the measurement of pressure differentials or can be manually controlled by the reactor operator.

Normally the emergency exhaust will be in the automatic mode during reactor operation. In this mode, emergency exhaust fan starts and its associated valve (valve-D) opens if the differential pressure between the containment building and ambient outside pressure reaches or exceeds a positive 0.25 +/- 0.05 inch water column. Operation continues until either:

- (a) the differential pressure drops to negative 0.25 +/- 0.05 inch water column, or,
- (b) the differential pressure rises to or exceeds positive 0.50 +/- 0.05 inch water column.

If either condition is met, the emergency exhaust fan stops and valve D closes. If condition (a) is met, the emergency exhaust remains shut down unless the differential pressure again rises to a positive 0.25 +/- 0.05 inch water column. If condition (b) is met, the emergency exhaust remains shut down until the pressure drops to a positive 0.50 +/- 0.05 inch water column, at which point the emergency exhaust fan starts and valve D opens.

The emergency exhaust system is intended to relieve small overpressures accompanied by airborne radioactivity in the containment building by passing contaminated air through high efficiency particulate filters and then through charcoal filters before releasing the air to the stack. Emergency exhaust air carried to the stack is diluted by the high volume of air being fed up the stack from the main intake supply fan through the bypass valve F.

Following a substantial pressure surge, unloading of the excess pressure through the charcoal filter is prohibited since the capacity and effectiveness of the filter is not intended for large volume releases. Thus, an overpressure in the building of greater than a half inch water column prohibits release through the stack, and full reliance is placed on containment.

6.2.5 Facility Filters

The four experimental facilities exhaust blowers, the emergency exhaust system, and the fume hood in the basement hot lab possess their own dedicated absolute or high efficiency particulate air (HEPA) filter. The HEPA filters have a minimum performance efficiency of 99.9% rated for particles 0.3 microns in diameter. The charcoal filter in the emergency exhaust system has a minimum performance efficiency of 95% for removal of elemental iodine.

6.2.6 Containment Integrity with Over-pressure

The containment building is a welded steel shell designed to be adequate for an internal gage pressure of [REDACTED] psi. A malfunction of ventilation system interlocks can be assumed which would result in the closure of the exhaust fan while leaving the main intake fan and valve open (AC-2 of Figure 6-2). Characteristic curves for the main intake fan indicate a static head pressure capability of [REDACTED] psi. Such an overpressure is a small fraction of the design specification and poses no problem with containment integrity.

It is informative to consider the building overpressure achievable from vaporization of the pool water as a result of a nuclear excursion. The most conservative point of view is to assume that the entire thermal output results in the formation of steam, with all the heat thus assigned to latent heat and none to sensible heat, so that building temperature is constant. The air volume of the building is [REDACTED] ft³. If the temperature is taken as [REDACTED] °F, then [REDACTED] x [REDACTED] moles of water must be vaporized to achieve an overpressure of 0.5 psi, and this requires an energy equivalent to an excursion of [REDACTED] MW-sec. This is nearly four times the [REDACTED] MW-sec achieved in the Borax experiments, in which 4% excess k was intentionally added as a step function by rapid control rod withdrawal, resulting in a minimum period of [REDACTED] msec, and a maximum power of [REDACTED] x [REDACTED]¹⁻⁵. Such an accident at the UMLRR is not considered credible and an excursion of four times this magnitude is not possible. Subsequently, an overpressure to [REDACTED] psig as a result of a reactor accident at the UMLRR, even a non-credible one, is not possible.

6.2.7 Containment Integrity with Under-pressure

Low barometric pressures are associated with storm conditions, and are extreme in the centers of tropical hurricanes. Pressures of the order of [REDACTED] inches of mercury are commonly found in the eyes of hurricanes, and [REDACTED] inches has been recorded.

Consider the following conservative case, in which the:

| | |
|-------------------------|-----------------------------------|
| Diameter of eye | = [REDACTED] miles, |
| Pressure at edge of eye | = [REDACTED] inches Hg, |
| Pressure at center | = [REDACTED] inches Hg, |
| Drift velocity | = [REDACTED] mile h ⁻¹ |

If the eye passed directly over the reactor, one [REDACTED] would be required for the barometric pressure to drop by [REDACTED] inches Hg, corresponding to a linear $\Delta P/\Delta T = [REDACTED]$ lb-in.⁻²-h⁻¹. If the further assumption is made that before the approach of the hurricane, the reactor building went into a condition of containment with internal pressure at approximately [REDACTED] atmosphere, then the internal overpressure would be [REDACTED] of Hg, or [REDACTED] psi, which is within the [REDACTED] psi design pressure.

These considerations apply only when the containment building is sealed. With the containment valves open, the excess internal pressure would be relieved through the stack. The stack is designed for a pressure drop of less than [REDACTED] inches water column when exhausting at [REDACTED] ft³-min⁻¹. Since this low pressure driving force is capable of exhausting such a large volume of air, the application of the much larger pressure drop (on the order of inches of Hg) postulated for the hurricane would lead to rapid equalization with the valves open.

The postulated hurricane is assumed to move at a velocity that would result in a pressure decrease rate of [REDACTED] in. Hg h⁻¹. If an assumption is made there is a loss of electrical power resulting in containment closure immediately prior to the hurricane, as the hurricane approaches and diminishes external pressure, the building is effectively becoming pressurized. Further assuming that the emergency electrical power is available (Chapter 8 of this SAR), at [REDACTED] inches water column building overpressure, the emergency exhaust system starts to remove air from the building (see Section 6.2.4). If the emergency exhaust blower is able to remove the overpressure in the containment building as the hurricane approaches, the rate of exhaust must be:

$$\left(\frac{\blacksquare \text{ in.Hg.h}^{-1}}{\blacksquare \text{ in.Hg.atm}^{-1}} \right) \left(\frac{\blacksquare \text{ ft}^3 \text{ atm}^{-1}}{\blacksquare \text{ h}^{-1}} \right) = \blacksquare \text{ ft}^3 \text{ min}^{-1}$$

of air through the blower (rated at $\blacksquare \text{ ft}^3 \text{ min}^{-1}$) to decrease the internal pressure at the same rate the external pressure is being lowered by the hurricane. No building overpressure results, but as the hurricane recedes and barometric pressure increased, the containment building will become under-pressurized, and this must be relieved by the vacuum breaker. If the hurricane is symmetrical and of constant linear velocity, the barometric pressure will increase at 2 in. Hg h^{-1} , and air must be supplied at this rate through the 6-inch diameter vacuum breaker pipe to equilibrate. This corresponds to an air velocity through the pipes of:

$$\frac{(\blacksquare \text{ ft}^3 \text{ min}^{-1})}{\pi(3)^2 \text{ in.}^2} = \blacksquare \text{ ft. min}^{-1},$$

or about \blacksquare miles per hour. This is not an excessive requirement.

It is also possible to conceive of a malfunction of the ventilation system interlocks that would result in the closure of the main intake valve-A while leaving the main exhaust fan and exhaust valves open. Characteristic curves for the exhaust fan indicate a static head pressure capability of \blacksquare psi. The six-inch diameter vacuum breaker opens at about \blacksquare inches water column, and thus this intake of air would tend to reduce the under-pressure of the building, so that the containment design for \blacksquare psi external pressure load is adequate.

6.2.8 Acceptance Testing

After the airlock doors, truck entrance door, vacuum relief device and miscellaneous penetrations for mechanical and electrical services were installed, the builder (Chicago Bridge & Iron Company) performed an acceptance leak test of the containment building. All welds in the bottom and all welds in the cylindrical shell were tested using vacuum box and soap film, and the airlock door systems were tested using a halogen leak detector.

Upon the completion of the reactor construction, the reactor staff performed several initial leak rate tests. The leak rate results varied from [REDACTED] ± [REDACTED] to [REDACTED] ± [REDACTED] building volume per day at [REDACTED] psig. After the initial acceptance tests, leak tests were periodically performed at [REDACTED] psig, with the results extrapolated to a leakage rate at [REDACTED] psig where the rate must be less than [REDACTED] per [REDACTED] hours. All tests to date have been shown to meet these criteria.

The Technical Specifications (Chapter 14) require the following ongoing tests:

- (1) Building pressure will be verified prior to reactor operation and at least every eight hours during reactor operation to ensure that it is less than ambient atmospheric pressure.
- (2) The containment building isolation system including the initiating system shall be tested annually. The test shall verify that valve closure is achieved in < [REDACTED] seconds after the initial signal (half the time for air under normal ventilation to travel from Valve B to Valve C, Figure 6-2)
- (3) Any additions or modifications to the containment building or its penetrations shall be tested to verify containment building integrity by performing an integrated leakage rate test of the containment building.
- (4) The emergency exhaust system including the initiating system shall be verified annually to be operable.
- (5) The filter trains in the emergency exhaust, facilities exhaust, and pneumatic sample exhaust shall be replaced or tested biennially to verify that they are operable.
- (6) The air flow rate in the stack exhaust duct shall be measured biennially.

6.3 Emergency Core Cooling System

In addition to the results of the accident analyses in Chapter 13, an emergency core cooling system has been shown not to be applicable to a 1MWth research reactor.

6.4 References

1. Hunt, C. H. and DeBevec, C. J., "Effects of Pool Reactor Accidents," General Electric, Atomic Power Equipment Department, GEAP-3277, November, 1959.
2. Dietrich, J. R., "Experimental Investigation of the Self-Limitation of Power Driving Reactivity Transients in a Subcooled, Water-Moderated Reactor," The Argonne National Laboratory ANL-5323, 1954.
3. "Reactors," *Nucleonics*, 13, 40 (September 1955).
4. Dietrich, J. R., "Experimental Determinations of the Self-Regulations and Safety of Operating Water-Moderated Reactors," *Proc. Intern. Conf. Peaceful Uses At. Energy*, Geneva, 1955, 13 88 (1955).
5. Zinn, W. H., et al., "Transient and Steady-State Characteristics of a Boiling Reactor, the Borax Experiments," 1953, the Argonne National Laboratory Report ANL-5211, 1954.

Table of Contents

7 Instrumentation and Control Systems..... 7-4

7.1 Summary Description 7-4

7.1.1 Reactor Control System 7-4

7.1.2 Reactor Protection System..... 7-5

7.1.3 Engineered Safety Features..... 7-5

7.1.4 Control Console Display Instruments..... 7-5

7.1.5 Radiation Monitoring System..... 7-6

7.1.6 Human-Machine Interface 7-6

7.2 Design of Instrumentation and Control System..... 7-7

7.2.1 Design Criteria 7-7

7.2.2 Design Basis Requirements 7-8

7.2.3 System Description..... 7-12

7.2.4 System Performance Analysis 7-16

7.2.5 Conclusion 7-16

7.3 Reactor Control System 7-17

7.3.1 Introduction..... 7-17

7.3.2 Drive Mechanisms 7-18

7.3.3 Control Blade Withdrawal Inhibit Circuit 7-19

7.3.4 Control Blade Drive Rundown Circuit 7-19

7.3.5 Regulating Rod Manual and Automatic Modes..... 7-20

7.4 Reactor Protection System..... 7-21

7.4.1 Nuclear Instrumentation System..... 7-22

7.4.2 Process Control and Instrumentation System 7-32

7.4.3 Scram Circuit 7-37

7.4.4 Alarm and Indicator System 7-39

7.4.5 [REDACTED] Mode Operation 7-40

7.5 Engineered Safety Features Actuation Systems 7-41

7.6 Control Console and Display Instruments 7-41

7.6.1 Human Machine Interface Displays..... 7-47

7.6.2 Performance Characteristics 7-50

7.7 Radiation Monitoring Systems 7-51

7.7.1 Introduction..... 7-51

7.7.2 Area Radiation Monitoring System 7-53

7.7.3 Detector Locations 7-56

7.7.4 Radiation Monitoring Computer Interface..... 7-57

7.7.5 Alarm Logic and Action Description..... 7-59

7.7.6 LREA Detector Combinations and Explanations 7-60

7.7.7 GREA Detector Combinations and Explanations..... 7-60

7.7.8 Gamma Cave Safety System and Interlocks..... 7-61

7.7.9 Beam Port Bunker Safety System and Interlocks 7-63

Table of Figures

Figure 7-1: I&C System Inter-relationship..... 7-16

Figure 7-2: Functional Block Diagram of RPS..... 7-22

Figure 7-3: Linear Power Channel Block Diagram 7-24

Figure 7-4: Log Power channel Block Diagram 7-24

Figure 7-5: Start-up Channel Block Diagram..... 7-32

Figure 7-6: Block Diagrams for Coolant Flow, Temperature, and Pool Height..... 7-36

Figure 7-7: I & C Layout for Control Console and Instrument Panel 7-42

Figure 7-8: Instrument Panel Layout 7-43

Figure 7-9: Control Console Layout 7-43

Figure 7-10: Block Diagram of Integrated ARM and RARM System Assemblies..... 7-58

Table of Tables

Table 7-1: Limiting Safety System Settings 7-11

Table 7-2: Linear Power Module Specifications 7-25

Table 7-3: Log-N Module Specifications 7-28

Table 7-4: Failure Analysis for each process variable..... 7-35

Table 7-5: RPS Safety Chain Scrams 7-38

Table 7-6: Radiological Protections Scrams..... 7-39

Table 7-7: I & C Components..... 7-44

Table 7-8: Radiation Monitoring Probes and Functions..... 7-53

Table 7-9: Detector Range and Sensitivities..... 7-54

Table 7-10: Main Chassis Area Radiation Monitoring (ARM)..... 7-56

Table 7-11: Remote Area Radiation Monitoring (RARM)..... 7-57

Table 7-12: GREA Detector Combinations and Explanations 7-61

7 Instrumentation and Control Systems

7.1 Summary Description

The Instrumentation and Controls (I&C) systems are comprised of the sensors, electronics, displays, and actuating devices used to provide information to the operator and to provide the means for safely operating the reactor. The I&C systems associated with the reactor include the following:

- (1) Reactor Control System
- (2) Reactor Protection System
- (3) Engineered Safety Feature Actuation System
- (4) Control Console and Instrumentation Panel Displays
- (5) Radiation Monitoring System
- (6) Human Machine Interface

The UMLRR began operating in 1975. Since then, most of the original components of the I&C systems for the UMLRR have been replaced and upgraded. The I&C components now mainly consist of analog-digital hybrids, whereby an analog signal is transmitted to an analog-to-digital converter. The digital output is then made available for display or other uses. The use of digital components is necessitated by the obsolescence of analog components, while providing the advantages of flexibility and reliability. In addition to meeting the single failure criterion, the I&C systems employ the principles of diversity, redundancy, and testability.

7.1.1 Reactor Control System

The reactor control system (RCS) consists of the drive mechanisms and control interface providing for the manual motion control of the safety blades, regulating rod, and startup counter. The RCS also provides for the automatic control of the regulating rod after a minimum critical power is attained. In manual mode, the operator may adjust the height of the four reactor control blades for start-up and shutdown of the reactor and to compensate for reactivity changes due to temperature and xenon effects. Fine control of the reactor power level is made by manually adjusting the height of the regulating rod. In automatic mode, the regulating rod height is adjusted by a proportional controller to maintain reactor power at a pre-set level.

With the exception of the isolated reactor power level signal used for automatic control, the instrumentation used by the RCS is separate and distinct from the reactor protection system. In addition, the RCS is equipped with a number of design features and interlocks to ensure safe operation. Among these are: (1) the limitation to withdraw only one control blade at a time, and (2) the automatic insertion of all four control blade drives upon a scram signal from the reactor protection system whereby the control blades have dropped by gravity into the reactor core.

7.1.2 Reactor Protection System

The reactor protection system (RPS) consists of two subsystems - the Nuclear Instrumentation (NI) system and portions of the Process Controls and Instrumentation (PCI) System. The relationship of the RCS to the RPS is shown in (Figure 7-1). The RPS is designed to ensure the reactor does not operate beyond the safety limits defined in the reactor license technical specifications (Chapter 14). This is accomplished by promptly placing the reactor in a sub-critical safe shutdown condition by the automatic initiation of a reactor scram. The scram circuits interrupt power to the control blade drive magnets, allowing the control blades to drop by gravity into the reactor core. A reactor scram may also be initiated manually by the reactor operator.

7.1.3 Engineered Safety Features

Engineered Safety Features (ESFs) are designed to (1) prevent or mitigate the consequences of fuel damage due to overpower or loss of cooling events, or (2) gain control of any radioactive material released by accidents. The results of design bases events analyzed for the UMLRR in Chapter 13 show that ESFs are not required for overpower or loss of cooling events. If an experiment containing radioactive material were to fail, the UMLRR containment isolation system described in Chapter 6 is designed to manually and automatically shut-down the containment building ventilation system and actuate ventilation isolation valves.

7.1.4 Control Console Display Instruments

The display instruments associated with the RCS and RPS consist of digital panel indicators, chart recorders, and display monitors. The instruments provide sufficient information to the operator to allow for the safe operation of the reactor. Figure 7-7 depicts the layout of the instrument cabinets in the control room. Figures 7-8 and 7-9 depict the layout of the display

instruments in each cabinet. The instrument locations provide for convenient viewing in either a seated or standing position.

The display instruments associated with the reactor protection system include the start-up neutron count rate, the reactor period and power level, the primary coolant temperature, primary coolant flow rate, and pool water level height. The display associated with the reactor control system includes the control blade position and status indicators.

7.1.5 Radiation Monitoring System

The Radiation Monitoring System (RMS) monitors and displays radiation readings at various locations within the reactor containment building and the building ventilation exhaust system. Radiation detectors are located in strategic areas to monitor radiation from the reactor and various experimental facilities. The RMS initiates warning alarms inside and outside the containment building and provides for automatic initiation of the containment isolation.

7.1.6 Human-Machine Interface

The I&C systems displays are assembled in three cabinets for effective operator interface: the instrumentation panel, the control console, and the radiation monitoring cabinet. All three cabinets are positioned in the Reactor Control Room (RCR), located on the third floor inside the reactor containment building (Figure 7-7).

The instrumentation panel positioned in the left of the RCR houses the digital indicators for instruments associated with primary coolant, including temperature, flow, and pool height. The instrumentation panel also houses the chart recorders for reactor power and primary coolant measurements, and the scram and alarm indicator panel. All the instrumentation panel indicators are sufficiently large, illuminated, and elevated for easy viewing by an operator seated at the control console. The control console occupies the center of the control room where the operator is typically seated during reactor operation. The control console left-hand side houses the amplifier modules having integrated displays for monitoring the reactor power and period. The console center houses the process controls display screen (PCS) for the display of retransmitted isolated analog output signals from the power monitors and primary coolant instruments. The PCS also provides an interface for on/off controls for the various pump motors, ventilation valves, and ventilation fans. The console right-hand side houses the drives control display screen

(DCS) for the display of the control blade position and status indicators. The DCS also provides an interface for selecting, withdrawing and inserting the drives for the control blades, regulating rod, and start-up counter.

The radiation monitoring cabinet is located to the right rear diagonal of the control console. The cabinet includes six ratemeter modules, each capable of displaying the digital readings of up to three radiation detectors. The ratemeters also provide visual indicator alarms for high radiation and component failure conditions. The radiation monitoring system display screen (RMS) is also located on the cabinet for the display of retransmitted isolated analog output signals from the ratemeters, and the remotely located constant air monitors and the stack monitor.

The positioning of the cabinets and the instrument layouts serve two main objectives. The first is to provide the operator with the information needed to monitor the reactor during start-up, steady-state, and power adjustment operations. The second is to provide the information needed to identify undesired conditions or trends. The first objective is met by placing the reactor power level and period and reactor control element position information directly in front of the operator. Primary coolant information is displayed both to the left and in front of the operator. The second is met by placing alarm indicators to the left and radiation indications in close proximity to the right.

7.2 Design of Instrumentation and Control System

7.2.1 Design Criteria

As a non-power research reactor, it is not necessary for the UMLRR to operate under adverse conditions such as severe natural phenomena, a seismic event, or fire. Administrative procedures require the reactor to [REDACTED]. In addition, a seismic sensor provides for an automatic shutdown should a seismic event occur. While it is anticipated that the UMLRR I&C systems would remain operable during such circumstances, once the reactor is shutdown, there is no safety reason for them to do so. As shown in the Chapter 13 accident analyses, the shutdown reactor does not pose a radiological hazard so long as the reactor pool integrity is maintained. A substantial additional layer of protection is provided by the containment building.

The containment building adequately protects the I&C from adverse external environmental conditions. Most of the I&C equipment is located in the control room which is a separate enclosed structure within the containment building. The control room is equipped with [REDACTED] and has a portable fire extinguisher.

The following criteria are applied the design of the Reactor Protection System:

- Single Failure – to ensure that no single failure or single maintenance action or any other single human action could disable the basic safety function of shutting down the reactor and maintaining it in a safe shutdown state for all operational states or design basis accidents (DBAs). The Single Failure Criterion is bolstered by the following additional criteria along with the use of fail-safe design concepts where practicable.
- Redundancy – incorporating any or combinations of the following: functional diversity (the monitoring of different reactor variables), equipment diversity (monitoring the same reactor variable using equipment of different principles of operation), simple redundancy (monitoring the same reactor variable using duplicate equipment).
- Independence – physical isolation such that any failure in one channel is isolated to the channel itself and does not affect other channels.
- Reliability – the use of technology that is qualified or proven by experience or testing or both.
- Testability – the capability for periodic checks, tests, and calibration.
- Manual Initiation – Providing a simple and direct means for the reactor operator to immediately shutdown the reactor.

- [REDACTED]

7.2.2 Design Basis Requirements

The I&C systems are designed with sufficient reliability and redundancy to ensure the reactor can be operated safely and so that design basis events are detected and the reactor can be automatically shut-down under the condition of any single failure in the system.

The I&C systems are designed to perform the following functions:

- Providing the reactor operator with information on the operating status of the reactor.

- Providing the means to control the reactivity of the reactor and to ensure that the reactor can be safely shut down.
- Providing the means to detect and measure radiation levels within the facility and in the air vented outside the facility.

7.2.2.1 Reactor Control System (RCS)

Reactivity is controlled in the UMLRR by means of a regulating rod and four shim safety control blades. The regulating rod has no scram capability. The four control blades can be scrammed manually or automatically by the RPS.

The RCS has two modes of operation: manual and automatic. Manual mode is used to start up and shutdown the reactor, and to change power levels. Automatic mode is used for steady-state operation. While manual mode allows the reactor operator to manipulate all reactivity control devices (four shim safety control blades and the regulating rod), automatic mode only moves the regulating rod. Several safety features are designed into the RCS.

These safety features include:

- (1) Only one control blade can be withdrawn at a time.
- (2) All four control blades can be scrammed from any height in the reactor.
- (3) All four control drives are automatically inserted at normal speed upon receipt of a rundown signal.
- (4) The reactor operator can take manual control of the regulating rod at any time by simply engaging the manual regulating rod control.

There are several interlocks associated with the RCS:

Start-up Interlock: The reactor control blades cannot be withdrawn unless (1) the key-locked operate switch is unlocked and placed into the on position by the reactor operator; (2) all limit switch contacts in the scram chain are in the normal position; (3) all relay contacts and in the scram chain are reset by the reactor operator and energized in the normal closed condition. This also energizes the control blade drive magnets for connection to the control blades. These interlocks ensure a reactor operator has enabled the RCS and RPS, and the operating conditions are normal prior to start-up.

Withdrawal Inhibit: The control blades cannot be withdrawn unless (1) the neutron count rate is greater than 2 CPS, and (2) the liner power channel indication is greater than 5%. This ensures the nuclear instrumentation for start-up is operating and there is adequate neutron indication for monitoring the start-up.

Automatic Regulating Rod Control: The regulating rod cannot be placed into automatic mode unless: (1) the reactor period is greater than 30 sec., (2) the regulating rod is not in the full-in or full-out position. This ensures the automatic control can compensate for small changes in reactivity. Once in automatic control, failure to meet any of these conditions causes a transfer to manual and an alarm.

Automatic Rundown: The control blade drives will automatically insert upon a scram signal. The control blades will drop by gravity into the reactor core and the control blade drives will follow at normal speed to verify all control blades are fully inserted.

The operator interface associated with the RCS is located on the right-hand side of the control console. The Drives Control display Screen (DCS) displays the control blade position and status indicators. The DCS also provides an interface for selecting, withdrawing and inserting the drives for the control blades, regulating rod, and start-up counter. The operator may also select the Automatic or Manual modes of regulating rod operation, once the reactor is critical at power level determined by the operator. An indicator informs the operator of the regulating rod control mode.

7.2.2.2 Reactor Protection System (RPS)

The RPS ensures that the limiting safety system settings (LSSS) are not exceeded as the result of transients of the type discussed in Chapter 13 of this SAR. For the UMLRR, these events are categorized as insertion of reactivity (including fuel mishandling), loss of coolant, and loss of coolant flow. The primary parameters of concern are the reactor power level, the primary coolant temperature, the primary coolant flow, and the reactor pool water level.

The reactor power level, the coolant temperature, and the coolant flow rate are interrelated variables used to establish the technical specification safety limits and the LSSS values. These limits and settings ensure the integrity of the fuel cladding is maintained and subsequently no consequence occurs for design bases events. Consequence in this regard means

the radiation dose to the public or to the reactor staff from an uncontrolled release of radioactivity.

The design bases analyses consider an automatic protective action (scram) occurs at the point where reactor power, coolant temperature, coolant flow, and coolant height reach technical specification LSSS values, either individually or in combination. In addition, the analyses consider the reactor scram begins within 210 milli-second of reaching the value. The set-points at which RPS action occurs are set conservative to the limiting safety system settings. This conservative approach provides further assurance that a safety limit will not be approached. Table 7.1 provides range of instrument readings (maximum and minimum) and the LSSS values. An analysis of the uncertainties in the instruments and measurements has been taken into account for the LSSS values.

Table 7-1: Limiting Safety System Settings

| Parameter | Max | Min | LSSS |
|--------------------------|-------|-------|-------|
| Reactor Power | █ MW | █ | █ MW |
| Temperature ¹ | █ F | █ F | █ F |
| Coolant Flow | █ GPM | █ GPM | █ GPM |
| Pool Height | █ ft | █ ft | █ ft |

1-Coolant Inlet

The RPS is both redundant and diverse as noted in Section 7.4 of this chapter. The RPS receives inputs from various sensors and switches that form the RPS safety chain scram circuit. In addition, the RPS receives inputs from several switches associated with radiological protection. The radiological protection scrams protect personnel and the environment from potential radiation exposure and are unassociated with reactor protection. Table 7-5 provides a full list RPS safety chain scrams and Table 7-6 lists the radiological protection scrams.

7.2.2.3 Engineered Safety Features (ESF)

The results of design bases events analyzed for the UMLRR in Chapter 13 show that ESFs are not required for overpower or loss of cooling events. If an experiment containing radioactive material were to fail (an event that is unrelated to reactor safety), the UMLRR containment isolation system described in Chapter 6 is designed to manually and automatically shut-down the containment building ventilation system and actuate the ventilation isolation valves. Certain combinations of detectors as listed in Section 7.7.5 will automatically isolate the

containment building if radiation measurements exceed set-point levels. In addition, a loss of electrical power to the building or the loss of either the main intake fan motor or main exhaust fan motor will cause building isolation.

7.2.2.4 Control Console Display Instruments

The design basis of the control console display instruments is that the reactor operators be provided with a central location from which they can safely monitor and operate the reactor. The design basis of the control console display instruments is to ensure adequate and reliable information from which the reactor operator can discern the condition of the reactor and take appropriate actions as necessary. Instrumentation associated with the reactor power, the primary coolant system, and auxiliary systems allow the operator to safely monitor and operate the reactor. User interfaces in the control room provide the operator with the ability to start and stop equipment throughout the facility. The I&C are grouped as described in Section 7.1.4. The instruments for monitoring parameters are both diverse and redundant. An annunciator alarm panel is provided to alert the operator to an abnormal condition and to facilitate both the diagnosis of the abnormal condition in the facility as well as the selection of the appropriate response to the condition.

7.2.2.5 Radiation Monitoring System (RMS)

The design basis of the RMS is to ensure adequate and reliable information from which the reactor operator can evaluate radiation levels in the building and air effluent leaving the building. The RMS provides continuous indication of gamma activity at selected locations in the facility and facility air exhaust. Indicators are provided for high alarms, alert alarms, and detector failure alarms. Relay contacts are provided for various audible and visible alarms and for building isolation. The RMS has redundant detectors for area radiation detection. Diversity is provided by area gamma, air particulate and gaseous monitors.

7.2.3 System Description

A summary of the I&C system is given here with emphasis on the relation between the five subsystems. Detailed descriptions are provided in Section 7.3 through 7.7 of this Chapter.

Figure 7-1 is a simplified diagram illustrating the important design aspects of the system and the interconnections and relationships among the five subsystems that comprise the I&C

System. The five subsystems are: the Reactor Protection System, the Reactor Control System, the Radiation Monitoring System, the Engineered Safety Features, and the control and display instruments that form the human machine interface.

Figure 7-2 provides a block diagram of the Reactor Protection System (RPS). The RPS is the composite of protective instrument channels and protective components designed to safely shutdown the reactor in response to a process variable or other condition having reached a limit specified in the design basis.

The Nuclear Instrumentation (NI) system (Section 7.4.1) monitors and displays reactor neutron flux from the subcritical source multiplication range through full power. Reactor period information also is provided beyond the critical power range to full power. The Process Control and Instrumentation (PCI) System (Section 7.4.2) monitors and displays the following process variables associated with the primary coolant system: temperature, flow rate, and pool water height.

The NI and PCI provide input signals to the alarm and indication system and the scram circuits. In addition, all parameters required by the technical specifications (Chapter 14, TS 3.2.3) to cause a reactor scram have an input to the reactor protection system. The “reactor safety chain” circuit (Section 7.4.3) is a series of relays with each relay corresponding to a scram condition. If any relay opens, electric power to the four control blade electromagnets is interrupted, causing a reactor scram. The actuating logic for the RPS is such that any one sensor indication exceeding its setpoint will cause a reactor scram.

The Reactor Control System (RCS) controls the operation of the control blade drives and the Regulating Rod (Section 7.3). A single HMI display screen provides the interface to monitor and operate the drive mechanisms for the control blade drives, regulating rod drive, and startup neutron counter drive.

The drive mechanisms employ DC motors. An optical encoder detects and transmits each revolution of the mechanism drive shaft. The optical signal pulses are counted and displayed in units of inches. The up and down position limits of the drives are protected by through-beam photosensors on the drives. The control blade drives are hard wired with mechanical relay logic, which prevents more than one control blade drive from operating in the up direction (blade withdrawal) at any one time. However, all four control blade drives can

operate simultaneously in the down direction (Section 7.3.4). The control blade drives are coupled to electromagnets, which when energized can attach to the control blades. Power for the electromagnets is governed by the reactor protection system (RPS).

The inhibit circuit (Section 7.3.3) prevents the actuation of the control blade drives and subsequent withdrawal of the control blades unless certain conditions are met. The circuit receives control power through contacts in the main scram relays. As a result, all scram conditions must be cleared and the scram relays reset in order to energize the individual control blade drive relays. The Start-up Channel, Logarithmic Power/Period channel, and signals from the Linear Power channels control the inhibit relay. In similar fashion to the scram relays, the inhibit relay independently will interrupt power to the control blade drive relays. This inhibit relay ensures that the reactor operator has sufficient indication of neutron count rate and reactor power level before any control blade is withdrawn.

The regulating rod is a low reactivity worth control element designed for making fine adjustments of the reactor power level once the reactor is critical. The regulating rod is mechanically coupled to its drive mechanism. The regulating rod drive may be controlled in either and automatic or manual mode selectable by the operator (Section 7.3.5). An indicator informs the operator of the regulating rod control mode. In automatic mode, the regulating rod is controlled by a proportional gain algorithm. When the operator places the regulating rod drive in automatic mode, the algorithm maintains the reactor power at a set-point level by controlling the output signal to the regulating rod drive servomotor. The set-point level is the reactor power level signal as measured by linear power channel No. 2 when servo system is placed in automatic mode. Any difference between the set-point value and the measured power level signal will generate an error value. The magnitude of the output signal to drive the servomotor, and thereby increase or decrease the reactor power level signal, is dependent on the error value. The auto control cannot be engaged or will disengage under the condition of a reactor scram, or if the reactor period is less than 30 seconds, or if the deviation between the setpoint and power level is too large.

The Radiation Monitoring System (RMS) consists of area monitors, constant air monitors, and a stack effluent monitor (Section 7.7). The area monitor detectors and readouts are capable responding to and indicating external radiation exposure levels. The constant air

monitors and stack effluent monitor respond to and indicate concentrations of airborne radionuclides. The reading of each monitor is displayed and recorded on the RMS panel. Alarm indicators are provided for warning and high alarm levels and for detector failure. Certain combinations of monitors having high level readings will trip area warning alarms and initiate isolation of the containment building.

The I&C human machine interface for the RPS and the RMS have redundant displays. The RPS process variables indications (flow, temperature, and pool level) are each located on the instrumentation panel cabinet and on the Process Control System (PCS) graphical user interface (GUI) display. The RMS area monitor readings are available on the RMS panel modules and on the RMS GUI display. The stack and constant air monitors have local displays in addition to the RMS GUI screen. The RCS control blade/regulating blade position indicators, status indicators, and controls are located on the Drive Controls System (DCS) GUI display.

When the reactor is operating, the instruments and displays associated with scram channels are checked and tested for acceptable performance each day in accordance with Technical Specification 4.2.2 (Chapter 14). The setpoints for the scram channels are set at levels that are more conservative than the limiting safety system settings used in the accident analyses in Chapter 13. Calibrations are performed at intervals in accordance with Technical Specification 4.2.2 and using procedures approved in accordance with Technical Specification 6.4.

operation of the reactor. Interlocks ensure that scram protection is enabled and that the related systems are operating normally before any reactor startup can occur. The RPS ensures that the reactor is automatically shut-down and placed in a safe condition should any of the parameters of concern generate a trip signal. These parameters are the reactor power level and reactor period signals from the Nuclear Instrumentation System and reactor pool level, primary coolant flow, and primary coolant temperature signals from the Process Controls and Instrumentation System. The Engineered Safety Feature ensures the safety of the public and the environment by preventing or mitigating the effects of radiological accidents and the potential of release of radioactive materials to the environment. The reactor is shutdown and placed in a safe condition and the containment building is isolated upon the receipt of elevated radiation signals. The I&C panels and displays provide the operator with all of the information and controls necessary to safely operate the reactor from a central location. Controls are grouped by systems. Meters, recorders, and annunciators provide the operator with indication of facility and reactor parameters. The RMS provides the reactor operator with radiation and activity levels throughout the facility.

7.3 Reactor Control System

7.3.1 Introduction

The Reactor Control System (RCS) controls the operation of the control blade drives and the Regulating Rod. A single HMI display screen provides the interface to monitor and operate the drive mechanisms for the control blade drives, regulating rod drive, and startup neutron counter drive.

These control elements are the primary means for the criticality control of the UMLRR. The RCS consists of an inhibit circuit, the control blade withdraw/insert circuits, the Regulating Rod withdraw/insert circuit, and the regulating rod automatic control circuit. A complete description of control blades, regulating rod and respective drive mechanisms is provided in Chapter 4.

The nuclear instrumentation system used by for monitoring the reactor neutron flux for both manual and automatic control of the reactor is described under the Reactor Protection

System (RPS) section 7.4.1. The process instruments used for monitoring primary coolant parameters are described under section 7.4.2.

Reactivity is controlled in the UMLRR by means of four shim safety control blades and a regulating rod. The RCS consists of the drive mechanisms, circuitry, and control interface providing for the manual motion control of the safety blades, the regulating rod, and the startup neutron counter. The RCS also provides for the automatic control of the regulating rod after a minimum critical power is attained. In manual mode, the operator may adjust the height of the four reactor control blades for start-up and shutdown of the reactor and to compensate for reactivity changes due to temperature and xenon effects. Fine control of the reactor power level is made by manually adjusting the height of the regulating rod. In automatic mode, the regulating rod height is adjusted by a proportional controller to maintain reactor power at a pre-set level.

With the exception of the inhibit signals from the nuclear instrumentation system and an isolated reactor power level signal used for automatic control, the RCS instrumentation and controls are separate and distinct from the RPS. The RCS is equipped with a number of design features and interlocks to ensure safe operation. Among these are: (1) the inhibit circuit, (2) the limitation to withdraw only one control blade at a time, and (3) the automatic insertion of all four control blade drives upon a scram signal from the reactor protection system whereby the control blades have dropped by gravity into the reactor core.

7.3.2 Drive Mechanisms

The drive mechanisms employ DC motors. An optical encoder detects and transmits each revolution of the mechanism drive shaft. The optical signal pulses are counted and displayed in units of inches. The up and down position limits of the drives are protected by through-beam photosensors on the drives. The control blade drives are hard wired with mechanical relays, whose logic prevents more than one control blade drive to operate in the up direction (blade withdrawal) at any one time. However, all four control blade drives can operate simultaneously in the down direction (rundown). The control blade drives are coupled to electromagnets which when energized can attach to the control blades. Power for the electromagnets is governed by the RPS. The drive mechanism hardware is further described in Chapter 4.

7.3.3 Control Blade Withdrawal Inhibit Circuit

The Inhibit Circuit is a relay logic system that prevents the actuation of the control blade drives and the subsequent withdrawal of the control blades, unless the following control system logic conditions have been satisfied:

1. The Master Control Switch is in the "ON" or "TEST" position;
2. All RPS limit switches are in the normal safe position and RPS scram relays are energized;
3. Linear power monitors are on-scale and reading above 5% of the selected range;
4. Source range level indication is greater than 2 cps.

A three-position ("Off-Test-On") key-locked Master Control Switch located on the instrumentation panel controls power to the RCS relays. Unauthorized operation of the RCS is prevented by the key-lock design which must be unlocked and switched to "Test" or "On" by the operator. The "Test" position allows the master scram relays to be reset and the ability to test the control blade drives without engaging the electromagnets. The master control switch must be turned to the "On" position to energize the control blade electromagnets.

The inhibit circuit design requires the limit switch contacts in the scram chain to be in the normal safe position and require that all relay contacts in the scram chain are reset and energized in the normal closed condition by the reactor operator. These interlocks ensure the reactor operator has enabled the RPS, and the operating conditions are normal prior to start-up.

The Start-up Channel and the Linear Power Channels control the drive mechanism inhibit relay. In similar fashion to the scram relays, the inhibit relay independently will interrupt power to the control blade drive relays. The inhibit function for a neutron count rate less than 2 CPS, and the linear power channel indication less than 5% ensures the nuclear instrumentation for start-up is operating and there is adequate neutron indication for monitoring the approach to critical.

7.3.4 Control Blade Drive Rundown Circuit

The Rundown Circuit is a relay logic system that actuates the simultaneous insertion of all four control blade drives. When a scram is initiated, either automatically or manually, a set of contacts on the main scram bus relays will open and de-energize the power supply to the

control blade electromagnets. As a result, the control blades drop by gravity into the reactor core. At the same time, a set of contacts will close that energizes the rundown circuit relays. These relays actuate the automatic insertion of all four control blade drives at normal speed to verify all control blades are fully inserted. A manual rundown also may be initiated by the operator at the control console. The rundown circuit is designed to override the control blade drive inhibit and withdraw signals.

7.3.5 Regulating Rod Manual and Automatic Modes

The RCS has two modes of operation: manual and automatic. Manual mode is used to start up and shutdown the reactor, and to change reactor power levels. Automatic mode is used for steady-state operation. While manual mode allows the reactor operator to manipulate all reactivity control devices (four safety control blades and the regulating rod), automatic mode only controls the regulating rod. Manual operation and automatic scram of the four control blades is not affected by the regulating rod automatic control.

The regulating rod is a low reactivity worth control element designed for making fine adjustments of the reactor power level once the reactor is critical. The regulating rod drive may be controlled in either the automatic or manual mode selectable by the operator. Automatic control is selected only after a minimum power level has been attained (typically 500 watts or greater) and is used for long term steady-state operation. In the automatic mode, the regulating rod provides continuous control of the reactor by the actuation of a proportional controller to compensate for small changes in reactivity. When the operator places the regulating rod drive in automatic mode, the proportional controller maintains the reactor power at a set-point level by controlling the output signal to the regulating rod drive servomotor. The set-point level is the reactor power level signal as measured by linear power channel No. 2 when servo system is placed in automatic mode. Any difference between the set-point value and the measured power level signal will generate an error value. The magnitude of the output signal to drive the servomotor, and thereby increase or decrease the reactor power level signal, is dependent on the error value.

The regulating rod cannot be placed into automatic mode unless: (1) the reactor period is greater than 30 sec., (3) the regulating rod is not in the full-in or full-out position. This ensures

the automatic control can compensate for small changes in reactivity. The regulating rod automatic mode will remain engaged unless any one of the following actions occur:

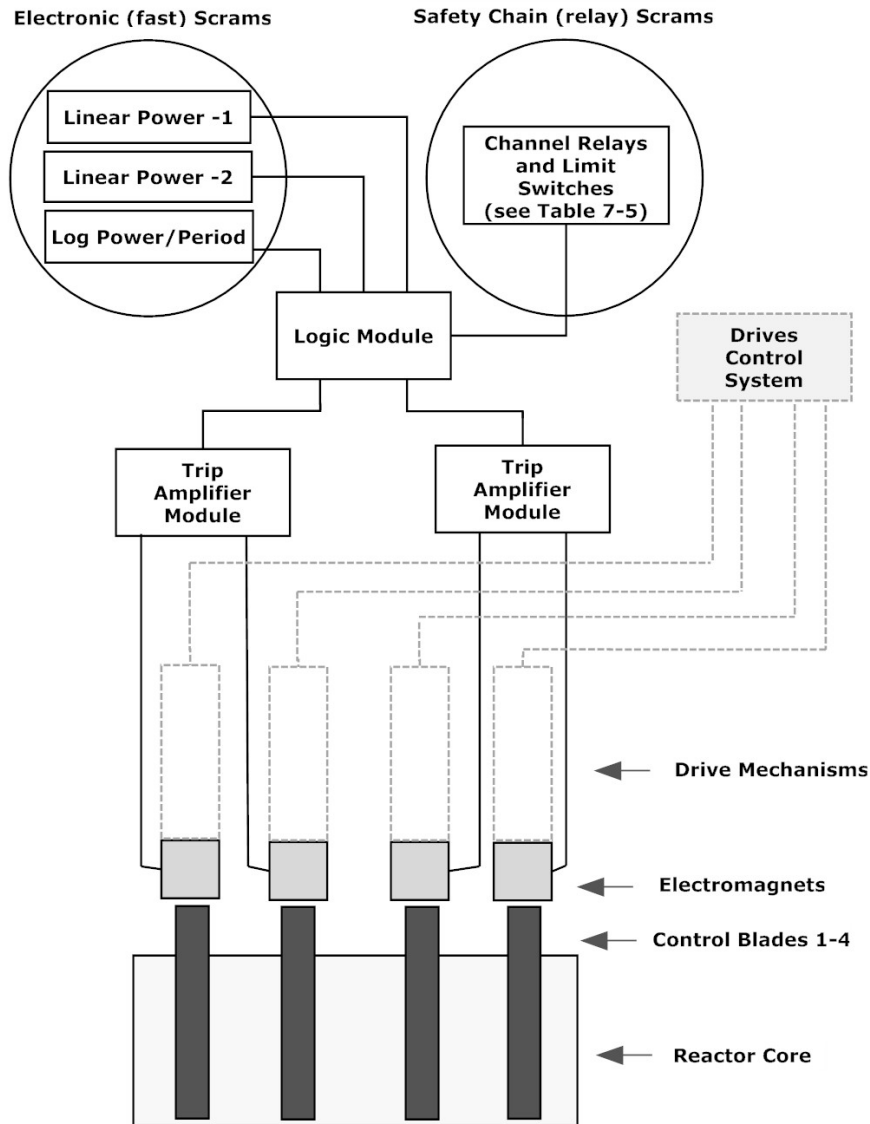
- (1) The operator selects manual control;
- (2) The deviation between the power set-point and actual power is greater than 2%;
- (3) The reactor period is less than 30 sec.;
- (4) The regulating rod reaches the full-in or full-out position;
- (5) A reactor scram occurs or the operator selects manual rundown of the control blades.

7.4 Reactor Protection System

The Reactor Protection System (RPS) consists of three subsystems - the Nuclear Instrumentation (NI) system, the Process Control and Instrumentation (primary coolant monitoring) system, and the scram chain circuit. The relationship of the RCS to the RPS is shown in Figure 7-2. The RPS is designed to ensure that the Technical Specification Safety Limits are not exceeded as the result of transients of the type discussed in Chapter 13 of this SAR. This is accomplished by the use of Limiting Safety System Settings (LSSS) which ensure the reactor is automatically and promptly placed into a sub-critical safe shutdown condition by the initiation of a reactor scram to prevent exceeding the Safety Limit.

The primary parameters of concern monitored by the RPS are the reactor power level, the primary coolant temperature, the primary coolant flow rate, and the reactor pool water height.

The RPS has two modes of operation – forced convection (1MW mode) and natural convection ([REDACTED] MW mode). In the [REDACTED] mode, the primary coolant flow scrams are bypassed and the linear power channel scrams are enabled on the [REDACTED] decade range.



Note: Dashed components are not part of the RPS

Figure 7-2: Functional Block Diagram of RPS

7.4.1 Nuclear Instrumentation System

Three separate nuclear instrument channels are designed for an accurate measurement and display of reactor power. Two multi-range linear power channels measure the neutron flux over 9 decade ranges. The third power measuring channel is wide-range logarithmic power and period channel capable of providing a continuous indication of period and reactor power over a logarithmic scale covering 10 decades of neutron flux. A fourth start-up nuclear instrument channel measures neutron counts from subcritical levels up to low critical power levels

overlapping the power channels. The neutron detectors for these channels are located exterior to the reactor core in the corner posts and subsequently measure the leakage neutron flux. The linear power and logarithmic power/period channels provide reactor power trip signals to the RPS. In addition, the isolated output signal from the linear channels is used to actuate a control drive inhibit relay for either too low or too high power indication. The logarithmic power/period channel provides a reactor period trip signal to the RPS. In addition, the logarithmic power/period channel provides a control blade drive inhibit signal for a short period and down-scale power indication. The start-up channel includes a relay that is part of the inhibit circuit. A neutron count rate below a threshold limit will open the relay preventing withdrawal of the control blades. Figure 7-3 and Figure 7-4 provide block diagrams for the reactor flux measuring channels.

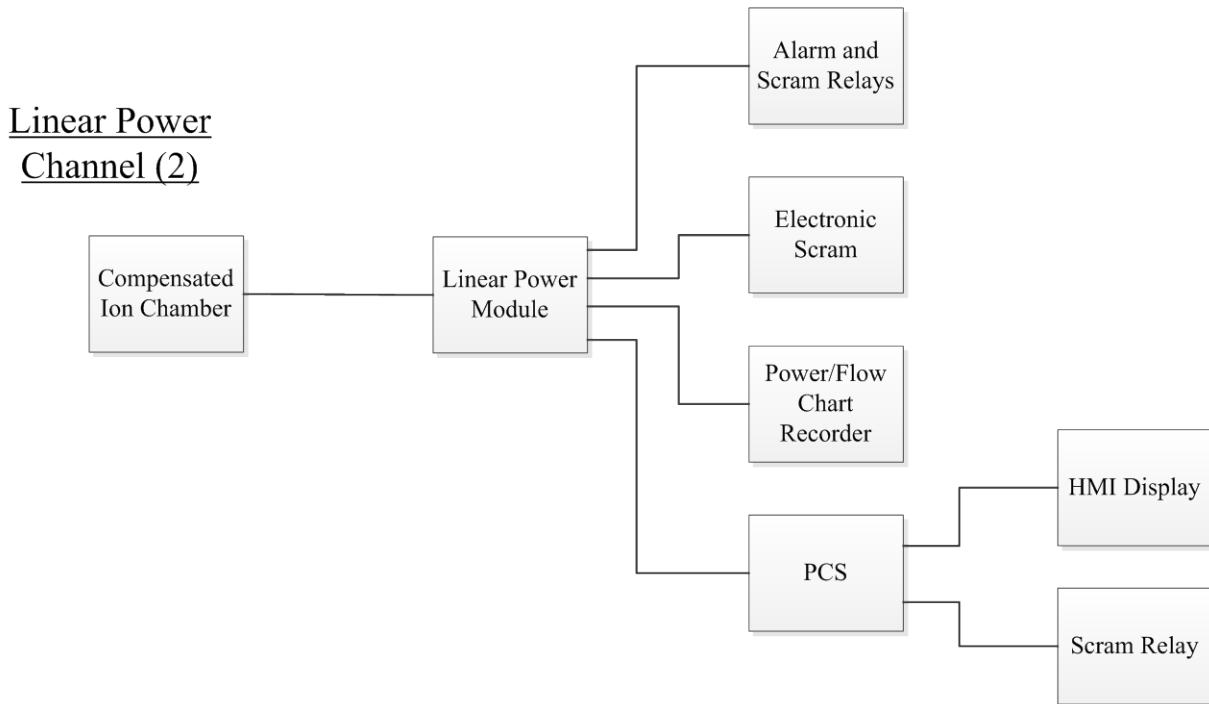


Figure 7-3: Linear Power Channel Block Diagram

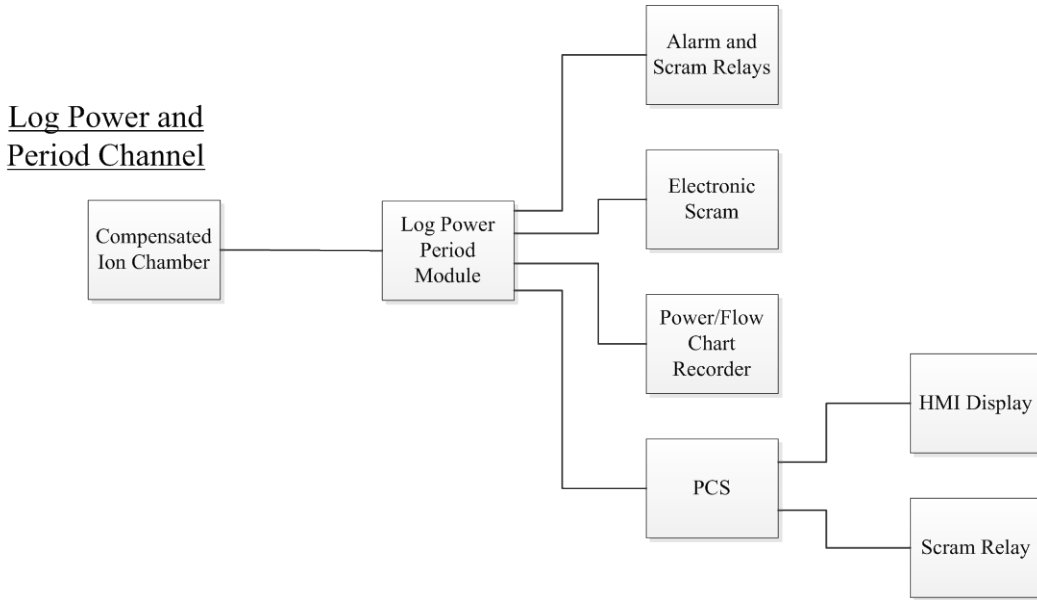


Figure 7-4: Log Power channel Block Diagram

7.4.1.1 Linear Power Channels

The function of each linear channel (Figure 7-9, C1 and C2) is to monitor the neutron fluence rate (power level) in ranges that overlap the start-up channel and cover the logarithmic power measuring channel. It also provides multiple trip functions for alarm and scrams. The linear channels are calibrated in units of watts and are capable of measuring power levels from 0.1 Watt up to 120% of the steady state licensed power level of 1MW.

Each of the two linear power channels consists of a neutron detector and a multi-range linear power module. The multi-range linear power modules are manufactured by General Atomics specifically for use in research reactors. Each module includes a display for percent reactor power indication, bi-stable trip circuits, detector high voltage and compensating voltage power, and isolated analog output signals for remote instrumentation. The module includes a test circuit to allow the user to test the proper performance of the electrometer and to ensure the functionality of all trip circuits. Table 7-2 provides specifications for the linear power modules.

Table 7-2: Linear Power Module Specifications

| | | |
|-------------------------|--|---|
| INPUT RANGE | 1 x 10 ⁻¹⁰ to 1 x 10 ⁻³ Amperes or 1 x 10 ⁻¹¹ to 1 x 10 ⁻⁴ Amperes | |
| LINEARITY | ± 1% of Full Scale on upper 5 ranges; ± 2.5% of Full Scale on lower 2 ranges | |
| TEMPERATURE | ± 0.15% / °C maximum in the range of 10 to 55 °C | |
| CALIBRATION/TEST | 2 fixed currents for calibration, 1 adjustable for multi-range function test and trip testing. HV trip test. | |
| RESPONSE TIME | 10 ⁻⁸ to 10 ⁻³ Amperes | 1 msec |
| | 10 ⁻⁹ to 10 ⁻⁸ Amperes | 10 msec |
| | 10 ⁻¹¹ to 10 ⁻⁹ Amperes | 100 msec |
| BISTABLE TRIPS | High Voltage, High Power and Alarm: User Configurable (increasing or decreasing) Logic Level output and two form "C" contacts per trip | |
| OUTPUTS | Front Panel | Linear Power (0 to 120%) and range indication High Voltage (0 to 1000 VDC) |
| | Remote meter | 0 -10 VDC or 0-1mA |
| | Recorder | 0 - 1 VDC or 0 – [REDACTED] VDC or 4-20mA |
| | High Voltage | 300 to 800 VDC @ 2.6 watts |
| | Compensation | 0 to 150 VDC |
| POWER REQUIRED | 117 VAC ± 10% 50/60 Hz @ 1 Amp | |

7.4.1.1.1 Amplifier Circuit

The incoming current signal from the neutron detector is accurately measured from 10pA to 1mA using a high input impedance operational amplifier. The analog amplifier circuit measures the detector current and converts it into a linear analog voltage in nine one-decade ranges. For every decade of current, the analog board returns a 0 to +10VDC signal for use in driving the module percent power indicator and the isolated analog signal for remote indication. The module is designed to measure power up to 120% of nominal. Subsequently, the amplifier output voltage of +10VDC represents 1.2 times nominal current. For every decade of current, a relay switches in the appropriate feedback resistor to generate the expected output signal. The 1E-11 decade is the default range and always active. Other ranges are switched into the circuit in parallel as determined by a microprocessor or manually by the user. Three test circuits are located on the amplifier board: calibration low, calibration high, and manual current adjust. The tests circuits allow the user to test the proper performance of the electrometer and to ensure the functionality of all trip circuits.

7.4.1.1.2 Trip Alarm Circuit

The trip/alarm circuit contains identical bi-stable circuits to generate trips for high voltage, high power, and alarm indications. Each circuit is jumper configurable for a rising or falling trip. A comparator monitors an incoming signal voltage from the amplifier circuit board and compares it to a reference voltage. The reference voltage (trip set-point) is user adjustable

via a potentiometer on the circuit board. When the circuit is configured for a rising trip, the comparator will switch states when the amplitude of the incoming signal exceeds the reference signal. A falling trip works the opposite way – when the incoming signal amplitude falls below the reference voltage, the comparator will switch states. Once a trip has occurred, the circuit latches in the tripped state. The only way to unlatch the circuit is for the user to apply a reset signal, even if all signal levels return to nominal prior to the reset. Each trip has both a DPDT (Form C) relay and an opto-isolator providing a trip logic signal. The relays are held energized in a fail-safe condition until a trip de-energizes the coil. Taking the module out of operate mode (such as during a self-test) will immediately activate the trip relay.

7.4.1.1.3 Isolation Amplifier Circuit

The isolation amplifier circuit provides two isolated outputs that can be jumper configured for either voltage or current output. Adjustment potentiometers on the circuit board allow the isolators to be calibrated for offset and span. A 0 to +10VDC input from the amplifier circuit will generate a 4 to 20mA or 0 to +10VDC isolated output that is available for remote indicators.

7.4.1.1.4 Display and Front Panel

The front of the module provides an LCD touch screen for display of linear power, range indication, and high voltage indication. The front panel also provides red LED indicators for Trip 1, Trip 2 and High Voltage. A potentiometer knob on the front panel allows the user to manually adjust the current in test mode. Two recessed potentiometers allow the user adjust the compensation power supply voltage to the detector.

The trip outputs are summarized as follows:

- (1) High Power Scram – Logic Level: A rising trip that switches an opto-isolated transistor conducting a 12 VDC signal to the scram logic unit when un-tripped and 0VDC when tripped (see also section 7.4.3).
- (2) High Power Scram – Relay: A rising trip providing an open relay contact output when measured power exceeds the scram set-point and a closed contact output when un-tripped. The relay coil associated with this contact is de-energized in the trip condition. This trip contact is used in the scram safety chain.

- (3) High Power Alarm – Relay: A rising trip providing a closed relay contact output when measured power exceeds the alarm set-point and an open contact output when un-tripped. The relay coil associated with this contact is de-energized in the trip condition. This trip contact is used to initiate the alarm annunciator. An additional relay contact actuated by this trip is opened to initiate the control blade drive inhibit.
- (4) High Voltage Scram – Relay: A decreasing trip providing an open relay contact output when the high voltage output drops below the trip set-point and a closed contact output when un-tripped. The relay coil associated with this contact is de-energized in the trip condition. This trip contact is used in the scram safety chain. An additional relay contact actuated by this trip is closed to initiate the alarm annunciator.

7.4.1.1.5 Failure Analysis

Failure of the power source or internal power supplies will cause all the trips to assume their tripped state. Relay contacts associated with trips (2), (3), and (4) above will open and the voltage output from (1) will drop to zero. Reactor scram and blade withdrawal inhibit will result.

A component failure in the amplifier circuit causing a false upscale signal output will cause trips (1), (2), and (3) to be actuated. Relay contacts associated with trips (2) and (3) will open and the voltage output of trip (1) will drop to zero. Reactor scram and blade withdrawal inhibit will result.

A component failure in the amplifier section causing a false downscale signal output will actuate the control drive inhibit relay.

A component failure in the amplifier section which would cause the output to neither increase nor decrease, yet not respond to an increase or decrease of signal input, is considered highly unlikely. However, since the linear power channels operate independently (1 out of 2 mode), reactor protection is provided by the second linear power channel. Additional reactor protection is provided by the Logarithmic Power/Period Channel.

7.4.1.2 **Logarithmic Power/Period Channel**

The function of the Logarithmic Power/Period (Log-N) channel (Figure 7-9, C3) is to monitor the neutron fluence rate (power level) in ranges that overlap the start-up channel and the

linear power measuring channels. In addition, the log-N channel provides the rate of change in reactor power (period) and provides multiple trip functions for alarm and scrams. The module combines count rate and current measuring techniques to cover 10 decades of neutron flux ranging from 0.3 to 1E10 n/cm²-s. The power measurement is calibrated in units of watts and is capable of measuring from sub-critical levels up to 120% of the steady state licensed power level of 1MW.

The Log-N channel consists of a fission chamber, pre-amplifier, and a wide-range logarithmic power module to provide percent reactor power indication, reactor period indication, detector high voltage, and bi-stable trip circuits. The wide-range logarithmic power module is manufactured by General Atomics specifically for use in research reactors. The module provides indications of reactor power, reactor period and detector high voltage. Isolated analog and digital outputs are provided for remote indicators. Bi-stable trip circuits provide for reactor scram and alarm indication. The module includes a test circuits to allow the user to test the proper performance of the current amplifier and differentiator circuit, and to ensure the functionality of all trip circuits. Table 7-3 provides specifications for the Log-N module.

Table 7-3: Log-N Module Specifications

| | | | | |
|--|--|----------|---|---------|
| INPUT RANGE | Counting - 0.1 C/sec to 3x10 ⁵ C/sec CURRENT 1x10 ⁻⁶ to 1x10 ⁻³ A | | | |
| LINEARITY (LOG CONFORMITY) + 1% OF THE LINEAR | Full scale equivalent covering the combined counting and current regions in the temperature range of 20 to 30 C | | | |
| TEMPERATURE COEFFICIENT | ± 0.15%/ C maximum over 10 to 55 C | | | |
| CALIBRATION/TEST | 2 fixed count rates, 2 fixed currents for calibration, 1 adjustable count rate, 1 adjustable current for trip testing, HV trip test, test modes selected sequentially by front panel control | | | |
| RESPONSE TIME CONSTANTS | 10 ⁻⁴ to 10 ⁻³ Amperes | <1 msec | 10 ² to 10 ³ Counts/sec | 30 msec |
| | 10 ⁻⁵ to 10 ⁻⁴ Amperes | <2 msec | 10 ¹ to 10 ² Counts/sec | 0.3 sec |
| | 10 ⁻⁶ to 10 ⁻⁵ Amperes | 2.5 msec | 10 ⁰ to 10 ¹ Counts/sec | 3 sec |
| | 10 ⁴ to 10 ⁵ Counts/sec | 15 msec | 10 ⁻¹ to 10 ⁰ Counts/sec | 30 sec |
| | 10 ³ to 10 ⁴ Counts/sec | 20 msec | | |
| OUTPUTS | Remote Meter: 0–10 V full scale Remote Meter: 0–1 mA full scale Recorder: 0–0.1 V full scale | | Recorder: 0–1 V full scale Optional: 4.0–20 mA full scale High Voltage: +300 to +800 VDC @2.6W | |
| BISTABLE TRIPS | High voltage High power level Low power level Period | | User configurable (increasing or decreasing) with Logic Level output and two form C contacts per trip | |
| POWER REQUIRED | 117 VAC + 10% 50/60 Hz @ 1.0 A | | | |

7.4.1.2.1 Log Count Rate/Current and Period Circuits

In the lower 7 decades, the log count rate circuitry counts pulses coming from the preamplifier. For the upper 3 decades, the current flowing in the fission chamber is processed by the log current amplifier circuit. The transition from pulse to current mode happens automatically. The combination of the pulse count and the current signal provides a logarithmic indication of the reactor power. Two test circuits are located on the Log Count Rate Board to simulate readings at a low count rate and a high count rate. The tests circuits allow the user to test the log count rate amplifier. Three test circuits are located on the Log Current Board: low current, high current, and manual current adjust. The tests circuits allow the user to test the log current amplifier and to ensure the functionality of the associated trip circuits.

The period signal is derived from the log power signal. A differentiator circuit monitors the log power signal and generates an output proportional to the rate of change in reactor power at any given instant. A test circuit is provided to produce a linear ramp output corresponding to a period of 3 seconds to test the circuit and to ensure the functionality of the period trip circuits.

7.4.1.2.2 Trip Alarm Circuit

The trip/alarm circuit contains identical bi-stable circuits to generate trips for high voltage, short period, high power, alarm, and low power indications. It is similar in design and operation as that used for the linear power channels. Once a trip has occurred, the circuit latches in the tripped state. The only way to unlatch the circuit is for the user to apply a reset signal, even if all signal levels return to nominal prior to the reset. Each trip has both a DPDT (Form C) relay and an opto-isolator providing a trip logic signal. The relays are held energized in a fail-safe condition until a trip de-energizes the coil. Taking the module out of operate mode (such as during a self-test) will immediately activate the trip relay.

The High Voltage Trip is configured as a decreasing trip when the high voltage is below the specified setpoint. The Period Trip is configured as an increasing trip when the period exceeds the specified setpoint. Trip 1 is configured as an increasing trip (scram) when the power level exceeds the specified setpoint. Trip 2 is configured as an increasing trip (alarm) when power level exceeds the specified setpoint. Trip 3 is configured as an increasing trip (inhibit)

when power level exceeds the specified setpoint. Trip 4 is configured as a decreasing trip (inhibit) when power level goes below the specified setpoint.

7.4.1.2.3 Isolation Amplifier Circuit Board

The isolation amplifier circuit board is similar in design and operation as that used for the linear power channels. Output A is factory set for power level, and Output B is factory set for period.

7.4.1.2.4 Display and Front Panel

The display and front panel is similar in design and operation as that used for the linear power channels. The front panel board houses the red LED indicators for all trips, activated by the trip/alarm board. A potentiometer lets the user manually control the current in test mode. This potentiometer is accessible with a knob on the front panel.

The trip outputs are summarized as follows:

- (1) Short Period Scram – Logic Level: A rising trip that switches an opto-isolated transistor conducting a 12 VDC signal to the scram logic unit when un-tripped and 0VDC when tripped (see also 7.4.3).
- (2) High Power Scram – Relay: A rising trip providing an open relay contact output when measured power exceeds the scram set-point and a closed contact output when un-tripped. The relay coil associated with this contact is de-energized in the trip condition. This trip contact is used in the scram safety chain.
- (3) High Power Alarm – Relay: A rising trip providing a closed relay contact output when measured power exceeds the alarm set-point and an open contact output when un-tripped. The relay coil associated with this contact is de-energized in the trip condition. This trip contact is used to initiate the alarm annunciator.
- (4) High Power Inhibit – Relay: A rising trip providing an open relay contact output when measured power exceeds the High Power Alarm (2) set-point. The relay coil associated

with this contact is de-energized in the trip condition. This trip contact is used in the control blade drive inhibit circuit.

(5) Low Power (Counts) Inhibit – Relay: A decreasing trip providing an open relay contact output when power drops below a value of $10E-6\%$ power (10 counts per second). The relay coil associated with this contact is de-energized in the trip condition. This trip contact is used in the control blade drive inhibit circuit.

(6) High Voltage Scram – Relay: A decreasing trip providing an open relay contact output when the high voltage output drops below the trip set-point and a closed contact output when un-tripped. The relay coil associated with this contact is de-energized in the trip condition. This trip contact is used in the scram safety chain.

7.4.1.2.5 Failure Analysis

Failure of the power source or internal power supplies will cause all the trips to assume their tripped state. Relay contacts associated with trips (2), (3), (4), (5), and (6) above will open and the voltage output from (1) will drop to zero. Reactor scram and blade withdrawal inhibit will result.

A component failure in the amplifier circuit causing a false upscale signal output will cause trips (1), (2), (3), (4) to be actuated. Relay contacts associated with trips (2), (3), and (4) will open and the voltage output of trip (1) will drop to zero. Reactor scram and blade withdrawal inhibit will result.

A component failure in the amplifier section causing a false downscale signal output will actuate the control drive inhibit relay.

A component failure in the amplifier section which would cause the output to neither increase nor decrease, yet not respond to an increase or decrease of signal input, is extremely remote. However, since the linear power channels are operated independently in a 1 out of 2 mode, reactor protection is provided by the two operating linear channels.

7.4.1.3 Start-up Channel

The startup channel components include a B-10 proportional counter detector, preamplifier, linear pulse amplifier and single channel analyzer, count-rate meter, and high-voltage power supply. The startup channel can be used to monitor flux levels from a minimum effective low range of \blacksquare n/cm²-s to a high of 5×10^4 n/cm²-s.

The ionization charge from the proportional counter detector is converted to pulse output by the preamplifier. The output pulse is shaped by the amplifier then directed to the pulse height analyzer for discrimination. The remaining pulse signals are converted a voltage logic signal processed by the ratemeter. The ratemeter provides a hard-wired relay to the control blade drive inhibit circuit which will de-energize if the count-rate drops below the set-point value. The ratemeter also provides an analog output signal for remote monitoring. Figure 7-5 provides a block diagram of the Start-up Channel and its individual elements.

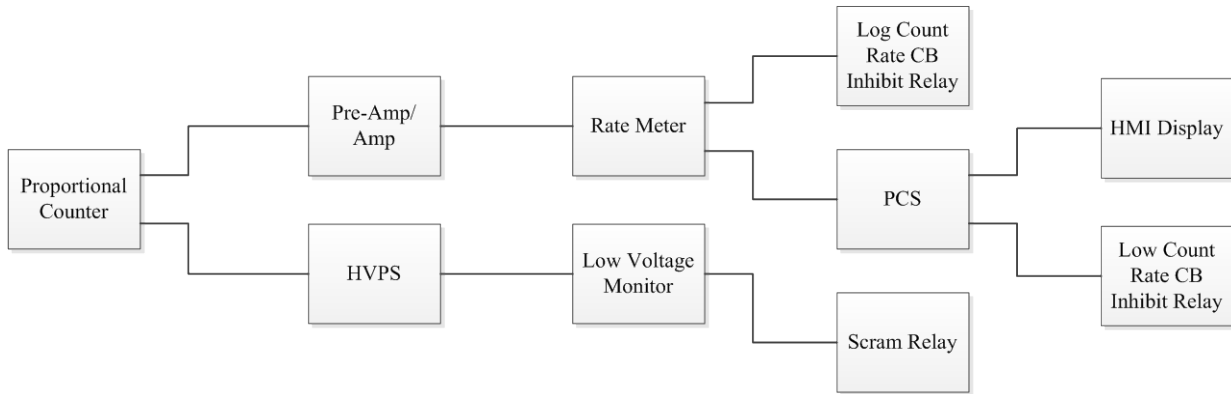


Figure 7-5: Start-up Channel Block Diagram

7.4.1.3.1 Failure Analysis

Failure of the power supply, preamplifier, or the amplifier will cause a downscale reading and will actuate the control drive inhibit relay. A component failure in the discriminator circuit causing a false upscale signal output will create a disproportionately high reading, alerting the operator to the malfunction.

7.4.2 Process Control and Instrumentation System

The Process Control and Instrumentation System is composed of the following channels: (1) primary coolant system flow, (2) reactor core flow, (3) primary coolant inlet temperature, (4)

primary coolant outlet temperature, (5) pool water temperature, and (6) pool water height. All six channels have readouts on individual digital panel meters (Figure 7-8, P1 – P6) located on the Instrumentation Panel in the control room. The meters are microprocessor-based universal temperature and process indicators with configurable features for calibration and alarm relay settings. The configuration setting is password protected. The programming embedded by the manufacturer is not alterable by the operator.

In addition to displaying the measured variable, each panel meter has two SPDT (Form C) relay outputs for alarm and scram, and an isolated analog output for retransmission of the measured variable. The relays are configured to be de-energized (fail-safe) for the trip condition. To test the proper performance of the meter and to ensure the functionality of the trip relays, each meter has an external test circuit consisting of a spring loaded momentary toggle switch and a potentiometer. Figure 7-8 shows the panel layout and Table 7-7 summarizes the function of each instrument. The Process Control and Instrumentation System includes a display screen on the control console for the display of the isolated analog output signals and the user interface for on/off controls for the various pump motors, ventilation valves, and ventilation fans.

7.4.2.1 Primary Coolant Flow Measurement

The primary coolant flow rate is measured using a stainless steel orifice plate installed in the primary piping after the heat exchanger. A differential pressure transmitter provides an analog output current signal that is proportional to differential pressure across the orifice plate. The signal is sent to the control room instrumentation panel Primary Flow indicator where the flow-rate is displayed in gallons per minute. The scram relay is configured as a decreasing trip, providing an open relay contact output when the flow-rate drops below the trip set-point and a closed contact output when un-tripped. The relay associated with this contact is de-energized in the trip condition. This trip contact is used in the scram safety chain. The alarm relay is configured as a decreasing trip, providing a closed relay contact output when the flow-rate drops below the trip set-point and an open contact output when un-tripped. The relay associated with this contact is de-energized in the trip condition. This trip contact is used to actuate the annunciator.

Measurement of the core flow provides a second method of monitoring the primary coolant flow rate. A turbine flow meter is mounted in a two-inch diameter sampling pipe located

between the discharge header beneath the core and the primary flow riser plenum. A magnetic pick-up sensor above the turbine rotor produces signal pulses at a frequency proportional to the flow rate. The frequency signal is amplified at the reactor bridge and the resultant logic pulse signal is sent to the control room instrumentation panel Core Flow indicator where the flow-rate is displayed as a percentage of the nominal flow rate. The scram and alarm relays are configured similar to the primary flow rate meter.

7.4.2.2 Primary Coolant Temperature Measurement

The temperature measuring channels consist of resistance temperature detectors (RTD). The temperature sensing resistance elements operate on the principle that resistance in a wire varies in relation to change of temperature. There are three independent temperature channels for the primary coolant system. The Core Outlet RTD measures the temperature of primary coolant in the piping exiting the reactor core. The Pool Inlet RTD measures the temperature of the primary coolant in the piping exiting the heat exchanger. The Pool RTD measures the temperature of the primary coolant in the pool near the surface of the water above the reactor. Each RTD is of the 3-wire configuration to provide resistance compensation and is connected to the respective temperature indicator on the control room instrumentation panel. Each temperature indicator displays the temperature in degrees Fahrenheit and has alarm and scram relays. The scram relay is configured as an increasing trip, providing an open relay contact output when the temperature reaches the trip set-point and a closed contact output when un-tripped. The relay associated with this contact is de-energized in the trip condition. This trip contact is used in the scram safety chain. The alarm relay is configured as an increasing trip, providing a closed relay contact output when the temperature reaches the trip set-point and an open contact output when un-tripped. The relay associated with this contact is de-energized in the trip condition. This trip contact is used to actuate the annunciator.

7.4.2.3 Pool Height Measurement

The pool water height above the core is measured by a non-contact ultrasonic transducer. An ultrasonic sound wave is pulsed from the base of the transducer. The sound wave reflects against the water surface and returns to the transducer. The time of flight between the sound generation and receipt is used to generate an analog output current signal. The current signal is inversely proportional the distance between the transducer and the water surface (increasing

distance, decreasing signal). The signal is sent to the control room instrumentation panel Pool Height indicator where the height is displayed in feet. The scram relay is configured as a decreasing trip, providing an open relay contact output when the height drops below the trip set-point and a closed contact output when un-tripped. The relay associated with this contact is de-energized in the trip condition. This trip contact is used in the scram safety chain. The alarm relay is configured as a decreasing trip, providing a closed relay contact output when the height drops below the trip set-point and an open contact output when un-tripped. The relay associated with this contact is de-energized in the trip condition. This trip contact is used to actuate the annunciator. An independent magnetic float switch having contacts connected in series to the reactor safety chain also monitors pool height. If the float drops to a predetermined level, the switch contacts will open causing a scram. Figure 7-6 provides the coolant flow, temperature, and pool height block diagrams.

7.4.2.4 Failure Analysis

The failure analysis for each process variable is summarized in Table 7-4.

Table 7-4: Failure Analysis for each process variable.

| Variable | Loss of Signal | Loss of Power |
|---------------------------|------------------------|----------------------|
| Temperature Pool | High reading and scram | Fail-safe scram |
| Temperature Pool Inlet | High reading and scram | Fail-safe scram |
| Temperature Core Outlet | High reading and scram | Fail-safe scram |
| Primary Flow | Low reading and scram | Fail-safe scram |
| Core Flow | Low reading and scram | Fail-safe scram |
| Pool Height (Transmitter) | Low reading and scram | Fail-safe scram |
| Pool Height (Float) | scram | n/a |

Loss of signal could be caused by a wire break, and/or failure of a transmitter in case of Primary Flow, Core Flow, and Pool Height. A break in a wire for an RTD provides an infinite resistance measurement resulting in a false high temperature reading exceeding the trip set-point. A break in a signal wire or failure of a transmitter for the Primary Flow, Core Flow, or Pool Height results in the loss of signal and a subsequent downscale reading below the trip setpoint.

A break in the wire for the Pool Height float results in loss of continuity in the safety chain scram bus and produces a scram. Loss of power could be the external power or the internal power supply for a meter or transmitter. The scram relay for each indicator is configured to switch to an open contact condition when the relay is de-energized. The pool height float provides a dry contact switch as part of the scram chain.

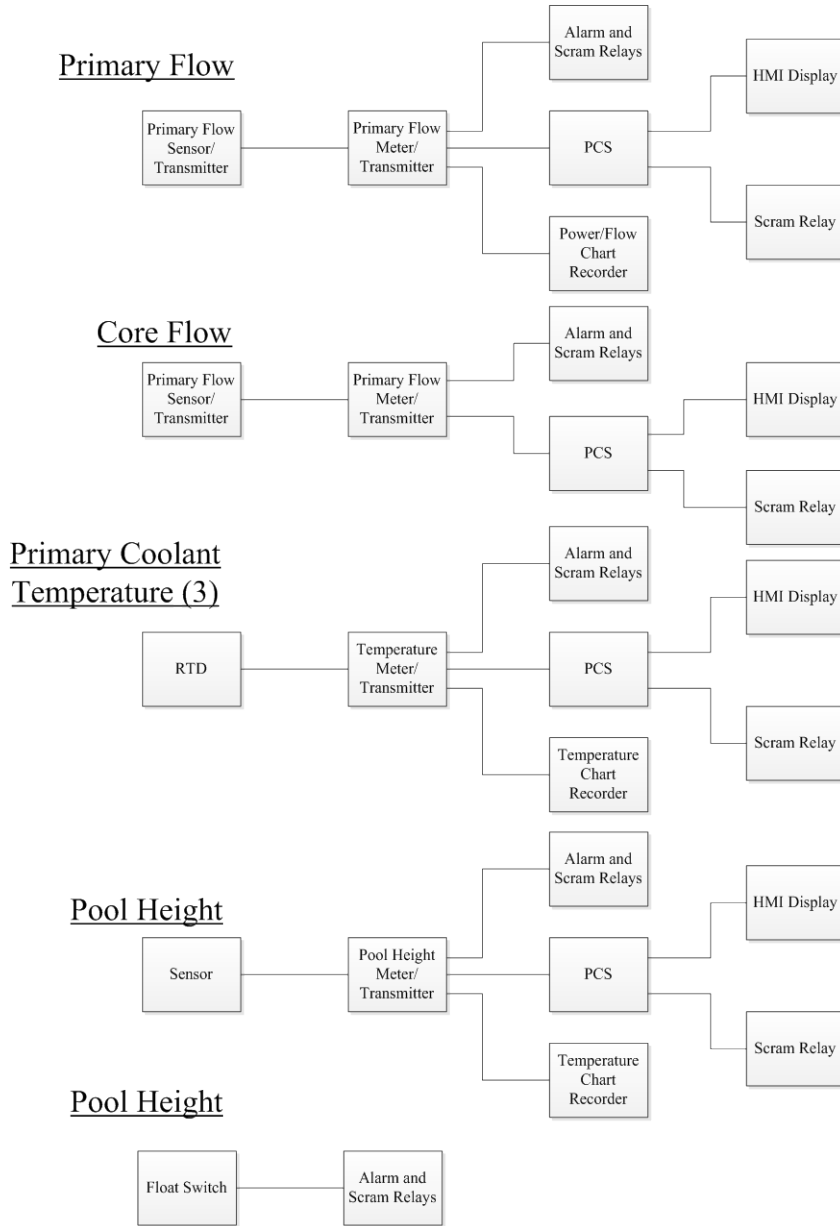


Figure 7-6: Block Diagrams for Coolant Flow, Temperature, and Pool Height

7.4.3 Scram Circuit

The automatic shutdown of the reactor can be initiated by any of the various relays, limit switches, and electronic input signals that comprise the scram circuit. The scram circuit includes the Logic Unit (LU) and the Trip Actuator Amplifiers (TAA). The LU monitors the 12 VDC logic output signals from the two linear power modules and the Log-N power/period module. The TAA contains a power supply for providing direct current to the electromagnets and two series-connected bi-stable amplifiers to allow fast switching of the current. Control of the switching action is provided by a 12VDC signal input from the LU. There are two independent TAA units. One TAA supplies and controls the current for the control blades No. 1 and No. 2 electromagnets. The second TAA supplies and controls the current for the control blade No. 3 and control blade No. 4 electromagnets. Electrical power for the TAA units is supplied through the main scram relays.

7.4.3.1 Relay Scram

The switches and relays listed in Table 7-5 are series connected to form a Safety Chain Scram Bus leading to the two master scram relays also connected in series. The master scram relays provide 120VAC power to the TAAs through a set of electrical contacts. Actuation of any switch or relay in the safety chain will open the electrical contacts supplying the 120VAC power to the TAA units, thereby terminating current to the electromagnets.

7.4.3.2 Electronic Scram

In addition to relay trips, both the linear power monitors and the log power/period monitor provide independent logic level trip signals via opto-isolated transistors. The Logic Unit (LU) monitors the logic level trip signals. In the normal un-tripped state a 12VDC signal is supplied through the transistor. When tripped, the 12VDC logic signal goes to zero. The LU incorporates two redundant comparator circuits for each of the logic level input signals. If the input signal to any one of the six comparators is terminated, a 12 VDC output signal sent from the LU to each TAA bi-stable amplifier is switched off. Loss of either 12VDC signal to the bi-stable amplifiers will trip the TAA, cutting off the output current to the electromagnets.

The type of scram (relay or electronic) has a significant impact on the control blade release time – the time from the initiation of a scram to when the control blade releases from the

magnet and begins to fall freely into the core. The release time for a relay scram is approximately 190 msec and the release time for a logic level fast scram is approximately 5 msec. The difference is due to the relatively slow decay of the magnetic coil in the relays versus the fast switching of the opto-isolated transistor. The more conservative relay scram time is used in the safety analysis in Chapter 13.

Table 7-5: RPS Safety Chain Scrams

| Scram Condition | Scram Setpoint |
|--|--|
| Key Operated Switch | Switch to Off or Test |
| Manual Scram Pushbuttons (9) | Pushbutton Depressed ⁽¹⁾ |
| Linear Module 1 High Power Relay | █ (forced flow) or █ (natural convection) |
| Linear Module 2 High Power Relay | 1.1MW (forced flow) or 110kW (natural convection) |
| Log /Period Module High Power Relay | █ |
| Log /Period Module Short Period Relay | ≤ █ seconds |
| Linear Module 1 High Voltage Relay | ≤ █ volts |
| Linear Module 2 High Voltage Relay | ≤ █ volts |
| Log /Period Module High Voltage Relay | ≤ █ volts |
| Startup Counter High Voltage Relay | ≤ █ volts |
| Primary Coolant Flow Indicator Relay | ≤ █ GPM |
| Core Flow Indicator Relay | ≤ 5 █ of nominal flow |
| Pool Height Float Switch | ≥ █ inches below full (24.5' above core CL) |
| Pool Height Sensor Transmitter Relay | ≤ █ feet |
| Pool Temperature Indicator Relay | ≤ █ |
| Core Outlet Temperature Indicator Relay | ≤ █ |
| Pool Inlet Temperature Indicator Relay | ≤ █ |
| Temperature Recorder (Pool, Outlet, Inlet) Relay | Same as above |
| Seismic Sensor Switch | ≥ █ Modified Mercalli Scale ⁽²⁾ |
| Primary Plenum Outlet Gate Switch | Switch Open (Forced Convection) ⁽³⁾ |
| Bridge Movement Limit Switch | Switch Open (Forced Convection) ⁽³⁾ |
| Bridge Position Limit Switch | Switch Open (Forced Convection) ⁽³⁾ |
| Inlet Pipe Swivel Limit Switch | Switch Open (Forced Convection) ⁽⁴⁾ |
| Outlet Pipe Swivel Limit Switch | Switch Open (Forced Convection) ⁽⁴⁾ |
| Primary Piping Valve Limit Switches (6) | Switch Open (Forced Convection) ⁽⁴⁾ |
| Process Control HMI WDT Relays (2) | ≥ █ second |
| Drive Control HMI WDT Relay | ≥ █ second |

Notes:

- (1) Manual Scrams - Manual scram is initiated at the operator discretion by actuation of the manual scram push button which breaks the safety chain scram circuit and de-energizes the main scram relays. Emergency manual scram pushbuttons are also located in strategic locations in the containment building and one located outside the building in the Reactor Supervisor's office.
- (2) Seismic Disturbance - Relay scram occurs when a seismic disturbance closes the seismic trip detector contact which short circuits the seismic trip relay coil.

- (3) Bridge, Coolant Gate - Relay scram occurs if the bridge is moved out of position, or if the riser plenum coolant gate opens under forced convection
- (4) Primary Piping - Relay scram occurs if primary piping is out of alignment or if pool inlet/outlet valves are unseated

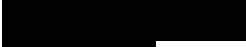
Table 7-6: Radiological Protections Scrams

| Scram Condition | Scram Setpoint |
|--|-----------------------|
| Area Radiation Monitoring System Relay | See section 7.7 |
| Thermal Column Door Limit Switch | Switch open |
| Beamport Door Limit Switch | Switch open |
| Third Floor Airlock Integrity | Both doors unsealed |
| First Floor Airlock Integrity | Both doors unsealed |
| Truck Door Seal Switch | Door unsealed |

Although the radiological protection scrams are part of the reactor protection system (RPS) scram circuit, these scrams have no function in reactor protection. They are solely incorporated into the scram chain to protect personnel, the public, and the environment from possible radiation exposures.

7.4.4 Alarm and Indicator System

The alarm system is divided into two sections: one for coolant variables and the other for nuclear variables. The section used for cooling system alarm will be operative with forced cooling. When an abnormal condition develops, a buzzer sounds and the appropriate light goes on. The operator may press the acknowledge button to silence the buzzer. When the alarm condition is corrected, the light may be reset. The following conditions will actuate the alarm and indicator system:

- (1) Short period inhibit
- (2) High neutron flux inhibit
- (3) Safety chain scram
- (4) Blade disengaged
- (5) Low pool level
- (6) Bridge unlocked
- (7) 
- (8) 
- (9) 
- (10) Low coolant flow (2 sensors)
- (11) High coolant temperature (3 sensors)
- (12) High conductivity

- (13) High voltage failure
- (14) Regulating blade at limit
- (15) Reactor core low flow
- (16) Demineralizer high temperature and low flow.

7.4.5 [REDACTED] Mode Operation

The reactor may be operated up to a steady-state power level of [REDACTED] when the primary pump is off and core cooling is maintained by natural convection (see analysis in Chapter 13). When the Power Select Switch P-18 is placed in the [REDACTED] position, a set of contacts provides a 24VDC signal that energizes the natural convection control relays associated with primary coolant indicators and the linear power channels.

When energized, the primary coolant natural convection control relay closes two sets of contacts. One set of contacts provides a logic status input to the Primary Flow Indicator and the second set of contacts provides a logic status input to the Core Flow Indicator. In both indicators, the status input disables the alarm and trip relays while status input is activated. This condition allows the scram circuit (Section 7.4.3) to be energized when primary pump is off and there is no primary flow. When the 24VDC signal is not present, the set of contacts on natural convection control relay reverts to the normally open position, deactivating the logic status inputs, and enabling the alarm and trip relays on the indicators.

In order to accommodate the need for a low-power ([REDACTED]) SCRAM when operating under Natural Convection mode, the linear power modules utilize two spare trips designed into the trip circuitry. The mode of operation of the bases the high power trip on a relay activated switch. The Normally Closed (NC) contact on the DPDT relay, with a make before break capacity, is used for Forced Convection Operation. The 24VDC signal generated during Natural Convection switches the relay contacts in use to the Normally Open (NO) poles. The Make/Break capacity ensures that the transient between switching from Natural Convection to Forced Convection does not produce an open circuit fault and the associated SCRAM. Each of the four trips, alarm and SCRAM for both Forced Convection and Natural Convection, have independent trip set points.

7.5 Engineered Safety Features Actuation Systems

Engineered Safety Features (ESFs) are designed to (1) prevent or mitigate the consequences of fuel damage due to overpower or loss of cooling events, or (2) gain control of any radioactive material released by accidents. The results of design bases events analyzed for the UMLRR in Chapter 13 show ESFs are not required for overpower or loss of cooling events. The UMLRR containment isolation system described in Chapter 6 is designed to manually and automatically shut-down the containment building ventilation system and actuate ventilation isolation valves.

7.6 Control Console and Display Instruments

The I&C systems are assembled in three cabinets: (1) the control console, (2) the instrumentation cabinet, and (3) the radiation monitoring cabinet. All three cabinets are positioned in the Reactor Control Room (RCR), located on the third floor of the reactor containment building (Figure 7-7).

The RCR is a wedged shaped enclosure measuring [REDACTED] feet ([REDACTED] m) along the side facing the reactor pool and [REDACTED] feet ([REDACTED] m) on the side with entry, and having an [REDACTED]-foot ([REDACTED] m) high suspended acoustical ceiling. The RCR serves as a centralized management point for monitoring and interfacing with the reactor controls and instruments, and other related systems. Windows on the south and west sides of the RCR provide the operator a wide view of the entire third floor area, including the reactor pool and reactor bridge. A door with [REDACTED] [REDACTED] floor airlock.

The control console provides the operator with a vantage point from which to conveniently observe reactor performance and adjust operating parameters to varying requirements when needed for experiments and other operations. The control console consists of a desk type cabinet 71 inches wide, 44 inches high, and 31 inches deep. The controls and instruments required for operation of the reactor are contained in a control panel, which slopes upward 45° from the rear of the desk.

The [REDACTED] Panel is located adjacent to the [REDACTED] console and angled towards the operator for easy viewing and access to the instrument readouts and controls.

The instrumentation panel is 70 inches wide, 83 inches high, and 26 inches deep. To the [REDACTED] of the [REDACTED] panel is the [REDACTED] panel.

The [REDACTED] [REDACTED] cabinet is located to the right rear diagonal of the control console. The cabinet is 29 inches wide, 60 inches high.

Figure 7-7 provides the [REDACTED] layout for the control console and instrumentation panel. Table 7-7 lists the I&C components depicted in Figure 7-8 & Figure 7-9.

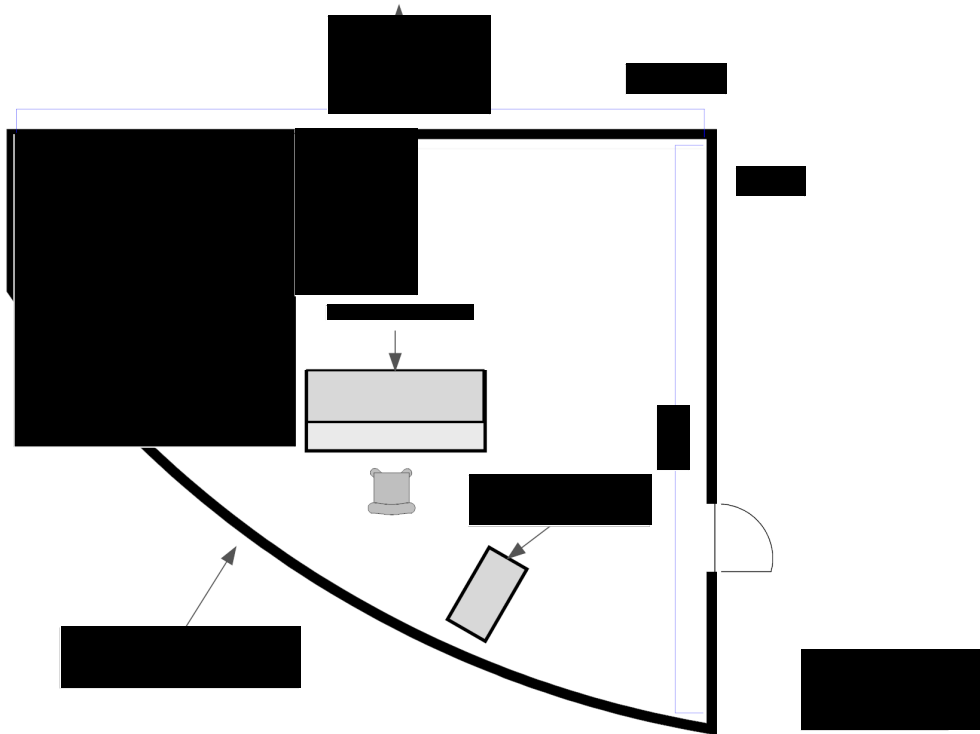


Figure 7-7: I & C Layout for [REDACTED] [REDACTED] and [REDACTED] Panel

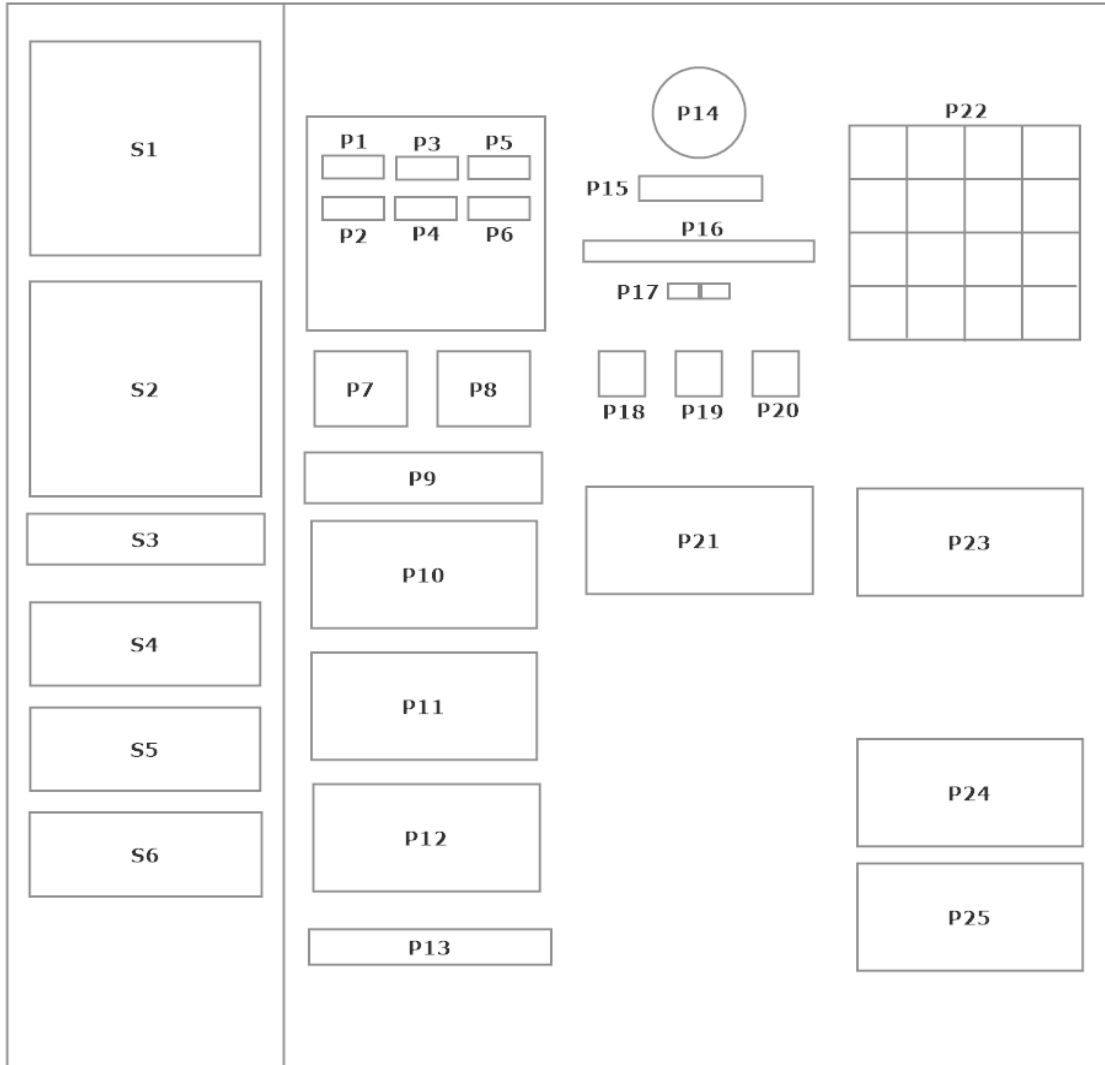


Figure 7-8: Instrument Panel Layout

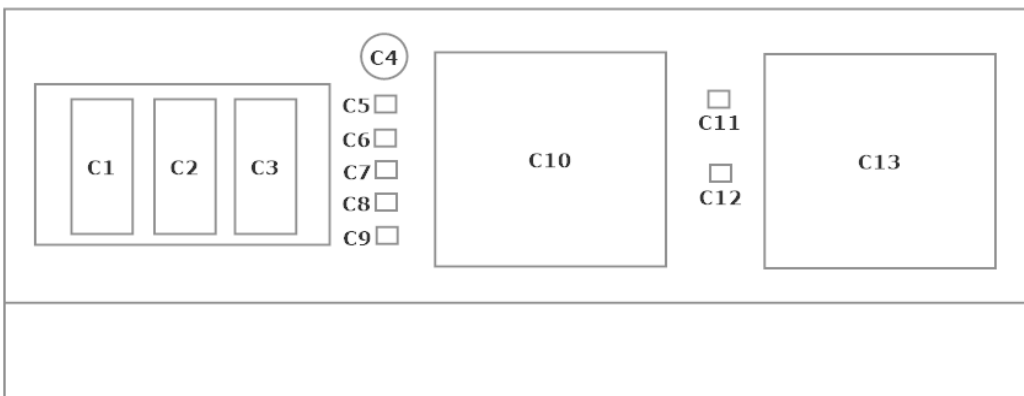


Figure 7-9: Control Console Layout

Table 7-7: I & C Components

| Reference Number | Description | Function |
|------------------|--------------------------------------|--|
| S1 | Camera Display - 1 | Displays internal/external facility camera feeds |
| S2 | Camera Display -2 | Displays internal/external facility camera feeds |
| S3 | Intercom | Master station internal/external intercoms |
| S4 | Computer -1 | Digital camera display software |
| S5 | Computer -2 | [REDACTED] |
| S6 | Digital Video Recorder | Records all internal camera video feeds |
| Reference Number | Description | Function |
| P1 | Primary Inlet Temperature Indicator | Converts and displays primary coolant inlet RTD temperature signal in °F. Provides relay outputs for alarm and scram. Provides 4-20mA output signal to recorder and PCS. Provides manual switch and potentiometer for trip function test. |
| P2 | Primary Outlet Temperature Indicator | Converts and displays primary coolant outlet RTD temperature signal in °F. Provides relay outputs for alarm and scram. Provides 4-20mA output signal to recorder and PCS. Provides manual switch and potentiometer for trip function test. |
| P3 | Pool Temperature Indicator | Converts and displays pool RTD temperature signal in °F. Provides relay outputs for alarm and scram. Provides 4-20mA output signal to recorder and PCS. Provides manual switch and potentiometer for trip function test. |
| P4 | Pool Height Indicator | Converts and displays pool height sensor signal in feet above the core center line. Provides relay outputs for alarm and scram. Provides 4-20mA output signal to PCS. Provides manual switch and potentiometer for trip function test. |
| P5 | Primary Flow Indicator | Converts and displays primary flow sensor signal in GPM. Provides relay outputs for alarm and scram. Provides 4-20mA output signal for recorder and PCS. Provides manual switch and potentiometer for trip function test. |
| P6 | Core Flow Indicator | Converts and displays core flow sensor signal in percentage of nominal flow. Provides relay outputs for alarm and scram. Provides 4-20mA output signal to PCS. Provides manual switch and potentiometer for trip function test. |
| P7 | Temperature Chart Recorder | Records primary inlet, outlet, and pool temperatures. Provides relay output for scram. |
| P8 | Power and Flow Chart Recorder | Records Linear Power 1, Log-power, and primary flow. Provides relay output for scram. |
| P9 | Back-up Display Drawer | Houses back-up for C-10 display |
| P10 | I/O Rack -1 | Refer to Section 7.6.1 |

| | | |
|-----|--------------------------------------|--|
| P11 | I/O Rack -2 | Refer to Section 7.6.1 |
| P12 | I/O Rack -3 | Refer to Section 7.6.1 |
| P13 | Local Ethernet switch | Provides interconnections hub for sub-systems. Refer to Section 7.6.1 |
| P14 | Clock | |
| P15 | Reactor On Indicator | Light indicates key-operated master switch (P18) is turned to ON position |
| P16 | Fuse Indicators | Fuses with various panel branch circuits |
| P17 | 115VAC/24VDC Indicators | 115VAC light indicates reactor control circuit is energized through 115VAC control power circuit breaker and Master Switch (P18). 24VDC light indicates DC power supply is energized for scram circuit and other interlocks |
| P18 | Power Level Selector Switch | █ position provides a 24VDC signal to energize relays which bypass forced convection trips (P4 and P5) and enable power level trips on the 100kW range (C1 and C2). Refer to Section 7.4.5 for more detail. |
| P19 | Key Operated Switch | OFF position de-energizes two fuse-protected branches of the reactor control circuit. TEST position energizes reactor control circuit without energizing scram magnets, thereby allowing test of control drives with blades disconnected. ON position energizes reactor control circuit and scram magnets; sounds warning bell for impending reactor start-up |
| P20 | Alarm Panel Switch | Energizes alarm indicator panel (P21) |
| P21 | Nuclear Instrumentation Module (NIM) | The NIM includes a high voltage power supply and voltage monitor for the start-up channel B-10 proportional counter, and a high voltage power supply for the N-16 ion chamber. An amplifier processes the signal from the proportional counter preamplifier (located on reactor bridge) and provides a pulsed signal output to the count ratemeter. Refer to Section 7.4.1 |
| P22 | Alarm Panel | Provides annunciator buzzer and annunciator lights for 16 monitored conditions. Refer to Section 7.2.2 |
| P23 | N-16 Power Module | Measures current from ion chamber located on primary coolant line. |
| P24 | Magnet Power Supply Indicators | Monitors individual magnet current to the four control blade scram magnets. |
| P25 | Logic Element and Trip Amplifiers | Receives signals from linear power modules (C1 and C2) and the log power/period module (C3), and cuts off power to the safety magnets on signals of excessive neutron flux or short period |

Table 7-7: continued

| Reference Number | Description | Function |
|------------------|--|---|
| C1 | Linear Power Module - 1 | The wide range linear power module measures detector current 1E-11 to 1E-3 amps. Relay and electronic trip outputs are provided for alarm and scram conditions. Isolated signal outputs are provided for remote indicators. Refer to Section 7.4.1 |
| C2 | Linear Power Module - 2 | Same as C1. |
| C3 | Log Power and Period Module | The wide range logarithmic power monitoring module measures 10 decades of neutron flux ranging from 0.3 to 1E10 nv. A period circuit generates an output proportional to the rate of change in power. Relay and electronic trip outputs are provided for alarm and scram conditions. Isolated signal outputs are provided for remote indicators. Refer to Section 7.4.1 |
| C4 | Manual Scram Pushbutton | De-energizes scram relays and produces a relay scram at the discretion of the operator. |
| C5 | Secondary System Remote Control Switch | Energizes circuit allowing for remote control of secondary cooling system motor operated valve and cooling tower fans. |
| C6 | Alarm Panel Reset Switch | An alarm condition is annunciated by a buzzer and lighted indicator on the alarm panel. |
| C7 | Alarm Acknowledge Switch | Alarm Panel Reset Switch clears the indicator when the alarm condition is cleared. Alarm Acknowledge Switch turns off the buzzer. Alarm Panel Test Switch turns on all the alarm indicators and buzzer. The Scram Reset Switch energizes the scram relays and scram circuit chain when the scram condition has been cleared. |
| C8 | Alarm Panel Test Switch | |
| C9 | Scram Reset Switch | |
| C10 | Process Controls Display | See section 7.6.1 |
| C11 | Third Floor Airlock Switch | Opens third floor outer airlock door. |
| C12 | First Floor Airlock Switch | Opens first floor outer airlock door. |
| C13 | Drives Controls Display | See section 7.6.1 |

7.6.1 Human Machine Interface Displays

7.6.1.1 Introduction

There are two human machine interface (HMI) display screens (C-10 and C-13) on the control console (Figure 7-9). The center display screen (C-10) is associated with the Process Controls and Instrumentation System and is designated as the PCS display. The display screen on the right side of the console (C-13) is associated with the control blade and regulating rod drive controls and is designated as the DCS display. A third display is associated with the Area Radiation Monitoring System (ARMS) and is located on the ARM cabinet. The PCS provides indicators for power level, various temperatures, flow rates, pressures, water purity, and on/off controls for various motors, valves, and fans. The DCS provides displays and controls for the drive mechanisms associated with the control blades, regulating blade, and start-up counter. The ARMS provides displays for alarms and test functions for the various area radiation monitors. The PCS, DCS, & ARMS each have separate hardware and software, and operate independently. The systems use control and input/output hardware manufactured for industrial process control, process monitoring, and data acquisition. The software used to operate the system is an integrated suite of industrial control and automation software provided by the same manufacturer of the hardware. The ARMS was installed in 1999, the PCS in 2001, and the DCS in 2003. Each system was installed under 10 CFR 50.59, and subsequently reviewed during routine inspections.

7.6.1.2 Hardware Description

Field devices, sensors, and isolated outputs for each system are connected to the input/output (I/O) modules located on I/O racks. Each I/O rack houses a microprocessor. The rack microprocessor communicates data from each I/O module to a single main microprocessor referred to as a controller. In addition to communication, the rack microprocessors are capable of providing independent local control of the output modules to perform simple tasks such as on/off control. The controller receives and processes the input from each rack microprocessor. The controller includes a programmed set of instructions to perform control actions by sending commands to the rack microprocessors. The controller also relays data to the Human Machine Interface (HMI) personal computers for display.

7.6.1.3 HMI Computers

Each HMI computer displays the information from the associated controller and provides a touch screen and a keyboard terminal for manual control of process functions. The PCS and DCS HMIs consist of 19-inch flat panel, touch screen displays connected to their respective PC. The ARMS use a standard 19-inch display and PC. Each PC contains the programmed display configuration developed for its particular application. The display configurations were developed using the integrated software package associated with the hardware. The configurations provide graphical interfaces for displaying data from the controller and the transfer of operator commands. Data trending (charts) and archiving are also accomplished on the PCs. The configurations are password protected to prevent unauthorized changes.

7.6.1.4 Process Controls Display

A number of display screens are available on the PCS to monitor and control various systems, record data, test various functions, and to allow adjustments to set-points and analog signal calibration.

The Reactor Power screen provides the linear percent power output from linear power channels 1 and 2, the logarithmic power and period outputs from the logarithmic power channel, the start-up count rate from the start-up count rate channel, the linear percent power from the nitrogen-16 detector, and a calorimetric determination which is based upon the primary coolant flow rate and core differential temperature.

The Coolant Systems screen displays detailed information about the various water systems processes. The screen allows the operator to START/STOP coolant pumps, START/STOP the cooling tower fans and to view the controls status. Indicators display the status of the motors and controls.

Complete information related to the coolant systems status includes indicators for coolant flow rates, coolant temperatures, conductivity, the heat exchanger temperatures and differential pressures, pool water height, make up water control status, pump room sump level, temperature and humidity outside containment, and difference in temperature across the core.

The Ventilation System screen displays detailed information about the containment building ventilation and isolation system. The screen allows the operator to START/STOP the

ventilation fans. The same controls concurrently operate and provide status of the associated air duct valves for the fans.

Several trend screens are available to view data plots of various parameters.

While no credit is taken in the technical specifications, the isolated outputs from the process variables are also monitored by the PCS, providing a redundant and parallel protection system. When a parameter safety set-point is reached, the PCS controller sends a signal to the independent I/O racks that each contains a trip relay. The relays are de-energized, opening contacts on the safety chain scram circuit.

7.6.1.5 Drives Control Display

The drives control display screen (DCS) displays the control blade position and status indicators. The DCS also provides an interface for selecting, withdrawing and inserting the drives for the control blades, regulating rod, and start-up counter. The operator may also select the Automatic or Manual modes of regulating rod operation, once the reactor is critical at power level determined by the operator. An indicator informs the operator of the regulating rod control mode. In addition, the following indicators are available:

7.6.1.6 Control Blade Drive Indicators

A control blade Disengaged/Engaged indicator informs the operator whether the control drive magnet is attached to the control blade. A digital positional indicator provides the control blade position in inches from the core bottom, measured to 1/100th of an inch. A bar graph also provides a visual indication of the control blade position. Other indicators provide an absolute indication of the control blade position as full in or full out, or if a drive motor malfunction exists. An Inhibit indicator signals if power to the drives has been disconnected due to a safety interlock.

7.6.1.7 Regulating Rod Drive Indicators

A digital positional indicator provides the regulating rod position in inches from the core bottom, measured to 1/100th of an inch. A bar graph also provides a visual indication of the regulating rod position. Other indicators provide an absolute indication of the regulating rod

position as full in or full out, or if a drive motor malfunction exists. An Inhibit indicator signals if power to the drives has been disconnected due to a safety interlock.

7.6.1.8 Regulating Rod Mode Indicators

A Manual/Auto indicator informs the operator whether the regulating rod in manual or automatic mode. The power level/setpoint indicator provides two bar-graphs: (1) along with a digital indicator, the power level bar graph provides the actual reactor power level, (2) the setpoint bar-graph indicates the power level for the reactor at the moment the automatic mode is engaged. While in automatic mode, the Auto Increase/Decrease controls allow the operator to make slight adjustments to power in increments of approximately 2%.

7.6.1.9 Startup Counter Drive Indicators

A digital positional indicator provides the start-up counter position in inches from the core bottom, measured to 1/100th of an inch. A bar graph also provides a visual indication of the start-up counter position. Other indicators provide an absolute indication of the start-up counter position as full in or full out, or if a drive motor malfunction exists.

7.6.1.10 Other Controls

The Auto Blade Position Schedule allows the operator to withdraw each control blade drive in a semi-automatic mode. The control blade drives are hard-wired such that only one drive can operate at one time. Using the Position Enter control, the operator enters the desired position of the control blade in inches. The operator selects the desired control blade and then uses the Start control to automatically drive the control blade to the desired position.

The Reset control places all six drives into the full in position, then resets all the digital indicators to zero

7.6.2 Performance Characteristics

The ARMS HMI was installed in 1999. The PCS HMI was installed in 2001 and the DCS HMI was installed in 2003. All three systems have performed normally and reliably to date. The analog/digital hybrid provided by the HMI systems provide more detailed, accurate, and reliable information than was available with the original I&C components.

Continued reliable performance is assisted by routine surveillance and maintenance. The performance of both the PCS and DCS HMI are checked thoroughly as part of the pre-startup reactor checkout procedure. In addition to performing the daily channel checks and tests required by the Technical Specifications (Chapter 14, TS 4.2.2), the operator performs administratively required checks that compare and record readings from stand-alone indicators and the HMI displays.

7.6.2.1 Failure Analysis

The availability of the HMI displays is not of paramount concern since the primary parameters of concern monitored by the RPS (reactor power level, primary coolant temperature, primary coolant flow rate, and reactor pool water height) are available on stand-alone indicators. Nonetheless, each HMI also employs a failsafe “watchdog” timer that activates trip relays in the scram circuit.

The failsafe watchdog timers ensure that any microprocessor or communication failure will result in a reactor failsafe shutdown condition. If communication is lost between a controller and the associated HMI computer display, within 1 second a command is given for the watchdog relay to open. If communication is lost between a controller and an I/O rack, within 1 second a command is given for the watchdog relay to open. The computer display also has a watchdog timer. If the computer fails to communicate with the controller within █ seconds, the controller will open the scram relay.

A failure with the DCS that results in lost control or positional information of the drives will result in a reactor scram. The operator can visually verify the reactor is shutdown by visual observation of the power measuring instruments and, if necessary, visually verifying the control blades are in the reactor core.

A failure of the PCS HMI will also result in a fail-safe shutdown of the reactor.

7.7 Radiation Monitoring Systems

7.7.1 Introduction

The installed Area Radiation Monitoring (ARM) system is designed to perform several important and diverse functions ensuring the safe operation of the UMLRR. These functions

include: measurement of the containment building internal radiation levels and measurement of the radioactivity levels within effluent releases.

Radiation and radioactivity measurements are made to demonstrate that exposures from radiation and gaseous effluent releases are within the established objectives of the UMLRR ALARA Program. The locations that have been selected to be monitored continuously include areas or systems where an increase in radiation level may indicate a change in facility conditions which could potentially have an adverse effect on the safe operation of the facility and may constitute an undue risk to the health and safety of the facility staff and the general public.

In addition, the ARM can initiate an automatic isolation of the reactor containment building should a high radiation level occur when a pre-set combination of detectors within the containment building unexpectedly experience high radiation levels. This function is described in greater detail in Chapter 6, Engineered Safety Features.

This section discusses the operating principles, designs, and the functional performance of the instrumentation and control (I&C) aspects of both required and permanently installed radiation monitoring equipment at the reactor facility. The UMLRR Radiation Protection Program establishes the radiation monitoring criteria for the reactor facility necessary to provide an acceptable level of radiation protection for the staff and general public. This program is discussed in detail in Chapter 11, Radiation Protection Program and Waste Management.

The UMLRR Radiation Monitoring System radiation detectors and monitors are structured to measure the radiation expected to be encountered in a research reactor environment. The detectors give reasonable assurance that all radiation sources will be identified and accurately evaluated. The Area Radiation Monitoring (ARM) System also provides reasonable assurance that dose rates and effluents present at the facility will be acceptably detected, and that the health and safety of the facility staff, the environment, and the public will be acceptably protected.

7.7.2 Area Radiation Monitoring System

7.7.2.1 Description

The Area Radiation Monitor (ARM) is used to continuously monitor gamma and beta radiation levels at strategic locations in the reactor facility, as well as any gaseous and particulate emissions. Radiation levels are displayed on six rate meters positioned in a centrally-located control chassis adjacent to the Reactor Control Panel (Figure 7-7), as well as remote rate meters strategically located through the facility. Each rate meter drives three detectors and is equipped with Double Pole Double Throw relays (DPDT) and a Single Pole Double Throw relay, as well as isolated 4-20 mA analog outputs and isolated RS-485 communication ports. The Analog Outputs are proportional to the dose rate for area monitors or the count rate/concentration for air monitors. These rate meters can drive a range of detector types that can include a mix of the following detectors:

Table 7-8: Radiation Monitoring Probes and Functions

| Type of Radiation Monitor | Radiation Detected | Use |
|---|--------------------|---|
| Gamma Detector (Geiger Counter) | Gamma | Area dose rate monitoring throughout containment |
| Neutron Detector (Proportional Counter) | Neutron | Fission product monitor |
| Ion Chamber Detector | Gamma | Area dose monitoring suitable for burst radiation |
| <i>Additional remote rate meter outputs available at the ARM control chassis include the following detector assemblies:</i> | | |
| Stack Effluent Monitor | Beta-Gamma | Monitor gaseous and particulate effluents released through the stack |
| Environmental Gamma | Gamma | Monitor environmental levels within UMLRR |
| Continuous Air Monitors | Beta-Alpha | Monitor air levels at pool level and on experimental level |
| Remote Ratemeter | Gamma / Neutron | Provide radiation monitoring and readouts at remote locations within containment. |

The Detector ranges and sensitivities are listed in Table 7-9. Detector Range and Sensitivities. This list provides details of the sensitivity for isotopes of interest as well as the potential ranges in which the detector is designed to function.

Table 7-9: Detector Range and Sensitivities

| Detector Type | Low Range | High Range | Detector Sensitivities, Low Range* | Detector Sensitivities, High Range* |
|-------------------------------|----------------------|------------|------------------------------------|-------------------------------------|
| Geiger | μR/h | R/h | CPM/mR/h | CPM/mR/h |
| Ion chamber | μR/h | R/h | μR/Pulse / 4 /Pulse | 0.4 /Pulse / nSv/Pulse |
| Proportional | μR/hr | R/hr | | |
| PIPS | | | α | β |
| Gaseous Extended Range Beta | μCi/cc | μCi/cc | Xe-133 sensitivity cpm/μCi/cc | |
| Particulate Extd. Range gamma | β 1E1cpm γ 1E1cpm | β γ | Cs-137 β sensitivity cpm/μCi/cc | Cs-137 γ sensitivity cpm/mR/hr |

*sensitivity as described for particular isotope and radiation type

For Geiger, Ion Chamber and Proportional detectors, the detector assemblies contains a high voltage power supply, a radiation detecting element, a pulse amplifier, a line driver. The pulse signal generated by the detecting element is amplified and processed, and then carried via cable to an electronics channel, where it is further processed and displayed on a meter in millirem per hour. Each electronics channel is equipped with an adjustable set point trips that initiate a visual alarm on detection of both an elevated radiation and high radiation level.

For PIPS, Gaseous and Particulate detectors, the detector, power supplies, amplifiers and readouts are co-located and are integrated into an assembly that contains both detector and readout.

Alarms may be latching or non-latching and while the alarm relays are configuration as normally energized (de-energized on alarm, failsafe) or normally de-energized (energize on alarm). In latching mode, the alarm indicators continue to indicate alarm until after the rate drops below the alarm set point and the operator has pressed the Reset button on the rate meter face plate. In non-latching (or tracking mode), the alarm indicators automatically reset when the rate drops below the alarm set point.

Adjustment to the alarm trip set points on the rate meter is accomplished using the panel of each electronics channel; the panel cannot be changed in any way without the use of a physical key lock on the channel. This key lock shifts the device from being changed with authorization from the appropriate personnel. This arrangement reasonably ensures that an inadvertent or unmonitored adjustment of the trip point is highly unlikely. The power required to operate the detector assembly is supplied by the rate meter through interconnecting wires.

7.7.2.2 Constant Air Monitor (CAM)

Monitoring for internal airborne contamination is performed using Constant Air Monitors (CAM). Technical Specifications (Chapter 14, TS 3.6.1) require that a CAM be functional on the experimental level (3rd Floor) of the facility while operating the reactor. The counting efficiency for the CAM for beta particles is about 0.23 counts per disintegration. This high efficiency is attained through the use of two solid state PIPS detectors. The first PIPS detector views the filter and therefore responds to alpha, beta, and gamma radiation from trapped particulates, as well as ambient gamma and cosmic ray radiations. The second PIPS detector is mounted above the first, and in this configuration it responds only to ambient gamma and cosmic ray radiations. Given that ambient gamma rays are isotropic, and ambient cosmic rays are directed downward through the atmosphere, the second PIPS detector is used to subtract gamma and cosmic ray response from the first detector.

The Passivated Implanted Planar Silicon (PIPS) detector, is fabricated in the form of a large area (450 mm²) silicon diode, produces a signal as the energized particle is slowed down or stopped in the depletion region through the formation of electron-hole pairs. Therefore, the front surface of the PIPS detectors are coated with aluminum to block the light, and one of the PIPS detectors is placed in close proximity to the air filter source.

Outputs from the CAM are hardwired to the ARM Chassis and read directly into the ARM Computer Data Acquisition System (CDAS) for both display and alarm purposes as described in Section 7.7.5. Local audible and visual alarm alerts the operator to high activity or abnormal air flow through the radiation detection equipment. The CAM system set points and programming are limited to a hardwire connection requiring a stand-alone computer to connect and program the unit, and are not readily modified or changed.

7.7.2.3 Stack Exhaust Air Monitor

The air exiting the facility through the ventilation system exhaust stack is continuously monitored for airborne radioactivity by the Stack Radiation Monitoring System. The maximum rate of discharge through the facility ventilation exhaust stack shall not exceed limits specified in the Technical Specifications (Chapter 14, TS 3.6.2). These limits ensure that exposure to the general public resulting from radioactivity released to the environment will not exceed the limits

of 10 CFR 20. The monitoring equipment of this system consists of a two-channel radiation detection system designed-to measure the airborne concentrations of radioactive particulate, and noble gas in the facility exhaust air which is sampled by an isokinetic probe located in the ventilation exhaust plenum. The detector characteristics are described in Table 7-9. The output from each radiation detector is displayed on a local meter in counts per minute (cpm) and on the ARM CDAS computer display. Local audible and visual alarm alerts remote users to high activity or abnormal air flow through the radiation detection equipment; while the ARM CDAS computer displays visual alarm conditions as well as the automate alarm responses to the reactor control room.

7.7.3 Detector Locations

The locations of the main chassis ratemeter detectors and the remote ratemeter detectors, as well as detector type, are shown in below in Table 7-10 Main Chassis Area Radiation Monitoring (ARM) and Table 7-11 Remote Area Radiation Monitoring (RARM). The Ratemeter – Detector identifies the individual ratemeter and the detectors associated with it.

Table 7-10: Main Chassis Area Radiation Monitoring (ARM)

| Ratemeter - Detector | Identifier / ARM Logic | Location | Type |
|----------------------|------------------------|-----------------------|---------|
| 1-1 | CONTROL ROOM (R) | 3 RD FLOOR | GM |
| 1-2 | HOT CELL | 2 ND FLOOR | GM |
| 1-3 | BULK POOL (AX-2) | 3 RD FLOOR | GM |
| 2-1 | RABBIT FILER | 2 ND FLOOR | GM |
| 2-2 | ELDRS-OUT (O) | 1 ST FLOOR | GM |
| 2-3 | THERMAL COLUMN (L) | 1 ST FLOOR | GM |
| 3-1 | RABBIT-1 (M) | 1 ST FLOOR | GM |
| 3-2 | RABBIT-2 | BASEMENT LEVEL | GM |
| 3-3 | PUMP ROOM | BASEMENT LEVEL | GM |
| 4-1 | EXHANUST PLENUM | 3 RD FLOOR | GM |
| 4-2 | GAMMA CAVE (AX-2) | 1 ST FLOOR | GM |
| 4-3 | FACILITIES FILER | 1 ST FLOOR | GM |
| 5-1 | DEMINERALIZER (S) | BASEMENT LEVEL | ION CH. |
| 5-2 | REACTOR BRIDGE (K) | 3 RD FLOOR | ION CH. |
| 5-3 | FISSION PRODUCTS (E) | BASEMENT LEVEL | NEUTRON |
| 6-1 | ELDRS IN-CAVE | 1 ST FLOOR | GM |
| 6-2 | SPARE | SPARE | GM |
| 6-3 | GAMMA CAVE IN-CAVE | 1 ST FLOOR | GM |

Table 7-11: Remote Area Radiation Monitoring (RARM)

| Detector | Identifier / ARM Logic | Location | Type |
|----------|---------------------------|----------|-----------------------|
| 8-1 | INTERNAL BUNKER (GAMMA) | FLOOR | GM |
| 8-2 | INTERNAL BUNKER (NEUTRON) | FLOOR | NEUTRON |
| 8-3 | THERMAL COL. BEAMLINER | FLOOR | ION CH. |
| 8-4 | SPARE | NA | NA |
| 9-1 | GAMMA CAVE SHELTER | FLOOR | GM |
| 9-2 | GAMMA CAVE EXTERIOR | FLOOR | GM |
| 9-3 | SPARE | NA | NA |
| 9-4 | SPARE | NA | NA |
| 10-1 | SAMPLE PREP | FLOOR | GM |
| 10-2 | N-16 AREA MONITOR | FLOOR | ION CH. |
| 10-3 | SPARE | NA | NA |
| 10-4 | SPARE | NA | NA |
| 11-1 | CAM 1 BETA (D) | FLOOR | PIP |
| 11-2 | CAM 1 ALPHA | FLOOR | PIP |
| 12-1 | CAM 2 BETA (C) | FLOOR | PIP |
| 12-2 | CAM 2 ALPHA | FLOOR | PIP |
| 13-1 | STACK PARTICULATE (A) | R | γ/β SCINT. |
| 13-2 | STACK GASEOUS (B) | R | β SCINT. |

7.7.4 Radiation Monitoring Computer Inte

Signals from both the panel mounted and remote ratemeters are acquired using optically isolated Input/Output modules. This data is then processed by a stand-alone computer connected to the ARM Computer Data Acquisition System (CDAS) controller. Programmed configurations provide graphical displays for operational data from the system’s controller (microprocessor) and provides for the transfer of operator commands and pre-programmed system responses. A complete description of the hardware and software can be found in Chapter 7, along with a more detailed description of the HMI and system architecture.

The system diagram of the Integrated ARMS is shown in Figure 7-10 Block Diagram of Integrated ARM and RARM System Assemblies.

NOTES

1. AX-2 DENOTES A REMOTE READOUT LOCATED ADJACENT TO DETECTOR LOCATION.
2. ALL RATEMETER MODULES ARE SUPPORTED BY BATTERY BACKUP POWER SUPPLY.
3. UNLESS NOTED, ALL DETECTORS ARE GEIGER DETECTORS.
4. ALL RATEMETERS ARE POWERED ON ELPL - EMERGENCY POWER CIRCUIT.
5. HIGH TRIPS BY PRESET COMBINATIONS OF DETECTORS ARE CAPABLE OF PRODUCING A GENERAL REACTOR OF THE VENTILATION SYSTEM.

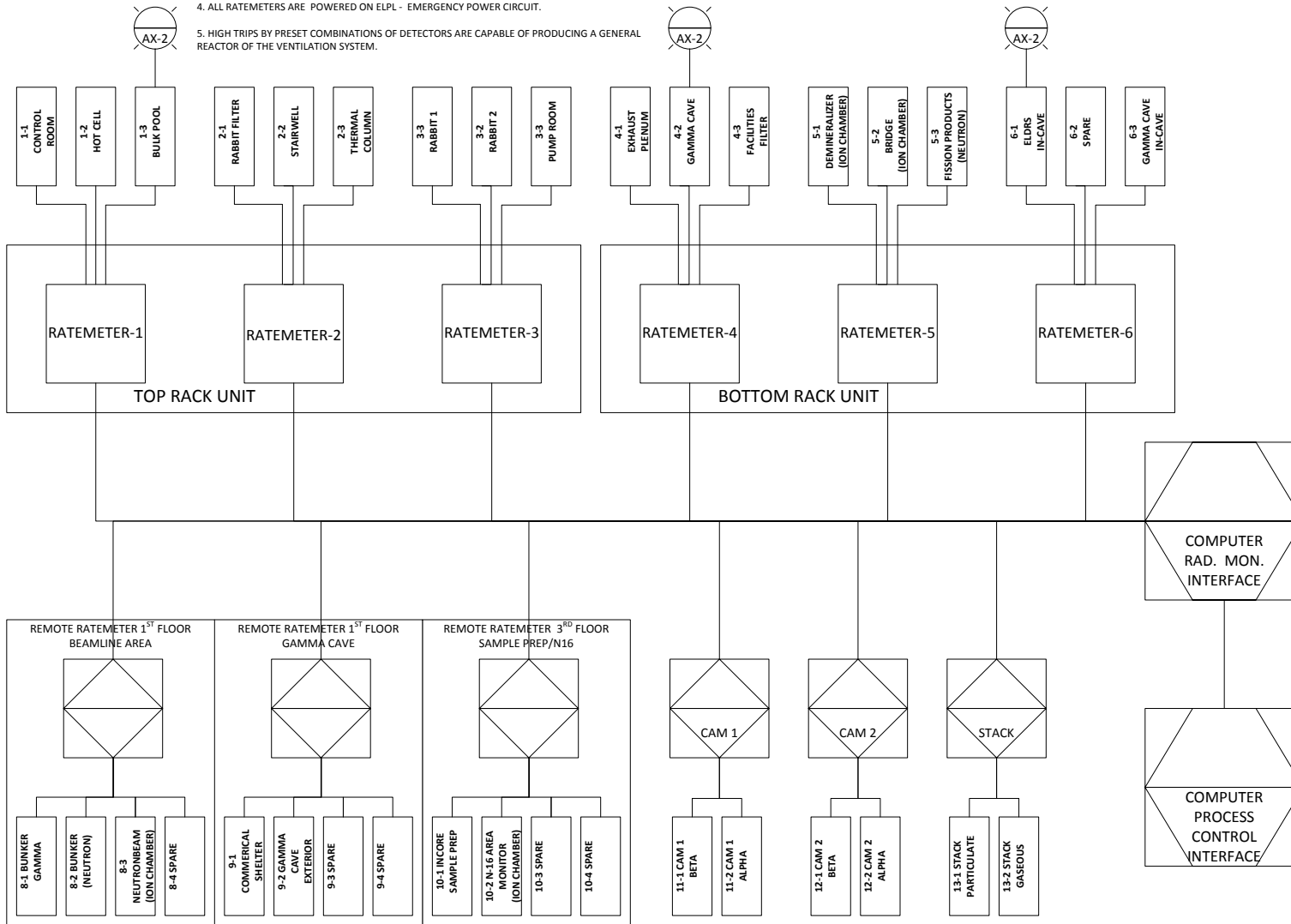


Figure 7-10: Block Diagram of Integrated ARM and RARM System Assemblies

7.7.5 Alarm Logic and Action Description

Readings producing high alarms on a certain combination of detectors may indicate the *potential* for either a *local* radiation hazard or a *general* radiation hazard. Local radiation hazards are considered for a specific area within the containment building. General radiation hazards correspond to a fission product release or other significant radioactivity release, where the release has or may occur outside of containment. Under a Potential Local Radiation Emergency Alarm (LREA), operator response is required to initiate containment isolation, a Potential General Radiation Emergency Alarm (P-GREA), in contrast automatically activates the containment isolation system. Alarm conditions are considered a potential emergency until the operator can verify the conditions and declare an actual emergency.

(Note: + indicates either/or, * indicates with/and)

7.7.5.1 Potential Local Radiation Emergency Alarm (P-LREA)

Logic: $(L * M * O) + (C * D) + (K * R) + (E * S)$

High readings on detectors associated with LREA Logic initiate the following actions:

1. P-LREA indicator on cabinet *and* display screen activated.
2. “Squee” alarms energized in the reactor building *and* laboratory building.
Pressing the *ALARM* pushbutton on the cabinet or clicking *Actuate Alarm* on the display screen declares an emergency and initiates the following additional actions:
3. LREA indicator on display screen activated.
4. Evacuation alarm horns energized in reactor building (only).
5. Reactor building ventilation is shutdown.
6. Reactor automatic shutdown (SCRAM).

7.7.5.2 Potential General Radiation Emergency Alarm (P-GREA)

Logic: $[(S+I+L+K+E+R) * (A+B+C+D)] + [(I+R+K) * (E+S)]$

High readings on detectors associated with GREA Logic initiate the following actions:

1. P-GREA indicator on cabinet and display screen activated.
2. “Squee” alarms energized in reactor building *and* laboratory building.
3. Reactor building ventilation shutdown.

Pressing the *ALARM* pushbutton on the cabinet or clicking *Actuate Alarm* on the display screen declares an actual emergency and initiates the following additional actions:

4. GREA indicator on display screen.
5. Evacuation alarm horns energized in reactor building *and* laboratory building.
6. Reactor automatic shutdown (SCRAM).

7.7.5.3 Emergency Team (ET) Alert

Pressing the ALARM pushbutton on the cabinet or clicking *Actuate Alarm* on the display screen, *when no GREA or LREA logic is present*, energizes the “squee” alarms in both the reactor and laboratory buildings and changes the status indicator to ET Alert on the display screen.

7.7.6 LREA Detector Combinations and Explanations

The combinations of detectors that result in a Local Radiation Emergency Alarm (LREA) will correspond to a specific area within the containment building. There are four combinations of detectors that produce an LREA alarm are as follows: (L*M*O) + (C*D) + (K*R) + (E*S)

1. (L)Thermal Column AND (M)Rabbit 1 AND (O) ELDRS-Out

This alarm combination indicates a wide area radiation hazard on the reactor first floor. (e.g., open beam port or open gamma facility shield).

2. (C)Cam2 AND (D)Cam1

This combination indicates an airborne contamination hazard within containment.

3. (K)Reactor Bridge AND (R)Control Room

This combination indicates a wide area radiation hazard on the reactor third floor. (e.g., a strong radioactive source near or above the pool surface).

4. (E)Fission Products AND (S)Demineralizer

While this combination indicates a fission product release confined to the primary coolant.

7.7.7 GREA Detector Combinations and Explanations

The combinations of detectors resulting in a General Radiation Emergency Alarm (GREA) may correspond to a fission product release or other significant radioactivity release, where the release has or may occur outside of containment. These combinations can be categorized into five broad groups: Group I indicates a significant radioactivity release detected in primary water and airborne radioactivity. Group II indicates a significant radioactivity release detected in primary water and as well as airborne radioactivity at the stack. Group III indicates a significant radioactivity release detected at an area monitor and in primary coolant. Group IV indicates a significant radioactivity release detected at an area monitor and in containment air. Group V indicates a significant radioactivity release detected at an area monitor and in air at the stack.

Table 7-12: GREA Detector Combinations and Explanations

| | | | |
|---|-----------------------|--|--|
| GREA DETECTOR COMBINATIONS: [(S+I+L+K+E+R) * (A+B+C+D)] OR [(I+R+K) * (E+S)] | | | |
| <i>Group I</i> – (Significant radioactivity detected in primary water and in containment air) | | | <i>Group II</i> – (Significant radioactivity detected in primary water and in air at the stack) |
| (S) Demineralizer | (C) Cam2 | | (S) Demineralizer (A) Stack Particulate |
| (S) Demineralizer | (D) Cam1 | | (S) Demineralizer (B) Stack Gaseous |
| (E) Fission Products | (C) Cam2 | | (E) Fission Products (A) Stack Particulate |
| (E) Fission Products | (D) Cam1 | | (E) Fission Products (B) Stack Gaseous |
| (K) Reactor Bridge | (C) Cam2 | | (K) Reactor Bridge (A) Stack Particulate |
| (K) Reactor Bridge | (D) Cam1 | | (K) Reactor Bridge (B) Stack Gaseous |
| | | | |
| <i>Group III</i> – (Significant radioactivity release detected at an area monitor and in primary coolant) | | | <i>Group IV</i> – (Significant radioactivity release detected at an area monitor and in containment air) |
| (I) Exhaust Plenum | (E) Fission Products | | (I) Exhaust Plenum (C) Cam2 |
| (I) Exhaust Plenum | (S) Demineralizer | | (I) Exhaust Plenum (D) Cam1 |
| (R) Control Room | (E) Fission Products | | (L) Thermal column (C) Cam2 |
| (R) Control Room | (S) Demineralizer | | (L) Thermal column (D) Cam1 |
| (K) Reactor Bridge | (E) Fission Products | | (R) Control Room (C) Cam2 |
| (K) Reactor Bridge | (S) Demineralizer | | (R) Control Room (D) Cam1 |
| | | | |
| <i>Group V</i> – (Significant radioactivity release detected at an area monitor and in air at the stack) | | | |
| (I) Exhaust Plenum | (A) Stack Particulate | | |
| (I) Exhaust Plenum | (B) Stack Gaseous | | |
| (L) Thermal column | (A) Stack Particulate | | |
| (L) Thermal column | (B) Stack Gaseous | | |
| (R) Control Room | (A) Stack Particulate | | |
| (R) Control Room | (B) Stack Gaseous | | |

7.7.8 Gamma Cave Safety System and Interlocks

The UMLRR Cobalt-60 sources are a Pool Irradiator used both as an underwater irradiator and as a panoramic wet-source storage irradiator as defined by 10CFR36. A gamma radiation facility, adjacent to the lower section of the bulk pool, is a “dry room” providing opportunity for bulk irradiation of experiments in air. This panoramic wet-source storage irradiator facility, is described in detail in Chapter 10.

The facility utilizes a redundant series of fixed radiation monitors, redundant key locks,

[REDACTED] to ensure the safety of operators. In addition to the

fixed radiation monitors, operators [REDACTED] dry room area, are equipped with portable radiation monitors to ensure an additional layer of radiation protection.

Local redundant readouts (Section 7.7.3) of the radiation levels in and around the facility are clearly visible to operators at the approach of this facility outside of the gated area. Additional light tree optical indicators of both door status and cobalt movement are also shown in the same approach area.

Based on existing Co-60 dose rates, the licensed Co-60 activity of [REDACTED] Ci is expected to produce a maximum dose rate at [REDACTED] from the source window of [REDACTED]/hr, and a dose rate of [REDACTED]/hr at a distance of [REDACTED] from the source window. The exterior walls of the facility serve as a permanent beam stop. There is one doorway into the facility.

The UMLRR configuration has been analyzed and granted site specific approval, by means different from the regulatory prescription, under §36.17. This is in addition to fact that the regulatory analysis for the promulgation of 10 CFR Part 36 (58FR7727) specifically states “other utilization facilities such as fuel fabricators, power reactors and research and training reactors will not be affected by the rule”. Exemptions from portions of 10 CFR Part 36 were granted primarily from §36.23 Access Control, §36.27 Fire Protection and §36.37 Power Failures.

The details of the point-by-point review and analysis¹ of the alternative compliance mechanisms can be summarized as follows:

Access Control – The door to the irradiation room is closed and p [REDACTED] [REDACTED]. A second barrier, [REDACTED] is closed as the experimenter leaves the Gamma Cave area. Thus, [REDACTED] are in place to prevent access to the Gamma Cave before any radiation sources are put into use. When the [REDACTED] [REDACTED] is put into use by removal of a [REDACTED] [REDACTED]

Fire Protection – UMLRR Technical Specifications prohibit explosive materials, cryogenic liquids, Pyrophoric materials and oxidizers from the reactor building, Quantities of flammable liquids are limited to that needed for day-to-day operations. All flammable materials

are stored in NFPA certified Flammable cabinet on the [REDACTED] to the [REDACTED]

Power failures – UMLRR has backup generator capacity (Chapter 8) for the access control systems associated with this facility. The control systems are also powered using commercial-grade un-interruptible power supplies, capable of powering the entire control system during the transient time between the power loss and the emergency generator start lag.

7.7.9 Beam Port Bunker Safety System and Interlocks

Several measures are in place to ensure that radiation levels in and around the beam ports are controlled, minimizing dose to experimenters and personnel, and isolating the radiation fields from non-radiation workers. The first physical barrier is a concrete shield structure, which surrounds the open end of the port nearest to the thermal column. The barrier creates a room with three exterior walls, a fourth interior wall to shield the entrance, and a partial concrete ceiling of twenty-four inch depth to prevent scatter toward the third floor catwalk. All concrete walls for this enclosure are twenty-four inches thick. The entrance is designed to mimic a simple labyrinth with walls on either side to prevent scatter of radiation through the shallow door. Two inches of borated plastic is attached to each side of the walls of the concrete enclosure and each side of the door. One inch of borated plastic is attached to the outside of the ceiling. Further shielding is accomplished through use of a beam stop composed of [REDACTED] inch-thick stack of borated polyethylene (Racorad). The shielding allows for the exterior surface area to be open to the general public during full power operations with the shield plug removed. Additional details of this facility can be found in Chapter 4. Entry into this area while the reactor is operating at powers above [REDACTED] will produce an automatic reactor s. An illustration of the general layout of the area can be seen in Figure 7-11.

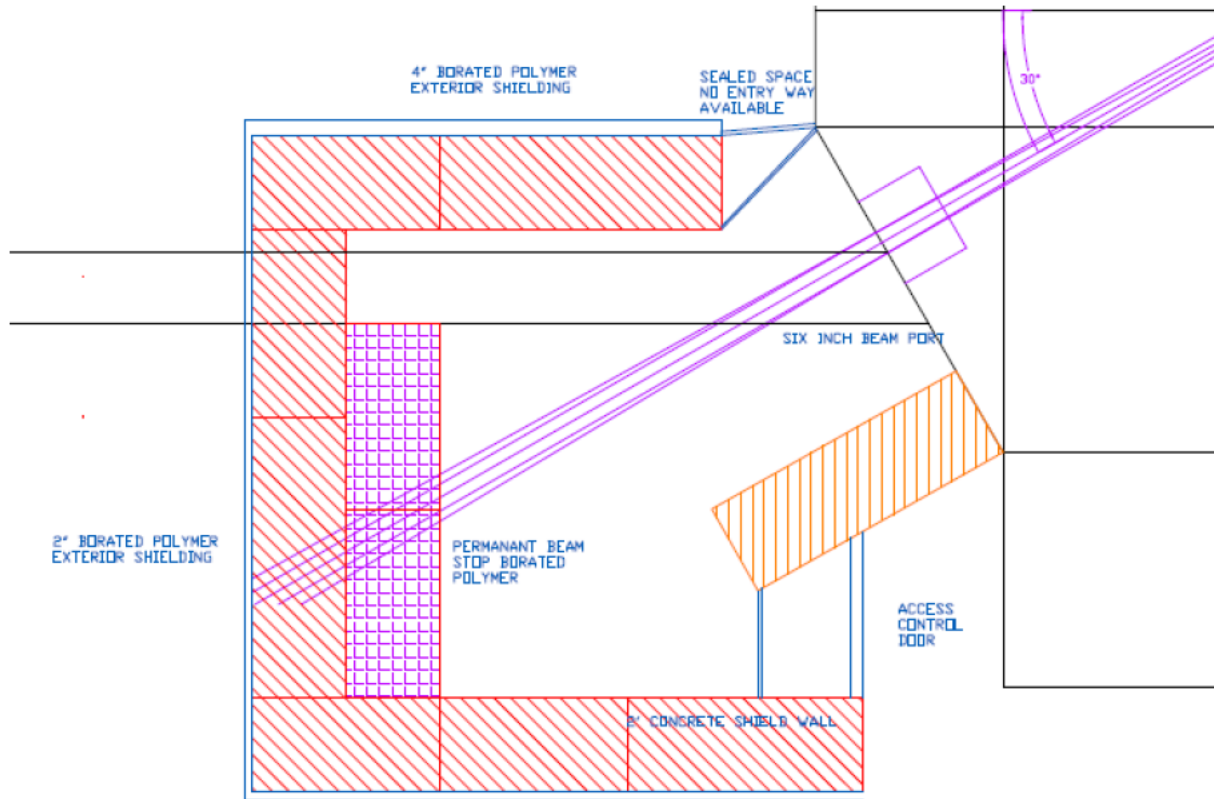


Figure 7-11: Beam Port Bunker Facility

Using the reference core configuration as a basis, the measured dose, at the center of the 6” beam along of the plane of the reactor exterior wall, was [REDACTED]ⁱⁱ. As per 10CFR20.1602, this dose rate categorizes the interior volume of the Beam Port Bunker as a “Very High radiation Area”. This area must first meet the requirements of 10CFR20.1601, as well as “the licensee shall institute additional measures to ensure that an individual is not able to gain unauthorized or inadvertent access to the area”. In order to meet the requirement of 10CFR20.1601 and 1602, the following provisions have been made:

- a. The entryway is key locked at all times, except when occupied. When occupied, the door must remain open. Access to the bunker is made using a key controlled by the licensed reactor operators.
- b. A control device energizes a conspicuous visible alarm signal whenever the radiation level inside of the Bunker exceeds the limits of 10CFR20.1601. The key locked door, limits the ability of an individual to enter the Bunker when the “Very High Radiation Area” condition exists. Should there be an unintended occupant within the bunker area

when reactor power is raised, either the open door interlock or a manual push button exercised by the occupant would shut down the reactor. The control device also provides a local readout, such that personnel are locally aware of any potential radiation fields in the Bunker Area.

- c. The interlocks provide a control device that, upon entry into the area, produces a reactor “SCRAM” causing the level of radiation to be reduced below that level [REDACTED] rem ([REDACTED]) in 1 hour at [REDACTED] centimeters from the radiation source.
- d. If the Bunker door opens, in addition to the reactor SCRAM, an 85 dB alarm and flashing light are also activated until such time that the radiation levels drop below those specified in 10CFR20.1601.

ⁱ UMLRR License No.R-125, Docket No. 50-223 February 4, 1994 through December 30, 1997

ⁱⁱ UML RSO survey and report dated 01/07/2014,